1. Report No.	2. Government Accession No.	3. Recipient's Catalog No.
FHWA/TX-06/5-1707-03-1		

4. Title and Subtitle	5. Report Date
IMPLEMENTATION OF AIMS IN MEASURING AGGREGATE RESISTANCE TO POLISHING, ABRASION AND BREAKAGE	August 2006 Pub: December 2006
	6. Performing Organization Code

7. Author(s)	8. Performing Organization Report No.
Eyad Masad, Anthony Luce, and Enad Mahmoud	Report 5-1707-03-1

9. Performing Organization Name and Address	10. Work Unit No. (TRAIS)
Texas Transportation Institute The Texas A&M University System College Station, Texas 77843-3135	11. Contract or Grant No. Project 5-1707-03

12. Sponsoring Agency Name and Address	13. Type of Report and Period Covered
Texas Department of Transportation Research and Technology Implementation Office P.O. Box 5080 Austin, Texas 78763-5080	Technical Report: September 2005 – May 2006
	14. Sponsoring Agency Code

15. Supplementary Notes

Project performed in cooperation with the Texas Department of Transportation and the Federal Highway Administration.

Project Title: Support for the Implementation of the AIMS Equipment in TxDOT Operations

URL: http://tti.tamu.edu/documents/5-1707-03-1.pdf

16. Abstract

The report presents efforts undertaken to help in the implementation of the Aggregate Imaging System (AIMS) in Texas Department of Transportation (TxDOT) operations. These efforts focus on measuring aggregate shape properties and texture of polishing coupons supplied by TxDOT, compilation of a database of aggregate properties measured at TxDOT and Texas Transportation Institute (TTI), and analysis of the aggregate properties. A comparison was conducted between the measurements from the TIT and TxDOT AIMS units, and it was found that there was no statistical difference between the measurements of the two AIMS units.

The current method used in the Wet Weather Accident Reduction Program (WWARP) relies on the terminal Polished Value (PV) and magnesium sulfate soundness to classify aggregates. A new method is proposed in this report to better classify aggregates. This method is based on the magnesium sulfate soundness and texture results from AIMS. This method is more sensitive than the current method and allows the aggregates to be spread more evenly in four different categories.

The report also includes the development of new methods for measuring aggregate resistance to polishing, abrasion, and breakage. These methods rely on measurements using the Aggregate Imaging System (AIMS) and Micro-Deval. The new method for measuring aggregate resistance to polishing monitors change in aggregate texture as a function of polishing time. The new method for measuring aggregate degradation is capable of distinguishing between breakage and abrasion. The new methods are shown to be rapid and accurate, and they require reasonable training.

17. Key Words	18. Distribution Statement
Aggregate, AIMS, Polishing, Skid, Abrasion, Imaging.	No restrictions. This document is available to the public through NTIS: National Technical Information Service Springfield, Virginia 22161 http://www.ntis.gov

19. Security Classif.(of this report)	20. Security Classif.(of this page)	21. No. of Pages	22. Price
Unclassified	Unclassified	232	

IMPLEMENTATION OF AIMS IN MEASURING AGGREGATE RESISTANCE TO POLISHING, ABRASION AND BREAKAGE

By

Eyad Masad
Assistant Research Scientists
Texas Transportation Institute

Anthony Luce
Graduate Assistant Research
Texas Transportation Institute

and

Enad Mahmoud
Graduate Assistant Research
Texas Transportation Institute

Report 5-1707-03-1
Project 0-1707-03
Project Title: Support for the Implementation of the AIMS Equipment in TxDOT Operations

Performed in cooperation with the
Texas Department of Transportation
and the
Federal Highway Administration

August 2006
Published: December 2006

TEXAS TRANSPORTATION INSTITUTE
The Texas A&M University System
College Station, Texas 77843-3135

DISCLAIMER

This research was performed in cooperation with the Texas Department of Transportation (TxDOT) and the Federal Highway Administration (FHWA). The contents of this report reflect the views of the authors, who are responsible for the facts and the accuracy of the data presented herein. The contents do not necessarily reflect the official view or policies of the FHWA or TxDOT. This report does not constitute a standard, specification, or regulation.

The United States Government and the State of Texas do not endorse products or manufacturers. Trade or manufacturers' names appear herein solely because they are considered essential to the object of this report.

ACKNOWLEDGMENTS

The authors wish to express their appreciation to the Texas Department of Transportation personnel for their support throughout this study, as well as the Federal Highway Administration. We would also like to thank the project director Mr. Edward Morgan and Ms. Caroline Herrera and Dr. German Claros for their valuable input throughout the project.

TABLE OF CONTENTS

Page

TABLE OF CONTENTS (Continued)

Page

TABLE OF CONTENTS (Continued)

Page

LIST OF FIGURES

Figure **Page**

LIST OF FIGURES (Continued)

Figure **Page**

LIST OF FIGURES (Continued)

Figure **Page**

LIST OF FIGURES (Continued)

Figure **Page**

LIST OF TABLES

Table **Page**

LIST OF TABLES (Continued)

Table **Page**

LIST OF TABLES (Continued)

Table **Page**

CHAPTER I
INTRODUCTION

PROBLEM STATEMENT

Aggregate properties influence several aspects of asphalt pavement performance. Angular and textured aggregates are desirable to improve aggregate resistance to permanent deformation. Aggregate polishing characteristics affect asphalt pavement microtexture, and consequently affect pavement surface frictional properties. Aggregate resistance to degradation (abrasion and breakage) is also an important property that influences performance. Abrasion is defined as the loss of aggregate surface angularity, while breakage refers to fracture of particles. Some aggregates experience significant abrasion and breakage during plant operations and compaction, leading to changes in aggregate characteristics critical to Hot Mix Asphalt (HMA) design. Consequently, HMA characteristics in the field would deviate from the designed mix.

New generation mixes such as Open Graded Friction Course (OGFC) and Stone Matrix Asphalt (SMA) rely on stone-to-stone contacts among coarse aggregates to sustain traffic loads. The stress transfer mechanisms in these mixes bear high contact stresses at the contact points, which could cause aggregate degradation at the contact points.

Recent studies at Texas A&M University have focused on developing imaging methods or characterizing aggregate shape characteristics and their influence on HMA performance. This study focuses on developing new test methods for quantifying aggregate resistance to polishing and degradation (abrasion and breakage).

Many test methods exist for measuring aggregate polishing and degradation. However, a critical review of these methods reveals that they suffer from being time consuming, are unable to differentiate between aggregates with distinct resistance to polishing, or are unable to differentiate between aggregate resistance to abrasion and breakage. For example, the Micro-Deval is repeatable in measuring aggregate degradation, but it is not able to differentiate between aggregate breakage and abrasion.

The new methodologies developed in this study rely on the Aggregate Imaging System (AIMS) and Micro-Deval measurements to quantify aggregate resistance to polishing and degradation. As part of this study, measurements conducted using two AIMS units and two Micro-Deval machines were analyzed to establish the reproducibility of these two methods using a wide range of aggregates.

OBJECTIVES OF THE STUDY

The objectives of this study are to:

- Measure the shape properties of aggregate samples and coupons supplied by TxDOT.
- Make necessary changes to the AIMS analysis methods to improve sensitivity to changes in aggregate properties and reduce variability.
- Compile a database of aggregate properties that include the AIMS measurements of aggregate shape, angularity, and texture characteristics.
- Assess the variability in the AIMS measurements conducted at TxDOT and Texas Transportation Institute (TTI).
- Develop a new method for classifying aggregates used in asphalt pavement surfaces as part of the wet weather accident reduction program (WWARP).
- Develop new experimental methods to measure aggregate resistance to polishing, abrasion, and breakage using the Aggregate Imaging System and Micro-Deval machine.

STUDY ORGANIZATION

This report is organized in seven chapters as follows:

- Chapter I introduces the main motivation of this study, followed by the objectives and the outline of the report.

- Chapter II contains a literature review that emphasizes the significance of aggregate resistance to polishing, abrasion, and breakage in asphalt pavement performance. In addition, this chapter includes a summary of the different test methods for measuring aggregate resistance to polishing, abrasion, and breakage.
- Chapter III discusses the analysis of variability in AIMS and Micro-Deval measurements. Measurements were conducted at the Texas Transportation Institute and Texas Department of Transportation.
- Chapter IV discusses the construction and analysis of a database of aggregate properties. This data was used as a basis for comparison of the measurements from the two AIMS units at TTI and TxDOT.
- Chapter V describes the classification of aggregates into three different levels for angularity, texture and sphericity. This chapter also proposes a new method to classify aggregates used in the surface of asphalt pavements as part of the wet weather accident reduction program.
- Chapter VI describes new experimental methods to assess aggregate resistance to polishing, abrasion, and breakage. The methods rely on the AIMS and Micro-Deval measurements.
- Chapter VII includes the conclusions and recommendations of this study.

CHAPTER II
LITERATURE REVIEW

This literature review focuses on the significance of aggregate resistance to polishing characteristics and degradation (abrasion and breakage) on HMA pavement performance. This chapter discusses the advantages and disadvantages of test methods that have been used for measuring these aggregate characteristics.

AGGREGATE POLISHING AND DEGRADATION CHARACTERISTICS

Aggregate properties influence different aspects of HMA performance. HMA performance parameters affected by aggregate properties are permanent deformation, fatigue cracking, frictional resistance, thermal cracking, and raveling (Kandhal and Parker 1998). Many aggregate properties are related to those performance parameters, such as gradation and size, aggregate particle shape and surface texture, porosity, cleanliness, toughness and abrasion resistance, durability and soundness, expansive characteristics, polish and frictional characteristics, and mineralogy and petrography (Kandhal and Parker 1998).

Research conducted under National Cooperative Highway Research Program (NCHRP) 4-30A has highlighted in detail the influence of aggregate shape characteristics on HMA properties and performance (Masad et al. 2005). This study showed that shape, angularity, and texture are all important characteristics that should be quantified to better predict pavement performance. McGahan (2005) conducted comprehensive statistical analyses that related aggregate shape characteristics to several HMA mechanical properties. He concluded that aggregate shape characteristics are very important in influencing these mechanical properties. In fact, McGahan (2005) found that aggregate shape characteristics have a stronger relationships with mechanical properties than other mix properties such as binder grade and voids in mineral aggregates (VMA).

HMA pavement skid resistance depends on the microtexture and macrotexture of its surface. Dahir (1979) and Forster (1989) referred to 0.5 mm as a dividing line between macrotexture and microtexture. Microtexture is mainly dependent on aggregate shape characteristics; while, macrotexture is a function of mix properties, compaction method, and aggregate gradation (Kandhal and Parker 1998, Crouch et al. 1995). Aggregate resistance to polishing affects asphalt pavement microtexture and skid resistance, which is considered a safety parameter. HMA surface frictional or skid resistance must maintain a minimum acceptable safe limit (Bloem 1971). One way that this safe limit can be achieved is through the use of aggregates with high resistance to polishing. Abdul-Malak et al. (1996) indicated that coarse aggregates at the surface are the main source of HMA pavement surface texture. He states that this is a result of the fact that the friction force is a result of the contacting points between vehicle tires and the HMA pavement surface, and coarse aggregates are responsible for developing these contacts points.

Henry and Dahir (1979) indicated that HMA macrotexture allows faster removal of water between the tire and the HMA pavement surface especially at high speeds; on the other hand, microtexture influences where water penetrates the surface and reduces skid resistance at both high and low speeds. Skid resistance of the HMA pavement surfaces is supposed to be adequate both right after construction and also after being opened to traffic, so aggregates that resist polishing and wear are desired (Bloem 1971).

Hogervorst (1974) reported that the change of skid resistance with vehicle speed depends on both its microtexture and macrotexture (see Figure 2.1). Microtexture defines the level of skid resistance, but skid resistance decreases as vehicle speed increases. Macrotexture will control the magnitude of reduction of skid resistance as speed increases.

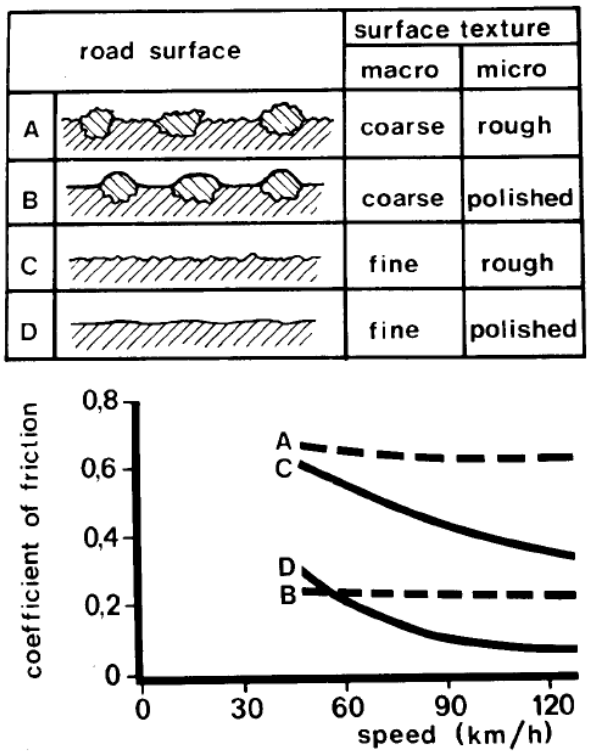

Figure 2.1. Skid Resistance Relationship with Surface Texture (after Hogervorst 1974).

Aggregate resistance to degradation (abrasion and breakage) is another important aggregate property that is related to several HMA performance parameters. Aggregates are exposed to degradation during production and construction before the pavement is in service. Degradation during construction affects the overall gradation; as such, the field produced mix will be different from the laboratory designed one (Wu et al. 1998).

New generations of asphalt mixes such as OGFC and SMA rely on stone-to-stone contacts in transferring applied stresses within the aggregate structure. This stress transfer mechanism imposes high contact stresses at the contact point that might lead to aggregate fracture and compromise the mix performance (Gatchalian 2005). Therefore, there is a need to develop test methods to assess aggregate resistance to fracture during compaction and under traffic loads. In a recent study, Gatchalian (2005) used conventional and imaging techniques to assess aggregate fracture in SMA mixes. He found that some aggregates do experience significant

crushing in SMA, and he recommended using the Aggregate Imaging System to measure change in aggregate angularity after Micro-Deval testing and changes in gradation after compaction as measures of aggregate resistance to fracture.

AGGREGATE POLISHING TESTS

There are different methods available for measuring aggregate resistance to polishing and loss of frictional characteristics. Some of these methods have been used widely for a long time, while others have only been used in certain countries and laboratories, and some have recently been developed and are still in the evaluation process.

The British wheel/pendulum method, also known as polished value (PV), is one of the most widely used methods for measuring frictional properties of aggregates. Critical review of this method showed that test procedures differ among countries and even among state highway agencies in the United States. ASTM E303 and ASTM D3319 document these test methods. ASTM provides two different specifications: one for the polishing procedure, and the other for the use of the British pendulum to measure friction. The Texas Department of Transportation procedure for this test is Tex-438-A under the name "Accelerated Polish Test for Coarse Aggregates." The general concept and steps are similar among the different procedures, although they differ in some details such as type of polishing machine used and polishing time.

The British wheel/pendulum method procedure relies on preparing aggregate coupons that consist of aggregates glued to a plate. These coupons are polished using a polishing wheel for a certain period of time. Then, the British pendulum measures the friction value of the aggregate coupons, which is called the polish value (PV). A higher PV indicates aggregates with higher frictional properties and better skid resistance.

Many studies evaluate the British wheel/pendulum test. Won and Fu (1996) evaluated the Tex-438-A test procedure and revealed many issues concerning this test. They found that the PV resulting from this test has very high variability. The study

results attributed the high variability to the dependency of the PV on several factors that include:

- Coupon curvature: This factor may result in a change of up to 2 PV.
- Aggregate arrangement: Heterogeneous aggregates such as gravel contain some sandy particles that will provide more friction than other particles. Up to a 10 PV decrease was obtained when sandy particles were grouped rather than dispersed.
- Slider load: A 4 PV change was reported due to changes in slider load within American Society for Testing and Materials (ASTM) limits.
- Number of swings: The slider itself polishes aggregates each time, and the polished value changes with the number of swings.
- Aggregate sampling techniques: Obtaining aggregates through proper sample splitting is recommended over the picking of aggregates.

Perry et al. (2001) studied the PV test and concluded that it is not a good test to predict the skid resistance of aggregates. This conclusion was based on findings that the test result depends on aggregate size. Smith and Fager (1991) pointed out some issues regarding the use of the British pendulum as a measure of polishing. They reported that changing the pendulum pad changes the results, although the two pads used in the study met the specification. Kandhal et al. (1993) presented the categorization of PV for both limestone and gravel aggregates as shown in Figures 2.2 and 2.3.

As shown in Figures 2.2 and 2.3, 59 percent of limestone aggregates are between the values 28 and 32, while 75 percent of gravel aggregate results are in this same small range. These results indicate that it is hard to distinguish between aggregates using this test.

Another test that has been used for measuring aggregate polishing is the Penn State Reciprocating Polishing Machine Method (Nitta et al. 1990). A schematic diagram of the polishing machine for this test is presented in Figure 2.4. This machine is portable and is capable of polishing aggregates or pavement mixtures in the laboratory or in the

in the field. The machine applies a rubber pad back and forth over a specimen surface to be polished, while water and abrasive are charged to the specimen surface.

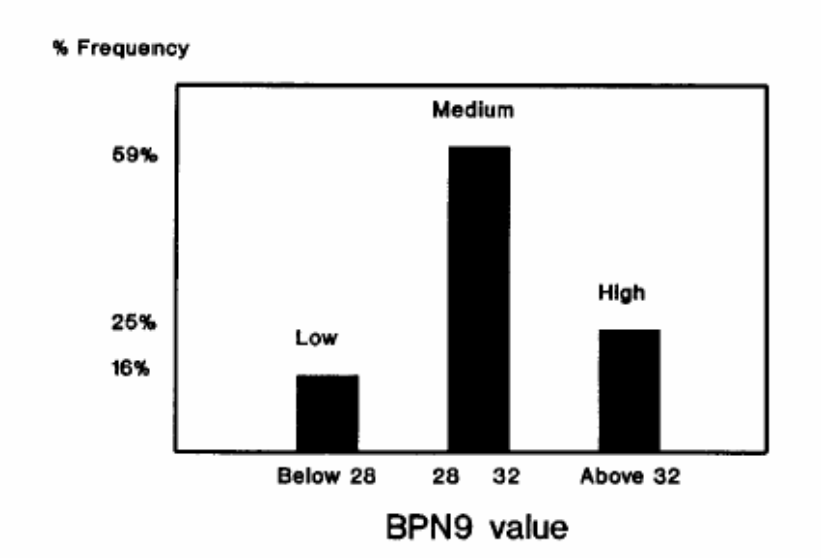

Figure 2.2. Polish Value Percentages Histogram for Limestone (after Kandhal et al. 1993).

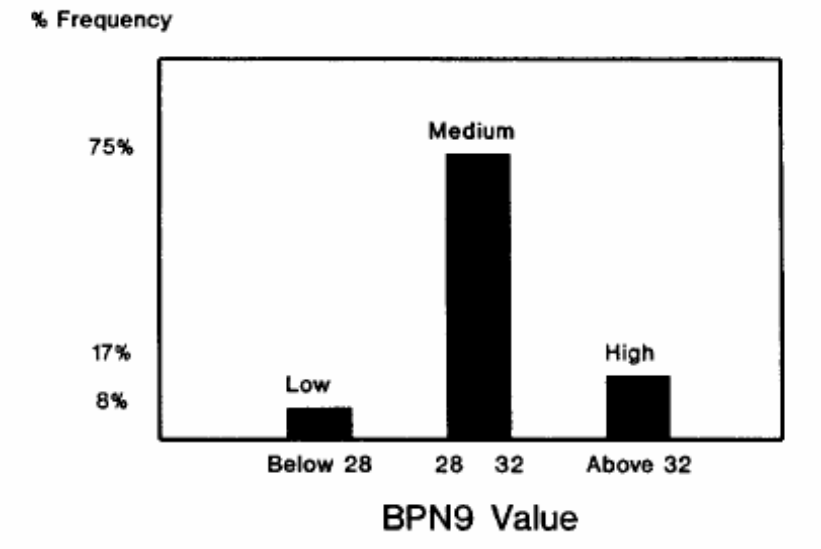

Figure 2.3. Polish Value Percentages Histogram for Gravel (after Kandhal et al. 1993).

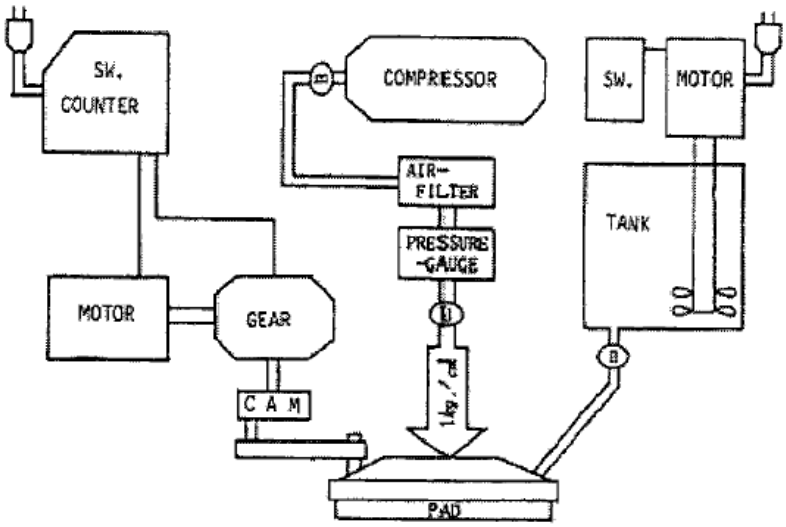

Figure 2.4. Schematic of Penn State Reciprocating Polisher (after Nitta et al. 1990).

Mullen et al. (1971) suggested two different laboratory methods for evaluating aggregate polishing. The first test is called the Circular Track Wear method. This method is based on polishing pavement samples prepared from aggregates that need to be evaluated. Subsequently, pavement samples are placed in a circular track, which are then polished for 16 hours using small-diameter tires. This process also uses the British pendulum to obtain the PV. Therefore, some of the limitations of the British pendulum are inherited in this test. The second test recommended by Mullen et al. (1971) is called the Jar Mill Wear method, which also uses the British pendulum to find the PV for pavement samples. However, the polishing method is different. Aggregates are polished first and then used to prepare pavement samples, which are tested using the British pendulum. Aggregate polishing is conducted using jar mill with flint pebbles as abrasive charge in dry condition. Some aggregates required about 120 hours of polishing to reach the terminal polishing.

As a result of a long-term multi-phase project initiated by Tennessee Department of Transportation (TDOT), Crouch et al. (1995, 1996, 2001, 2005) developed two methods for evaluating aggregate resistance to polishing in asphalt surfaces. The first method is called the Tennessee Terminal Textural Condition Method (T^3CM). This method is based on the idea of polishing an aggregate sample until it reaches its terminal texture condition. The terminal texture condition represents the state in which aggregate particles reach their minimum angularity and surface roughness. The T^3CM uses the Los Angeles abrasion and impact machine to achieve the terminal texture condition. However, no steel balls are used as in the case for the standard Los Angeles test, and the test continues until terminal texture condition is reached. The texture condition of the aggregate sample is assessed using the T^3CM uncompacted voids content apparatus (Figure 2.5). This apparatus measures the percent of uncompacted voids in an aggregate sample. The percent of voids is used as an indication of aggregate angularity and texture.

Crouch et al. (2005) also developed the Micro-Deval Voids at 9 hours (MDV9). This method was developed as a replacement of the T^3CM test. The changes were conducted to achieve:

- Smaller sample size (60 kg for T^3CM),
- Reduced laboratory time (30 to 47 hours for T^3CM), and
- Specified stopping point (no specified stopping time for T^3CM).

The Micro-Deval machine polishes aggregates in the MDV9 test. An aggregate sample of 4500 g is polished for 9 hours.

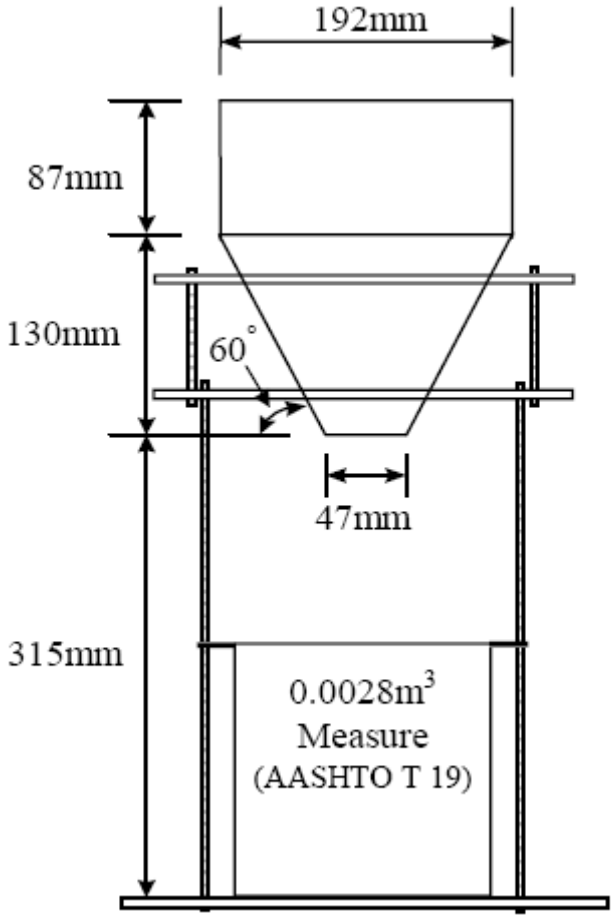

Figure 2.5. Schematic of T^{3}CM Uncompacted Voids Content Apparatus (after Crouch et al. 2005).

AGGREGATE ABRASION TESTS

The Los Angeles (L.A.) Abrasion and Impact Test (Association of American State and Transportation Officials [AASHTO T 96]) is the most widely used method for measuring aggregate resistance for abrasion and aggregate toughness (Kandhal and Parker 1998). In this test aggregates are mixed with steel balls of specific size and weight in a steel drum. Drum rotation promotes interaction between aggregates and steel, which introduces different mechanisms of abrasion, impact, and grinding. The lifting and dropping action of aggregates introduces very high impact forces, which

makes the test a measure of impact resistance rather than abrasion resistance. Originally, the test name was the L.A. Abrasion Test, but the addition of 'impact' to its name was to recognize that this test measures aggregate resistance to impact rather than abrasion (Rogers 1998). According to the AASHTO T 96, this test is a measure of aggregate degradation due to abrasion, impact, and grinding. However, Rogers (1998) indicated that studies revealed that this test measures mostly aggregate resistance to mechanical breakdown. Table 2.1 presents the specific details of the test according to the AASHTO T 96 procedure.

Table 2.1. AASHTO T 96 Los Angeles Test Specifications Summary.

Aggregate Material Size	Many gradings (max. size up to 3 inch)
Rotation Speed	30 to 33 rpm
Total Revolutions	500 (1000 for large aggregate size grading)
Steel Ball Size	46.8 mm diameter
Abrasion Charge	2500 to 5000 g—6 to 12 steel balls—(varies with aggregate size)
Determining the Loss	Percent passing sieve No. 12

The Micro-Deval test (AASHTO TP 58-00) is the second test that has been used for measuring abrasion resistance. This test was originally developed in the 1960s in France. The test measures the durability and abrasion resistance of aggregates through abrasion between aggregate particles and between aggregate particles and steel balls in the presence of water (Cooley and James 2003). The Micro-Deval test is standardized in AASHTO TP 58-00 "Standard Test Method for Resistance of Coarse Aggregate to Degradation by Abrasion in the Micro-Deval Apparatus," and in Tex-461-A procedure, "Degradation of Coarse Aggregate by Micro-Deval Abrasion." Table 2.2 presents the specific details of the test according to the AASHTO TP 58-00 procedure. Figure 2.6 shows schematic cross section of interaction between aggregates and steel balls in presence of water in the Micro-Deval.

Table 2.2. AASHTO TP 58-00 Micro-Deval Test Specifications Summary.

Aggregate Material Size	4.75 to 16.0 mm (3 grading types)
Rotation Speed	100 ± 5 rpm
Total Revolutions	9500 to 12000
Steel Ball Size	9.5 mm diameter
Abrasion Charge	5000 ± 5 g
Determining the Loss	Percent passing sieve No. 16

Figure 2.6. Schematic of Interaction between Aggregates and Steel Balls in Presence of Water in the Micro-Deval.

Several studies have compared the Micro-Deval and L.A. Abrasion and Impact Tests. A few points summarizing these studies are given herein:

- The L. A. Test is believed to measure the impact resistance of aggregates rather than abrasion resistance (Lane et al. 2000).
- The wet conditions in the Micro-Deval test give it the ability to simulate the field condition of aggregates better than the dry state in the L.A. Test (Rogers 1998).
- The interaction between aggregates and steel balls in the Micro-Deval jar induces more tumble action than impact (Meininger 2004).

- Los Angeles Test results have poor correlation with field performance (Senior and Rogers 1991).
- Micro-Deval results had mixed correlations with aggregate performance histories (Cooley and James 2003). This mixed correlation could be attributed to the difficulty of ranking aggregates performance simply based on experience with these aggregates.

Other tests for measuring aggregate resistance to abrasion are the "Aggregate Abrasion Test" and the "Nordic Ball Mill Test." These two tests are more widely used in Europe than in the United States. The Aggregate Abrasion Test is a dry test and it uses a flat rotating steel plate to abrade aggregates, while the Nordic Ball Mill Test has minor differences from the Micro-Deval test. Table 2.3 provides a comparison between the two tests (Hunt 2001).

Table 2.3. Comparison of Micro-Deval and Nordic Ball Mill Tests Specifications.

	Micro-Deval	**Nordic Ball Mill**
Aggregate Material Size	4.75 to 16.0 mm (3 grading types)	11.2 to 16.0 mm
Rotation Speed	100 ± 5 rpm	90 ± 3 rpm
Total Revolutions	9500 to 12,000	5400
Steel Ball Size	9.5 mm diameter	15.0 mm diameter
Abrasion Charge	5000 ± 5 g	7000 ± 10 g
Determining the Loss	Percent passing sieve No. 16	Percent passing 2 mm sieve
Cylinder Dimensions (Inside Diameter, Inside Length)	194 ± 2.0 mm, 170 ± 2.0 mm	206.5 ± 2 mm, 335 ± 2 mm

AGGREGATE IMAGING SYSTEM

AIMS determines shape characteristics of aggregate through image processing and analysis techniques. AIMS equipment consists of a computer automated unit which includes an aggregate measurement tray with marked grid points at specified distances along x and y axes. Coarse aggregate sample is placed on the specified grid points, while fine aggregate sample is spread uniformly on the entire tray. The system is also equipped with top lighting, back lighting and a camera unit. The AIMS software analyzes the aggregate images and produces measurements of their shape, angularity, and surface texture. Aggregate texture is quantified using wavelet analysis method (Texture index); aggregate angularity is described by measuring the irregularity of a particle surface using the gradient and radius methods (Angularity index); and shape is described by 2D form and 3D form (Sphericity). All details of AIMS and the analysis principals are given by Al-Rousan (2004).

SUMMARY

The literature review findings indicate that current methods for measuring aggregate resistance to polishing have several drawbacks. Among these drawbacks are the length of time it takes to prepare and polish aggregate specimens, and the influence of other factors besides texture on the results. For example, the British wheel/pendulum method results depend on the coupon curvature and size of aggregates.

Several studies have reported that the Micro-Deval test is a good method for assessing aggregate resistance to abrasion. However, the weight loss measured in this test could be attributed to either abrasion or breakage. Therefore, the Micro-Deval alone cannot separate the influence of abrasion from breakage.

CHAPTER III
ANALYSIS OF VARIABILITY IN AIMS AND MICRO-DEVAL MEASUREMENTS

OVERVIEW

AIMS repeatability and reproducibility have been evaluated in previous studies through the analysis of multiple measurements conducted by the same operator, and measurements conducted by three operators (Bathina 2005). However, these measurements were conducted using the same AIMS unit. This chapter documents the results of analyzing variability in measurements conducted using two AIMS units located at the TTI and TxDOT laboratories. In addition, this chapter analyzes variability in Micro-Deval measurements conducted in two different laboratories. The variability analysis is necessary since the methods recommended in Chapter IV rely on the results from the AIMS and Micro-Deval tests. The reliability of these methods obviously depends on the level of variability in the test methods used.

INTRODUCTION

Bathina (2005) conducted a statistical analysis of AIMS measurements in order to determine their repeatability, reproducibility, and sensitivity. The results of this study indicated that AIMS is highly repeatable. The maximum coefficient of variation (COV) was 13.9 percent when measuring the texture of random samples from the same aggregate and 4.9 percent when measuring the same aggregate sample, while the COV of reproducibility (variation among three operators) was 16.3 percent when measuring random samples. All measurements by Bathina (2005) were conducted using a single AIMS unit. This project also found that AIMS was sensitive to changes in aggregate properties. In the same study, AIMS results were compared with other test methods in terms of repeatability and reproducibility, and the conclusion was that AIMS has excellent repeatability and reproducibility compared to other test methods.

Bathina (2005) implemented a statistical method to compare AIMS results for two aggregates using aggregate shape classification categories developed by Al-Rousan (2004). Categories for texture and gradient angularity are shown in Table 3.1. Details of the mathematical derivation of the image analysis methods are given by Al-Rousan (2004).

Table 3.1. Gradient Angularity and Texture Categories.

Aggregate Property	Sub Class				
	1	**2**	**3**	**4**	**5**
Gradient Angularity	Rounded	Sub Rounded	Sub Angular	Angular	
Texture	Polished	Smooth	Low Roughness	Medium Roughness	High Roughness

VARIABILITY BETWEEN TWO AIMS UNITS

Angularity and Texture of Aggregates

Materials and Experiment

In this experiment, the same aggregates were scanned using the two AIMS units by the same operator. Aggregates that were used in this evaluation are listed in Table 3.2.

Table 3.2. List of Aggregates Used in Assessing AIMS Variability.

Aggregate Number	TxDOT Label	Aggregate Type	After Micro-Deval (AMD) or Before Micro-Deval (BMB)
1	05-0213	Crushed Limestone	AMD
2	05-0231	Crushed Gravel	AMD
3	05-0519	Crushed Limestone	AMD
4	05-0532	Crushed Limestone	AMD
5	05-0543	Partly Crushed Gravel	BMD
6	05-0545	Crushed Limestone	BMD
7	05-0643	Crushed Limestone	BMD
8	05-0649	Crushed Limestone	BMD
9	05-0693	Crushed Gravel	BMD
10	05-0708	Crushed Sandstone	BMD

As shown in this table, some of the aggregates used in this analysis were subjected to the Micro-Deval abrasion. These aggregates were included in order to ensure that a wide range of aggregate characteristics are accounted for in the analysis.

Three different sizes (1/2"—3/8", 3/8"—1/4", 1/4"—#4) of each of the aggregates in Table 3.2 were scanned and analyzed for angularity and texture. That is, a total of 60 scans were conducted at each location (30 scans for angularity and 30 scans for texture). Aggregate size will be referred to in this study by the retaining sieve (3/8", 1/4", and # 4).

Statistical Methods and Results

Three statistical analysis methods were used to compare the results from the two AIMS units by using SPSS software version 11.5. The first analysis calculates the average characteristics for each aggregate type, plotting the averages of the two AIMS units, and calculating the fitted line equation with its R^2. Such plots will give a general idea of how good the results are. Figures 3.1, 3.2, 3.3, and 3.4 represent the texture analysis results, while Table 3.3 shows the fitting equations. It can be seen that the R^2 values in Table 3.3 indicate an excellent correlation between the TTI and TxDOT measurements. Also, the equations in Table 3.3 show that the measurements are close to the equality line with small biases.

Figures 3.5, 3.6, 3.7, and 3.8 show the gradient angularity results. Very good correlation exists between the angularity measurements, but the correlation is not as good as the texture results. The R^2 and fitting equations in Table 3.4 clearly show this. It is important to mention that the higher intercept numbers for angularity compared with texture are expected as the magnitude of gradient angularity is in the thousands, while the magnitude for texture is in the hundreds.

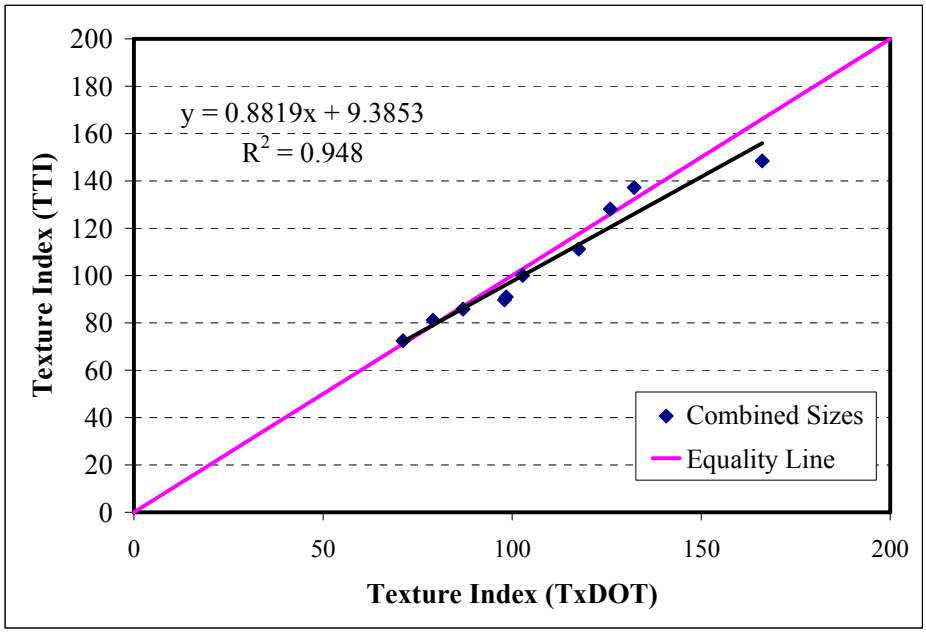

Figure 3.1. AIMS Analysis of Variability: Combined Sizes Texture Results.

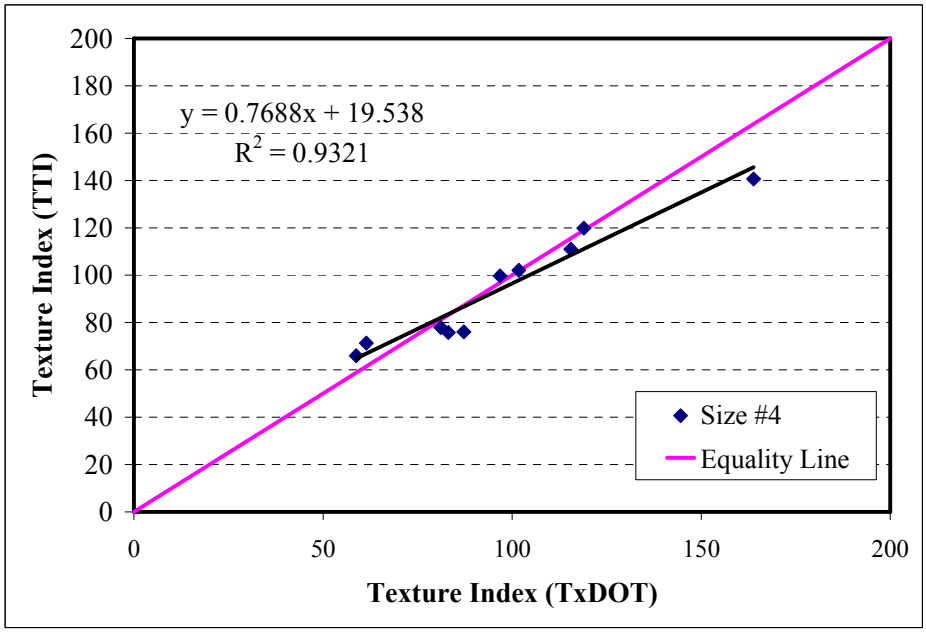

Figure 3.2. AIMS Analysis of Variability: #4 Size Texture Results.

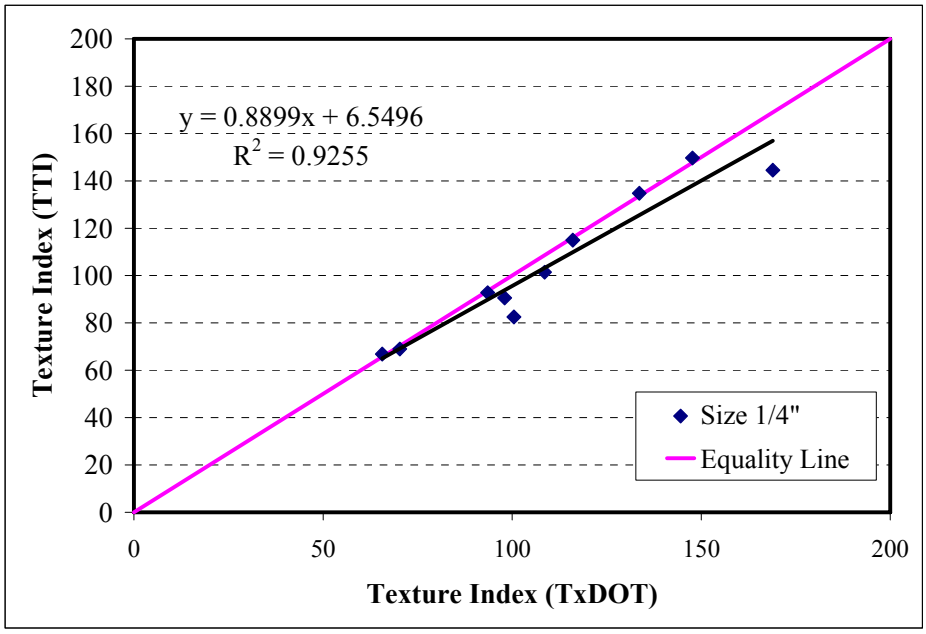

Figure 3.3. AIMS Analysis of Variability: 1/4" Size Texture Results.

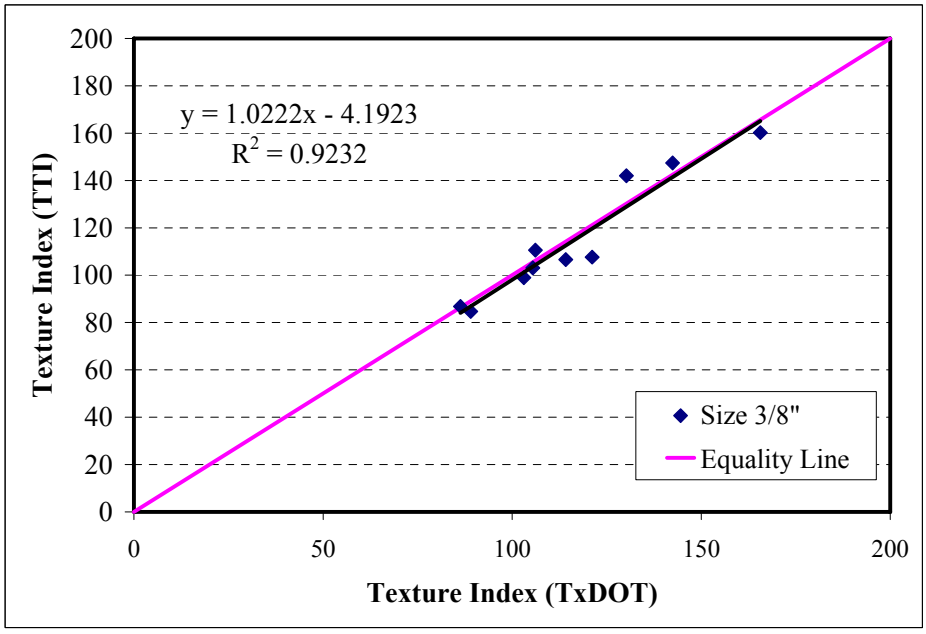

Figure 3.4. AIMS Analysis of Variability: 3/8" Size Texture Results.

Table 3.3. Linear Model Results for Texture Analysis.

	R^2	Linear Equation
Combined 3 sizes	0.948	TTI = 0.8819 × TxDOT + 9.3853
1/4"size	0.9255	TTI = 0.8899 × TxDOT + 6.5496
3/8" size	0.9232	TTI = 1.0222 × TxDOT – 4.1923
#4 size	0.9321	TTI = 0.7688 × TxDOT + 19.538

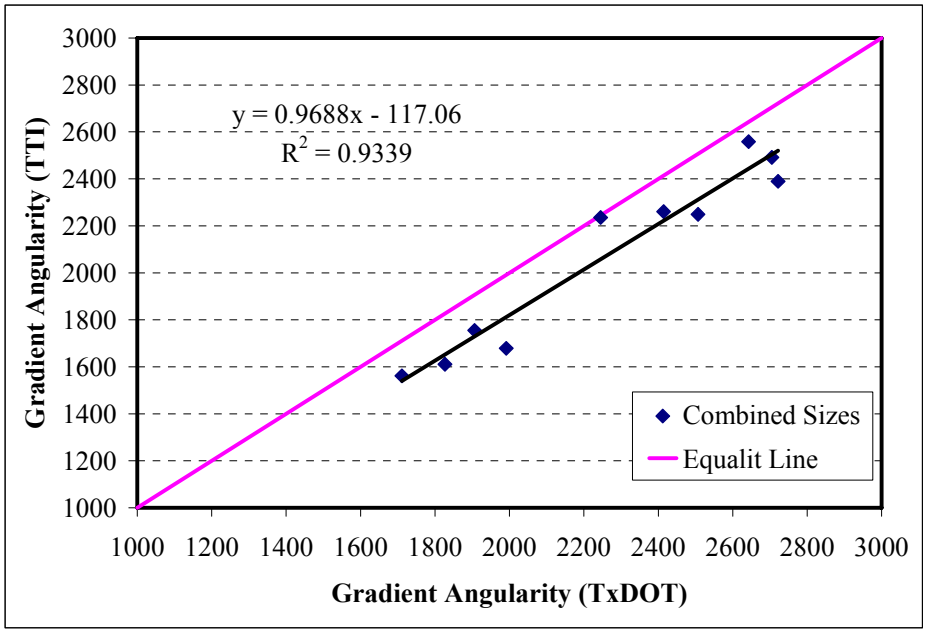

Figure 3.5. AIMS Analysis of Variability: Combined Sizes Gradient Angularity Results.

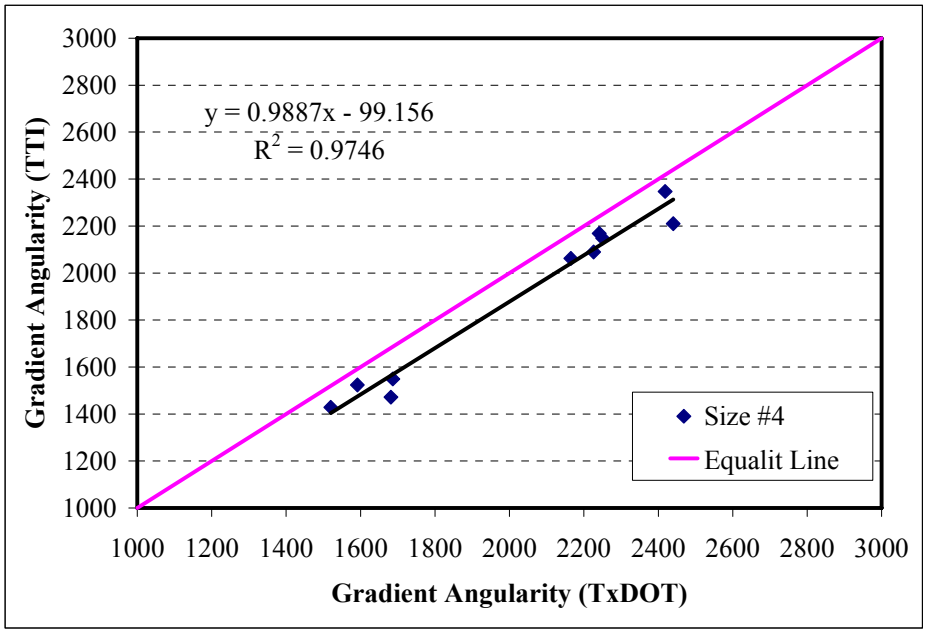

Figure 3.6. AIMS Analysis of Variability: #4 Size Gradient Angularity Results.

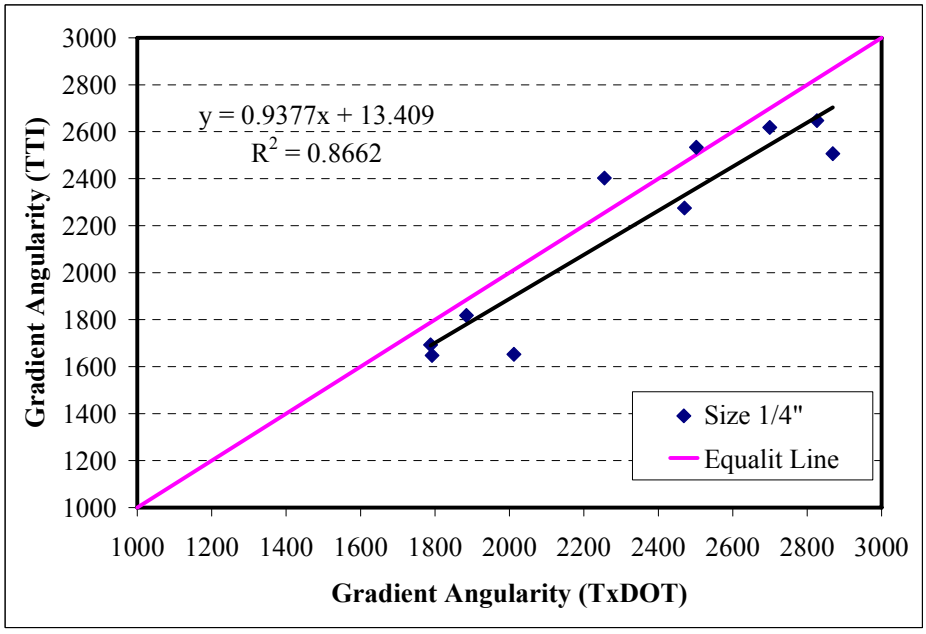

Figure 3.7. AIMS Analysis of Variability: 1/4" Size Gradient Angularity Results.

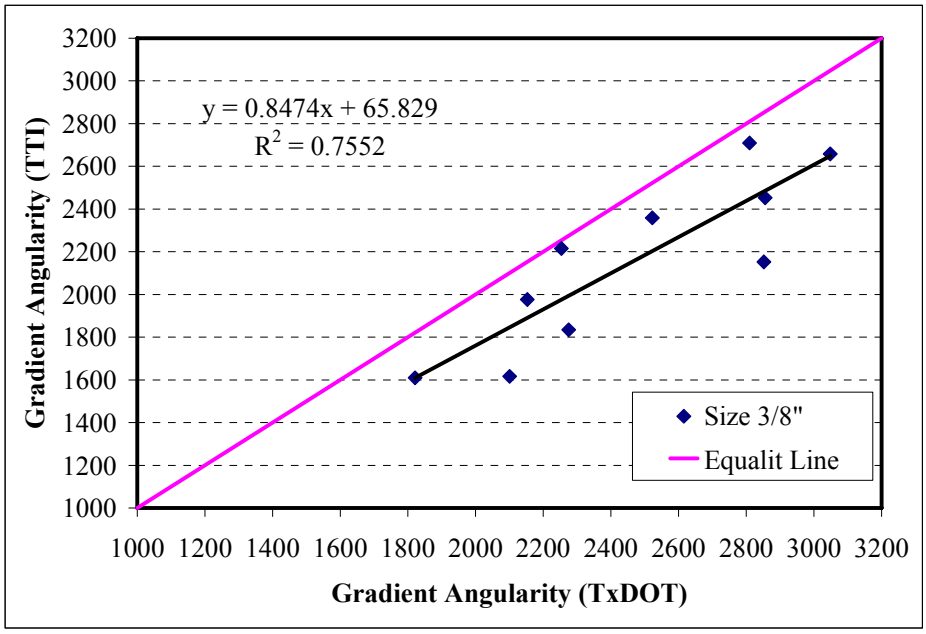

Figure 3.8. AIMS Analysis of Variability: 3/8" Size Gradient Angularity Results.

Table 3.4. Linear Model Results For Gradient Angularity Analysis.

	R^2	Linear Equation
Combined 3 sizes	0.9339	TTI = 0.9688 × TxDOT – 117.06
1/4" size	0.8662	TTI = 0.9377 × TxDOT + 13.409
3/8" size	0.7552	TTI = 0.8474 × TxDOT + 65.829
#4 size	0.9746	TTI = 0.9887 × TxDOT – 99.156

The second statistical analysis method involved calculating the confidence interval (C.I) for the difference between the means using the following equation:

$$(\overline{X}_{TTI\,i,j} - \overline{X}_{TxDOT\,i,j}) \pm 1.96 \times \sqrt{(\sigma^2_{TTI\,i,j} + \sigma^2_{TxDOT\,i,j})} \qquad (3.1)$$

where

$\overline{X}_{TTI\,i,j}$ = estimated value of the mean for aggregate property scanned at TTI

$\overline{X}_{TxDOT\,i,j}$ = estimated value of the mean for aggregate property scanned at TxDOT

$\sigma_{TTI\,i,j}$ = standard error in estimation of the mean for aggregate property at TTI

$\sigma_{TxDOT\,i,j}$ = standard error in estimation of the mean for aggregate property at TxDOT

i = aggregate number with values of 1, 2, …, 10

j = aggregate size with values of 1, 2, 3, 4, where 4 indicates the combined sizes.

The interval in Equation 3.1 is at 95 percent confidence. If the C.I contains zero, then the difference between the mean values of the aggregate property between TTI and TxDOT can be considered zero and the two measurements have the same mean value.

The estimated means and standard errors are given in Appendix A, and the C.Is for the difference in means between the TTI and TxDOT results are in Appendix B. Table 3.5 summarizes the C.Is' results for texture. It is obvious that in most cases the C.Is' contain zero indicating that the TTI and TxDOT texture measurements have the same mean value.

Table 3.5. Texture C.Is Results Summary.

	Number of C.I Containing Zero
Combined 3 sizes	9
1/4" size	8
3/8" size	9
#4 size	10

Table 3.6 shows a summary of the C.Is for angularity. Most of the C.Is contain zero. For the combined three sizes, the reason for three intervals not containing zero is attributed to the 3/8" size results. The correlation for the 3/8" size was not as good as the other results. Nevertheless, the results are still acceptable from a practical point of view.

Table 3.6. Gradient Angularity C.Is Results Summary.

	Number of C.I Containing Zero
Combined 3 sizes	7
1/4" size	10
3/8" size	6
#4 size	10

The third statistical analysis was in accordance with the categorical analysis employed by Bathina (2005). This chapter uses the chi-square goodness of fit test to analyze differences in measurements conducted in each of the aggregates listed in Table 3.2. The analysis used the following hypotheses:

- Null hypothesis: the two aggregates are not different in at least one subclass.
- Alternative hypothesis: the two aggregates are different in at least one subclass.

The p-value of the Pearson chi-square provides the test for the null hypothesis using 95 percent confidence. If the p-value is less than 0.05, then the null hypothesis is rejected; on the other hand, if the p-value is higher than 0.05, the null hypothesis cannot be rejected. Further knowledge of the difference in each subclass can be obtained by observing the standard residual. If the standard residual for a subclass is greater than 1.96, the difference in that subclass is believed to be a contributing factor.

An example of the texture and angularity results for aggregate 5 are shown in Tables 3.7 and 3.8, respectively. In aggregate 5, all the chi-square p-values are higher than 0.05 and all the standard residuals are less than 1.96. Therefore, all the subclasses are not different from each other. The same table is generated for each of the aggregates and all are given in Appendix D. Appendix E contains examples of full chi-square tables.

Tables 3.9 and 3.10 provide a summary of the categorical analysis results for the 10 aggregates. It is evident that the majority of measurements indicated that the p-values are higher than 0.05, and the standard residuals are less than 1.96. Again, this analysis

supports the main finding that the texture and angularity measurements in both the TTI and TxDOT AIMS units are similar.

Table 3.7. Chi-Square Summary Table for Texture Results of Aggregate 5.

Aggregate 5	Size Compared	Standard Residual Subclass					Chi-Square p-value
Texture		1	2	3	4	5	
TxDOT	**Combined**	0.4	-0.6	0.5	-0.4	-0.7	0.580
TTI		-0.4	0.6	-0.5	0.4	0.7	
TxDOT	**3/8"**	0.4	-0.4	0.3	-1.4		0.184
TTI		-0.4	0.4	-0.3	1.4		
TxDOT	**1/4"**	0.2	-0.6	0.6	0.3	-1.0	0.429
TTI		-0.2	0.6	-0.6	-0.3	1.0	
TxDOT	**#4**	0.3	-0.9	0.6			0.297
TTI		-0.3	0.9	-0.6			

Table 3.8. Chi-Square Summary Table for Gradient Angularity Results of Aggregate 5.

Aggregate 5	Size Compared	Standard Residual Subclass				Chi-Square p-value
Gradient Angularity		1	2	3	4	
TxDOT	**Combined**	-0.1	0.4	-0.4	-1.0	0.450
TTI		0.1	-0.4	0.4	1.0	
TxDOT	**3/8"**	-0.1	0.2	0.4	-1.0	0.504
TTI		0.1	-0.2	-0.4	1.0	
TxDOT	**1/4"**	0.5	0.2	-1.5	-1.0	0.073
TTI		-0.5	-0.2	1.5	1.0	
TxDOT	**#4**	-0.3	0.6	-0.4		0.547
TTI		0.3	-0.6	0.4		

Table 3.9. Categorical Analysis Results Summary for the 10 Aggregates' Texture.

	Number of Cases with p<0.05	Number of Cases with Standard Residuals > 1.96
Combined 3 sizes	0	0
1/4" size	1	0
3/8"size	0	0
#4 size	0	0

Table 3.10. Categorical Analysis Results Summary for the 10 Aggregates' Angularity.

	Number of Cases with p<0.05	Number of Cases with Standard Residuals > 1.96
Combined 3 sizes	1	1
1/4" size	3	1
3/8"size	3	1
#4 size	1	0

For each aggregate, a plot of columns that represent the percent of aggregate that belongs to each subclass of aggregate texture is useful to compare the results between TTI and TxDOT. Figures 3.9 and 3.10 present the plots of angularity and texture for aggregate 5. The same plot was generated for all 10 aggregates, and these plots are in Appendix C. In general, the results support the statistical results that the majority of TTI and TxDOT measurements are similar.

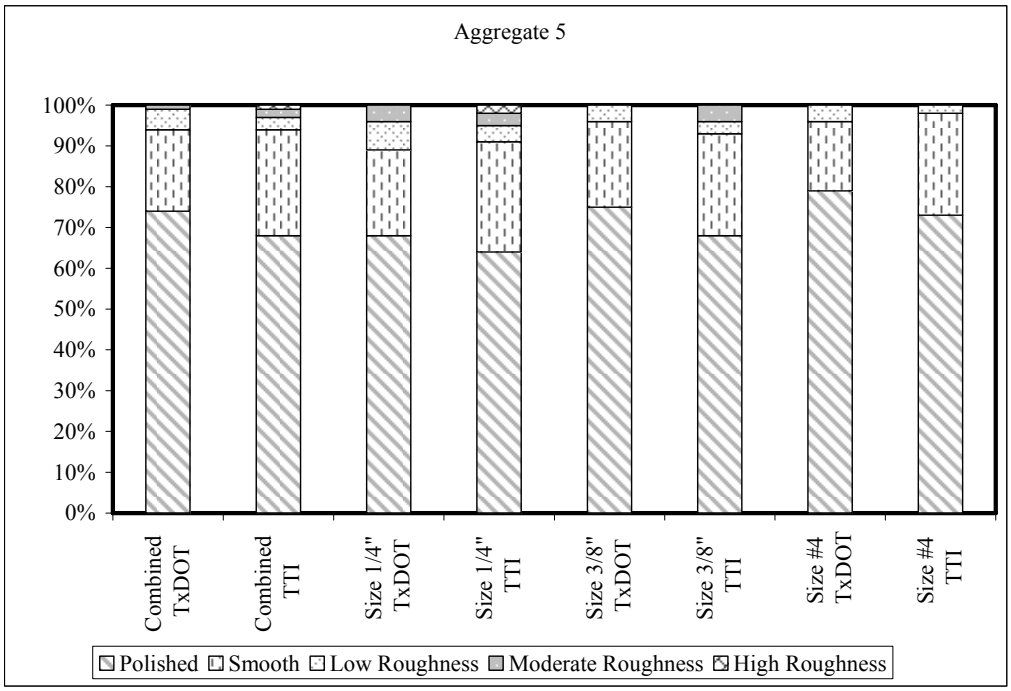

Figure 3.9. Aggregate 5 Texture Subclasses.

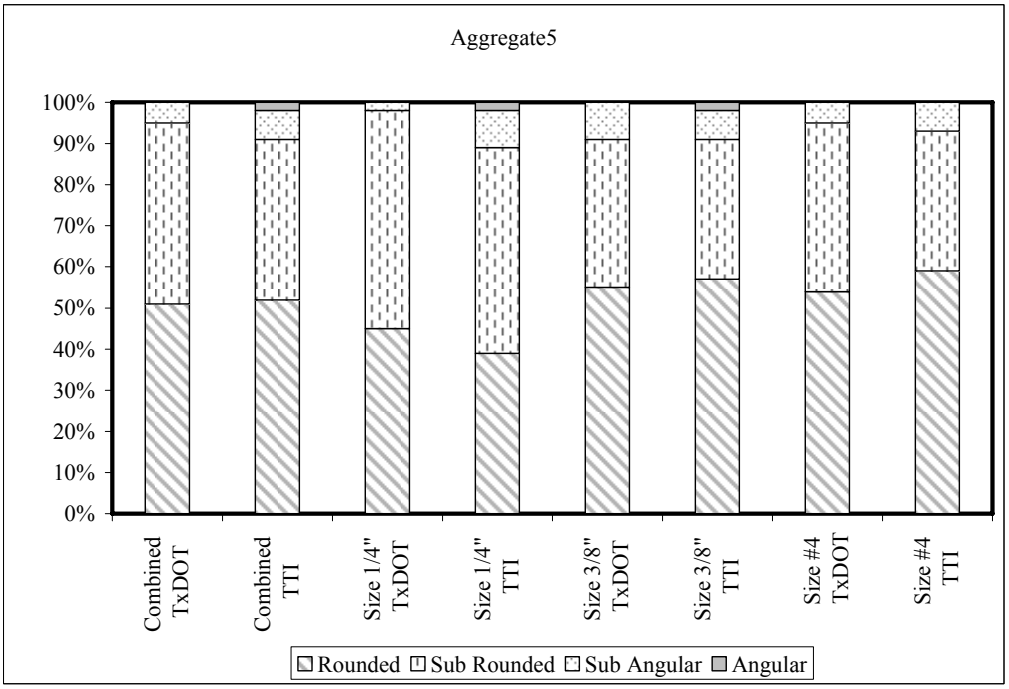

Figure 3.10. Aggregate 5 Gradient Angularity Subclasses.

SUMMARY

In this chapter, the results from two AIMS measurements were compared. Ten aggregates were measured using the two AIMS units, and statistical analysis was conducted to determine the correlations between the measurements. The first analysis was based on calculating the average characteristics of each aggregate type, plotting the averages from the two AIMS units, and calculating the fitted equation with its R^2. The R^2 for texture comparison was higher than 0.92, while the R^2 for the angularity comparison was higher than 0.75. As will be discussed in the following chapter, the angularity method was modified to reduce variability and enhance the correlation. The second statistical analysis involved calculating the confidence interval for the difference between the means. In most cases, the results showed that the TTI and TxDOT measurements had the same mean value. The third analysis method was based on the categorical analysis and the Pearson chi-square goodness of fit test. These results further support the main finding that the texture and angularity measurements from the TTI and TxDOT AIMS systems are similar.

CHAPTER IV
DEVELOPMENT AND ANALYSIS OF TXDOT AGGREGATE DATABASE

OVERVIEW

Throughout the implementation process of AIMS, 106 aggregate samples were sent to and tested at the Texas Transportation Institute laboratory. Table G.1 in Appendix G summarizes the aggregate mineralogy, TxDOT classification, and TxDOT laboratory sample number. These aggregates were scanned using AIMS before Micro-Deval (BMD), tested in the Micro-Deval and scanned again after Micro-Deval (AMD). The data from these tests were cataloged and compared to the results obtained by testing similar samples at the TxDOT laboratories. Table 4.1 shows a summary of the number of samples tested, where the "BOTH" column denotes the same aggregate sample tested at both the TxDOT and TTI laboratories. The measurements are included in the electronic database accompanying this database.

Table 4.1. Summary of Tests Run between the Two Labs.

	TTI	TxDOT	BOTH
Angularity BMD	106	108	104
Angularity AMD	110	97	96
Texture BMD	75	108	72
Texture AMD	83	99	72
Sphericity BMD	75	106	74
Sphericity AMD	83	100	72
Micro-Deval	105	134	98

The aggregate database was analyzed to determine the correlation between the TTI and TxDOT measurements and explore relationships between the aggregate properties included in the database. Statistical clustering analysis was conducted on the

AIMS data to determine new bounds for the classification of aggregates in either low, medium or high categories for texture, angularity, and sphericity. The method for calculating the angularity of particles and the texture scale were modified in order to enhance their accurate portrayal of aggregate shape properties.

A new method is proposed in order to better classify aggregates as part of the wet weather accident reduction program. This proposed method uses the texture results obtained from AIMS and the magnesium sulfate soundness to classify aggregates for pavement skid performance.

AGGREGATE TESTS AND PROCEDURES

In the NCHRP 539 study, Prowell et al. (2005) noted several consensus aggregate properties and source properties that played a major role in the performance of HMA pavements. Superpave defined the four important consensus aggregate properties to be coarse aggregates angularity, flat and elongated particles, uncompacted voids in fine aggregates, and sand equivalents. Aggregate durability and deleterious material content are the two different source properties that were discussed by Prowell et al. (2005). These properties are related to the transport, compaction, and continuous wear of aggregates throughout the life of the pavement. Although specifications for the consensus aggregate properties have been uniformly adopted through different agencies, the source properties vary due to regional differences in geology.

In order to assess the quality of aggregates used within the state of Texas, TxDOT initiated the Aggregate Quality Monitoring Program (AQMP). The AQMP sets forth a method to ensure the quality and consistency of aggregates produced within the state. It also allows for the expedited use of aggregates for a project since quality tests have been run on them at regular intervals. The TxDOT standard Tex-499-A states which tests and the frequency of testing are required. The specific tests required for asphalt pavements are L.A. abrasion, magnesium sulfate soundness, and polish stone value. The database developed in this study includes a number of consensus aggregate

properties, durability properties and AIMS measurements. The following sections discuss these aggregate properties and associate test methods.

Aggregate Consensus Properties

Crushed Face Count

The crushed face count test was run according to TxDOT procedure Tex-460-A. This test allows for the assessment of the percentage of the aggregates that have at least two crushed faces. This index is usually used as a measure of the angularity of a particle since it is assumed that a particle having at least two crushed faces has an acceptable level of angularity. This test is done by manual inspection in order to determine unweathered faces that constitute at least one quarter of the projected area of the rock. Table G.6 of Appendix G summarizes the results from this test.

Flat and Elongated Particles

High proportions of flat and elongated particles are believed to be detrimental to asphalt pavement performance. The flat and elongated particles are specified by their length to thickness ratio and are determined using TxDOT procedure Tex-280-F. For this test, the length is defined as the maximum dimension of the particle, the width is the maximum dimension perpendicular to the length, and the thickness is the maximum dimension perpendicular to the length and width.

An aggregate sample is obtained using a sampling technique according to TxDOT procedure Tex-221-F. Approximately 100 particles of each of sieve sizes 5/8 inch, 1/2 inch, and 3/8 inch are obtained using sieve analysis. The particles retained on 7/8 inch and those passing 3/8 inch sieve are not considered for this test. The number of particles with length to thickness ratios above a certain value are then determined (typically ratios of 3:1 or 5:1 are used for specifications). The percent of particles in each sieve size classified into each group is reported to the nearest 0.1 percent. The percent of flat and elongated particles within each sieve group are multiplied by its weight percent to determine the total flat and elongated percent of the aggregate blend.

Figure 4.1 shows a calculation example from the TxDOT Bituminous Test to compute the percent flat and elongated particles for one size. The total percent flat and elongated is the summation of the percentage for each size. The results from this test are summarized in Appendix G Table G.6.

Calculation Example

Sieve	%	%	%	%	adjusted %
7/8 in.	4.8				
5/8 in.	17.8 ➔	17.8	17.8 ÷	88.5 =	20.1
1/2 in.	42.1 ➔	42.1	42.1 ÷	88.5 =	47.6
3/8 in.	28.6 ➔	28.6	28.6 ÷	88.5 =	32.3
No. 4	6.7 ➔	0.0	0.0 ÷	88.5 =	0.0
		88.5			100.0

Suppose the 5/8 in. sieve has a flat and elongated % of 5.2 for the ratio 5:1, then:

$$\frac{\text{Adjusted \%} \times \text{flat and elongated \%}}{100} = \text{weighted percentage}$$

$$\frac{20.1\% \times 5.2\%}{100} = 1.05\%$$

Figure 4.1. Calculation Example to Compute Percent Flat and Elongated Particles.

Sand Equivalent Test

There is a TxDOT procedure for this test (Tex-203-F) but it was not conducted in this study. Clay-like fines in an aggregate blend used in an asphalt pavement cause the mix to be susceptible to moisture damage. The portion of the aggregate blend that passes the #4 sieve is mixed together to make a sample of 500 g. This sample is placed into a graduated cylinder and mixed with water to form a solution that has an exact height of 15 inches. This solution is agitated and then left to rest allowing the sand to settle and the clay to remain in solution. The height of the clay and sand level are then measured and used to calculate the sand equivalent using Equation 4.1.

$$\text{Sand Equivalent Value} = 100 \times \frac{\text{Sand Height Reading}}{\text{Clay Height Reading}} \quad (4.1)$$

Flakiness Index

The flakiness index is a measure of the percentage of particles in a coarse aggregate mix that has a shortest dimension less than half of the nominal size. The test is conducted according to TxDOT procedure Tex-224-F. In this test, aggregates are first sieved into sizes 7/8 inch (22.4 mm), 5/8 inch (16.0 mm), 3/8 inch (9.5 mm), and 1/4 inch (6.3 mm). Those aggregates retained on 7/8 inch and passing 1/4 inch are discarded and not included in determining the flakiness index. The total number of particles remaining needs to be more than 200. The aggregate retained on the 5/8 inch particles that also pass through a 3/8 inch gauge and particles from those retained on 3/8 inch that pass through 1/4 inch gauge are used to determine the number of aggregates with a shortest dimension less than half of the nominal size. These particles are combined and are considered the passing sample. The flakiness index is calculated using Equation 4.2 and is reported to the nearest whole number. Table G.6 in Appendix G summarizes the results for the flakiness index for the aggregates tested in this study.

$$\text{Flakiness Index} = \frac{\text{Passing Sample Particle Count}}{\text{Total Number of Particles}} \qquad (4.2)$$

Durability and Deleterious Materials Tests

Micro-Deval

The Micro-Deval test allows for the assessment of aggregate resistance to abrasion and weathering. This test was run according to TxDOT specification Tex-461-A. The aggregate blend with a total weight of 1500 ± 5 g, summarized in Table 4.2, is soaked in 2000 ± 500 mL of water for a minimum of one hour. This mixture is then placed in a steel cylinder with 5000 ± 5 g of steel ball bearings. This mixture of water, aggregate, and ball bearings are rotated for 105 minutes at 100 ± 5 rpm as illustrated previously in Chapter 2 Figure 2.6. After abrasion, the aggregates are washed, and the weight loss is considered to be that passing the #16 sieve. Equation 4.3 calculates the percent of weight loss, and Appendix G Table G.5 summarizes the results for all aggregates.

Table 4.2. Weight Specifications for Micro-Deval Test.

Passing	Retained On	Weight (g)
1/2 inch	3/8 inch	750 ± 5
3/8 inch	1/4 inch	375 ± 5
1/4 inch	#4	375 ± 5

$$PercentLoss = \frac{(\text{Weight Before} - \text{Weight After})}{\text{Weight Before}} \qquad (4.3)$$

Los Angeles Abrasion

The Los Angeles Abrasion Test allows for the assessment of an aggregate resistance to degradation during transport, mixing, and compaction. This test was run according to TxDOT procedure Tex-410-A. In this test, 5000 ± 5 g of an aggregate mix are placed into a steel cylinder with six to twelve 46.8 mm steel spheres, depending on the gradation used for the mix. The aggregates and steel spheres are then rotated at 30 to 33 rpm until the total rotations reach 500. The weight loss is measured as passing the #12 sieve, and the percent weight loss is calculated using Equation 4.4. The L.A. Abrasion Test differs from the Micro-Deval because the steel spheres used are much larger and it is a dry method. The L.A. abrasion is therefore more of an assessment of aggregate breakage than abrasion due to wear. Table G.5 of Appendix G summarizes the results from this test.

$$\text{Percent Loss} = \frac{(\text{Weight Before} - \text{Weight After})}{\text{Weight Before}} \qquad (4.4)$$

Magnesium Sulfate Soundness

The Magnesium Sulfate Soundness test, run according to TxDOT procedure Tex-411-A, allows for the assessment of an aggregate's resistance to freeze—thaw cycles, and this test therefore, examines the durability of the aggregates.

The gradation of the aggregate blend used for this test depends upon the type of pavement mix that the aggregate is to be used in. According to the test procedure, the aggregate mix is placed into a specified concentration of a magnesium sulfate solution. The aggregates are left in the solution for 16 to 18 hours, and then removed and dried in an oven. This cycle is repeated five times, and then the samples are washed thoroughly. Weight loss is determined based on the size of aggregate before and after the test. For example, a particle initially retained on a 2 inch sieve must pass a 1.5 inch sieve to be considered weight loss after testing while a #4 particle must pass a #5 sieve to be considered weight loss. The percent loss is calculated for each size and then multiplied by its gradation percent and summed to determine the total percent loss of the aggregate blend. The results from the magnesium sulfate soundness test are summarized in Table G.5 of Appendix G.

British Polish Value

The British Polish Value (BPV) or Polished Stone Value provides an indication of the aggregate resistance to polishing which is an important property in controlling asphalt pavement skid resistance. To determine the terminal value of the BPV, accelerated polishing tests for aggregate are conducted using TxDOT procedure Tex-438-A. In this test, aggregates are arranged into resin coupons with an arched shape, as shown in Figure 4.2. Once the resin has fully cured, the coupons are placed on a rotating wheel and polished for nine hours. The polished coupons are then skidded with a rubber pad while wet to determine the terminal British Polish Number (BPN). The reported BPN is the average of five consecutive skid measurements. The results from the accelerated polishing tests run at the TxDOT lab are summarized in Table G.6 of Appendix G.

Aggregate Imaging System Data

Many of the current methods used for aggregate classification are based on indirect methods of measuring aggregate properties. Analyzing aggregate using AIMS

offers direct measures of an aggregate particle's angularity, texture and shape. Capabilities of AIMS are extensively discussed in the NCHRP 4-30 study and as well as TxDOT Implementation Report 5-1707-01-1. A brief discussion of the AIMS analysis methods follows.

Figure 4.2. Coupon before and after Polishing.

Aggregate Angularity

To measure the angularity of a particle, a black particle projection is captured by using back-lit table where aggregate particles are placed. The particle projection is then used to determine the angularity index. The angularity index is the average of the change in the angles of the gradient vectors around the particle circumference (Masad et al. 2005). Basically, the circumference is divided into segments, and the gradients are calculated for these segments. As shown later, the segment length is important in determining the accuracy and variability of the analysis method. The angularity index is calculated using Equation 4.5. The previous analysis using this method calculated the gradient orientation (θ) using adjacent pixels (segment = 2 pixels), and then calculated the difference in the gradients separated by 3 pixels (Δ in equation 4.5 is equal to 3). The maximum value of the gradient angularity index was set

at 10,000 by Al-Rousan (2004) and was used during the course of this study. Examples of gradient vectors for smooth and angular particles are shown in Figure 4.3.

$$\text{Gradient Angularity Index} = \frac{1}{\frac{N}{\Delta}-1}\sum_{i=1}^{N-\Delta}\left|\theta_i - \theta_{i+\Delta}\right| \qquad (4.5)$$

where:

i is the i^{th} pixel on the perimeter of the particle

N is the total number of pixels in the perimeter, and

θ is the orientation of the gradient at a given pixel

Δ is number of pixels between gradients used in the calculations

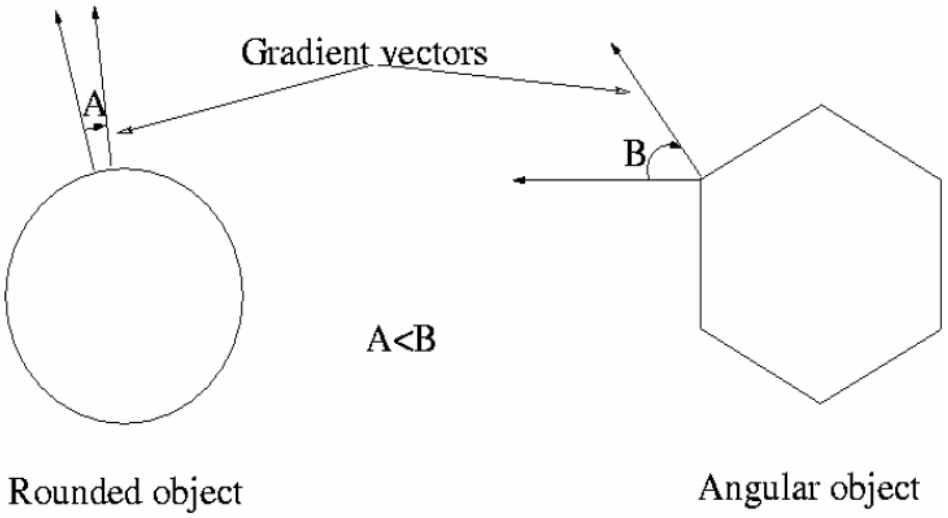

Figure 4.3. Illustration of Angle Differences between Gradients for Smooth and Angular Particles.

Texture

AIMS offers a method to analyze the surface texture of aggregate particles as well as the polishing coupons. The texture index is determined by taking a grayscale image of the surface of the aggregate particle. This image is then analyzed using the wavelet method to determine the texture of the particle. The wavelet method is

discussed in depth in the NCHRP 4-30 study (Masad et al. 2005). Six different scales of texture on a particle surface can be analyzed by this method. Level 1 corresponds to the smallest scale texture while Level 6 corresponds to the largest texture scale. The current method used to compare the texture of aggregates uses texture Level 6 (Al-Rousan 2004). As shown later in this study, different texture levels are recommended based on the results obtained from analyzing the comprehensive database of aggregates.

Sphericity

Sphericity is a measure of how close in length the three dimensions of an aggregate particle are. A sphericity index of 1.0 denotes that a particle is a perfect sphere or cube while sphericity decreases as a particle becomes more flat and/or elongated. The AIMS software uses Equation 4.6 to calculate the sphericity index. The three dimensions of a particle are determined using only two scans by one camera. Two of the dimensions for this calculation are obtained using the image projection used in angularity analysis, while the third dimension is obtained by determining the distance that the camera has to move vertically from a reference point in order for the image to be in focus.

$$Sphericity = \sqrt[3]{\frac{d_s * d_i}{d_l^2}} \qquad (4.6)$$

where:

d_s is the shortest dimension

d_i is the intermediate dimension

d_l is the longest dimension

COMPARISON BETWEEN TxDOT AND TTI AIMS RESULTS

The data collected for the database were used in the comparison between the two AIMS units since aggregate samples from the same sources were scanned at TxDOT and TTI. The comparison included the shape characteristics (angularity, texture and

sphericity) of individual aggregate particles and the texture of aggregates glued to the polishing coupons.

Coarse Aggregate Angularity

Aggregate particles from three size groups (retained on 3/8", 1/4", and #4 sieves) were scanned both before and after abrasion in the Micro-Deval test. In order to simplify the analysis, the average angularity of the three sizes combined was used as the basis for comparison between the two systems. Table G.2 of Appendix G contains all data for the gradient angularity.

The average angularity results from the two systems are shown in Figure 4.4. Linear regression was conducted in order to determine the R^2 value for the comparison between the two systems. The results indicate some positive correlation between the angularity measured using the two devices. However, this correlation is not sufficient, and it was decided that the analysis method should be modified to improve the correlation.

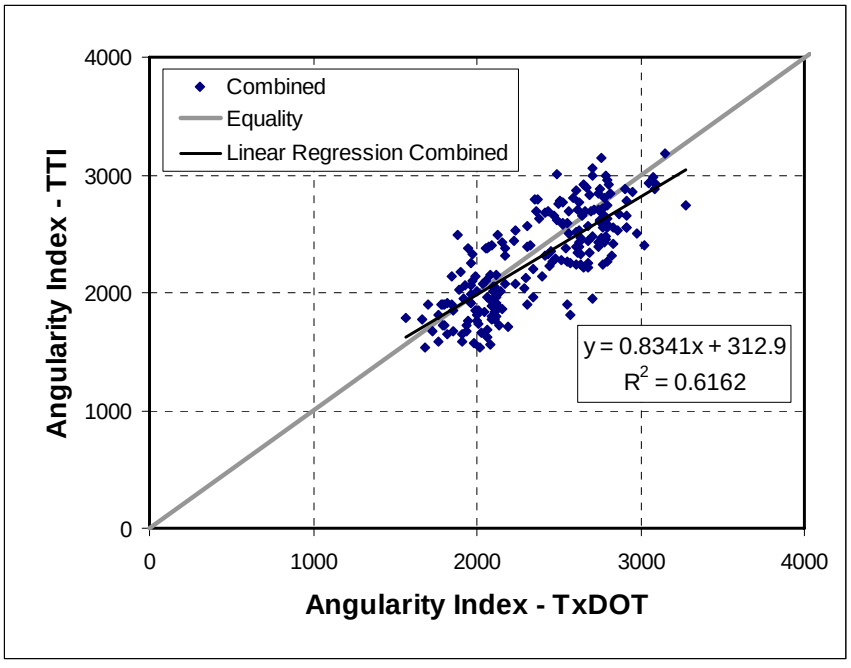

Figure 4.4. Combined BMD and AMD Average Gradient Angularity Index Comparison.

Modification of Coarse Aggregate Angularity

As discussed earlier, the angularity analysis (Equation 4.5) has been conducted using adjacent pixels (segment = 2 pixels) in order to determine the gradient orientation (θ), and the difference between gradients was taken to be 3 pixels (Δ in Equation 4.5 is equal to 3). Analysis has revealed the parameters used in the angularity method to be sensitive to slight changes in the surface angularity. However, it was found that the method was highly influenced by the noise at the surface boundary, which was thought to be the main problem in reducing the correlation between the AIMS units. As such, the researchers decided to examine the angularity analysis results using different numbers of segments at the circumference. The analysis focused on comparing the sensitivity and variability of the angularity results of the 10 aggregates listed in Table 3.2. Fifty-six particles from each of the aggregates were analyzed using the current method and by dividing the circumference of each particle to 30, 35, 40, 45, and 50 segments. Table 4.3 summarizes the average, standard deviation, and coefficient of variation for each aggregate using the different analysis methods.

The results in Table 4.3 and Figure 4.5 show that using 30 segments resulted in the minimum COV for all the ten aggregates. Plotting the results of the current method versus the method with 30 segments (Figure 4.6) showed a good correlation with $R^2 = 0.83$, with the results very close to the equality line. Therefore, using 30 segments is as sensitive as the current method in distinguishing between aggregates, but it has much less variability within the same aggregate source. Due to these favorable results, 30 was chosen as the number of segments to be used in the determining the gradient angularity index. This new method will be referred to as the modified angularity method as opposed to the current method employed in AIMS.

Table 4.3. Summary of Varying the Number of Steps Used to Calculate the Gradient Angularity Index.

Aggregate		Current Method	Number of Segments in Proposed Method				
			30	35	40	45	50
1	Average	3592.47	3292.28	3474.75	3682.51	3809.04	4374.16
	Standard Deviation	1307.72	617.01	719.96	789.30	942.90	1019.02
	COV	36.40%	18.74%	20.72%	21.43%	24.75%	23.30%
2	Average	2602.91	2540.38	2438.71	2371.94	2126.29	2181.82
	Standard Deviation	1200.68	773.18	895.48	930.30	892.48	924.85
	COV	46.13%	30.44%	36.72%	39.22%	41.97%	42.39%
3	Average	2792.79	2829.80	2792.00	2712.64	2756.26	2759.74
	Standard Deviation	1060.30	763.08	833.93	863.67	923.00	969.80
	COV	37.97%	26.97%	29.87%	31.84%	33.49%	35.14%
4	Average	2219.15	2460.80	2249.07	2096.33	1985.97	1911.80
	Standard Deviation	975.16	719.35	744.04	728.63	778.55	714.90
	COV	43.94%	29.23%	33.08%	34.76%	39.20%	37.39%
5	Average	2826.94	3062.20	3032.74	2942.41	2953.89	3019.68
	Standard Deviation	1414.78	613.26	672.12	620.42	785.40	941.13
	COV	50.05%	20.03%	22.16%	21.09%	26.59%	31.17%
6	Average	3098.19	2912.00	2968.55	3130.62	3211.91	3285.79
	Standard Deviation	1295.32	601.10	902.24	831.61	1022.47	997.80
	COV	41.81%	20.64%	30.39%	26.56%	31.83%	30.37%
7	Average	2632.05	2558.25	2518.84	2484.33	2469.78	2479.70
	Standard Deviation	1055.36	902.15	1133.02	1217.45	1142.68	1308.58
	COV	40.10%	35.26%	44.98%	49.01%	46.27%	52.77%
8	Average	1811.29	1734.50	1436.17	1192.33	1061.85	1027.76
	Standard Deviation	1072.38	465.96	553.38	575.10	535.23	604.32
	COV	59.21%	26.86%	38.53%	48.23%	50.40%	58.80%
9	Average	1892.66	2155.42	1873.35	1667.55	1512.83	1421.17
	Standard Deviation	952.44	704.09	737.64	685.42	714.89	662.32
	COV	50.32%	32.67%	39.38%	41.10%	47.25%	46.60%
10	Average	2441.17	2828.37	2692.90	2658.03	2639.98	2499.97
	Standard Deviation	1366.33	756.68	842.27	892.24	890.41	1006.38
	COV	55.97%	26.75%	31.28%	33.57%	33.73%	40.26%

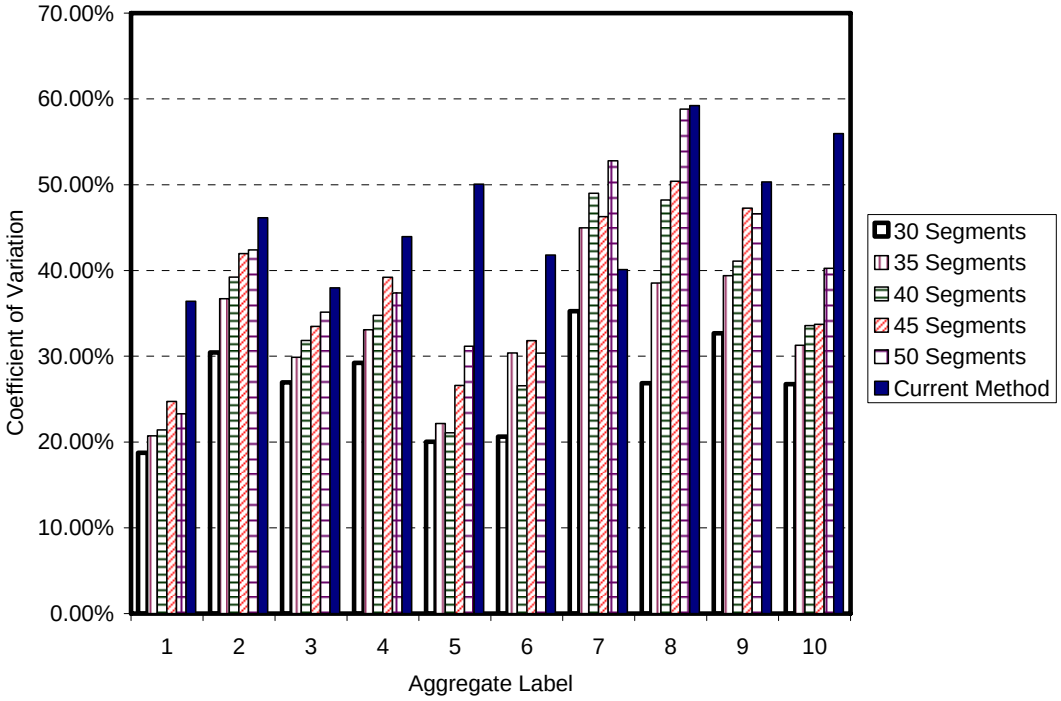

Figure 4.5. Comparison of COV versus Number of Steps in Angularity Analysis for 10 Test Aggregates.

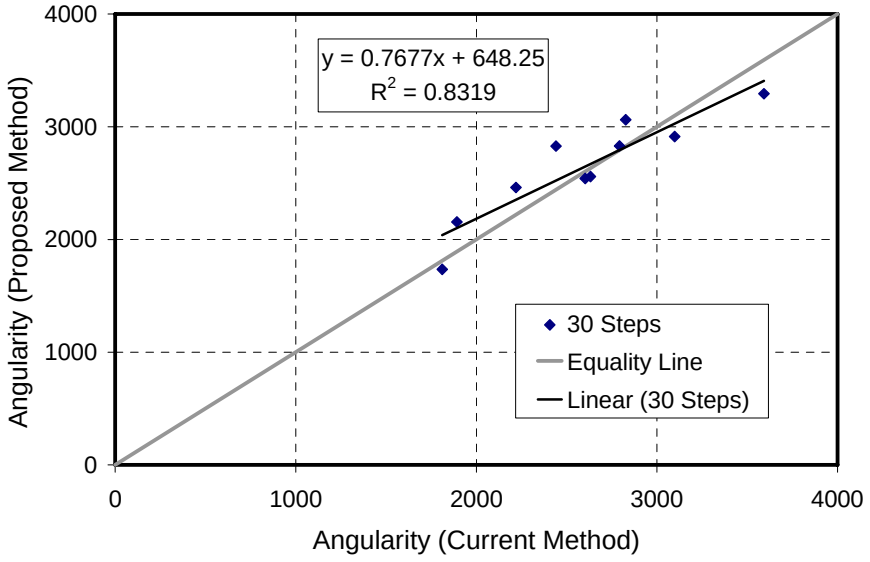

Figure 4.6. Comparison of Current and Proposed Angularity Methods.

Comparison of Modified and Original Angularity Methods for Database Aggregates

All of the database aggregates were analyzed using the modified angularity method. Using the TTI results, the modified angularity was compared to the original angularity index. Figure 4.7 shows the comparison for aggregates before and after Micro-Deval.

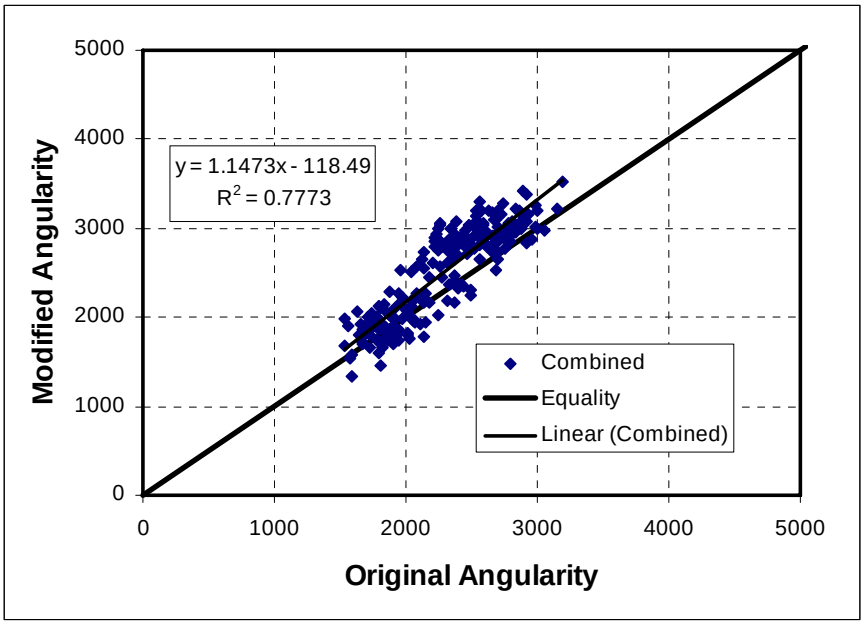

Figure 4.7. Combination of BMD and AMD Comparison between Modified and Original Angularity.

The results support that the two methods are close in their overall results. As discussed above, the method with 30 segments was chosen because it had the lowest coefficient of variation among the methods using different number of segments. In order to validate this point, the COV was calculated for all aggregates in the database. Figures 4.8 and 4.9 show the results of plotting the COV of the modified angularity versus the original angularity. The modified angularity gives a considerably lower COV in nearly all cases.

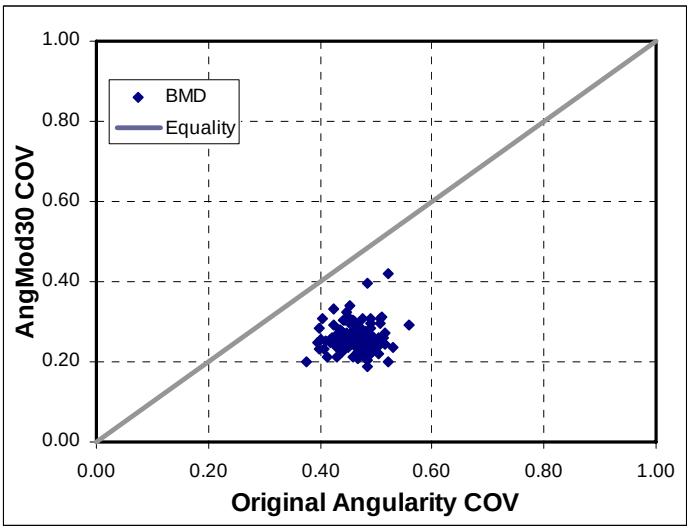

Figure 4.8. BMD Comparison between Modified and Original Angularity COV.

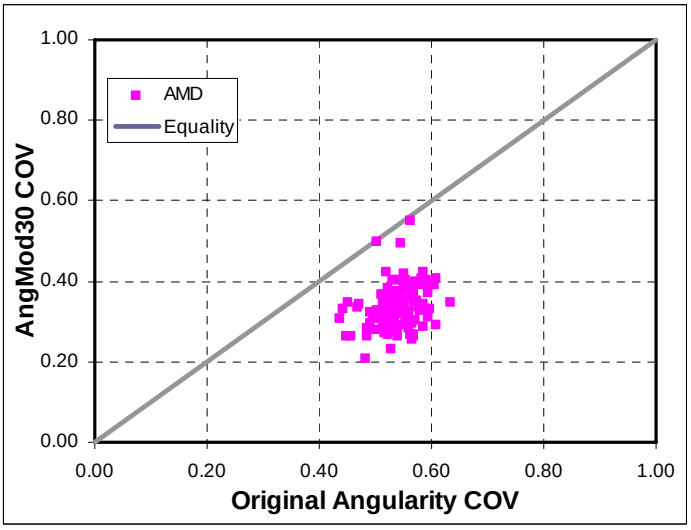

Figure 4.9. AMD Comparison between Modified and Original Angularity COV.

Comparison of AIMS Units Using Modified Angularity

Graphs for the comparison between the TTI and TxDOT AIMS units are given in Figures 4.10, 4.11 and 4.12 for aggregates BMD, AMD, and combined, respectively.

The regression equations are given in Table 4.4. The modified angularity values are all given in Table G.7 of Appendix G.

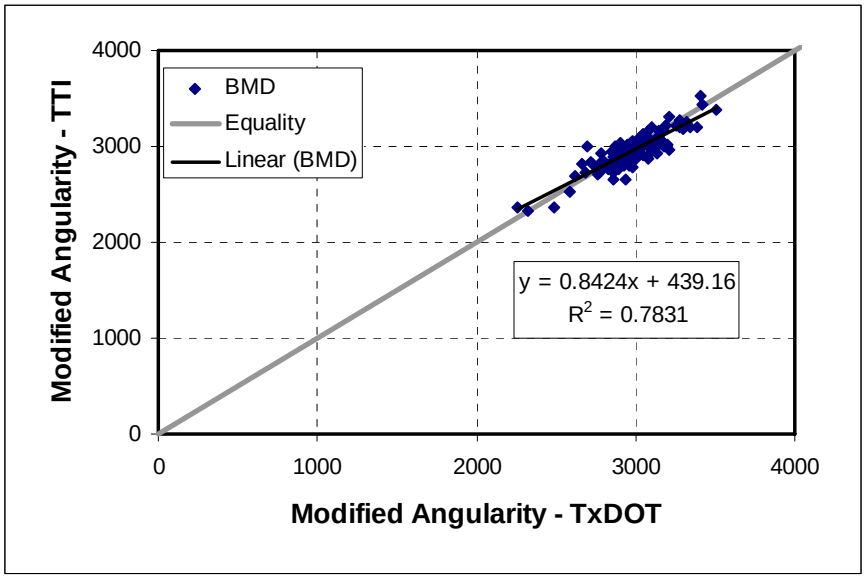

Figure 4.10. Modified Angularity Comparison BMD.

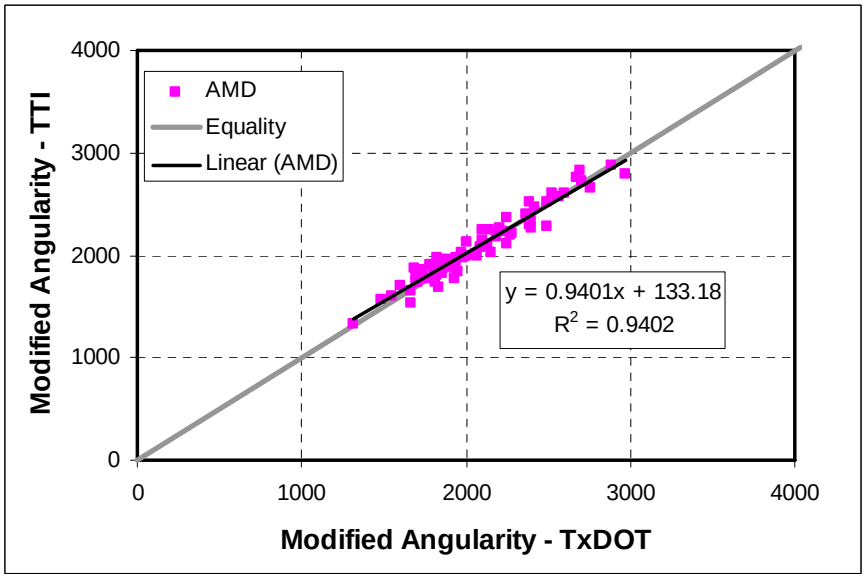

Figure 4.11. Modified Angularity Comparison AMD.

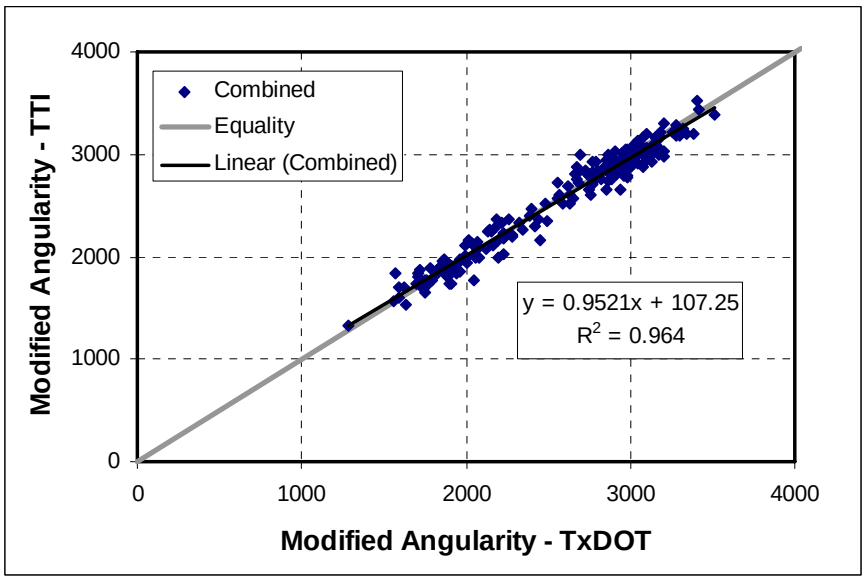

Figure 4.12. Modified Angularity Comparison Combined BMD and AMD.

Table 4.4. Modified Angularity Regression Summary.

	Equation	R^2 value
BMD	TTI = 0.8424*TxDOT + 439.16	0.7831
AMD	TTI = 0.9401*TxDOT + 133.18	0.9402
Combined	TTI = 0.9521*TxDOT – 107.25	0.9640

The modified angularity index shows a much better correlation between the two AIMS units. The combination of BMD and AMD results gives an R^2 value of 0.96 with very small bias indicating that the two units give nearly the same results. This is a much more favorable comparison than the original angularity method that had an R^2 value of 0.62. Also, the modified method offers a lower coefficient of variation than the original method.

Aggregate Particle Texture Comparison

As discussed earlier, the wavelet method is capable of analyzing the different texture scales on a particle surface. The AIMS analysis software provides six levels of texture; however, only level 6, representing the largest scale of texture in the analysis, has been used thus far in classifying the aggregates. The comparison of the texture indices given by the two AIMS units is shown in Figures 4.13, 4.14 and 4.15 for aggregates BMD, AMD, and combined, respectively. Table 4.5 summarizes the regression analysis results for these comparisons. All texture data are summarized in Table G.3 of Appendix G. The two systems are highly correlated, with R^2 values greater than 0.88.

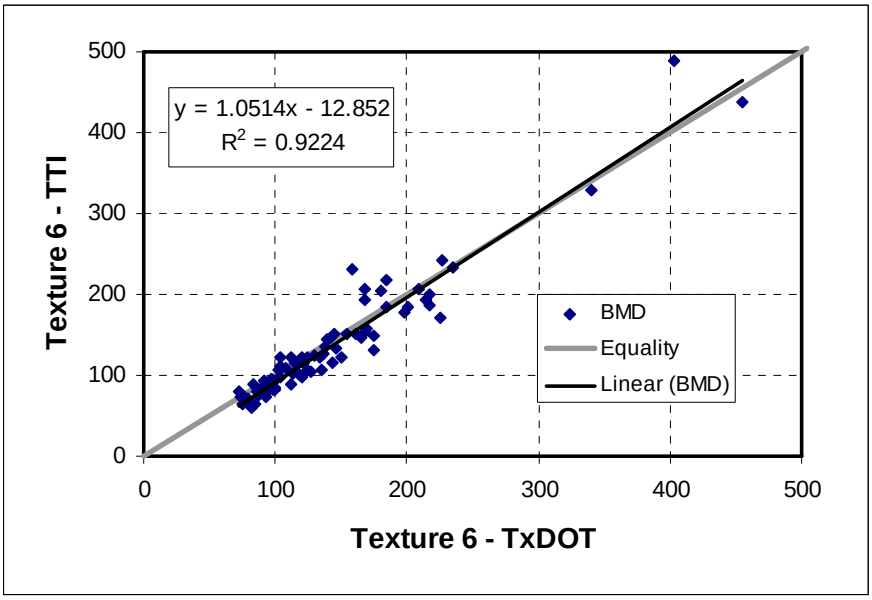

Figure 4.13. Texture Level 6 Comparison of BMD Aggregates.

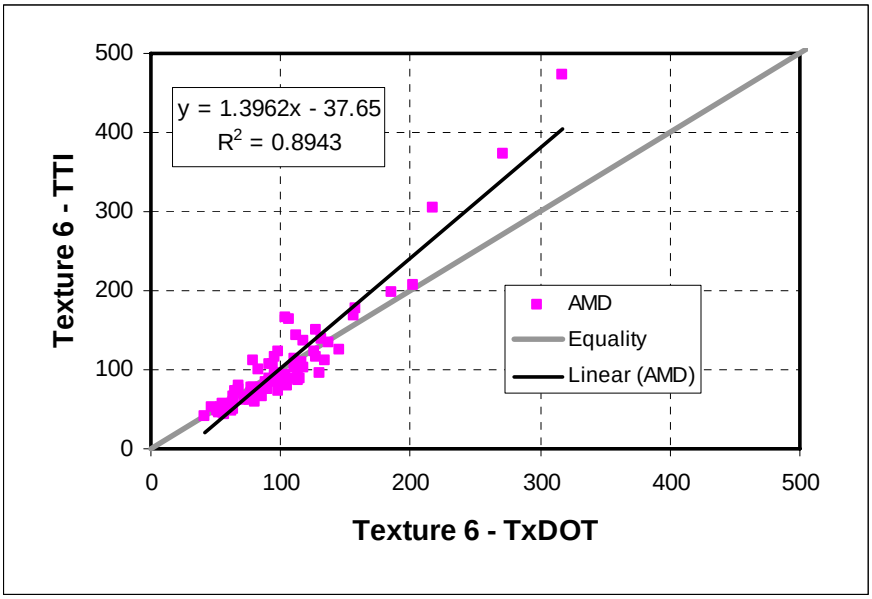

Figure 4.14. Texture Level 6 Comparison of AMD Aggregates.

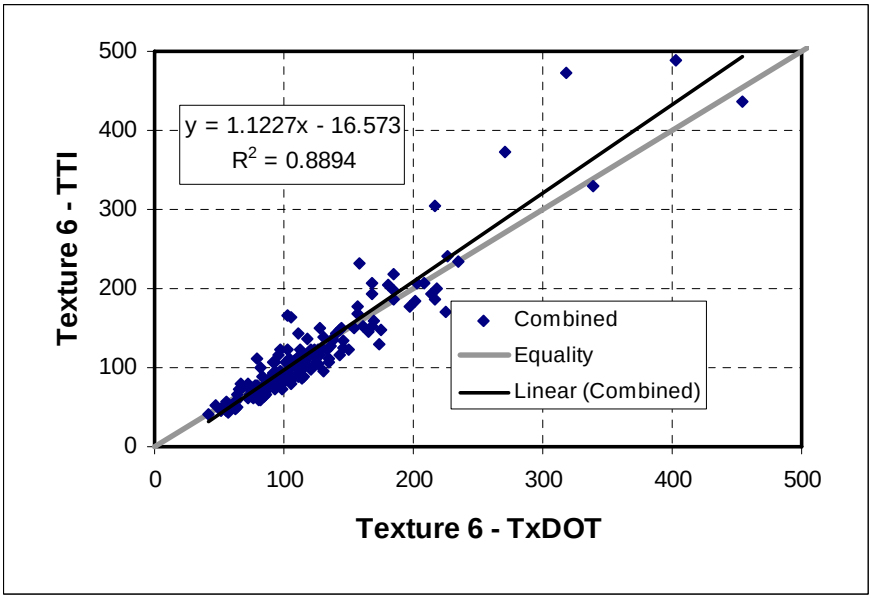

Figure 4.15. Texture Level 6 Comparison of Combined AMD and BMD Aggregates.

Table 4.5. Texture Level 6 Regression Results.

	Equation	R^2 value
BMD	TTI = 1.0514*TxDOT – 12.85	0.9224
AMD	TTI = 1.3962*TxDOT – 37.65	0.8943
Combined	TTI = 1.1227*TxDOT – 16.57	0.8894

Modification of Texture Method

During the course of the construction of the database and the comparison of its results, the texture values for aggregates with fine texture such as some sandstones were thought to be low compared to aggregates that have coarse surface texture. Also, some of these sandstones had a history of good performance in terms of texture and the retention of texture under traffic loading. Based on this observation, it was decided to conduct further analysis to examine the influence of the texture level on ranking of aggregates.

The texture analysis was conducted on six sandstone aggregates, a granite, a quartzite and two limestone aggregates. Table 4.6 lists the aggregate names used for this portion of the study as well as their corresponding TxDOT lab number in the database. The aggregates were passing 3/4"sieve and retained on sieve #4.

The different texture levels were captured using three different magnifications (9x, 12x an 16x), using two different objective lenses (0.25 objective lens, 0.5 objective lens), and the assessment of three texture levels (4, 5, and 6). In the AIMS procedure, the 0.25 objective lens is used to analyze the coarse aggregates, while the 0.5 objective lens is used to analyze the fine aggregates. However, they are both used in this experiment to analyze coarse aggregates to examine the influence of magnification on the analyzed texture scale. The 56 particles from each of the aggregates listed in Table 4.6 were analyzed. The results from levels 1 and 2 were not able to discriminate among the different aggregates sources; the results were within a small range of the same six sandstones. Level 3 correlated highly to level 4.

Table 4.6. Summary of Sample Names and TxDOT Lab Numbers.

Sample	Study Name	TxDOT Lab Number
Sandstone 1	SS-1	05-0771
Sandstone 2	SS-2	05-0828
Sandstone 3	SS-3	05-1190
Sandstone 4	SS-4	05-1210
Sandstone 5	SS-5	05-1221
Sandstone 6	SS-6	05-1222
Granite	Granite	N/A*
Limestone 1	LS-1	N/A*
Quartzite	Qtz	05-0946
Limestone 2	LS-2	05-0251

**These materials were not used to construct the database and therefore do not have TxDOT Lab numbers.*

Figure 4.16 shows the results of analyzing the six sandstone aggregates using level 6 texture, three magnifications and coarse (0.25 objective) and fine (0.5 objective) lenses. Table 4.7 shows a summary of the variables used in this analysis. For the sandstones tested, the average texture index generally increased with the use of the fine lens compared with the coarse lens due to capturing smaller scale of texture. Changing the magnification level for the same lens did not have considerable effect on texture. However, in general the highest texture index was either for the 12x and 16x magnifications. These findings support the assumption that sandstones have a finer texture than what is typically measured using the current AIMS procedure.

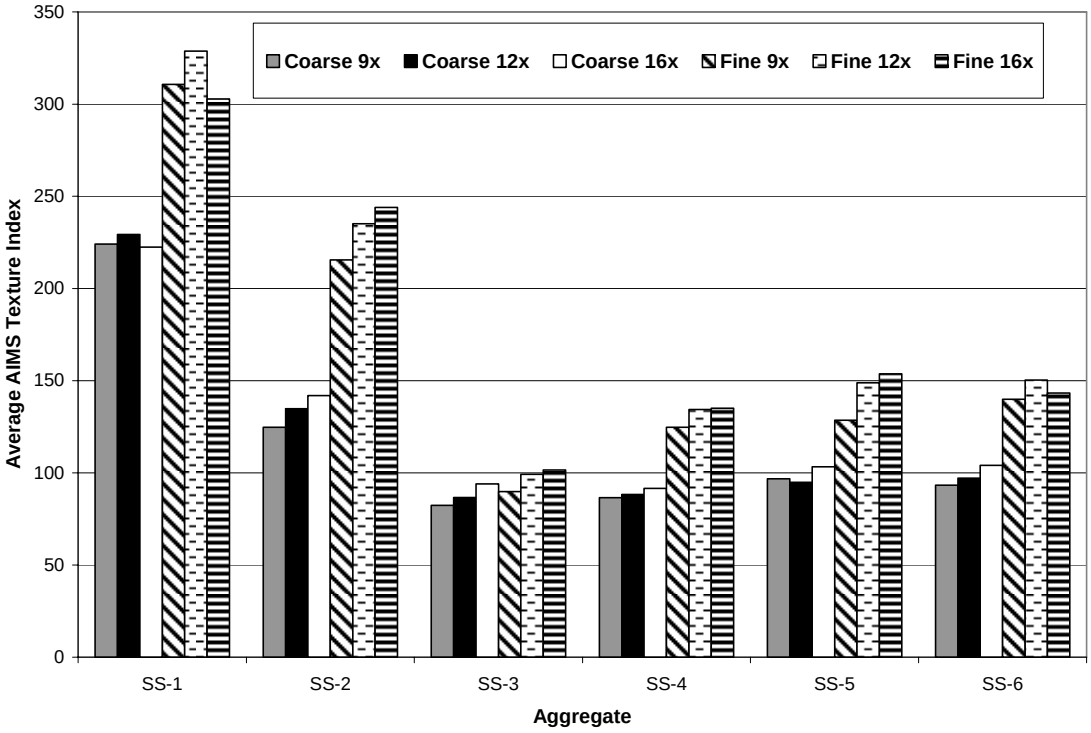

Figure 4.16. Average Level 6 Texture Indices of Six Sandstones with Varying Magnification and Objective Lens.

Table 4.7. Summary of Texture Scale versus Magnification Level.

Relative Texture Scale	Lenses	Magnification	Texture Level
Fine	0.50 objective	16	4
Medium	--	12	5
Coarse	0.25 Objective	9	6

Using texture levels 4, 5, and 6, the effect of texture scale was compared among the different aggregates as well. As shown in Figure 4.17, the granite and limestone aggregates exhibited an increase in texture index as the texture level increased. The sandstones and quartzite each had a lower texture index for level 6 than the other two

levels. This again shows that most of the texture in the tested sandstones was of a small scale (fine texture), while the texture in the tested granite and limestone was more pronounced in the large scale (coarse texture).

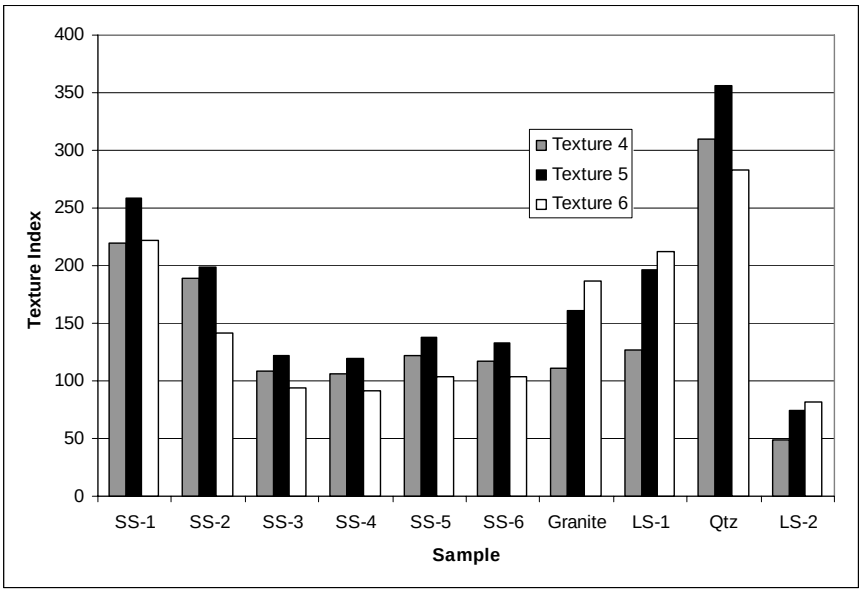

Figure 4.17. Comparison of Texture Levels of Six Sandstones, One Granite, One Highly Textured Limestone, One Quartzite, and One Low Texture Limestone.

As the data suggest, the sandstone and quartzite aggregates both have a much finer texture than what is typically considered in the AIMS procedure. It is therefore decided to use the average of levels 4 and 5 in analyzing aggregate texture. The results from averaging these two levels were also found to be consistent with the experience of skid resistance of these aggregates in asphalt pavement surfaces. The change to the new texture levels requires minimal software modification and no changes to the hardware of the system. Using texture levels 4 and 5 with the same coarse lens (0.25 lens) gave very good correlation with using the fine lens (0.5 objective) and level 6. However, the first alternative is more favorable than using the fine lens as this would make it difficult to achieve automated focusing and control of top lighting intensity on aggregate surface. The average of texture levels 4 and 5 will be used as a basis of comparison between the

two AIMS units. The level 6 texture was plotted against the average texture for levels 4 and 5 for all aggregates in the database. These plots are shown in Figure 4.18 for BMD samples and in Figure 4.19 for AMD samples.

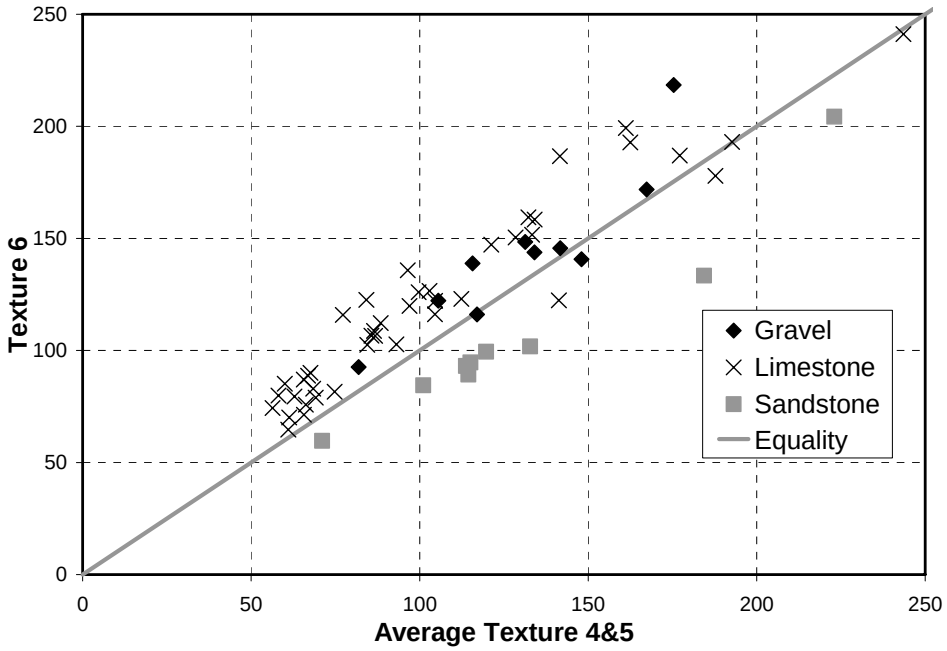

Figure 4.18. Texture Level Comparison for BMD Samples.

The values for the average of texture levels 4 and 5 is higher than level 6 for the sandstones as shown in Figures 4.18 and 4.19. The majority of the limestone and gravel samples exhibited a higher level 6 texture than the averages of levels 4 and 5. The COV was also studied to determine the variability of the texture within the aggregate samples, and the results are shown in Figure 4.20 for BMD samples and Figure 4.21 for AMD samples. It can be seen by looking at Figures 4.20 and 4.21 that the sandstones generally had the lowest COV. These results lead to the conclusion that sandstone aggregates have a more uniform texture compared with the gravels and limestones.

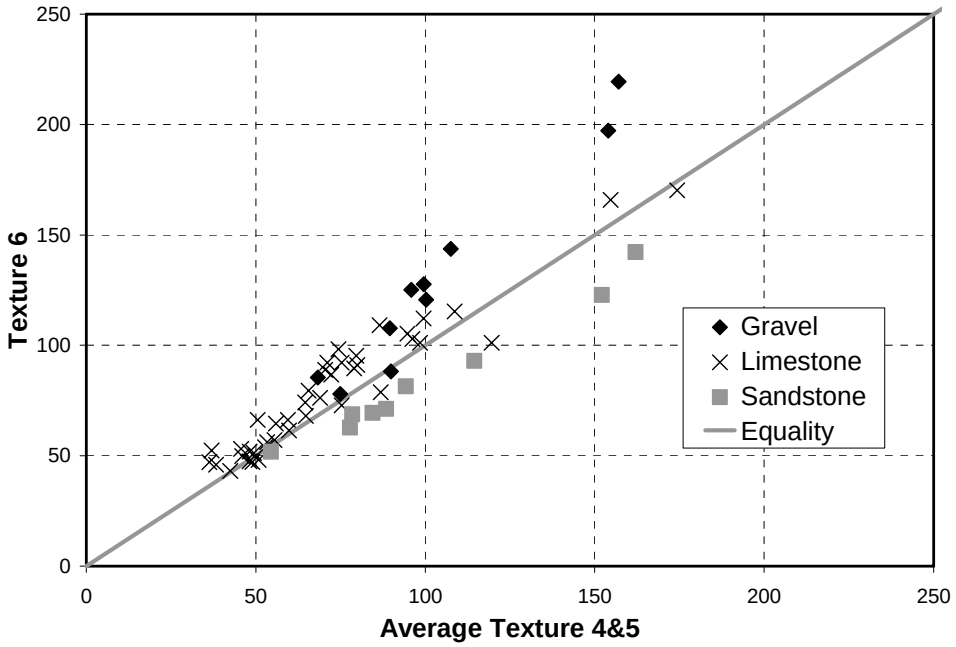

Figure 4.19. Texture Level Comparison for AMD Samples.

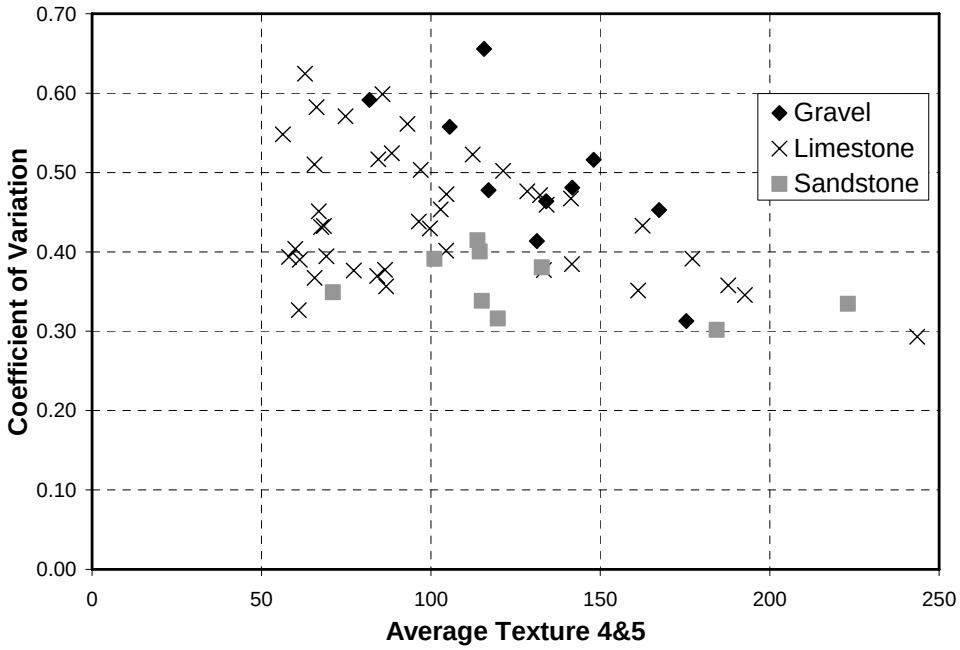

Figure 4.20. Coefficient of Variation Comparison for BMD Samples.

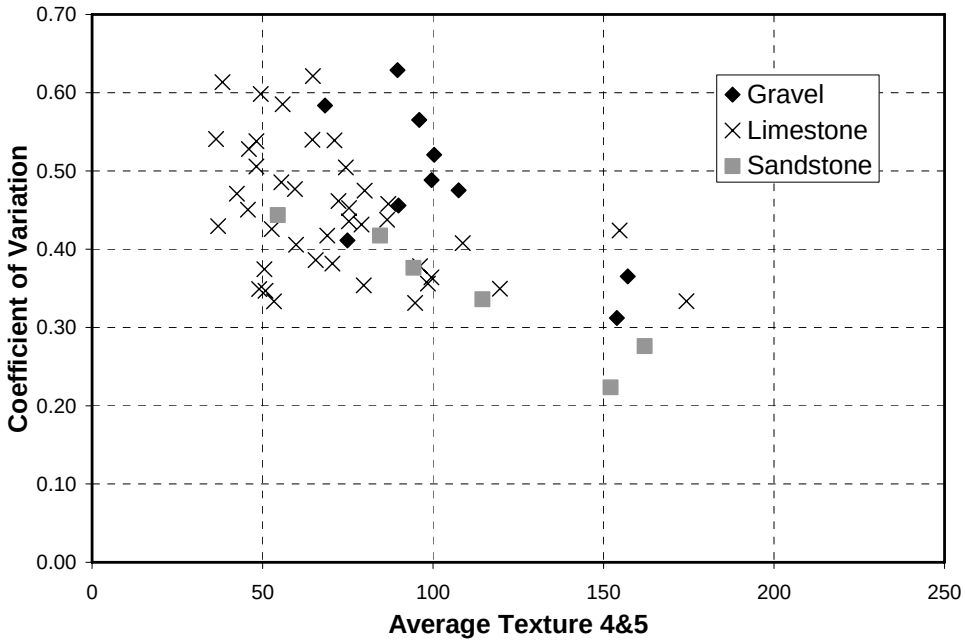

Figure 4.21. Coefficient of Variation Comparison for AMD Samples.

Comparison of AIMS Units Using Average Texture Levels 4 and 5

The correlation between the two AIMS units is assessed using the average of texture levels 4 and 5. The graphs for this comparison are shown in Figure 4.22 for the BMD samples, in Figure 4.23 for the AMD samples, and in Figure 4.24 for the combination of BMD and AMD samples. Table 4.8 shows the linear regression results for the comparison. The regression results show that there is a high correlation between the systems with an R^2 value of 0.92 for the combined samples. All of the average of texture levels 4 and 5 are available in Table G.8 of Appendix G.

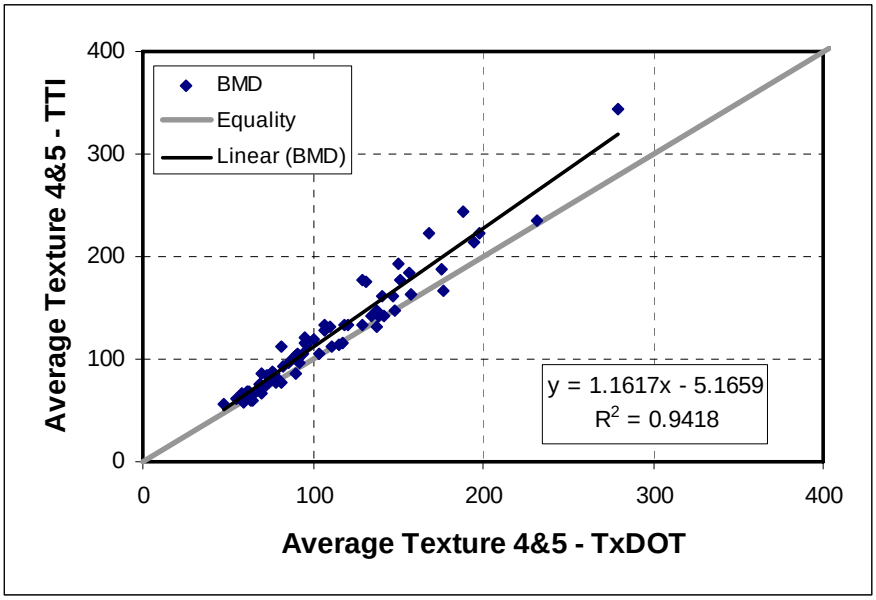

Figure 4.22. Average of Texture Levels 4 and 5 Comparison of BMD Samples.

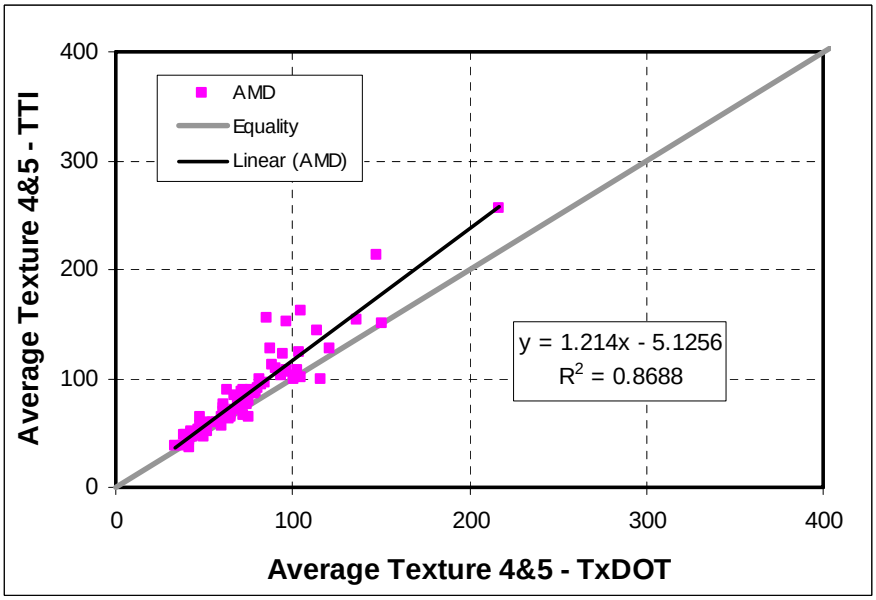

Figure 4.23. Average of Texture Levels 4 and 5 Comparison of AMD Samples.

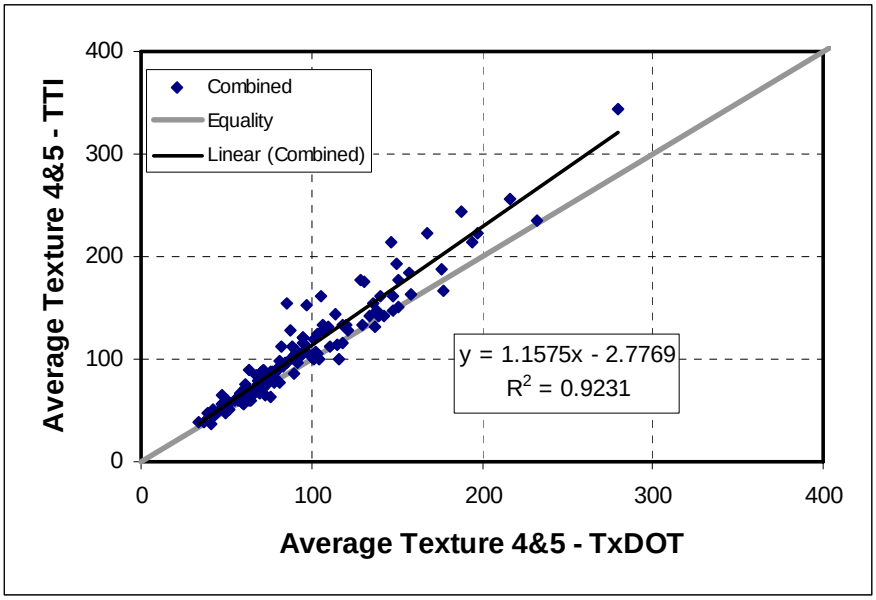

Figure 4.24. Average of Texture Levels 4 and 5 Comparison of Combined BMD and AMD Samples.

Table 4.8. Average of Texture Levels 4 and 5 Regression Results.

	Equation	R^2 value
BMD	TTI = 1.1617*TxDOT – 5.1659	0.9418
AMD	TTI = 1.2140*TxDOT – 5.1256	0.8688
Combined	TTI = 1.1575*TxDOT – 2.7769	0.9231

Sphericity Comparison

The sphericity index of the two AIMS unit was cataloged in the database and used for comparison of the units. The comparison of the two systems is shown in Figure 4.25 for BMD samples, Figure 4.26 for AMD samples and Figure 4.27 for the combination of BMD and AMD samples. The regression results are also summarized in Table 4.9. Table G.4 in Appendix G contains all data for the sphericity.

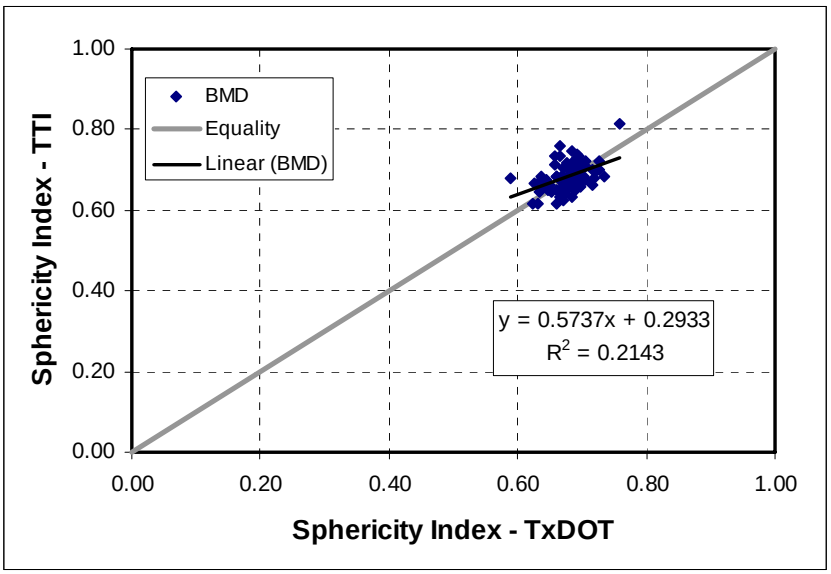

Figure 4.25. Sphericity Comparison for BMD Samples.

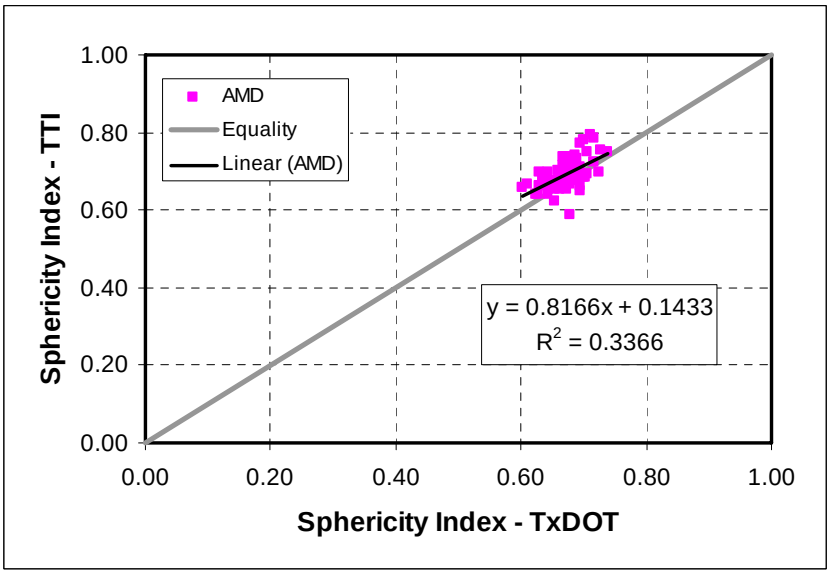

Figure 4.26. Sphericity Comparison for AMD Samples.

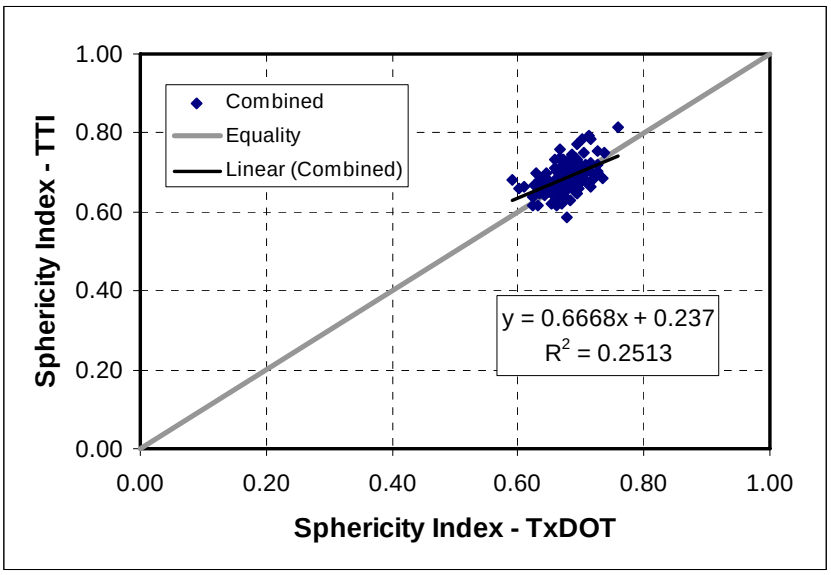

Figure 4.27. Sphericity Comparison for Combined BMD and AMD Samples.

Table 4.9. Sphericity Regression Results.

	Equation	R^2 value
BMD	TTI = 0.5737*TxDOT + 0.2933	0.2143
AMD	TTI = 0.8166*TxDOT + 0.1433	0.3366
Combined	TTI = 0.6668*TxDOT + 0.2370	0.2513

Most of the values of sphericity are between 0.6 and 0.7. There is not enough spread in the data, which contributed to the low correlation between the TxDOT and TTI sphericity values. In general most of the data are close together, and the variation in between the two units would not cause the average to be in another category. The distribution of the sphericity values within a sample is a better way to compare the TxDOT and TTI measurements.

Comparison of the Texture of Polishing Coupons

Aggregate coupons were polished using the British polishing wheel at the TxDOT lab. These coupons were then scanned at both of the laboratories. The coupon texture measurements consist of placing four coupons on the lighting table, then performing texture analysis at magnification 12 with a moving interval of 12 mm in the x-direction and 8 mm in the y-direction. A total 120 images on the surface of aggregates in four coupons are captured in this analysis method. Images are analyzed using the same wavelet method used for aggregate particles. Seventy-five coupons of various aggregates were used in this analysis. Table 4.10 summarizes the aggregate types used in these coupons.

Table 4.10. Aggregate Types Used in Coupons.

Aggregate Type	Number of Coupons
Limestone	50
Gravel	14
Lightweight Aggregate	1
Igneous Rock	1
Sandstone	7
Miscellaneous	2

The average texture results are compared as shown in Figure 4.28. It is obvious an excellent correlation exists between the coupon measurements using the two AIMS units. The R^2 is equal to 0.9137, and the equation of linear fit is TTI = 1.1051×TxDOT-9.8133. The deviation from the equality line is accepted due to variation in the samples and orientation on the scanning table.

The confidence interval for the difference between the means was calculated using Equation 4.8. Tabulated results of estimated means and standard errors are given in Appendix A, and the confidence intervals for the difference in means between TTI and TxDOT results are shown in Appendix B. Based on these results, it can be seen that

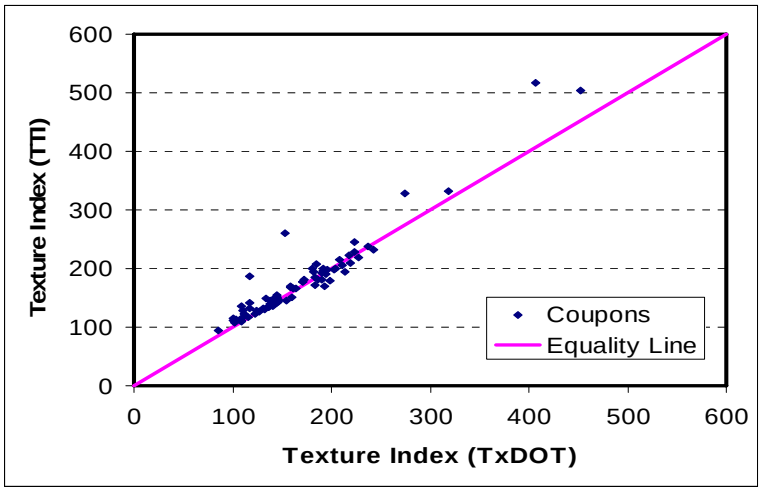

Figure 4.28. Aggregate Polished Coupons Texture Results.

only 11 C.Is out of 75 do not contain zero. The C.I containing zero indicates that the TTI and TxDOT texture measurements have the same mean value. It must be kept in mind that for the statistical analysis with 95 percent confidence level, there is always a chance for five percent of the data analyzed to be rejected (C.I do not contain zero) while in reality it should not be rejected (C.I contain zero). The categorical analysis indicated that only six cases have a p-value less than 0.05. Plots and tables for categorical analysis results are given in Appendices C and D, respectively.

$$(\overline{X}_{TTI\,i,j} - \overline{X}_{TxDOT\,i,j}) \pm 1.96 \times \sqrt{(\sigma^2_{TTI\,i,j} + \sigma^2_{TxDOT\,i,j})} \qquad (4.8)$$

where:

$\overline{X}_{TTI\,i,j}$ = estimated value of the mean for aggregate property scanned at TTI

$\overline{X}_{TxDOT\,i,j}$ = estimated value of the mean for aggregate property scanned at TxDOT

$\sigma_{TTI\,i,j}$ = standard error in estimation of the mean for aggregate property at TTI

$\sigma_{TxDOT\,i,j}$ = standard error in estimation of the mean for aggregate property at TxDOT

i = aggregate number with values of 1, 2, …, 10

j = aggregate size with values of 1, 2, 3, 4, where 4 indicates the combined sizes

Comparison of the Micro-Deval Results

Aggregates were tested in the Micro-Deval at both the TTI and TxDOT laboratories. In the Micro-Deval test, aggregates are subjected to abrasion, polishing, and breakage. Consequently, the same exact sample cannot be tested in both machines. One hundred aggregate samples were included in the comparison. Aggregate types and weight loss results are listed in Table G.5 of Appendix G.

The data plotted in Figure 4.29 show that the two Micro-Deval machines produce almost the same results, except for a few cases. The statistical analysis involves fitting a linear model to the data and then determining the confidence intervals for the slope and the intercept of this model. The liner regression model is summarized in Table 4.11.

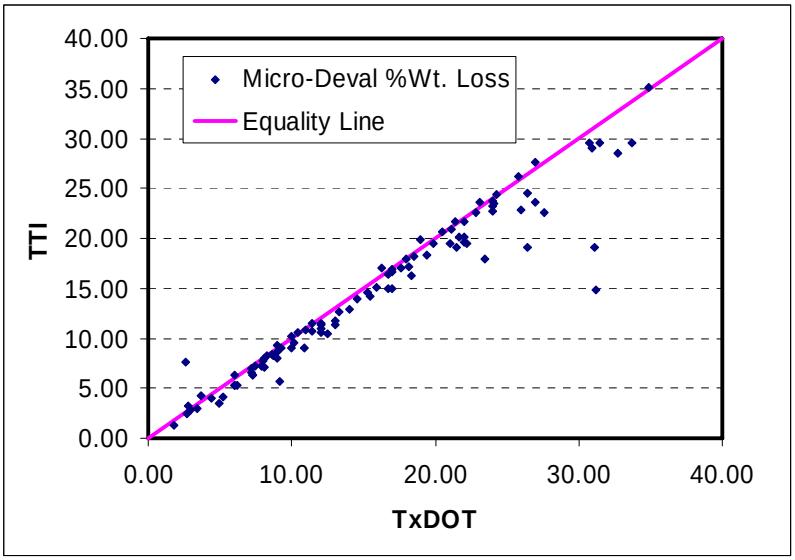

Figure 4.29. Micro-Deval Analysis of Variability: Weight Loss Results (All Data Points).

Table 4.11. Micro-Deval Analysis of Variability: Weight Loss Linear Model Results (All Data Points).

		Confidence Interval	
		Lower Limit	**Upper Limit**
Slope	0.872	0.822	0.922
Intercept	0.812	-0.08	1.705
R^2	0.923		

Figure 4.29 shows that there are two points that do not follow the general trend. These two points were investigated, and it was found that the TTI measurements of these two aggregates were not accurate as the number of revolutions at the end of the Micro-Deval test were below the lower acceptable limit. According to the Micro-Deval test specification those two results must be discarded. Therefore, the statistical analysis was repeated after removing the two points with results as shown in Figure 4.30. The new linear regression model is summarized in Table 4.12. The R^2 increased from 0.923 to 0.970, while the intercept decreased from 0.812 to 0.234. This intercept became closer to zero, which is the intercept of the equality line. Although the confidence intervals for the intercept contained zero for the two cases, the second case is closer to equally spread around zero. The slope value increased from 0.872 to 0.924, indicating that data became closer to the equality line. Neither confidence intervals for the slope in the two cases contained one, but the confidence interval is closer to one in the second case.

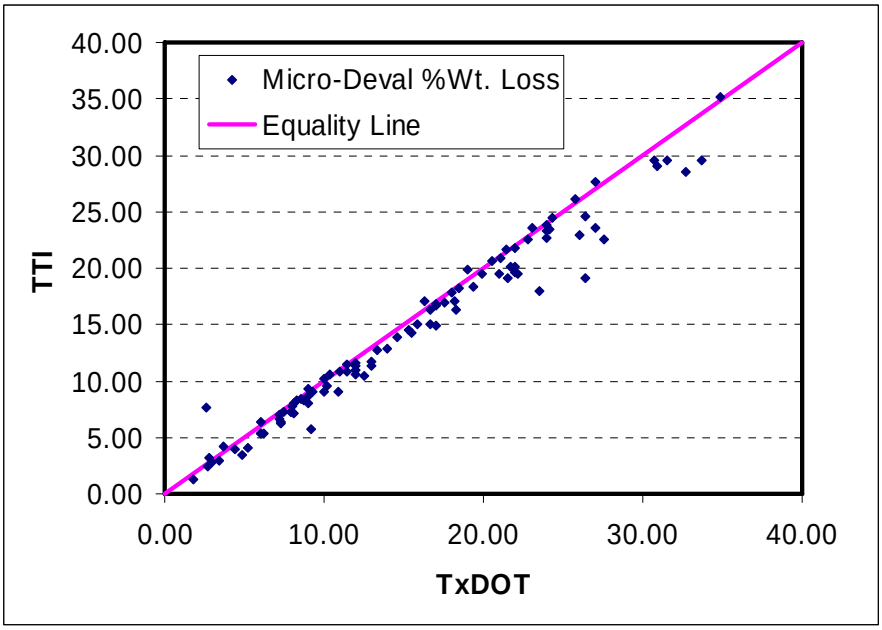

Figure 4.30. Micro-Deval Analysis of Variability: Weight Loss Results (Excluding Outliers).

Table 4.12. Micro-Deval Analysis of Variability: Weight Loss Linear Model Results (Excluding Outliers).

		Confidence Interval	
		Lower Limit	**Upper Limit**
Slope	0.924	0.891	0.957
Intercept	0.234	-0.335	0.804
R^2	0.970		

The statistical analysis results are presented in Appendix F. Residual analysis is important as it provides the proof for the goodness of fit using the linear model. Residual analysis for the two fitted models showed that the second one is much better, as the residual is more spread out and closer to the normal distribution than the first model.

Correlation of Micro-Deval and Magnesium Sulfate Soundness

Many literature sources indicate that there is often a relationship between the percent loss between the Micro-Deval test and the sulfate soundness test (Wu et. al. 1998, Rogers 1998, and Prowel et. al. 2005). This relationship was tested using the measurements conducted in this study. The magnesium sulfate soundness test was conducted according to TxDOT standard Tex-411-A, and the Micro-Deval test was conducted according to TxDOT standard Tex-461-A. The percent loss of each test was plotted against each other and a linear regression analysis was conducted to assess the correlation between the two properties. The relationship between the two test results is shown in Figure 4.31.

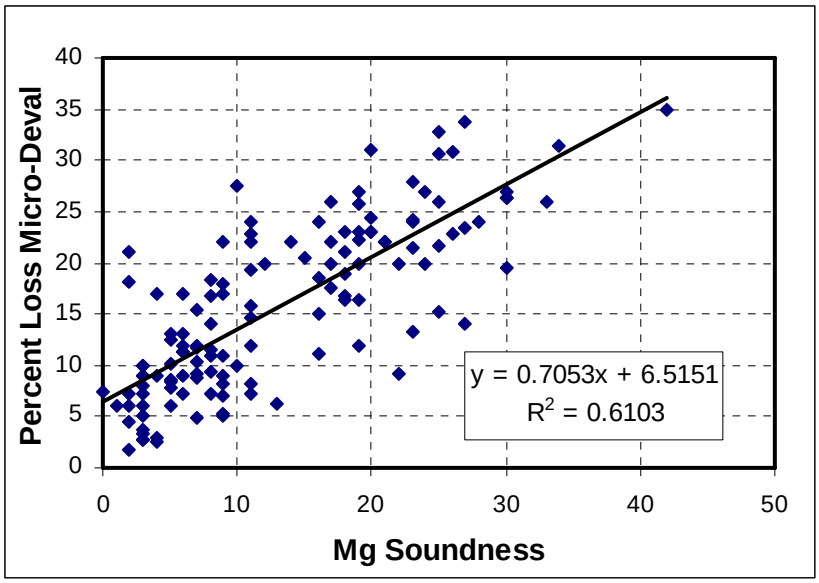

Figure 4.31. Correlation of Percent Loss of Sulfate Soundness and Micro-Deval.

A reasonable correlation exists between the two aggregate properties as both tests measure an aggregates resistance to wear and weathering. The R^2 coefficient of 0.61 is very near that of Rogers (1998) and Prowel et. al. (2005) who noted R^2 values of 0.66 and 0.76 respectively. The relationship found by Cooley and James (2003) was considerably lower than this with an R^2 value of 0.10, but this value seemed to be

influenced by two outlying points. Without these values, the correlation would most likely be much closer to the value obtained in other studies. Although the Micro-Deval is typically considered a measure of mechanical degradation and magnesium sulfate soundness is considered a measure of an aggregate's susceptibility to weathering, this and other studies clearly indicate a relationship between the results from these tests for an aggregate source.

Analysis of Accelerated Polish Test

The accelerated polish test results using Tex-438-A were analyzed and grouped into different ranges as shown in Table 4.13. As given in Table 4.13 and Figure 4.32, the results were within a very small range, where 80 percent of the data were between a PV of 21 and 30. Kandhal et al. (1993) reported that 59 percent of limestone aggregates are between the values of 28 and 32, while 75 percent of gravel aggregate's results are in the same range. With such a large percentage of aggregates falling within a small range, distinguishing between similar aggregates becomes difficult. The other drawback of this test, which is presented in the literature review, is that this test result (PV) is a function of many factors other than texture. The AIMS texture measurements of aggregates are therefore preferred to the PV method due to the shorter testing time and more sensitive results.

Table 4.13. PV Frequency Percentages Distribution.

Range	Frequency	Percentage (%)
$16 \leq PV \leq 20$	2	2
$21 \leq PV \leq 25$	57	52
$26 \leq PV \leq 30$	31	28
$31 \leq PV \leq 35$	16	15
$36 \leq PV \leq 40$	2	2
$41 \leq PV \leq 45$	0	0
$46 \leq PV \leq 50$	1	1
Total	**109**	**100**

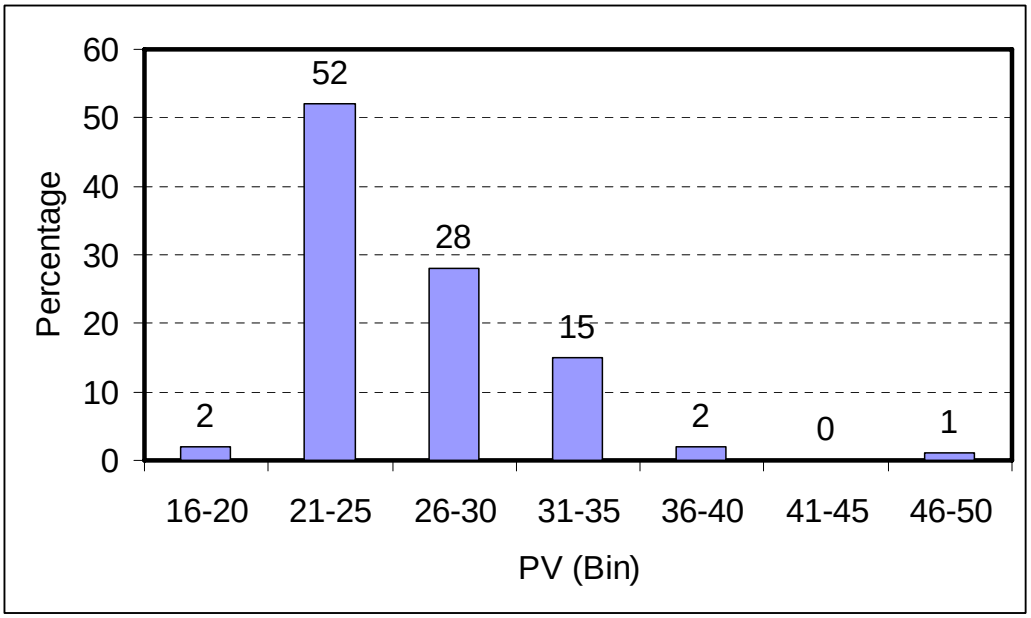

Figure 4.32. PV Percentages Histogram.

SUMMARY

This chapter presents the data produced and cataloged in the database as part of this project. These data were used to compare the AIMS units that are in use at the TTI and TxDOT laboratories. The comparison of the two AIMS units confirmed the findings in Chapter 3 that the two AIMS units provide very similar results.

The angularity analysis method was improved in order to reduce the variability in the measurements within the same aggregate source. The texture analysis method was also enhanced in order to increase the sensitivity of the method to fine texture (smaller scale texture).

The difference in Micro-Deval measurements conducted using two machines was also analyzed in this chapter. Excellent correlation was found between the measurements of the two machines. Correlation between the two properties of percent loss due to Micro-Deval and magnesium sulfate soundness was also assessed. This resulted in a moderate correlation.

Finally, the results from the accelerated polishing test of the database aggregates were analyzed. The majority of the residual PV measurement fell within a very small range. This makes distinguishing between like aggregates difficult, and the AIMS texture method is therefore preferred due to its increased sensitivity and decreased time requirements.

CHAPTER V
CLASSIFICATION OF AGGREGATES

OVERVIEW

The current AIMS software allows for each aggregate particle to be classified into one of four or five levels, depending upon the property being studied. Table 5.1 summarizes the classifications used for each of the AIMS measured properties. These classifications were originally developed as part of NCHRP 4-30 study (Masad et. al. 2005). The original classification was based on testing thirteen aggregate sources with a wide range of characteristics. The Ward's Linkage clustering method in SPSS was used in classifying these aggregates.

Table 5.1. Summary of Aggregate Properties and Classifications.

	Aggregate Property		
	Angularity	Texture	Sphericity
Classification Groups	Rounded	Polished	Flat/Elongated
	Sub-Rounded	Smooth	Low Sphericity
	Sub-Angular	Low Roughness	Moderate Sphericity
	Angular	Moderate Roughness	High Sphericity
	---	High Roughness	---

During the course of this study, the researchers decided that the classification system should be simplified into only three categories for each aggregate property: low, medium, and high. Also, a larger number of aggregate samples have been tested than was originally tested in the NCHRP 4-30 study. This chapter presents the method used to determine the bounds for each of the aggregate properties.

The chapter also revisits the aggregate classification method used by TxDOT as part of the wet weather accident reduction program. A new method that relies on AIMS texture measurements and magnesium sulfate soundness is recommended. The threshold values used in this proposed classification method are not supported by performance data, and future research should focus on accurate determination of these threshold values.

Classification Using Clustering Analysis

To determine the original clusters, the Ward's Linkage clustering method within SPSS was used. The Ward's Linkage clustering method is based upon minimizing the distance between each individual measurement and its cluster. For the NCHRP study, the Euclidean distance was set as the distance that was to be minimized for clustering the cases. This distance is calculated using equation 5.1.

$$Dist = \frac{\sum_{i=1}^{n}(x_i - \bar{x})(y_i - \bar{y})}{\sqrt{\sum_{i=1}^{n}(x_i - \bar{x})^2 \sum_{i=1}^{n}(y_i - \bar{y})^2}} \qquad (5.1)$$

where:

x and y represent two p-dimensional observations (items)

x = [x1, x2,…, xp] and

y = [y1, y2,…, yp].

Ward's Linkage method tries to make the similarity or distance measures sum of squares within groups as small as possible (Al-Rousan 2004).

For this study, the K-mean clustering method in SPSS was used. K-mean clustering is a non-hierarchical clustering method. A specified number of clusters is chosen, which is three in this case. Each of the data points is randomly assigned to one of the clusters until each of the clusters has approximately the same number of data points. The distance between each data point and each cluster is then calculated. A data point is in the correct cluster if it is closest to its own cluster, otherwise the point is

moved to the cluster it is closest to. This process is repeated until no data points change clusters after calculating the distance from the clusters. This method is very helpful in quickly analyzing a large number of data points but depends upon the initial clusters chosen to come up with the final clustering results (Lingras and Huang 2005).

Clustering was conducted for the modified angularity method, the average of texture levels 4 and 5, and sphericity. The analysis was done for all particles from the three sizes (3/8", 1/4", and #4) analyzed BMD, AMD and combined for the TTI data. The clustering results for the angularity index are summarized in Table 5.2, while the results for the average of texture levels 4 and 5 are summarized in Table 5.3 and the sphericity results are summarized in Table 5.4. The percentages of particles that fell within each of the categories are summarized in Tables 5.5 through 5.7.

Table 5.2. Bounds for Modified Gradient Angularity.

	Low	Medium	High
Angularity – BMD only	< 2590.26	2590.26 – 3615.90	> 3615.90
Angularity – AMD only	< 1738.04	1738.04 – 2717.17	> 2717.17
Angularity – Combined	< 2056.82	2056.82 – 3193.55	> 3193.55

Table 5.3. Bounds for Average of Texture Levels 4 and 5.

	Low	Medium	High
Texture – BMD only	< 118.5	118.5 – 238.5	> 238.5
Texture – AMD only	< 106.5	106.5 – 274.5	> 274.5
Texture – Combined	< 111.5	111.5 – 243.5	> 243.5

Table 5.4. Bounds for Sphericity.

	Low	Medium	High
Sphericity – BMD only	< 0.549	0.549 – 0.717	> 0.717
Sphericity – AMD only	< 0.592	0.592 – 0.739	> 0.739
Sphericity – Combined	< 0.573	0.573 – 0.729	> 0.729

Table 5.5. Percentage of Particle Falling Within Each Category for Angularity.

	Low	Medium	High
Angularity – BMD only	33.51 %	48.33 %	18.16 %
Angularity – AMD only	35.16 %	47.64 %	17.20 %
Angularity – Combined	31.62 %	47.75 %	20.63 %

Table 5.6. Percentage of Particle Falling Within Each Category for Texture.

	Low	Medium	High
Texture – BMD only	57.95 %	32.50 %	9.55 %
Texture – AMD only	70.63 %	26.86 %	2.51 %
Texture – Combined	63.73 %	30.04 %	6.23 %

Table 5.7. Percentage of Particle Falling Within Each Category for Sphericity.

	Low	Medium	High
Sphericity – BMD only	11.01 %	48.52 %	40.46 %
Sphericity – AMD only	16.53 %	48.13 %	35.34 %
Sphericity – Combined	13.93 %	48.59 %	37.48 %

As shown in Tables 5.2 and 5.3, the AMD samples have lower cluster bounds than the BMD samples for both texture and angularity. This difference would be expected since the particles have been abraded and would therefore have less texture and more rounded edges. Due to the AMD particles being more rounded, it would be reasonable that the sphericity clusters are higher, which is the case for these results, as evident in Table 5.4. As expected, in each aggregate property the bounds of the combined sample fall between those of the individual AMD or BMD bounds.

Classification Using Quartile Analysis

The clustering analysis used in the previous section gave bounds for the three categories of aggregates. However, a small percentage of aggregates (less than 10 percent) fell under the high texture category. For the angularity analysis, the percentages of aggregates classified as high angularity were less than 25 percent. It is believed that this classification would penalize aggregates with relatively high texture and angularity. The aggregates used in this study represented a wide range of mineralogy. Visual inspection of these aggregates revealed that they included materials with the highest angularity and texture that can be encountered. Therefore, classification was proposed to be based on quartiles. In this approach, the bounds are selected such that 25 percent of all aggregate particles are low, 50 percent are in the medium range, and 25 percent are in the high range. These bounds based upon individual particle measurements are shown in Tables 5.8, 5.9. and 5.10 for angularity, texture and sphericity, respectively.

Table 5.8. Individual Particle Angularity Quartiles.

	First Quartile	Median	Third Quartile
BMD Only	2420.46	2885.91	3417.84
AMD Only	1528.24	2017.96	2508.22
Combined	1880.73	2463.79	3060.59

Table 5.9. Individual Particle Texture Quartiles.

	First Quartile	Median	Third Quartile
BMD Only	65.0	103.5	161.5
AMD Only	46.5	74.0	115.5
Combined	54.5	87.0	138.5

Table 5.10. Individual Particle Sphericity Quartiles.

	First Quartile	Median	Third Quartile
BMD Only	0.615	0.691	0.763
AMD Only	0.624	0.698	0.772
Combined	0.620	0.694	0.767

It is sometimes desirable to classify an aggregate sample based on average properties. Therefore, the bounds for the average properties were determined based on the quartile analysis (25 percent of aggregates within the low range, 50 percent in the medium range, and 25 percent in the high range). The bounds based on average aggregate properties are presented in Tables 5.11, 5.12, and 5.13 for angularity, texture, and sphericity, respectively. In the case of sphericity, aggregates have a very small range for average angularity. It may therefore be desirable to classify sphericity based upon distribution, such as percent flat and elongated or some other measure such as percent less than 0.6.

Table 5.11. Average Angularity Quartiles.

	First Quartile	Median	Third Quartile
BMD Only	2838.18	2939.01	3056.53
AMD Only	1832.14	1981.01	2239.57
Combined	1981.33	2656.14	2938.13

Table 5.12. Average Texture Quartiles.

	First Quartile	Median	Third Quartile
BMD Only	77.71	113.14	147.42
AMD Only	56.24	79.00	103.36
Combined	67.77	92.08	132.09

Table 5.13. Average Sphericity Quartiles.

	First Quartile	Median	Third Quartile
BMD Only	0.661	0.681	0.705
AMD Only	0.667	0.687	0.713
Combined	0.664	0.682	0.709

Figure 5.1 shows the angularity versus texture for the BMD samples with the AMD samples plotted in Figure 5.2 and the combination of BMD and AMD shown in Figure 5.3. The igneous aggregates generally have the highest angularity, as seen in Figures 5.1, 5.2 and 5.3. The limestones have a wide spread in texture. The gravels have a narrower spread than the limestones in texture, but have both moderate levels of angularity and texture. The previous chapter, discussed the low variability in the sandstone samples which is considered an important factor contributing to the abrasion resistance of these aggregates.

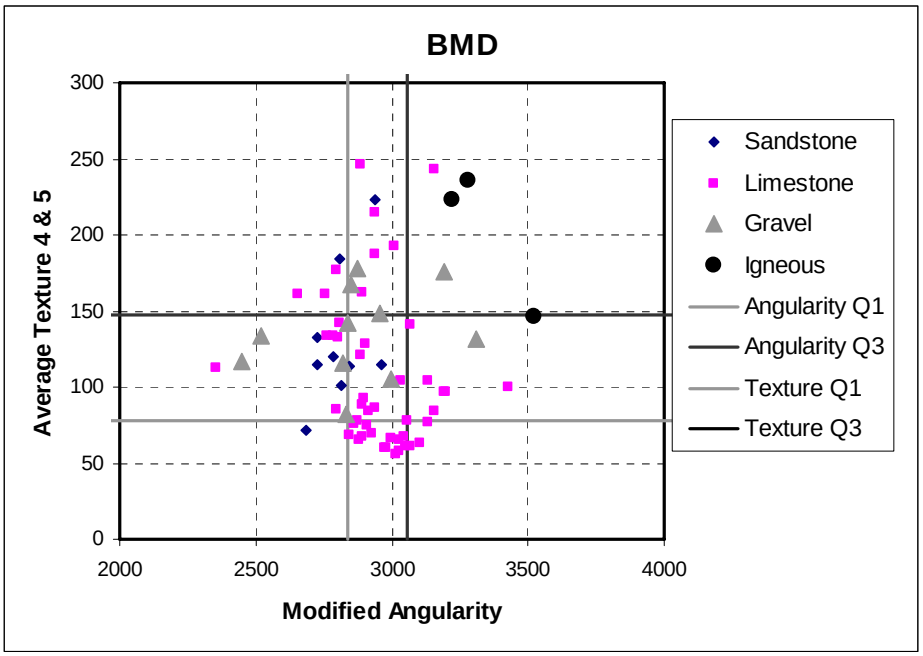

Figure 5.1. Clustering Comparison Based on Mineralogy for BMD Samples.

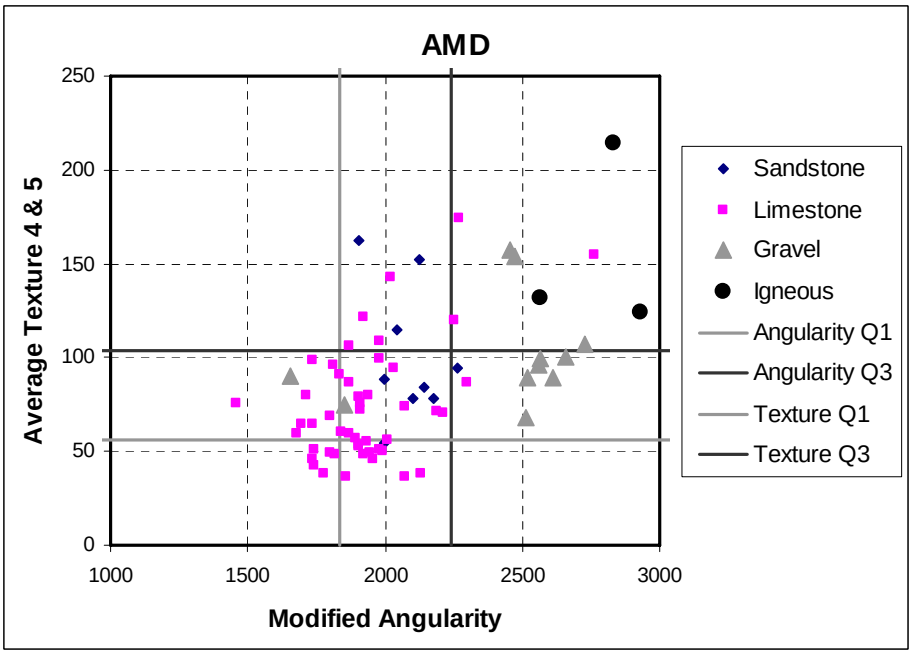

Figure 5.2. Clustering Comparison Based on Mineralogy for AMD Samples.

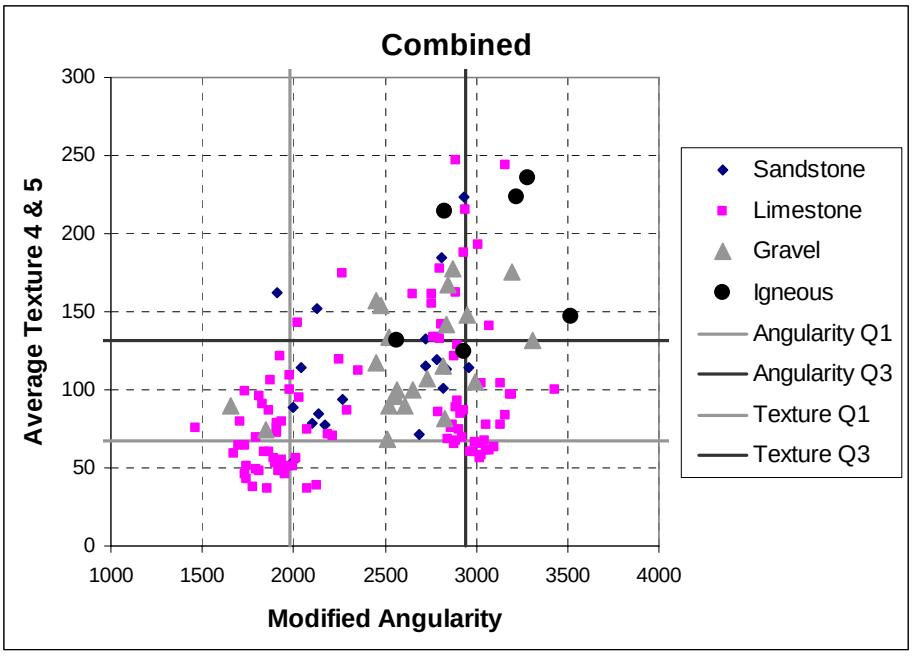

Figure 5.3. Clustering Comparison Based on Mineralogy for Combined Samples.

CLASSIFICATION OF AGGREGATES USED IN ASPHALT PAVEMENT SURFACES

TxDOT has implemented the WWARP, which is aimed at reducing the number of accidents due to inadequate surface friction of pavement in wet weather situations. To determine the surface friction demand, several inputs are studied. These inputs include, but are not limited to, precipitation, traffic volume and speed, accident history, and skid performance. Once these and several other inputs are evaluated, an aggregate is chosen based upon its classification to fit the surface friction needs of the roadway. The aggregates are classified as A, B, C, and D with A as the best and D as the worst. The method of classification is based upon the magnesium sulfate soundness test and the residual polished stone value. The chart used for classification purposes is shown in Figure 5.4.

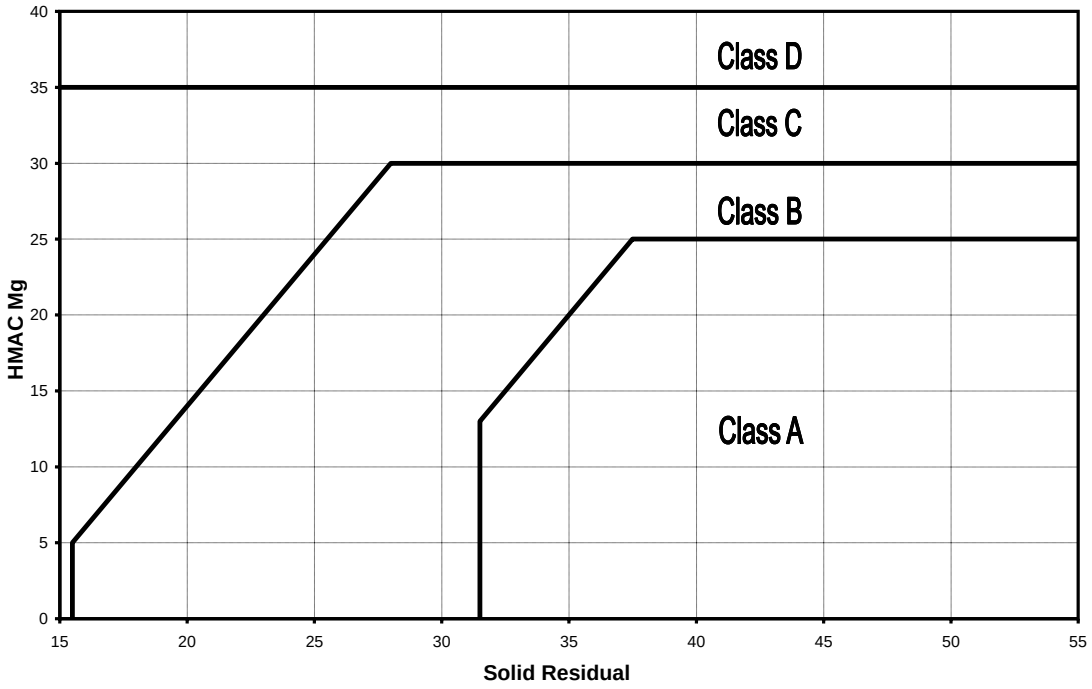

Figure 5.4. Surface Aggregate Classification for WWARP.

As shown earlier in this report, as well as in other studies, a great percentage of the values for the residual PV fall within a small range (see Table 4.13 and Figure 4.32). The classification method currently used, places the vast majority of aggregates in a classification of B or worse. Therefore, a new method needs to be developed using a measure of texture with more sensitivity than the PV as well as a measure of weather resistance.

The proposed method is based on the average of AIMS texture levels 4 and 5 of the AMD aggregates, the COV of the texture measurements, and a measure of aggregate's soundess. Since the current method used in the WWARP is the magnesium sulfate soundness rather than the Micro-Deval the magnesium sulfate soundness test will be used. However, it is believed that classification can be done using the Micro-Deval when more data become available on the relationship between Micro Deval results and

resistance to weathering. Texture measurements replace the PV because the PV is not sensitive enough to distinguish between aggregates, whereas the AIMS results offer a more sensitive assessment of aggregate texture. The time required to obtain AIMS results is also significantly less than that required to obtain the residual PV.

Aggregates were classified using the original method to determine a baseline for comparison. Of all aggregates tested, only 36 had all the data necessary to classify them using the original method and the proposed method. These data include the terminal PV, magnesium sulfate soundness, percent loss due to Micro-Deval, average texture, and texture COV. These properties as well as the original and proposed surface classification are included in Table 5.14. Figure 5.5 shows the new classification chart. The changes in the number of aggregates classified within each category are summarized in Table 5.15.

The aggregates within the shaded area in Figure 5.5 are classified as A or B based on texture COV. A COV of less than 0.4 classifies an aggregate as A while a COV greater than 0.4 classifies an aggregate as B. The aggregates within the A section have texture in the top 25 percent among all aggregates while aggregates in the shaded region have texture values in the third quartile among all aggregates. The maximum magnesium sulfate level for an aggregate to be classified as A was set at 18 percent, which Kandhal (1998) denoted as the dividing lines between good and poor performing aggregates. The dividing line between B and C as well as between C and D were according to the current TxDOT method.

Table 5.14. Aggregate Surface Classification Properties.

Sample Number	Class	PV Final	Sulfate Soundness	% Loss MD	Ave. Txtr.	COV	Prop. Class
05-0041	A	48	10	27.6	88.18	0.225	A
05-1002	A	37	19	22.2	81.74	0.339	B
05-1260	A	32	2	18.2	80.14	0.644	B
05-0129	B	25	8	11	100.95	0.369	A
05-0149	B	24	11	15.9	68.95	0.428	B
05-0178	B	27	25	21.7	41.42	0.552	C
05-0213	B	21	8	16.7	61.3	0.483	B
05-0235	B	26	3	2.7	105	0.507	A
05-0245	B	25	3	2.8	116.15	0.482	A
05-0247	B	26	3	3.7	102.64	0.491	B
05-0251	B	21	6	11.4	96.34	0.345	A
05-0350	B	33	25	15.3	78.57	0.42	B
05-0368	B	27	25	32.7	39.18	0.483	C
05-0397	B	24	11	19.4	56.73	0.497	B
05-0399	B	26	20	23.1	43.37	0.486	C
05-0519	B	23	16	18.5	75.3	0.49	B
05-0532	B	28	22	19.9	72.46	0.373	B
05-0535	B	35	26	22.8	216.34	0.315	B
05-0545	B	27	27	33.7	41.88	0.354	C
05-0768	B	23	3	10	67.08	0.379	B
05-0828	B	30	5	6	96.63	0.197	A
05-0832	B	27	11	12	90.98	0.415	B
05-0922	B	25	23	24	59.69	0.629	C
05-0938	B	26	2	4.4	147.21	0.196	A
05-0941	B	30	3	3.4	63.25	0.603	B
05-0992	B	24	6	17	60.83	0.475	B
05-1183	B	25	23	24.1	42.14	0.52	C
05-1201	B	31	7	8.7	75.53	0.435	B
05-1207	B	32	23	13.3	71.14	0.559	B
05-1223	B	25	19	25.8	47.56	0.531	C
05-1235	B	25	2	21.1	47.67	0.554	B
05-0347	C	26	34	31.5	59.82	0.622	C

Table 5.14. Aggregate Surface Classification Properties (Continued).

Sample Number	Class	PV Final	Sulfate Soundness	% Loss MD	Ave. Txtr.	COV	Prop. Class
05-0365	C	25	30	26.4	65.3	0.535	C
05-1205	C	26	30	27	44.03	0.357	C
05-0496	D	35	57	31.2	50.62	0.439	D

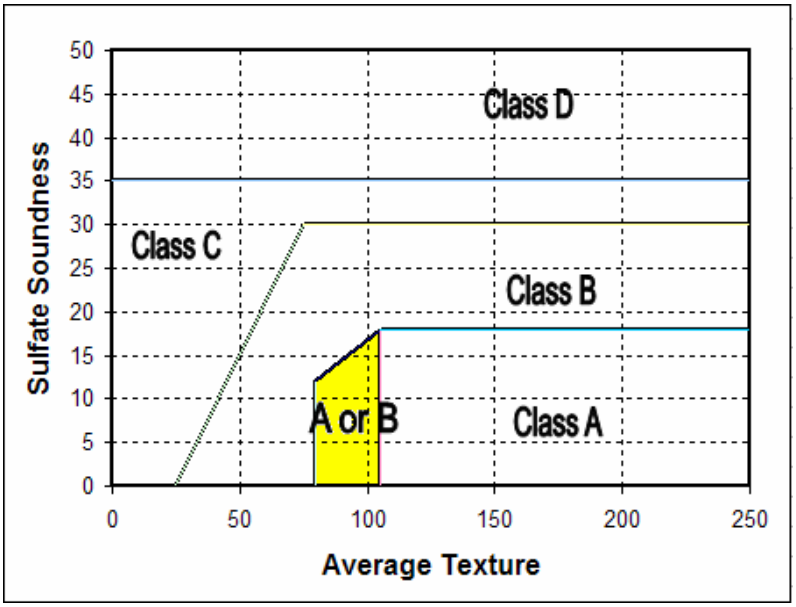

Figure 5.5. New Surface Aggregate Classification Method.

Table 5.15. Changes in Aggregates Classification.

Current Classification		Proposed Classification Count			
	Count	A	B	C	D
A	3	1	2		
B	29	6	16	7	
C	3			3	
D	1				1
Total	36	7	18	10	1

Many of the aggregates tested fell into the B aggregate surface classification based on the current method. This result would be expected due to the limited range observed in the terminal PV value used for classification purposes. Likely, many of these aggregates would change classification by using the new method, especially since this method is more sensitive to differences in aggregate properties than the current method.

The summary results in Table 5.15 show that many aggregates changed classification using the new method. Although many aggregates change classification, none change more than one level. Therefore, no aggregates initially classified as A are now classified as C, or vice versa. The majority of the changes came in those aggregates classified as B. The end result of the new classification is a more sensitive classification that allows for the aggregates to be more spread out over the groups instead of having the majority classified as B.

It should be noted that no performance testing or field evaluation was done to assess the results of this new classification. Future research will be necessary to validate the method and refine the cutoff values for classification. Classification methods using the percent loss due to Micro-Deval instead of or along with magnesium sulfate soundness should be investigated as well.

SUMMARY

This chapter documented the refinements of the aggregate shape classification method used in AIMS. The bounds for the new categorization of low, medium and high were determined using the Ward's Linkage clustering analysis. The clustering results were found to penalize the aggregates with high texture as only 10 percent of aggregates were classified as having a high texture. Consequently, quartiles analysis was conducted to classify aggregates in groups that belong to low (lowest 25 percent of the data), medium (middle 50 percent of the data), and high (top 25 percent of the data) categories. The aggregate surface classification for the wet weather accident reduction program was also revised to incorporate AIMS results in the classification of aggregates.

CHAPTER VI
DEVELOPMENT OF A METHODOLOGY FOR MEASURING AGGREGATE RESISTANCE TO POLISHING, ABRASION, AND BREAKAGE

OVERVIEW

This chapter includes the development of new methodologies for measuring aggregate resistance to polishing and degradation (abrasion and breakage). Polishing is the loss of aggregate surface texture, and abrasion is the reduction in aggregate size due to the loss of the surface angularity and texture, while breakage is the fracture of aggregate particle. The developed methodologies utilize the AIMS and Micro-Deval measurements.

Aggregates are expected to encounter degradation during production, transportation, construction, and compaction. In addition, some new generation mixes such as Stone Matrix Asphalt and Open Graded Friction Course rely on stone-to-stone contacts in transferring applied stresses through the aggregate structure. This stress transfer mechanism applies high contact stresses that can cause aggregate fracture. Therefore, it is desirable to use coarse aggregates that are able to sustain these contact stresses without fracture.

Aggregate resistance to polishing is mainly related to HMA pavement surface skid resistance. As pointed out in the literature review, there are several drawbacks of current methods for measuring aggregate degradation. Among these drawbacks are the length of time it takes for preparing and polishing specimens, and the influence of other factors besides texture on the results. The Micro-Deval test results cannot distinguish between aggregate abrasion and breakage.

INTRODUCTION

Asphalt pavement frictional resistance, which is also known as skid resistance, is one of most important performance parameters due to its effect on travel safety.

Frictional resistance of HMA must maintain a minimum acceptable safe limit. Skid resistance is a function of both the microtexture and macrotexture of the surface (Dahir 1979). The microtexture depends mainly on the aggregate shape characteristics; on the other hand, macrotexture is a function of mix design, compaction method, and aggregate gradation. According to Abdul-Malak et al. (1996), coarse aggregates at the surface are the main source of HMA pavement surface texture.

There are many methods available for measuring aggregate polishing resistance. The most widely used is the British wheel/pendulum method (ASTM E303 and ASTM D3319). However, many studies showed that the PV measured using the British pendulum is a function of many other factors besides aggregate texture (Won and Fu, 1996). These factors include the coupon curvature and aggregate size. In addition, most of the PV results of this test for a wide range of aggregates vary within a small range of 4 PV (Kandhal et al. 1993), which makes it difficult to distinguish among aggregate polishing resistance.

Crouch and Dunn (2005) developed two methodologies for measuring aggregate polishing. The first one is the Tennessee Terminal Textural Condition Method in which the uncompacted voids content is measured in aggregates before and after abrasion in the Los Angeles machine. The second test is the Micro-Deval Voids at 9 hours. In this test, uncompacted voids content is measured in an aggregate sample before and after 9 hours of abrasion in the Micro-Deval test.

Another important characteristic of aggregate that affects HMA properties is the resistance to degradation (abrasion and breakage). Aggregates are exposed to degradation during plant operations and under compaction. Degradation affects the overall gradation, so the field produced mix will be different from the laboratory designed one (Wu et al. 1998). Therefore, it is important to control aggregate degradation during construction.

Asphalt mixes such as OGFC and SMA rely on stone-to-stone contacts in transferring applied stresses within the aggregate structure. High contact stresses are present at the contact points which lead to aggregate fracture and reduction in load

carrying capacity (Gatchalian 2005). Therefore, there is a need to develop a test method to assess aggregate resistance to fracture during compaction and under traffic loads. Gatchalian (2005) recommended the use of the Aggregate Imaging System to measure change in aggregate angularity after Micro-Deval testing, and changes in gradation after compaction as measures of aggregate resistance to fracture.

A METHODOLOGY FOR MEASURING AGGREGATE RESISTANCE TO POLISHING

Aggregate polishing is defined as the aggregate's loss of its surface texture. The development of a methodology to measure aggregate resistance to polishing can be achieved by three steps: (1) measure the initial aggregate texture, (2) polish the aggregates, and (3) measure their texture after polishing. The simplicity of the methodology will depend on the techniques used to perform these steps and the time to carry out these steps.

In the developed methodology, AIMS is used to measure the aggregate texture. The operator needs only to do some simple steps to calibrate the system, and then the AIMS unit will operate through computer control to obtain images and analyze texture. AIMS takes 15 to 20 minutes to scan a set of aggregates for texture and angularity, which is considered a short time. The Micro-Deval test is introduced as the polishing mechanism in this study. The Micro-Deval test is conducted according to the Tex-461-A procedure.

Preliminary Evaluation of the Proposed Methodology

Prior to the development of the new methodology, it was necessary to examine the ability of the Micro-Deval to polish aggregates, and the relationship between polishing of coupons using the Accelerated Polish Test (Tex-438-A) and aggregate polishing using the Micro-Deval.

Aggregate coupons and Micro-Deval aggregate samples were all prepared at the TxDOT laboratory. The TxDOT laboratory conducted the AIMS texture measurements

on the coupons before and after polishing and on aggregate samples before and after the Micro-Deval. The TxDOT laboratory measured the PV using the British pendulum on the coupons.

The coupons were sent to the TTI laboratory after polishing where they were measured again using AIMS. Aggregate samples were also shipped to the TTI laboratory where they were measured using the Micro-Deval test and AIMS. Aggregates used in the two experiments were all from the state of Texas. Most of the aggregates are limestone and gravel, with some other types like sandstone, igneous rock, and lightweight aggregate were included.

Figure 6.1 shows a plot of the aggregate texture index before Micro-Deval against aggregate texture index after Micro-Deval. Most of the aggregates fall to the right of the equality line, which is proof that most of the aggregates had a higher texture index BMD and that AIMS is capable of detecting changes in texture due to polishing by the Micro-Deval. Figure 6.2 shows examples of images on one of the aggregates before and after Micro-Deval polishing. The loss of texture can even be seen visually in these images.

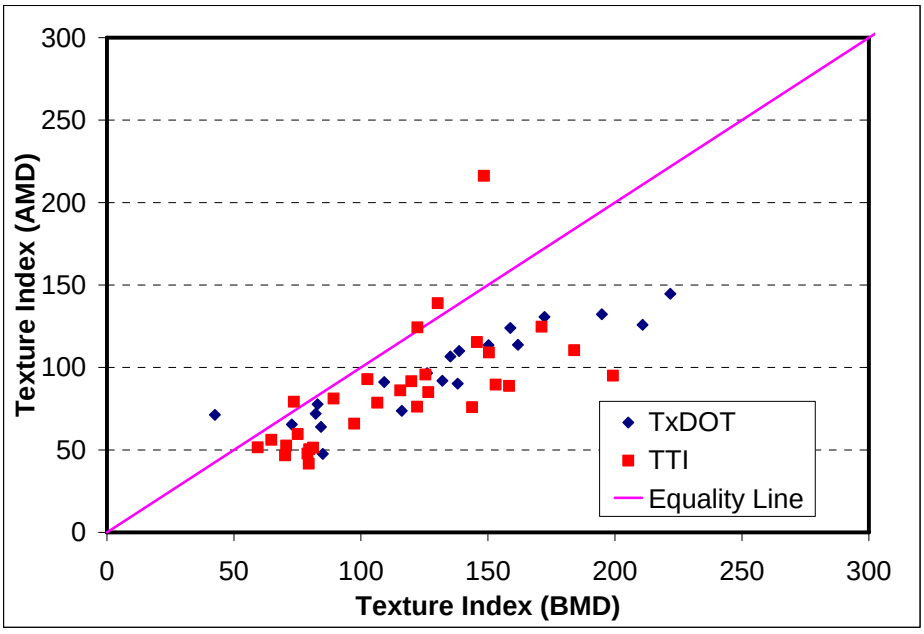

Figure 6.1. Comparing Aggregate Texture before and after Micro-Deval.

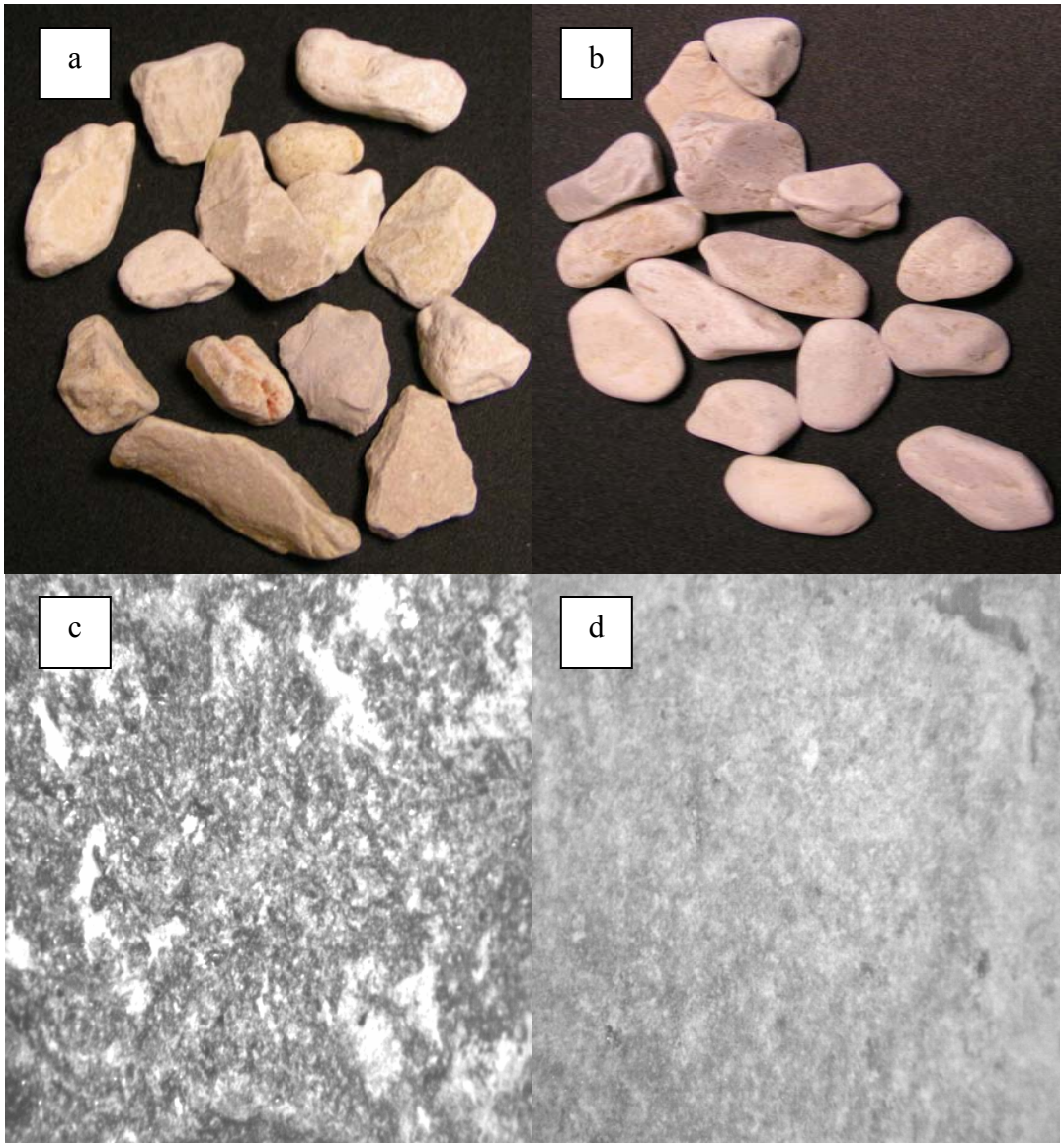

Figure 6.2. Aggregate Images: a) Aggregate Particles before Micro-Deval, b) Aggregate Particles after Micro-Deval, c) Aggregate Surface Texture before Micro-Deval, d) Aggregate Surface Texture after Micro-Deval.

Figure 6.3 shows the texture index of aggregates BMD versus the texture of coupons before polishing (BP); while the after polishing (AP) results are shown in Figure 6.4. There is very good correlation between texture of aggregates and texture of coupons in both the before polishing and after polishing cases. This result supports the claim that the Micro-Deval is able to polish aggregates, and this polishing effect is captured well by AIMS. Example images of polishing coupons before and after polishing were given in Chapter 4 Figure 4.2.

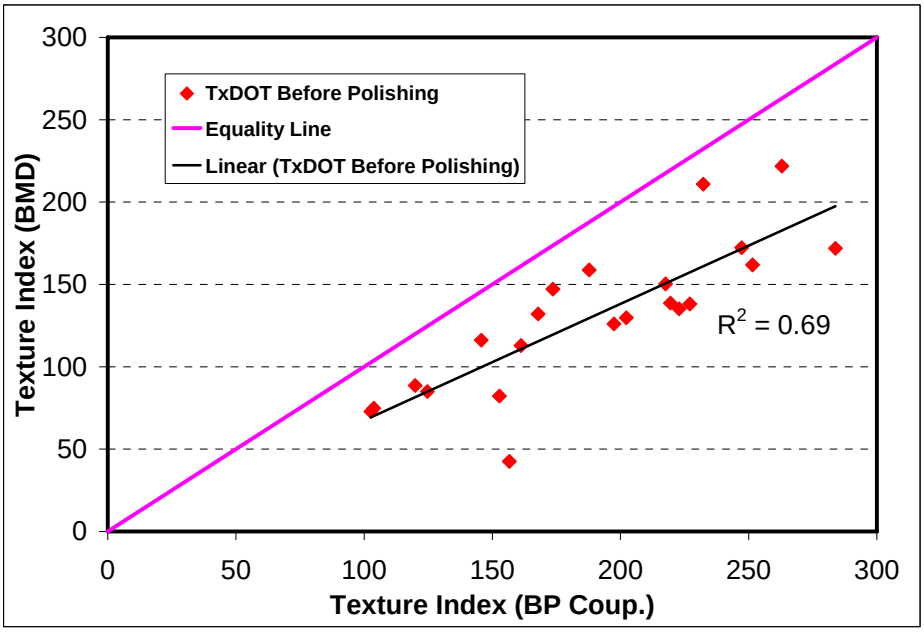

Figure 6.3. Relationship between Coupons and Aggregate Particles Texture.

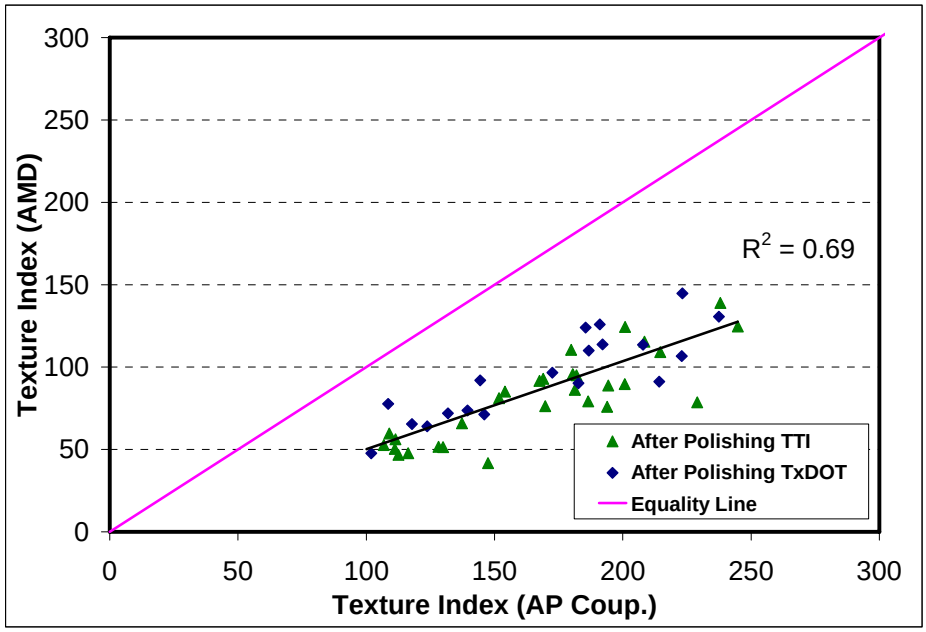

Figure 6.4. Relationship between Polished Coupons and Polished Aggregate Particles Texture.

Comparison of Aggregate Polishing Using the Proposed Methodology

An experiment was conducted to examine the effect of polishing time in the Micro-Deval on the texture index and to determine the time needed for the texture to reach its terminal value. The six different aggregates listed in Table 6.1 were subjected to Micro-Deval polishing for different lengths of time of 15, 30, 45, 60, 75, 90, 105, and 180 minutes.

Table 6.1. Aggregate Types Used in Polishing Experiment.

Aggregate Number	Description
1	Crushed Gravel
2	Hard Crushed Limestone
3	Soft Crushed Limestone
4	Traprock
5	Quartzite
6	Crushed Granite

Two different procedures were followed in order to determine whether it is necessary to use different aggregate samples for the different polishing time durations or if the same sample can be used for all time durations. In the first procedure, an aggregate sample was scanned using AIMS, and then it was tested in the Micro-Deval for 15 minutes. The sample was removed from the Micro-Deval and scanned in AIMS again. The same aggregate sample was returned to the Micro-Deval and tested for 15 more minutes, after which it was scanned using AIMS. This process was repeated until the cumulative time summed to 105 minutes, then the sample was returned to the Micro-Deval for another 75 minutes.

In the second procedure, eight different samples from each aggregate were used. Each aggregate sample was tested for a certain time duration and was discarded after this time duration. An example of the comparison between these two procedures is shown in Figure 6.5. As can be seen, the two procedures yielded very similar results. The second method is recommended in spite of the fact that it requires more material. The second procedure with different samples requires less time. Also, this procedure ensures that the Micro-Deval test is conducted at the same conditions for each of the time intervals irrespective of aggregate type. If the same aggregate sample is used for the different time durations, the washing of the fines after each interval affects the interaction between steel balls and aggregates.

Figure 6.6 shows the change of texture as a function of polishing time in the Micro-Deval for all six aggregates. Aggregate 1 is crushed gravel with low texture. The texture of this aggregate did not follow a certain trend with polishing time. The slight changes in texture can be attributed to the small differences among aggregate samples. Visual inspection of aggregates after the different time intervals showed that the aggregate texture changed very little, as the results in Figure 6.7 indicate. This aggregate lost only 2.68 percent of its weight after 105 minutes, but 1 percent of its weight was lost after 15 minutes and 1.47 percent of its weight was lost after 30 minutes.

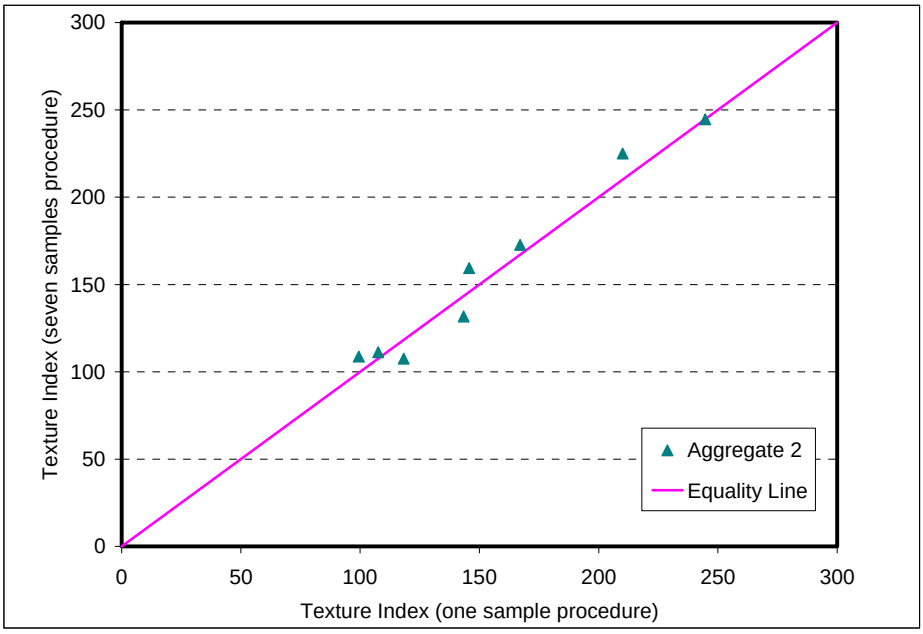

Figure 6.5. Comparing Results for Two Different Procedures of Proposed Methodology.

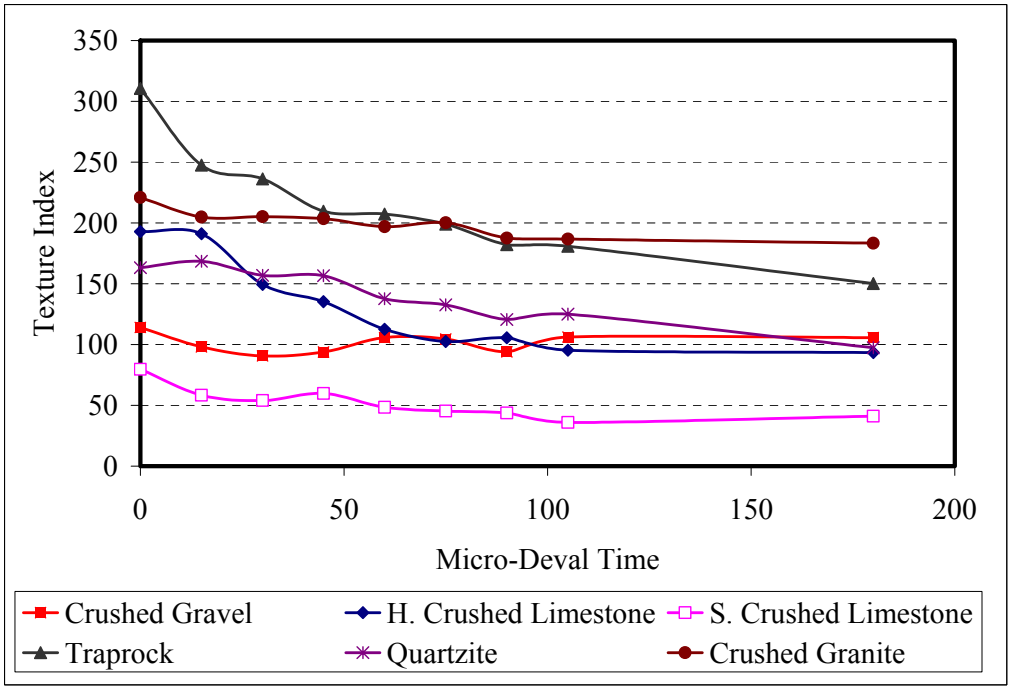

Figure 6.6. Aggregate Texture as Function of Micro-Deval Time.

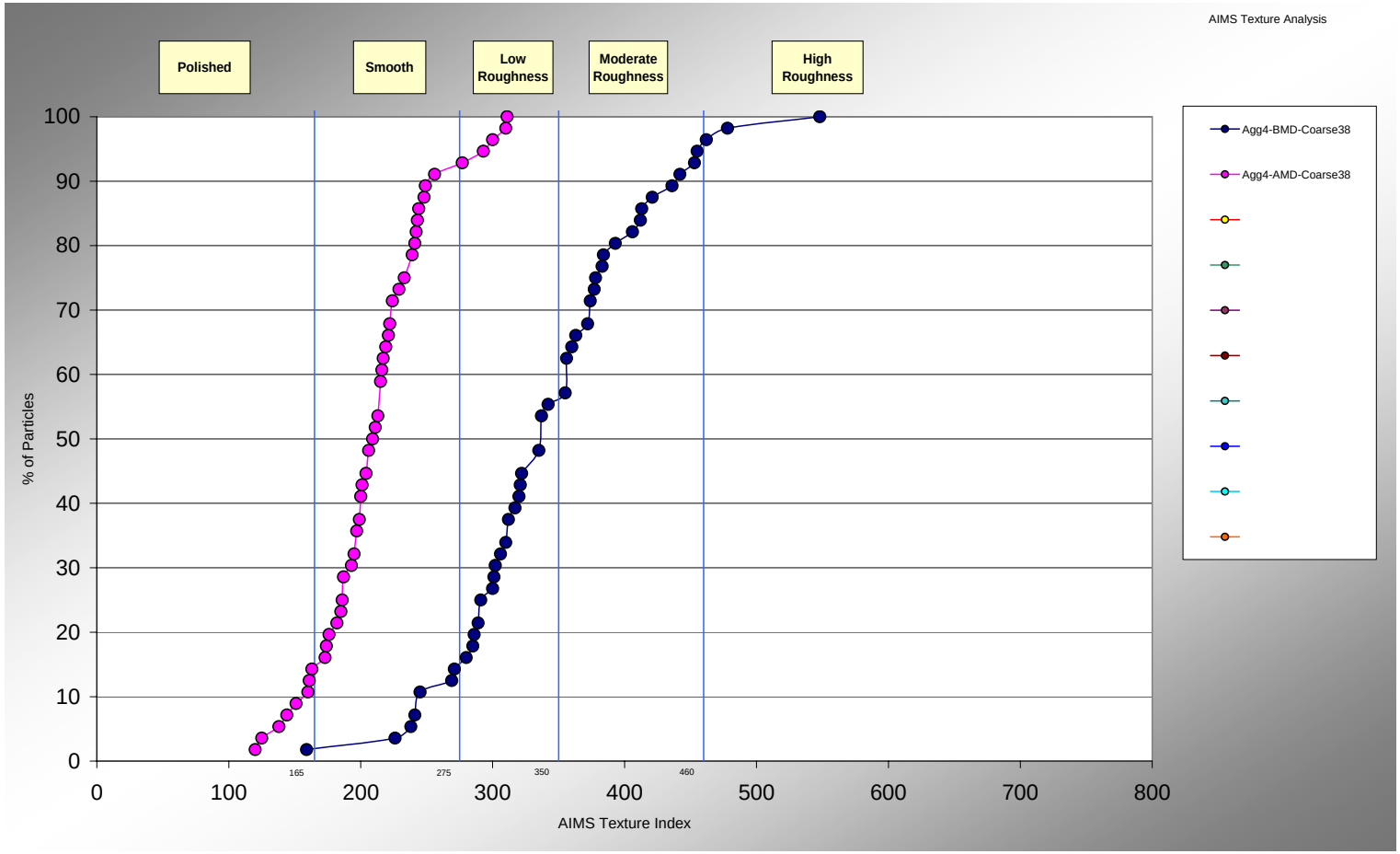

Figure 6.7. Texture Distribution of Aggregate 4 before and after Micro-Deval.

Aggregate 2 is a crushed hard limestone. Aggregate texture started at 200 and changed slightly after 15 minutes of polishing. However, texture dropped rapidly afterward until it reached a texture value around 100. Aggregate 3 is a crushed soft limestone. The trend for this aggregate is similar to the trend for aggregate 2 as the texture value stabilizes around value of 40. The Micro-Deval weight loss of this aggregate was 20.4 percent after 105 minutes in the Micro-Deval, which is the highest among all the six aggregates.

Aggregate 4 is a crushed traprock aggregate. The initial texture was 311, and it experienced rapid loss of texture until about 45 minutes, but the rate of texture loss decreased after that. Finally, texture stabilized in the last 30 minutes around a value 150.

Aggregate 5 is a quartzite aggregate, and did not lose much of its texture in the first 45 minutes. Aggregate 5 started losing texture for the following 45 minutes to reach a value around 120 and kept losing texture with time. Aggregate 6 is a crushed granite. This aggregate did not lose much of its texture, and its texture reached a value of 184. Figure 6.7 represents the texture distribution for aggregate 4 before and after the Micro-Deval. Figure 6.8 represents the texture distribution for aggregate 6 before and after the Micro-Deval. The figures show how the Micro-Deval polishing changed the texture distribution and that aggregate 4 was more affected by the Micro-Deval than aggregate 6.

The results in Figure 6.6 indicate that the Micro-Deval test is able to affect the aggregate texture within the 180-minute period. Therefore, the Micro-Deval is considered a good mechanism to polish aggregates, and it requires less time and effort than the polishing used in the Accelerated Polishing Test. A summary of texture before and after the Micro-Deval is shown in Table 6.2. The aggregates differed significantly in the amount of texture lost due to polishing. Also, initial texture cannot be relied on alone to characterize aggregates. As shown in Table 6.3, aggregates rank differently based on texture before polishing, texture after polishing, and percent loss of texture.

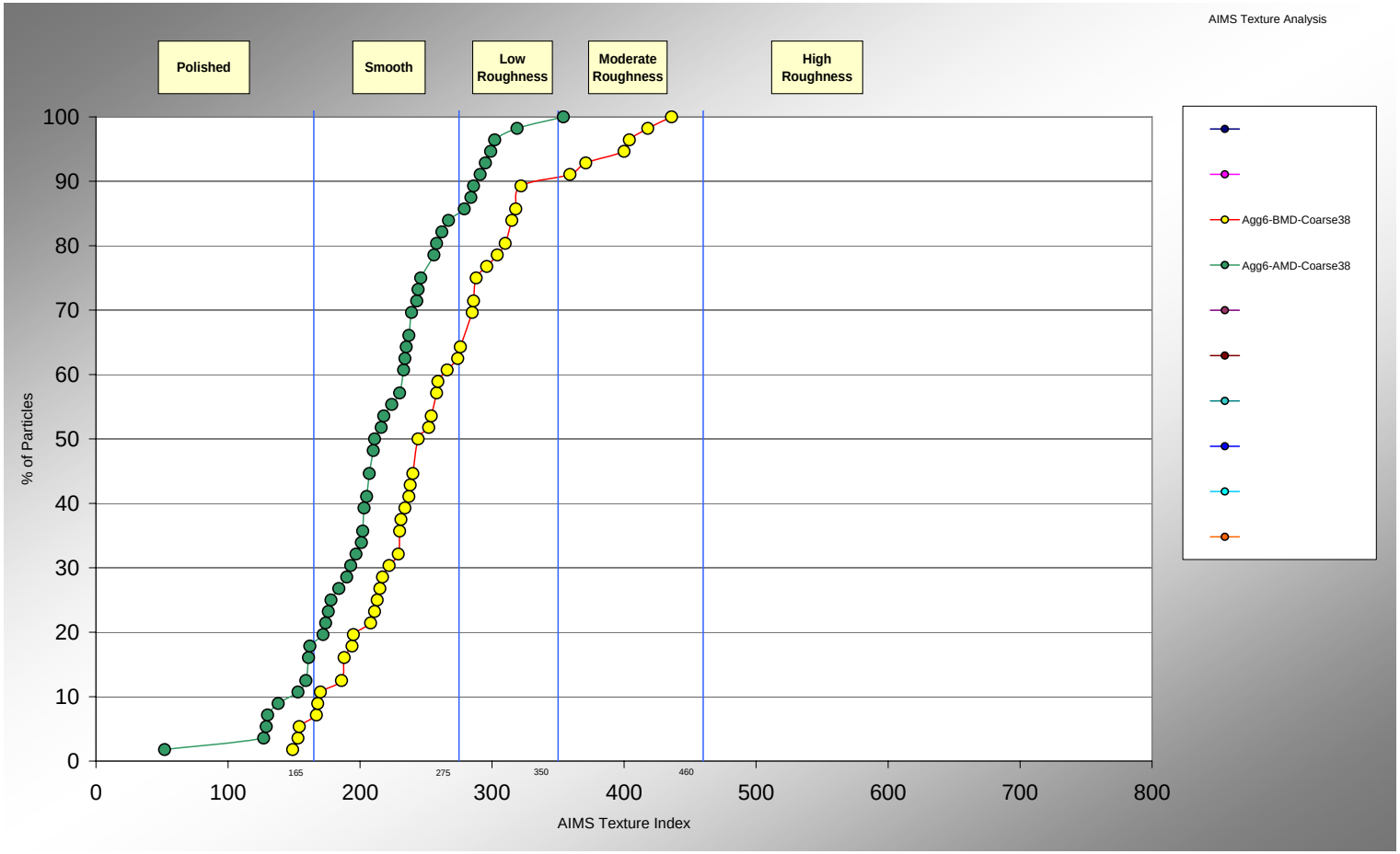

Figure 6.8. Texture Distribution of Aggregate 6 before and after Micro-Deval.

The use of BMD texture as the ranking criterion would lead to misleading results. For example, aggregate 4 started with very high texture but ended up ranked number two after polishing. The use of percent loss of texture can also be misleading. Aggregate four ranked sixth using this criterion while it had the highest BMD texture and the second highest AMD texture. Also, aggregate 1 ranked as the best using the percent loss of texture, and it had the second lowest initial texture and ranked third in AMD texture.

Table 6.2. Aggregate Texture, before and after Micro-Deval.

Aggregate Number	BMD Texture	AMD Texture	Percent Loss of Texture
1	114.10	105.67	7.39
2	192.77	93.37	51.57
3	79.70	41.03	48.53
4	310.58	150.20	51.64
5	163.18	97.36	40.34
6	220.93	183.35	17.01

Table 6.3. Ranking of the Aggregates Using Three Different Criteria.

Rank	BMD Texture Criteria	AMD Texture Criteria	Percent Loss of Texture Criteria
1 (Highest Texture)	4 (310.58)	6 (183.35)	1 (7.39)
2	6 (220.93)	4 (150.20)	6 (17.01)
3	2 (192.77)	1 (105.67)	5 (40.34)
4	5 (163.18)	5 (97.36)	3 (48.53)
5	1 (114.1)	2 (93.37)	2 (51.57)
6 (Lowest Texture)	3 (79.70)	3 (41.03)	4 (51.64)

The results discussed above prompted the development of an analytical method that can capture initial texture, final texture, and the change in texture. Two function were used to fit the data as shown in Equations 6.1 and 6.2.

$$Texture(t) = a + b \times e^{-ct} \quad (6.1)$$

$$Texture(t) = a - \frac{t}{b + c \times t} \quad (6.2)$$

where

Texture(t) = aggregate texture as function of time

t = time in minutes, and

a, b and c = parameters determined through fitting data.

Equation 6.2 was used by Kandhal et al. (1993). Table 6.4 shows the fitting parameters using Equation 6.1, while Table 6.5 shows fitting parameters for Equation 6.2

Table 6.4. Equation 6.1 Fitted Parameters.

Aggregate	a	b	c
1	99.81	14.29	1.59999
2	83.53	119.93	0.01987
3	39.13	37.46	0.02505
4	154.31	145.29	0.01877
5	0*	170.57	0.00317
6	178.69	39.02	0.01254

* The parameter "a" represents the final texture, and it must be equal to or larger than zero.

Table 6.5. Equation 6.2 Fitted Parameters.

Aggregate	a	b	c
1	101.40	1,061,649.63	53,687,091.2
2	202.63	0.369	0.00624
3	78.54	0.635	0.02180
4	30.63	0.250	0.00539
5	170.30	1.878	0.00300
6	218.45	1.656	0.01881

Figures 6.9, 6.10, 6.11, 6.12, 6.13, and 6.14 show the two fitting functions for aggregates 1, 2, 3, 4, 5, and 6, respectively. Only aggregate 1 did not fit well with the two functions. As discussed previously, aggregate 1 did not lose its texture with time in the Micro-Deval. For the other five aggregates, the two function fit the data points very well. All aggregates tended to reach a constant texture value, except for aggregate 5 which continued to lose texture with the testing time. Such behavior was also reported by Crouch et al. (2005) who stated that some aggregates continue to polish and do not reach a terminal point.

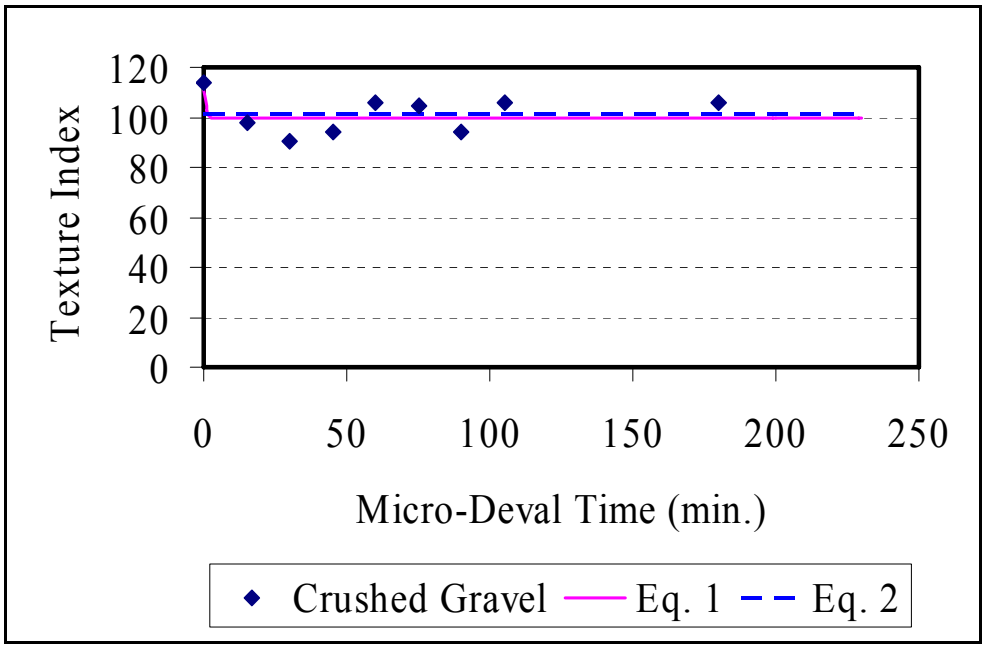

Figure 6.9. Equations 6.1 and 6.2 Fitting Plots for Crushed Gravel.

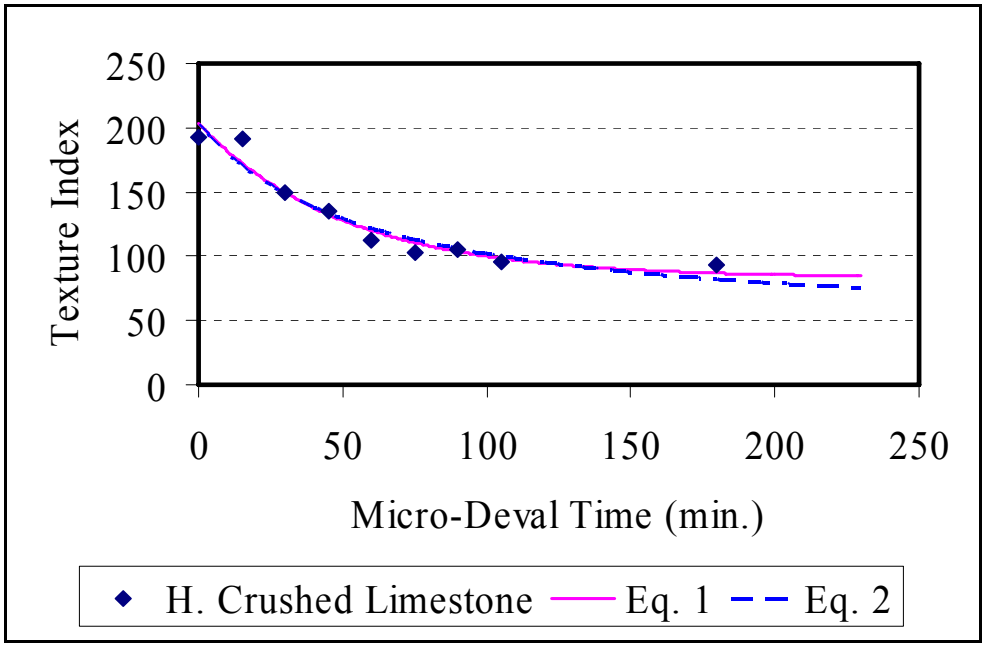

Figure 6.10. Equations 6.1 and 6.2 Fitting Plots for Hard Crushed Limestone.

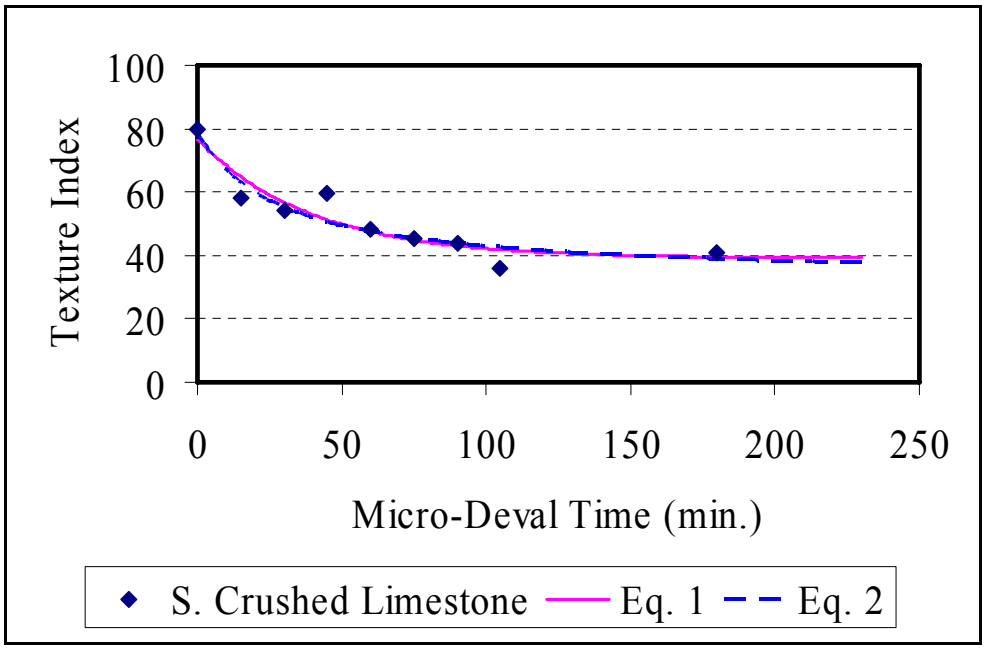

Figure 6.11. Equations 6.1 and 6.2 Fitting Plots for Soft Crushed Limestone.

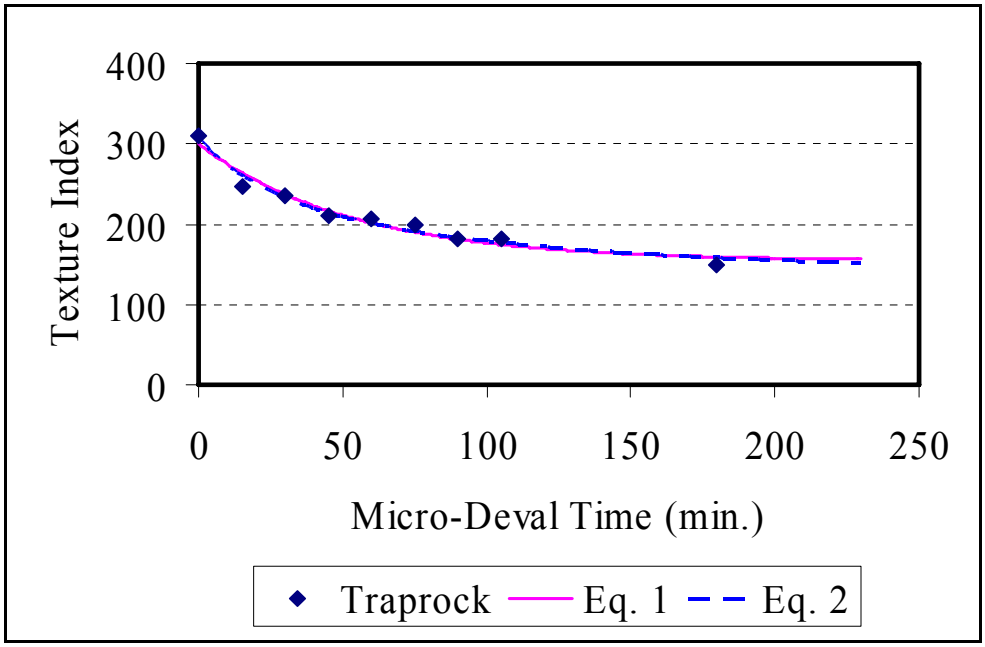

Figure 6.12. Equations 6.1 and 6.2 Fitting Plots for Traprock.

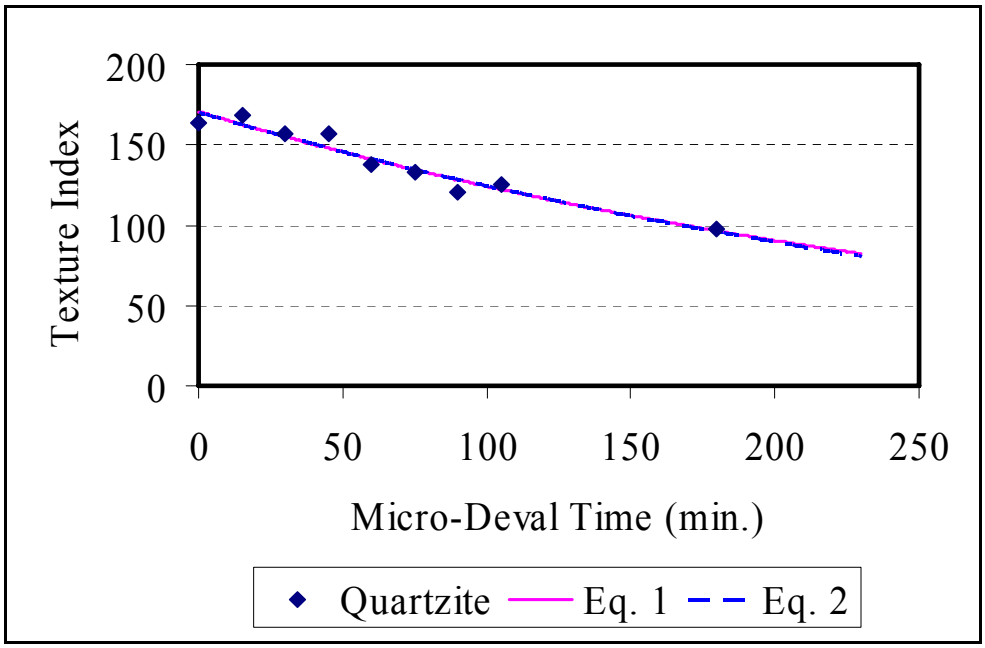

Figure 6.13. Equations 6.1 and 6.2 Fitting Plots for Quartzite.

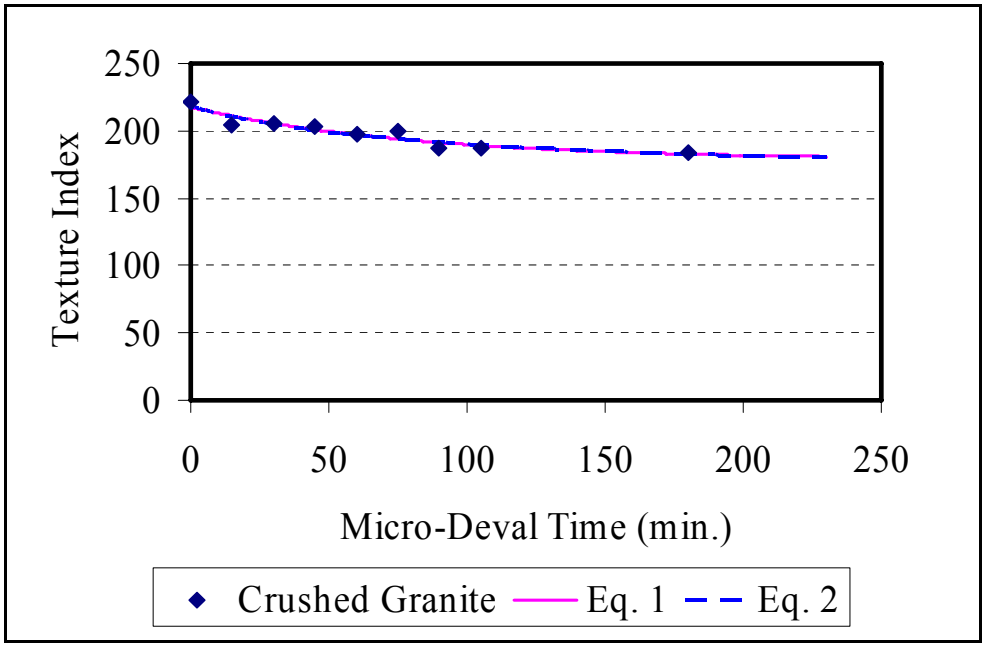

Figure 6.14. Equations 6.1 and 6.2 Fitting Plots for Crushed Granite.

All the analysis discussed above was conducted using 9 data points including the aggregate texture before polishing. Further analysis was conducted to determine whether similar results can be obtained by using only three data points (0, 105 min, and 180 min). The comparisons between the data fitting using Equation 6.1 for all nine points and for only three points are shown in Figures 6.15, 6.16, 6.17, 6.18, 6.19, and 6.20. The results in these Figures show that using only three points gives a fitting function similar to that obtained using nine data points. The standard error values for the three parameters in the two analysis cases (nine and three points) are given in Table 6.6.

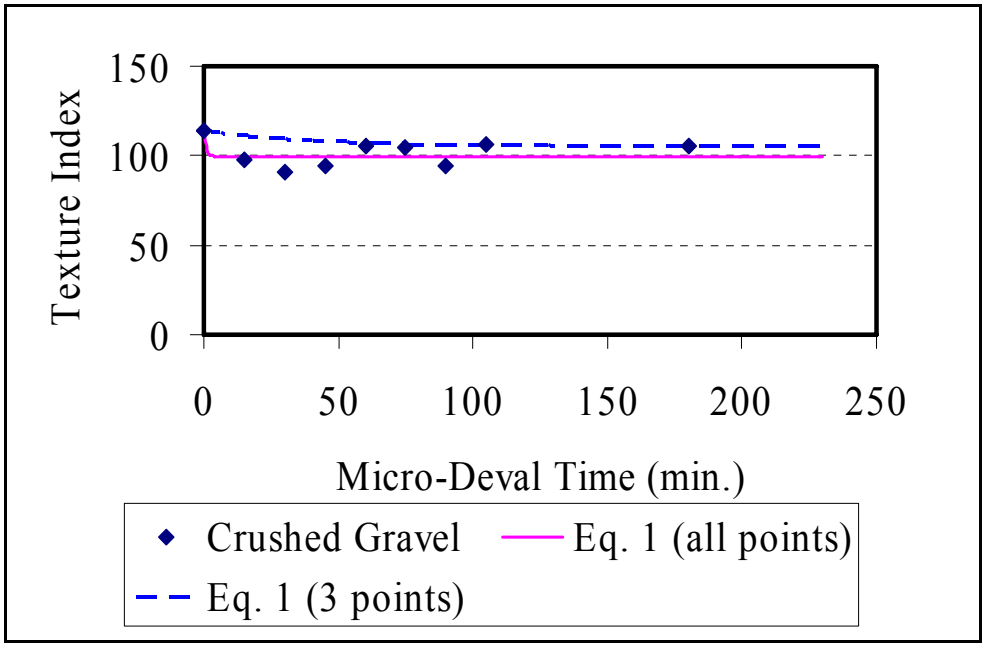

Figure 6.15. Fitting of Equation 1 to Experimental Measurements Using Three and Nine Data Points for Crushed Gravel.

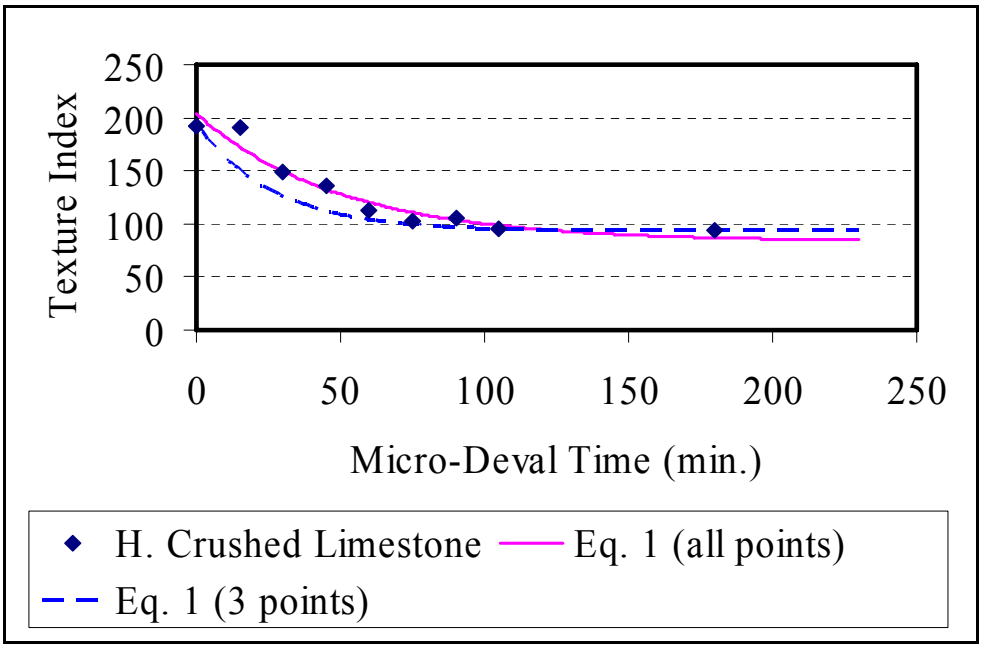

Figure 6.16. Fitting of Equation 1 to Experimental Measurements Using Three and Nine Data Points for Hard Crushed Limestone.

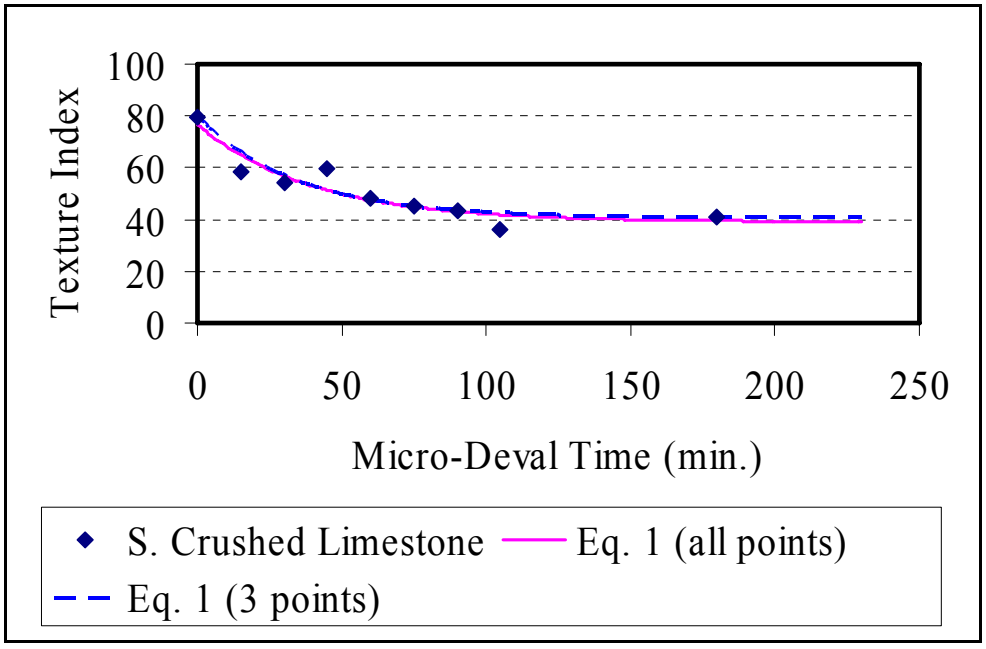

Figure 6.17. Fitting of Equation 1 to Experimental Measurements Using Three and Nine Data Points for Soft Crushed Limestone.

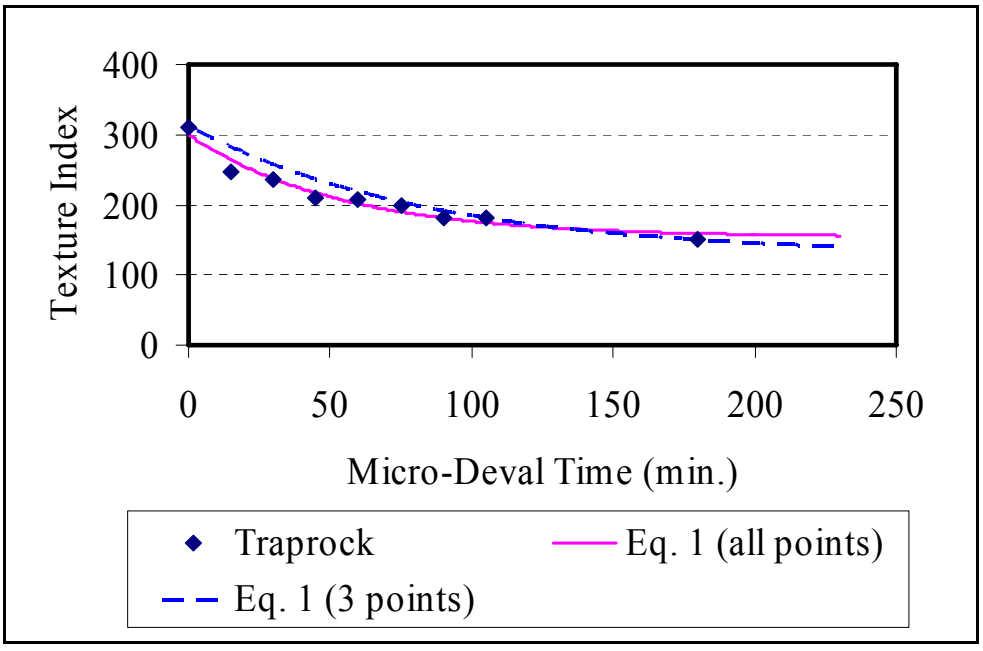

Figure 6.18. Fitting of Equation 1 to Experimental Measurements Using Three and Nine Data Points for Traprock.

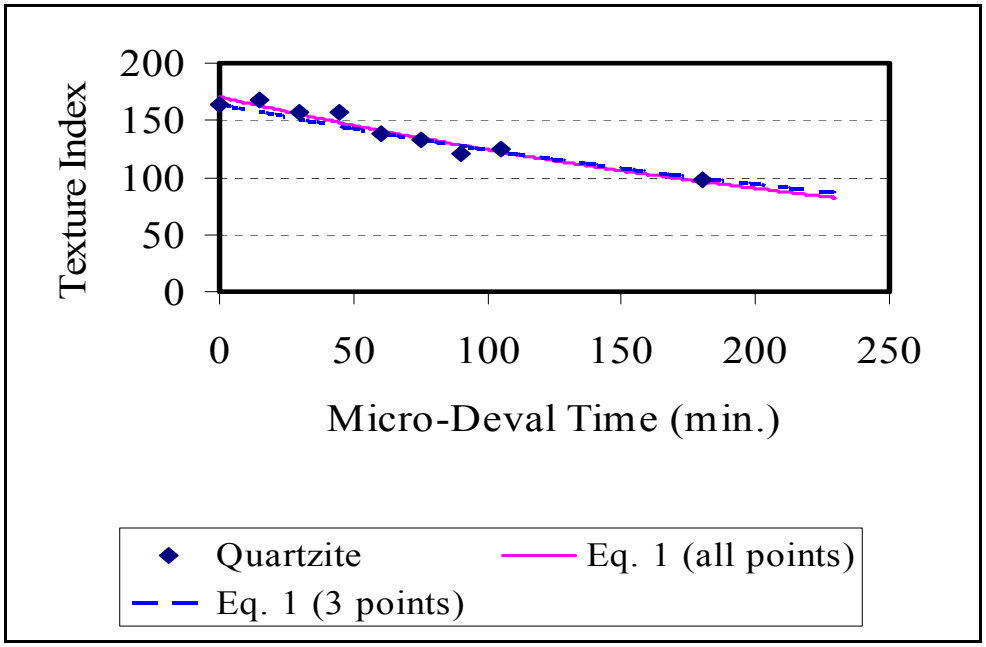

Figure 6.19. Fitting of Equation 1 to Experimental Measurements Using Three and Nine Data Points for Quartzite.

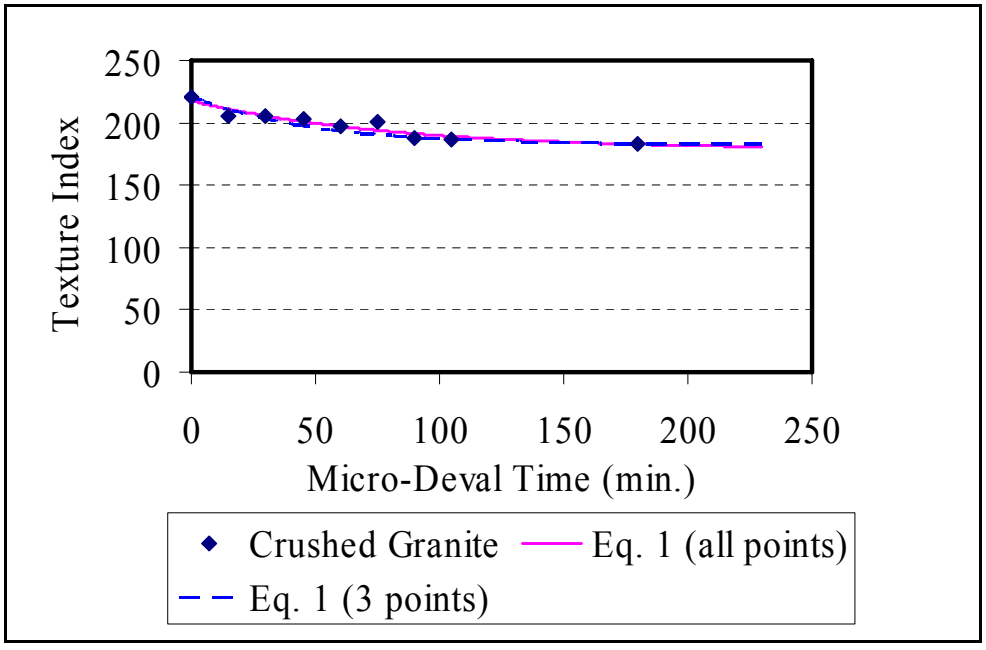

Figure 6.20. Fitting of Equation 1 to Experimental Measurements Using Three and Nine Data Points for Crushed Granite.

Table 6.6. Standard Errors of Equation 1 Parameters.

Aggregate Number	Parameter "a" standard error	Parameter "b" standard error	Parameter "c" standard error
	All points (Three Points)	All points (Three Points)	All points (Three Points)
1	2.44 (9.85)	7.32 (13.20)	0.00 (0.11)
2	11.50 (14.00)	12.56 (23.07)	0.01 (0.02)
3	4.72 (4.30)	5.92 (5.98)	0.01 (0.01)
4	12.64 (41.47)	13.44 (38.47)	0.00 (0.01)
5	N/A (N/A)	3.68 (4.40)	0.00 (0.00)
6	8.49 (5.79)	7.92 (6.48)	0.01 (0.01)

Figure 6.21 shows a comparison between the Micro-Deval weight loss and the texture loss. It is interesting to note that there is no unique relationship for all aggregates. This finding indicates that weight loss cannot be correlated to texture loss using the same relationship for all aggregates. Figure 6.22 presents the plot of only aggregates 2 and 6, and it is obvious how the magnitude of weight loss is not an indicator of texture loss. For example at 8 percent weight loss aggregate 6 lost around 15 percent of its texture, while aggregate 2 lost 30 percent of texture.

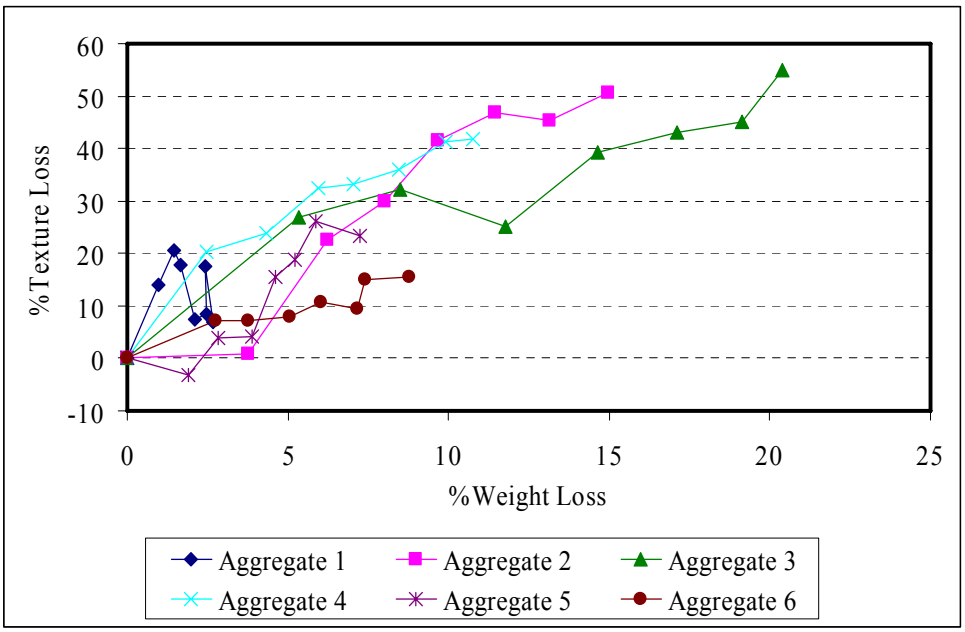

Figure 6.21. Comparison between Weight Loss and Texture Loss (All Aggregates).

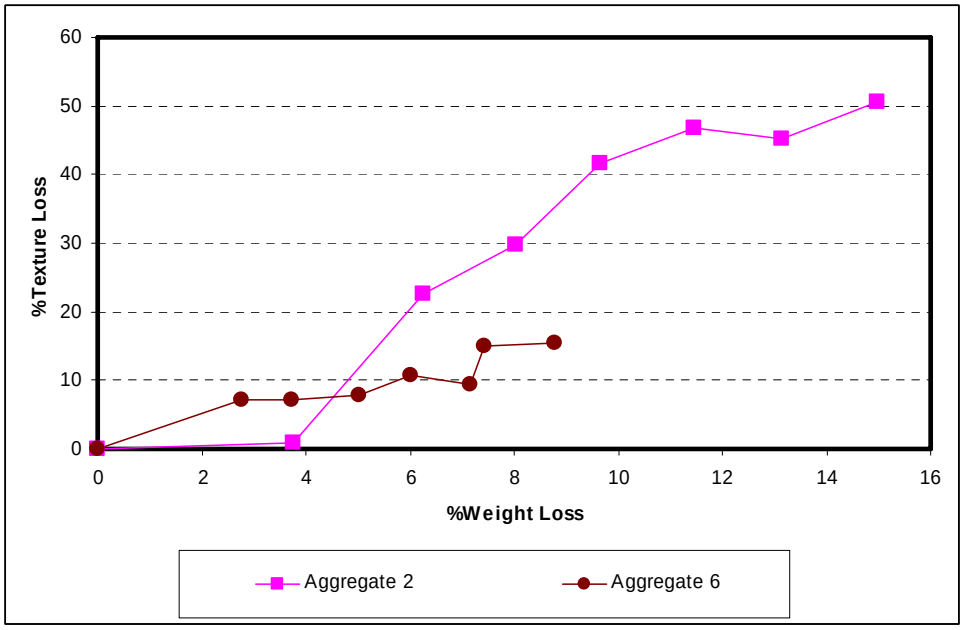

Figure 6.22. Comparison between Weight Loss and Texture Loss (Aggregates 2 and 6).

A METHODOLOGY FOR MEASURING AGGREGATE RESISTANCE TO ABRASION AND BREAKAGE

Aggregate abrasion is defined in this study as the aggregate loss of its surface angularity. In the Micro-Deval test, aggregates are subjected to both abrasion and breakage, and both of these mechanisms are associated with weight loss. Visual inspection of aggregates after Micro-Deval testing indicated that some of the aggregates were only abraded, while others experienced breakage with minimal change in their surface angularity. In this section, a procedure is developed to distinguish between aggregate breakage and abrasion. This procedure consists of three steps: (1) measure aggregate initial angularity, (2) test the aggregate in the Micro-Deval, and (3) measure its angularity and weight loss after the Micro-Deval.

A comparison between angularity before and after the Micro-Deval is shown in Figure 6.23. This plot is a good source of information on how angularity changes as a result of abrasion in the Micro-Deval. Figure 6.23 also shows that AIMS is capable of detecting changes in angularity, as all aggregates plot to the right of the equality line indicating loss of angularity or abrasion.

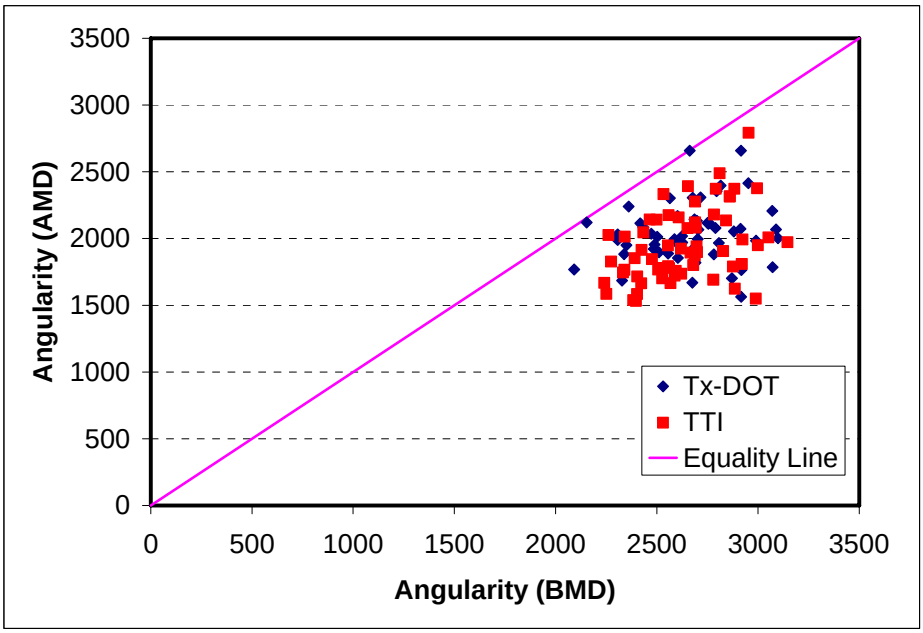

Figure 6.23. Comparing Aggregate Angularity before and after Micro-Deval.

The percent change in angularity is plotted against Micro-Deval weight loss (aggregate passing sieve #16) in Figure 6.24 to distinguish between abrasion and breakage. Aggregates with high weight loss but low angularity loss experienced high breakage and low abrasion. Aggregates that had high angularity loss and high weight loss encountered both high abrasion and high breakage. On the other hand, low values of weight loss and angularity loss were associated with low abrasion and breakage. Finally, aggregates with high angularity loss but low weight loss had high abrasion and low breakage.

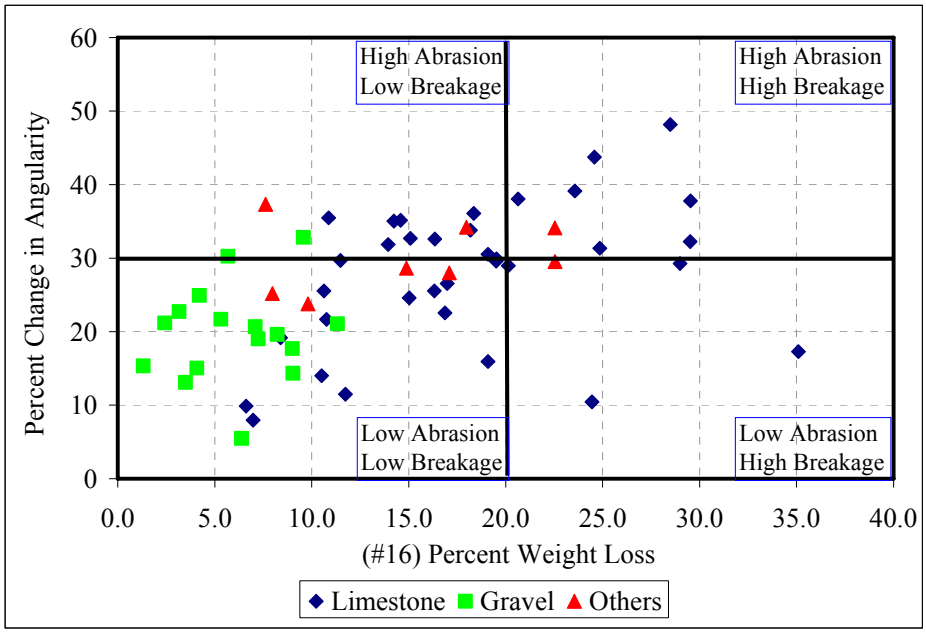

Figure 6.24. Percent Weight Loss (#16) against Percent Angularity Change.

It can be argued that the use of Micro-Deval weight loss is not a good indicator for breakage as it only includes the loss of aggregates smaller than the #16 sieve. Therefore, it was decided to explore whether the use of weight loss of particles passing the #4 sieve would change the relationship in Figure 6.24. It was found that excellent correlation exists between loss of aggregates passing the #16 sieve and aggregates

passing the #4 sieve (see Figure 6.25). Of course, the weight of aggregates passing the #4 sieve would be expected to be larger than the weight passing the #16 sieve, and this would shift the angularity loss versus weight loss relationship in Figure 6.26 compared to Figure 6.24. It is recommended to use loss of weight passing sieve #16 in accordance to the current Micro-Deval test procedure, and to avoid adding an unnecessary extra step to the test.

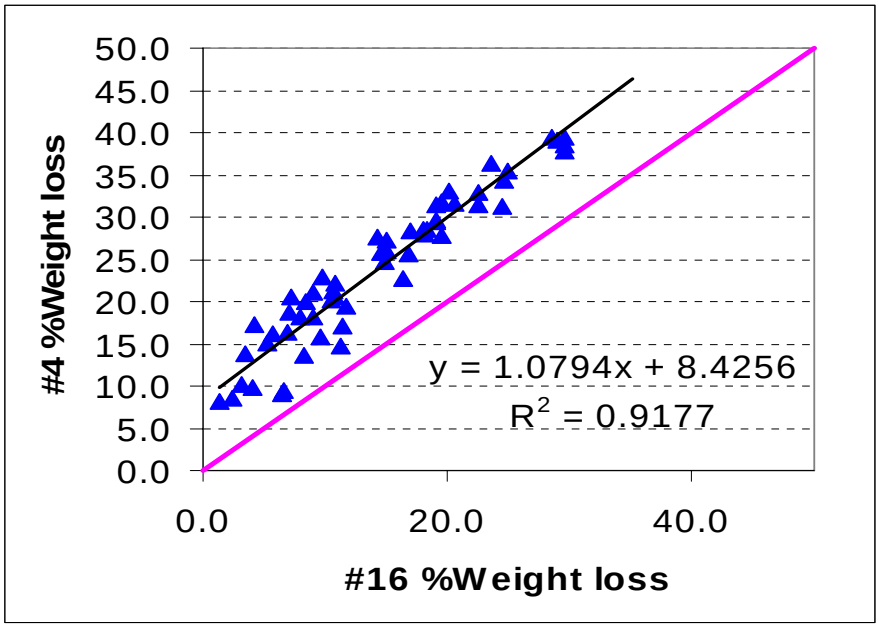

Figure 6.25. Correlation between #4 Percent Weight Loss and #16 Percent Weight Loss.

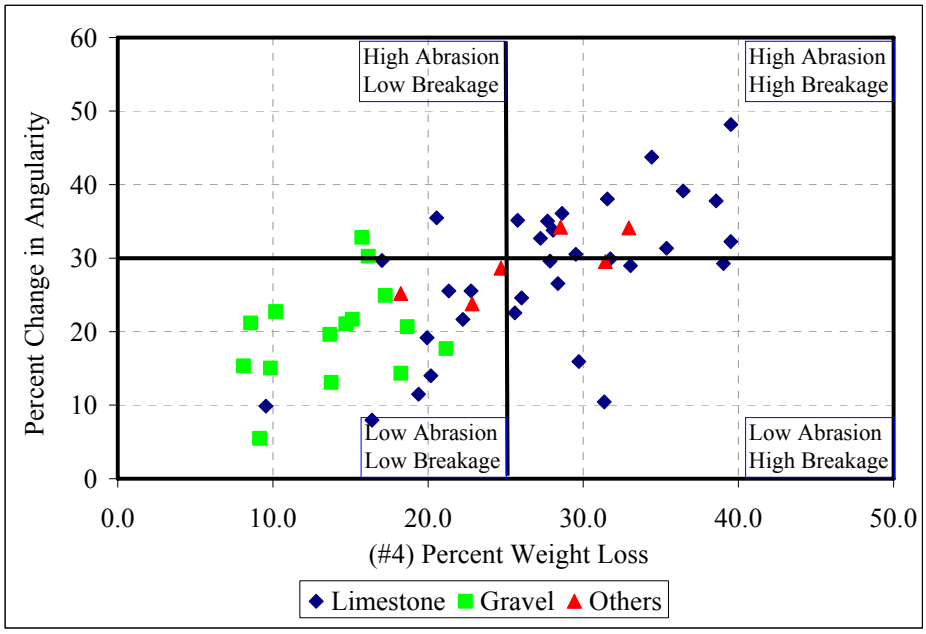

Figure 6.26. Percent Weight Loss (#4) against Percent Angularity Change.

SUMMARY

This chapter included the development of a methodology for measuring aggregate resistance to polishing. The methodology relies on measuring aggregate texture using AIMS before and after polishing in the Micro-Deval.

The results indicated the capability of the Micro-Deval to polish aggregates until they reach their final texture condition. An analytical procedure was also developed to analyze the loss of texture as a function of polishing time. This procedure allows for estimating the initial texture, the rate of texture loss, and the final texture. These factors should be considered when aggregate characteristics are related to pavement frictional or skid resistance.

A new methodology was also developed for measuring aggregate resistance to abrasion and breakage. The Micro-Deval was found to cause both aggregate abrasion and breakage. Plotting percent change in angularity, which is a measure of abrasion versus weight loss, made it possible to distinguish between aggregate abrasion and

degradation. It was also found that weight loss defined as weight passing sieve #16 is correlated with weight loss defined as weight passing the #4 sieve. The use of weight loss passing the #16 sieve is recommended to avoid adding an extra step to the test.

The procedure is useful if one is interested in determining aggregate resistance to abrasion and/or breakage. This procedure will be valuable for determining whether aggregates used during the mix design would be different than those used in the field due to abrasion and/or breakage in the plant and under compaction. Also, the procedure would be useful to select aggregates that can be used in mixes that rely heavily on stone-to-stone contacts. If one is interested in the effect of angularity on performance, then the initial angularity should also be taken into consideration. Some aggregates can have high loss of angularity, but their initial angularity is high enough to warrant acceptable remaining angularity for performance. However, the high loss of angularity of these aggregates remains a concern for changes in mix design irrespective of their contribution to mix performance.

CHAPTER VII
CONCLUSIONS AND RECOMMENDATIONS

CONCLUSIONS

This study focused on providing support for the implementation of the aggregate imaging system in TxDOT operations. The following points summarize the main efforts undertaken in this study and the main conclusions:

- Detailed statistical analyses were conducted to compare the AIMS measurements collected at the TxDOT and TTI laboratories. All statistical analysis methods supported the main finding that measurements from the two AIMS units were not statistically different. The texture measurements on polishing coupons were also compared. The two AIMS units scanned the same exact coupons. More than 80 percent of samples were not statistically different when measured using the two AIMS units.
- There was excellent correlation between the measurements of the two Micro-Deval machines at TTI and TxDOT. The results from the two machines are not different statistically.
- A database of aggregate properties was developed based on the measurements conducted at TxDOT and TTI. The database includes the following test results:
- AIMS measurements of texture, angularity and shape (sphericity). Tests were conducted according to procedures published in TxDOT implementation report 5-1707-01-1;
    - ❖ Crushed face count of coarse aggregates (Tex-460-A);
    - ❖ Flat and elongated particles (Tex-280-F);
    - ❖ Flakiness index (Tex-224-F);
    - ❖ Micro-Deval weight loss (Tex-461-A);
    - ❖ Los Angeles Abrasion (Tex-410-A);
    - ❖ Magnesium sulfate soundness (Tex-411-A); and
    - ❖ British polish value (Tex-438-A).

- The database was further used to compare the AIMS units that are in use at the TTI and DOT laboratories. The comparison between the two AIMS units confirmed the findings in Chapter 3 that the two AIMS units provide very similar results.
- The correlation between percent loss due to Micro-Deval and magnesium sulfate soundness was assessed. Moderate correlation was found between these tests.
- The results from the accelerated polishing test were analyzed and it was found that the majority of the residual PV measurement fell within a very small range. The small range of PV measurements makes it difficult to distinguish between aggregates.
- The AIMS angularity analysis method was improved in order to reduce the variability in the measurements within the same aggregate source. The new method was found to have a much smaller coefficient of variation than the previous method.
- The texture analysis method was also enhanced in order to increase the sensitivity of the method to fine texture (smaller scale texture). The texture levels used in the new AIMS analysis are more in agreement with the previous experience of aggregate performances in pavement surfaces.
- The AIMS aggregate classification method was revised based on the data collected on the TxDOT aggregates. The new limits were used to determine the percentage of particles in an aggregate sample that fall into the low, medium and high categories for each of the shape characteristics (texture, angularity and sphericity). Also, new limits were calculated in order to classify an aggregate sample based on the average measured properties. The limits were selected based on quartile analysis of the data such that 25 percent of the aggregates belong to the low category, 50 percent of the aggregates belong to the medium category, and the remaining 25 percent belong to the high category.

- A new method for aggregate classification was developed for use as part of the Wet Weather Accident Reduction Program. This method relies on AIMS texture measurements and magnesium sulfate soundness. This method allows for direct measurement of aggregate wear resistance and terminal texture. This method is also more sensitive than the current method and it relies on the average aggregate texture as well as the variation of texture in an aggregate sample. The new method was found to change the classifications of some the aggregates compared with the current method. However, none of the aggregates was found to change from A to C, B to D, or vice versa. All changes shifted an aggregate sample from one category to either one of its adjacent categories. The classification limits used in this proposed method are not supported by performance data, and future research should focus on accurate determination of these limits.
- A new method was developed for measuring aggregate resistance to abrasion and breakage. The methodology relies on measuring aggregate angularity using AIMS before and after abrasion in the Micro-Deval, in addition to the weight loss percent in the Micro-Deval. The Micro-Deval was found to cause both aggregate abrasion and breakage. Plotting percent change in angularity (abrasion measure) versus weight loss made it possible to distinguish between aggregate abrasion and breakage. The new methodology for measuring aggregate resistance to abrasion and breakage can be used in the selection of aggregates for mixes that rely on stone-to-stone contacts, and in the assessment of changes in aggregates characteristics during mix production and compaction.

RECOMMENDATIONS

- The reproducibility of AIMS measurements using more than two units should be studied.
- The limits used in the new method for classification of aggregates as part of the WWARP should be further examined based on the performance of aggregates in asphalt pavement in terms of skid resistance.
- It is also recommended to implement the new developed methods for measuring aggregate resistance to polishing, abrasion, and breakage in routine operations of TxDOT testing and specifications.

REFERENCES

1. Abdul-Malak, M., D. Fowler, and C. Constantino, (1996). "Aggregate Characteristics Governing Performance of Seal Coat Highway Overlays." *Transportation Research Record* 1547, Transportation Research Board, Washington, D.C., 15-22.

2. Al-Rousan, T.M. (2004). "Characterization of Aggregate Shape Properties Using a Computer Automated System." PhD Dissertation, Texas A&M University, College Station, Texas.

3. Bathina, M. (2005). "Quality Analysis of the Aggregate Imaging System (AIMS) Measurements." MS Thesis, Texas A&M University, College Station, Texas.

4. Bloem, D. (1971). "Skid Resistance—The role of Aggregates and Other Factors." *National Sand and Gravel Association Circular* 109, Silver Spring, Maryland, 1-30.

5. Cooley, L. Jr., and R. James, (2003). "Micro-Deval Testing of Aggregates in the Southeast." *Transportation Research Record* 1837, Transportation Research Board, Washington, D.C., 73-79.

6. Crouch, L., and T. Dunn, (2005). "Identification of Aggregates for Tennessee Bituminous Surface Courses." Tennessee Department of Transportation TDOT *Project Number TNSPR-RES1149, Final Report*, Cookeville, Tennessee.

7. Crouch, L., H. Sauter,, G. Duncan, and W. Goodwin, (2001). "Polish Resistance of Tennessee Bituminous Surface Aggregates." *ASTM Special Technical Publication* 1412, American Society for Testing and Materials, 185-199.

8. Crouch, L., G. Shirley, G. Head, and W. Goodwin, (1996). "Aggregate Polishing Resistance Pre-Evaluation." *Transportation Research Record* 1530, Transportation Research Board, Washington, D.C., 103-110.

9. Crouch, L., J. Gothard, G. Head, and W. Goodwin, (1995). "Evaluation of Textural Retention of Pavement Surface Aggregates." *Transportation Research Record* 1486, Transportation Research Board, Washington, D.C., 124-129.

10. Dahir, S. (1979). "A Review of Aggregate Selection Criteria for Improved Wear Resistance and Skid Resistance of Bituminous Surfaces." *Journal of Testing and Evaluation,* 7, 245-253.

11. Forster, S. (1989). "Pavement Microtexture and Its Relation to Skid Resistance." *Transportation Research Record* 1215, Transportation Research Board, Washington, D.C., 151-164.

12. Gatchalian, D. (2005). "Characterization of Aggregate Resistance to Degradation in Stone Matrix Asphalt Mixtures." MS Thesis, Texas A&M University, College Station, Texas.

13. Henry, J., and S. Dahir, (1979). "Effects of Textures and the Aggregates that Produce them on the Performance of Bituminous Surfaces." *Transportation Research Record* 712, Transportation Research Board, Washington, D.C., 44-50.

14. Hogervorst, D. (1974). "Some Properties of Crushed Stone for Road Surfaces." *Bulletin of The International Association of Engineering Geology* 10, 59-64.

15. Hunt, E. (2001). "Micro-Deval Coarse Aggregate Test Evaluation." Oregon Department of Transportation ODOT *Report OR-RD-01-13 Final Report,* Salem, Oregon.

16. Kandhal, P., and F. Parker, Jr. (1998). "Aggregate Tests Related to Asphalt Concrete Performance in Pavements." *National Cooperative Highway Research Program Report* 405, Transportation Research Board, National Research Council, Washington, D.C.

17. Kandhal, P., F. Parker, Jr., and E. Bishara, (1993). "Evaluation of Alabama Limestone Aggregates for Asphalt Wearing Courses." *Transportation Research Record* 1418, Transportation Research Board, Washington, D.C., 12-21.

18. Lane, B., C. Rogers, and S. Senior, (2000). "The Micro-Deval Test for Aggregates in Asphalt Pavement." Presented at the *8th Annual Symposium of International Center for Aggregate Research*, Denver, Colorado.

19. Lingras, P. and X. Huang, (2005). "Statistical, Evolutionary, and Neurocomputing Clustering Techniques: Cluster-Based vs Object-Based Approaches." *Artificial Intelligence Review*, Vol. 23, Issue 1, 3.

20. Masad, E., T. Al-Rousan, J. Button, D. Little, and E. Tutumluer, (2005). "Test Methods for Characterizing Aggregate Shape, Texture, and Angularity" *National Cooperative Highway Research Program NCHRP Project 4-30A Final Report*, Washington, D.C.

21. McGahan, J. (2005). "The Development of Correlations between HMA Pavement Performance and Aggregate Shape Properties." MS Thesis, Texas A&M University, College Station, Texas.

22. Meininger, R. (2004). "Micro-Deval vs. L.A. Abrasion." *Rock Products* 107, 33-35.

23. Mullen, W., S. Dahir, and B. Barnes, (1971). "Two Laboratory Methods for Evaluating Skid-Resistance Properties of Aggregates." *Highway Research Record* 37, 123-135.

24. Nitta, N., K. Saito, and S. Isozaki, (1990). "Surface Characteristics of Roadways: International Research and Technologies." *ASTM Special Technical Publication* 1031, American Society for Testing and Materials, 113-126.

25. Perry, M., A. Woodside, W. Woodward, (2001). "Observations on Aspects of Skid-Resistance of Greywacke Aggregate." *Quarterly Journal of Engineering Geology and Hydrology* 34, 347-352.

26. Prowel, B. D., J. Zhang, and E.R. Brown, (2005). "Aggregate Properties and the Performance of Superpave-Designed Hot Mix Asphalt." *National Cooperative Highway Research Program Report* 539, Transportation Research Board, National Research Council, Washington, D.C.

27. Rogers, C. (1998). "Canadian Experience with the Micro-Deval Test for Aggregates." *Advances in Aggregates and Armourstone Evaluation* 13, 139-147.

28. Senior, S. and C. Rogers, (1991). "Laboratory Tests for Predicting Coarse aggregate Performance in Ontario." *Transportation Research Record* 1301, Transportation Research Board, Washington, D.C., 97-106.

29. Smith, B., and G. Fager, (1991). "Physical Characteristics of Polish Resistance of Selected Aggregates." *Transportation Research Record* 1301, Transportation Research Board, Washington, D.C., 117-126.

30 Won, M., and C. Fu, (1996). "Evaluation of Laboratory Procedures for Aggregate Polish Test." *Transportation Research Record* 1547, Transportation Research Board, Washington, D.C., 23-28.

31 Wu, Y., F. Parker, and P. Kandhal (1998). "Aggregate Toughness/Abrasion Resistance and Durability/Soundness Tests Related to Asphalt Concrete Performance in Pavements." *Transportation Research Record* 1638, Transportation Research Board, Washington, D.C., 85-93.

APPENDIX A

ESTIMATED MEANS AND STANDARD ERRORS

Aggregate Particles

Texture

Combined Data	TxDOT		TTI	
Aggregate	$\overline{X}$	**σ**	$\overline{X}$	**σ**
1	87	4.369957	85.78571	4.0975
2	97.96429	4.3214	89.71429	4.036317
3	98.44643	3.976485	90.96429	3.309351
4	102.8214	3.130676	100.006	2.822416
5	132.2976	6.13047	137.1607	6.924273
6	71.16071	2.56208	72.4881	2.623592
7	125.9583	4.601192	128.0655	4.68568
8	79.07143	2.967479	81.13095	3.170636
9	166.1548	5.991713	148.4345	5.490775
10	117.5833	2.569943	111.1786	2.807015

#4 Size	TxDOT		TTI	
Aggregate	$\overline{X}$	**σ**	$\overline{X}$	**σ**
1	81.14286	7.328225	77.85714	5.467105
2	87.25	8.130081	76.07143	5.733693
3	83.14286	6.28048	75.73214	4.605579
4	96.80357	5.782723	99.69643	5.099142
5	118.9643	9.131505	119.8393	9.398217
6	58.78571	4.128434	65.96429	3.808139
7	101.7857	6.95345	102.0536	5.061403
8	61.44643	3.370028	71.32143	4.519518
9	163.875	11.26805	140.625	10.32324
10	115.5357	4.147755	110.9821	5.390015

1/4" Size	TxDOT		TTI	
Aggregate	$\overline{X}$	**σ**	$\overline{X}$	**σ**
1	93.51786	8.150133	92.76786	7.115284
2	100.4821	6.075285	82.53571	6.33886
3	98.01786	6.285599	90.57143	5.076612
4	108.5714	5.099329	101.4107	5.145909
5	147.7143	12.81957	149.6607	14.06315
6	65.66071	2.471431	66.85714	3.463486
7	133.6429	8.742471	134.7679	9.749525
8	70.28571	4.106592	68.98214	3.109004
9	168.9643	8.635962	144.5179	7.849766
10	116.0536	4.491942	114.9464	4.796605

3/8" Size	TxDOT		TTI	
Aggregate	$\overline{X}$	**σ**	$\overline{X}$	**σ**
1	86.33929	7.240187	86.73214	8.388981
2	106.1607	7.979754	110.5357	7.946328
3	114.1786	7.504808	106.5893	6.642092
4	103.0893	5.345606	98.91071	4.474624
5	130.2143	9.326603	141.9821	11.91315
6	89.03571	5.243918	84.64286	5.671496
7	142.4464	7.171232	147.375	7.708848
8	105.4821	5.679708	103.0893	6.948478
9	165.625	11.19063	160.1607	10.12672
10	121.1607	4.735935	107.6071	4.384423

Angularity

Combined Data	**TxDOT**		**TTI**	
Aggregate	$\overline{X}$	**σ**	$\overline{X}$	**σ**
1	1711.16	72.80331	1561.809	61.42769
2	1906.381	75.13533	1755.364	78.72513
3	1991.437	88.23072	1678.677	69.57869
4	1826.684	87.01019	1611.032	73.32052
5	2244.948	78.66324	2235.911	86.7982
6	2721.797	84.07584	2389.612	82.00073
7	2506.474	92.07075	2249.302	79.23181
8	2705.053	93.62201	2491.412	92.19736
9	2642.442	86.91391	2558.39	86.86291
10	2414.389	86.90446	2261.021	85.6606

#4 Size	**TxDOT**		**TTI**	
Aggregate	$\overline{X}$	**σ**	$\overline{X}$	**σ**
1	1519.953	108.1026	1428.536	94.42703
2	1681.689	120.5955	1471.738	106.4672
3	1686.712	123.8221	1549.088	112.2663
4	1591.276	125.5387	1523.967	104.3966
5	2226.19	132.9655	2089.579	138.1625
6	2440.186	137.5143	2210.119	144.6464
7	2164.916	129.6707	2062.447	118.8924
8	2241.268	130.4764	2168.94	137.8082
9	2418.078	135.459	2347.757	115.3158
10	2250.313	163.64	2148.842	142.2363

1/4" Size	TxDOT		TTI	
Aggregate	$\overline{X}$	**σ**	$\overline{X}$	**σ**
1	1792.197	114.2936	1647.533	115.2003
2	1884.615	124.786	1818.316	150.0946
3	2012.197	166.2619	1652.556	113.9799
4	1788.176	139.8855	1692.741	128.4724
5	2255.336	126.3916	2403.009	153.4569
6	2869.138	154.186	2506.476	140.314
7	2502.458	155.3485	2533.601	150.2915
8	2825.931	150.3462	2647.113	150.7583
9	2699.375	158.9219	2618	169.7125
10	2470.303	131.9993	2275.423	159.1191

3/8" Size	TxDOT		TTI	
Aggregate	$\overline{X}$	**σ**	$\overline{X}$	**σ**
1	1821.33	150.0903	1609.359	108.1049
2	2152.84	138.845	1976.039	142.0254
3	2275.403	157.3975	1834.387	133.211
4	2100.601	176.7376	1616.39	145.9658
5	2253.317	150.6715	2215.146	158.3809
6	2856.067	139.7926	2452.24	140.48
7	2852.049	178.8228	2151.857	134.848
8	3047.961	184.1179	2658.183	181.3123
9	2809.873	154.0166	2709.413	159.1967
10	2522.55	154.3842	2358.798	144.5119

Aggregate Coupons

Texture

Coupons	TxDOT		TTI	
Aggregate	$\overline{X}$	**σ**	$\overline{X}$	**σ**
05-0009	189.9412	7.892186	191.8917	7.414525
05-0017	191.6239	7.742266	196.3417	7.244765
05-0020	203.9381	7.132993	199.1417	7.491221
05-0041	117.7727	4.350306	186.5417	5.503766
05-0048	182.8417	7.509219	172.6167	6.790999
05-0093	137.1333	6.782474	134.275	6.167469
05-0109	126.9667	7.56453	127.2521	6.692278
05-0129	198.675	7.604069	179.8583	8.158714
05-0143	161.275	6.497144	165.6	6.840606
05-0149	214.2333	8.148626	194.3417	6.327671
05-0151	194.9496	7.063724	191.325	6.388706
05-0178	145.9833	7.205769	147.4583	6.835296
05-0213	144.4417	6.290291	154.0667	5.188286
05-0216	109.275	5.962065	111.125	4.951198
05-0231	186.7	7.830618	181.325	7.571001
05-0235	185.513	8.45972	208.45	7.598152
05-0238	182.7311	6.611569	193.875	8.793719
05-0239	227.661	8.987146	219.7917	9.179511
05-0245	223.2035	8.852059	244.7917	9.180999
05-0247	237.4348	9.823699	238.05	9.181395
05-0251	191	5.978064	181.95	5.0777
05-0317	153.4505	6.05683	260.7167	7.673923
05-0320	318.5882	14.68651	331.3248	12.34344
05-0321	183.2167	6.56265	184.1417	7.376892
05-0337	218.3898	9.90563	223.275	9.644805
05-0338	202.4746	8.961267	197.25	8.368996
05-0347	108.55	5.82511	108.95	5.645154
05-0350	207.8583	6.81038	214.6167	6.304018
05-0365	172.5583	6.390083	180.4583	6.770693
05-0368	101.95	5.111513	106.8167	5.26075
05-0397	139.4333	6.290157	137.275	5.759756
05-0399	131.8583	6.282053	129.9417	5.517293
05-0493	103.8917	5.639556	112.5583	5.249741
05-0494	158.2417	6.473324	167.55	6.06713
05-0496	123.775	5.079955	128.175	5.185868
05-0519	192.1167	7.565153	200.7583	7.294006

Coupons	TxDOT		TTI	
Aggregate	$\overline{X}$	**σ**	$\overline{X}$	**σ**
05-0521	406.5519	15.83243	516.6833	19.44254
05-0532	222.9917	6.723423	229.0252	6.844189
05-0534	219.9	7.793433	209.2333	7.117302
05-0535	452.5392	15.27214	502.8958	13.28046
05-0543	181.0847	8.269257	200.8833	9.589744
05-0545	100.1083	4.804917	111.3727	5.247389
05-0630	160.05	4.735273	151.7667	4.844179
05-0643	158.55	6.90965	169.7667	6.714337
05-0649	115.8083	5.563918	116.3333	4.888839
05-0693	274.7155	12.08329	327.7227	12.84997
05-0708	193.7395	4.717458	168.9667	4.58123
05-0715	108.3333	5.307417	115.8333	4.89847
05-0716	100.1681	5.34788	115.6583	5.339083
05-0719	146.2333	6.469274	144.25	6.009065
05-768	164.0833	5.738166	165.675	4.936022
05-800	171.4833	7.801924	176.75	7.131284
05-921	109.6167	6.135323	135.125	6.913021
05-922	138.35	6.589086	145.2333	5.386878
05-995	85.26667	5.075311	95	5.303651
05-1002	210.3833	5.690872	206.2712	5.4987
05-1183	140.6083	7.11589	147.2333	6.655706
05-1184	242.4333	7.911412	232.4083	7.985443
05-1190	145.5	5.752116	140.775	5.027786
05-1201	144.35	7.42167	150.7583	6.205277
05-1207	135.8	6.426699	134.3917	6.012595
05-1210	131.1083	4.604997	131.5833	4.623281
05-1221	141.225	4.319675	136.05	4.555906
05-1222	153.9083	5.98944	145.375	4.4523
05-1223	137.6833	5.727788	138.8833	5.671964
05-1235	141.6	5.669954	145.1417	5.171042
05-1236	110.4917	6.099869	128.0167	5.936793
05-1260	117.7583	5.683851	132.8	5.536619
05-1262	195.8917	5.997266	197.5417	5.848075
05-1269	133.6917	5.140189	148.775	5.97459
05-1314	171.6	6.926307	177.9333	6.0776
05-1319	117.7667	5.864802	141.6667	5.560658
05-1360	123.2667	5.944641	121.9917	4.510888
06-0009	144.55	5.881306	151.4	6.147788
06-0086	112.175	5.986231	121.85	6.48739

APPENDIX B

CONFIDENCE INTERVALS

Aggregate Particles

Texture

Combined Data	TTI – TxDOT Confidence Interval		
Aggregate	**Lower Limit**	**Upper Limit**	**Center**
1	-12.9557	10.52708	-1.21429
2	-19.8399	3.339942	-8.25
3	-17.622	2.657752	-7.48214
4	-11.0771	5.446143	-2.81548
5	-13.2633	22.98946	4.863095
6	-5.8601	8.51486	1.327381
7	-10.7643	14.97862	2.107143
8	-6.45213	10.57118	2.059524
9	-33.6493	-1.79119	-17.7202
10	-13.8641	1.054562	-6.40476

#4 Size	TTI – TxDOT Confidence Interval		
Aggregate	**Lower Limit**	**Upper Limit**	**Center**
1	-21.2057	14.63432	-3.28571
2	-30.6777	8.320567	-11.1786
3	-22.6756	7.854124	-7.41071
4	-12.2184	18.00408	2.892857
5	-24.8085	26.55854	0.875
6	-3.82991	18.18706	7.178571
7	-16.5891	17.1248	0.267857
8	-1.1748	20.9248	9.875
9	-53.2026	6.702627	-23.25
10	-17.8839	8.776754	-4.55357

1/4" Size	TTI – TxDOT Confidence Interval		
Aggregate	**Lower Limit**	**Upper Limit**	**Center**
1	-21.9553	20.45535	-0.75
2	-35.1554	-0.73742	-17.9464
3	-23.2825	8.389686	-7.44643
4	-21.36	7.038607	-7.16071
5	-35.351	39.24382	1.946429
6	-7.14307	9.535924	1.196429
7	-24.5416	26.79158	1.125
8	-11.399	8.791856	-1.30357
9	-47.3204	-1.57241	-24.4464
10	-13.9873	11.77305	-1.10714

3/8" Size	TTI – TxDOT Confidence Interval		
Aggregate	**Lower Limit**	**Upper Limit**	**Center**
1	-21.3265	22.11221	0.392857
2	-17.6975	26.44747	4.375
3	-27.2323	12.05374	-7.58929
4	-17.8421	9.484999	-4.17857
5	-17.8864	41.42212	11.76786
6	-19.5325	10.74674	-4.39286
7	-15.7076	25.56477	4.928571
8	-19.9827	15.19703	-2.39286
9	-35.0454	24.11683	-5.46429
10	-26.2031	-0.90402	-13.5536

Angularity

Combined Data	TTI – TxDOT Confidence Interval		
Aggregate	**Lower Limit**	**Upper Limit**	**Center**
1	-336.052	37.35069	-149.351
2	-364.315	62.28066	-151.017
3	-532.996	-92.5255	-312.761
4	-438.667	7.363766	-215.652
5	-238.632	220.558	-9.03685
6	-562.374	-101.997	-332.185
7	-495.252	-19.0936	-257.173
8	-471.182	43.89846	-213.642
9	-324.894	156.7906	-84.0518
10	-392.537	85.8015	-153.368

#4 Size	TTI – TxDOT Confidence Interval		
Aggregate	**Lower Limit**	**Upper Limit**	**Center**
1	-372.747	189.9145	-91.4164
2	-525.252	105.3508	-209.951
3	-465.218	189.9692	-137.624
4	-387.327	252.7095	-67.3089
5	-512.445	239.2214	-136.612
6	-621.247	161.1127	-230.067
7	-447.283	242.346	-102.469
8	-444.291	299.6335	-72.3287
9	-418.996	278.3547	-70.3209
10	-526.431	323.4878	-101.472

1/4" Size	TTI – TxDOT Confidence Interval		
Aggregate	**Lower Limit**	**Upper Limit**	**Center**
1	-462.729	173.4005	-144.664
2	-448.876	316.2771	-66.2993
3	-754.737	35.45567	-359.641
4	-467.696	276.8264	-95.435
5	-241.987	537.3324	147.6725
6	-771.271	45.94633	-362.662
7	-392.51	454.7966	31.14304
8	-596.128	238.492	-178.818
9	-537.084	374.3346	-81.3748
10	-600.096	210.3371	-194.879

3/8" Size	TTI – TxDOT Confidence Interval		
Aggregate	**Lower Limit**	**Upper Limit**	**Center**
1	-574.512	150.5686	-211.972
2	-566.093	212.4901	-176.801
3	-845.172	-36.8613	-441.017
4	-933.484	-34.9386	-484.211
5	-466.629	390.2868	-38.1713
6	-792.266	-15.3875	-403.827
7	-1139.17	-261.216	-700.193
8	-896.253	116.6974	-389.778
9	-534.611	333.6911	-100.46
10	-578.227	250.7228	-163.752

Aggregate Coupons

Texture

Coupons	TTI – TxDOT Confidence Interval		
Aggregate	Lower Limit	Upper Limit	Center
05-0009	-19.2739	23.17484	1.95049
05-0017	-16.0647	25.50014	4.717735
05-0020	-25.0706	15.47782	-4.79639
05-0041	55.01865	82.51923	68.76894
05-0048	-30.0691	9.619073	-10.225
05-0093	-20.8263	15.1096	-2.85833
05-0109	-19.5104	20.08131	0.285434
05-0129	-40.6763	3.042956	-18.8167
05-0143	-14.1663	22.81631	4.325
05-0149	-40.1129	0.329562	-19.8917
05-0151	-22.2922	15.04299	-3.62458
05-0178	-17.9917	20.9417	1.475
05-0213	-6.35664	25.60664	9.625
05-0216	-13.3398	17.03976	1.85
05-0231	-26.7236	15.97359	-5.375
05-0235	0.649872	45.22404	22.93696
05-0238	-10.4199	32.70768	11.14391
05-0239	-33.0485	17.30976	-7.86935
05-0245	-3.40857	46.58483	21.58813
05-0247	-25.7395	26.96997	0.615217
05-0251	-24.4232	6.323234	-9.05
05-0317	88.10484	126.4276	107.2662
05-0320	-24.8655	50.33863	12.73655
05-0321	-18.4271	20.27715	0.925
05-0337	-22.2128	31.9831	4.885169
05-0338	-29.2571	18.80796	-5.22458
05-0347	-15.4989	16.29893	0.4
05-0350	-11.4308	24.9475	6.758333
05-0365	-10.3475	26.14753	7.9
05-0368	-9.51004	19.24338	4.866667
05-0397	-18.8748	14.55816	-2.15833
05-0399	-18.304	14.4707	-1.91667
05-0493	-6.4348	23.76813	8.666667
05-0494	-8.08096	26.69763	9.308333
05-0496	-9.82846	18.62846	4.4
05-0519	-11.9555	29.23884	8.641667

Coupons	TTI – TxDOT Confidence Interval		
Aggregate	Lower Limit	Upper Limit	Center
05-0521	60.98741	159.2754	110.1314
05-0532	-12.771	24.83804	6.033543
05-0534	-31.3531	10.01979	-10.6667
05-0535	10.68858	90.02466	50.35662
05-0543	-5.02029	44.61747	19.79859
05-0545	-2.68088	25.20967	11.26439
05-0630	-21.5606	4.993967	-8.28333
05-0643	-7.66715	30.10049	11.21667
05-0649	-13.992	15.04196	0.525
05-0693	18.4351	87.57924	53.00717
05-0708	-37.6615	-11.8841	-24.7728
05-0715	-6.65599	21.65599	7.5
05-0716	0.678886	30.30165	15.49027
05-0719	-19.2892	15.32252	-1.98333
05-768	-13.2437	16.42705	1.591667
05-800	-15.4506	25.9839	5.266667
05-921	7.392161	43.62451	25.50833
05-922	-9.79793	23.56459	6.883333
05-995	-4.65466	24.12132	9.733333
05-1002	-19.6224	11.3981	-4.11215
05-1183	-12.4721	25.72211	6.625
05-1184	-32.0572	12.00716	-10.025
05-1190	-19.6989	10.24887	-4.725
05-1201	-12.5527	25.36941	6.408333
05-1207	-18.6579	15.8412	-1.40833
05-1210	-12.3148	13.26477	0.475
05-1221	-17.4803	7.130284	-5.175
05-1222	-23.1608	6.094146	-8.53333
05-1223	-14.5994	16.99944	1.2
05-1235	-11.4991	18.58242	3.541667
05-1236	0.841506	34.20849	17.525
05-1260	-0.51045	30.59378	15.04167
05-1262	-14.7681	18.06811	1.65
05-1269	-0.36431	30.53098	15.08333
05-1314	-11.7275	24.39417	6.333333
05-1319	8.059511	39.74049	23.9
05-1360	-15.9012	13.35123	-1.275
06-0009	-9.82556	23.52556	6.85
06-0086	-7.6265	26.9765	9.675

APPENDIX C

CATEGORICAL PLOTS

Aggregate Particles

Texture

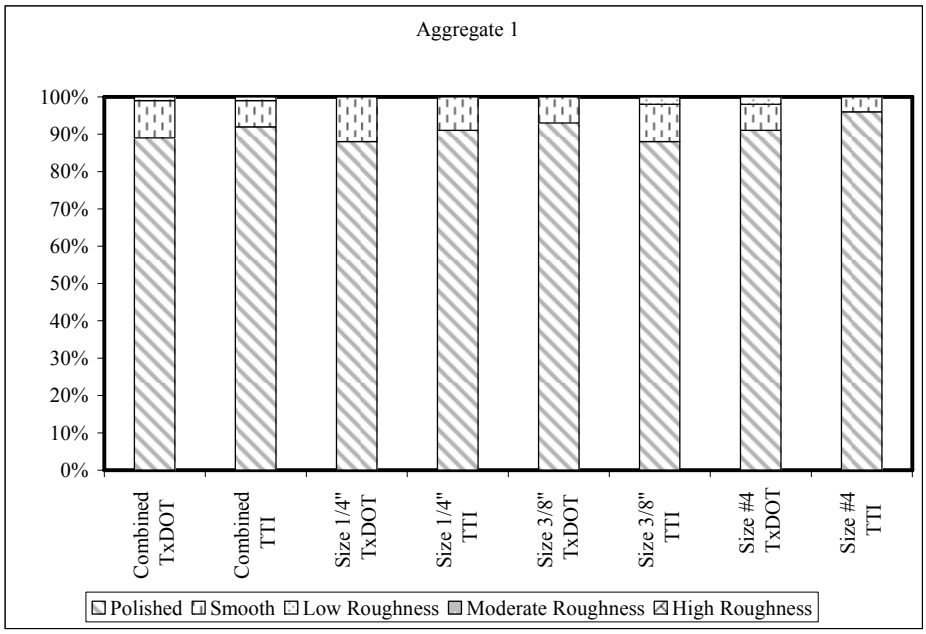

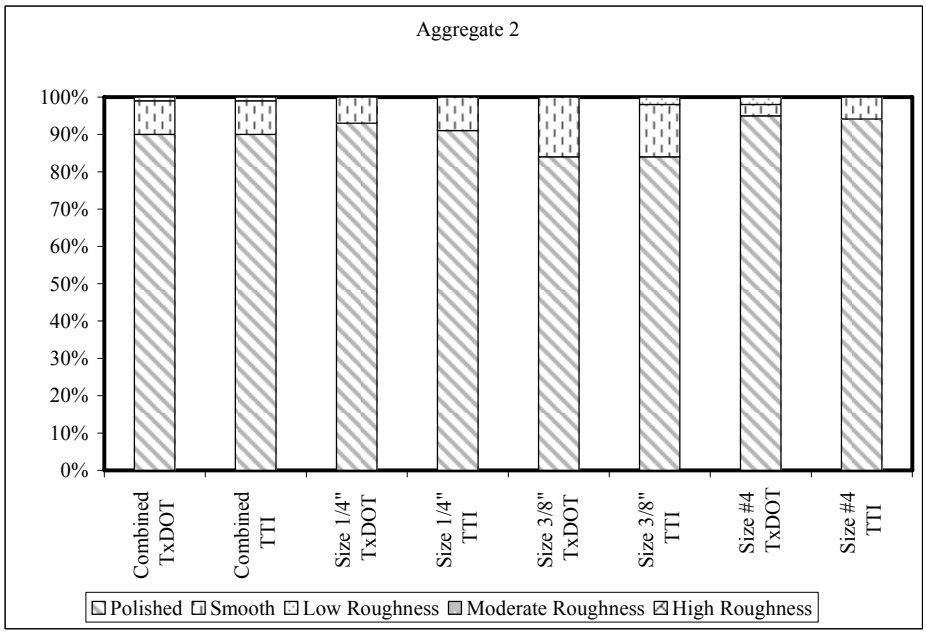

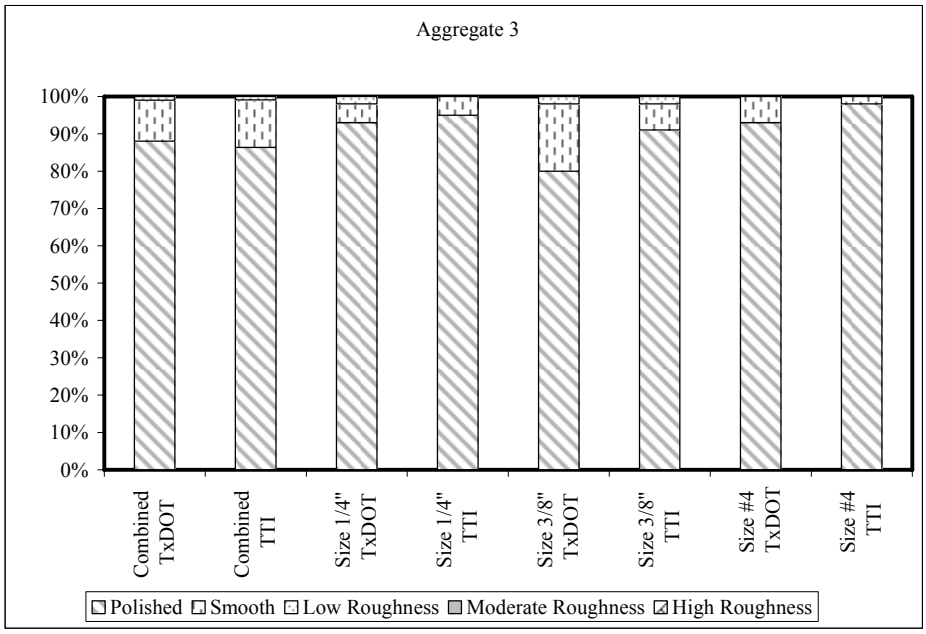
Aggregate 3
100%
90%
80%
70%
60%
50%
40%
30%
20%
10%
0%
Combined TxDOT
Combined TTI
Size 1/4" TxDOT
Size 1/4" TTI
Size 3/8" TxDOT
Size 3/8" TTI
Size #4 TxDOT
Size #4 TTI
Polished
Smooth
Low Roughness
Moderate Roughness
High Roughness

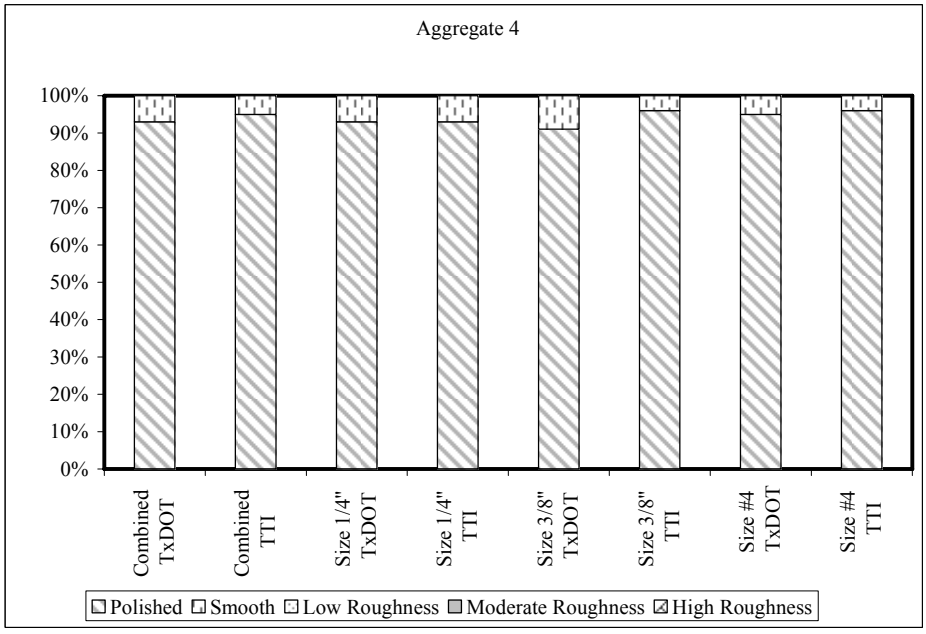
Aggregate 4
100%
90%
80%
70%
60%
50%
40%
30%
20%
10%
0%
Combined TxDOT
Combined TTI
Size 1/4" TxDOT
Size 1/4" TTI
Size 3/8" TxDOT
Size 3/8" TTI
Size #4 TxDOT
Size #4 TTI
Polished
Smooth
Low Roughness
Moderate Roughness
High Roughness

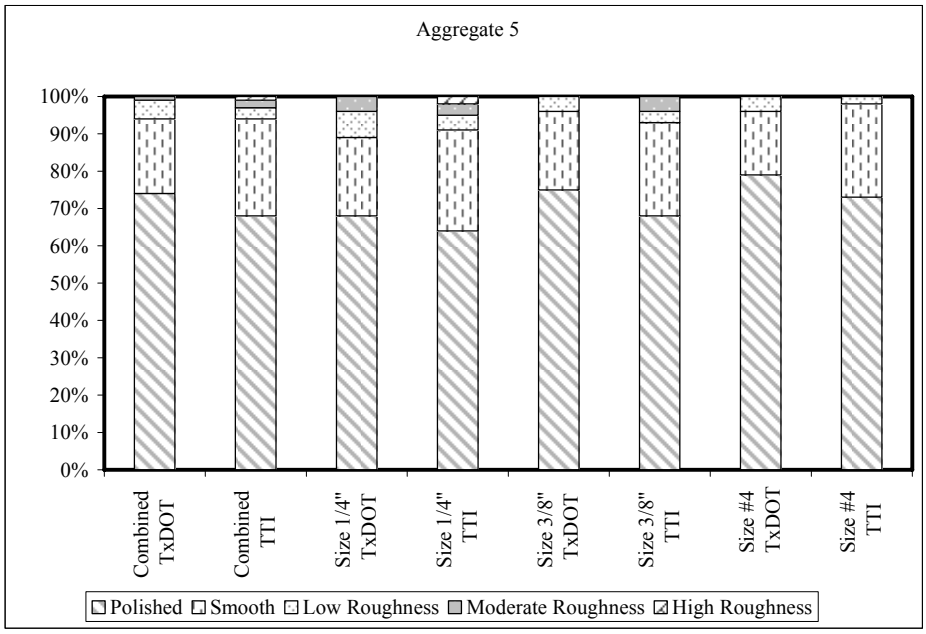
Aggregate 5
100%
90%
80%
70%
60%
50%
40%
30%
20%
10%
0%
Combined TxDOT
Combined TTI
Size 1/4" TxDOT
Size 1/4" TTI
Size 3/8" TxDOT
Size 3/8" TTI
Size #4 TxDOT
Size #4 TTI
Polished
Smooth
Low Roughness
Moderate Roughness
High Roughness

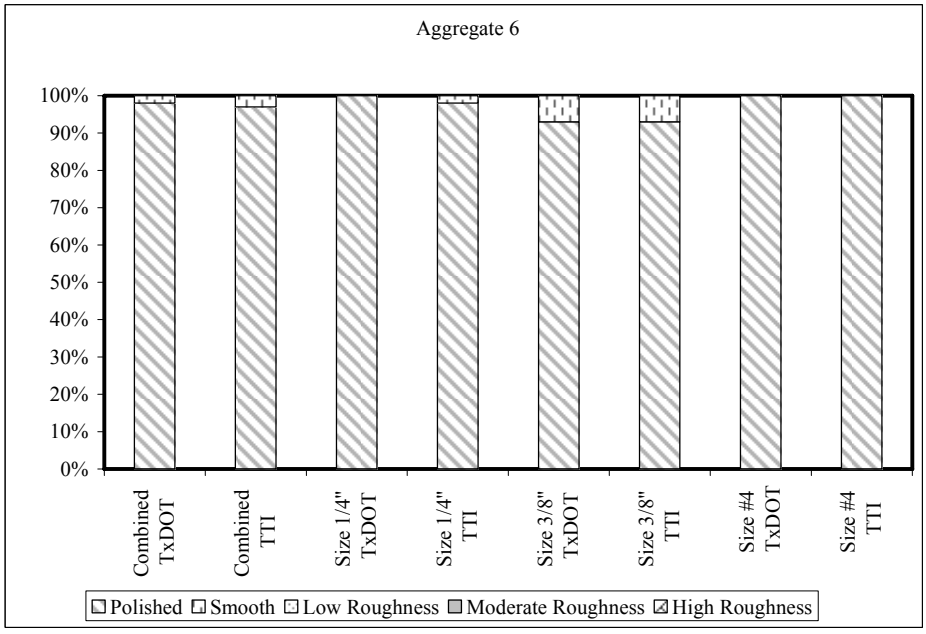
Aggregate 6
100%
90%
80%
70%
60%
50%
40%
30%
20%
10%
0%
Combined TxDOT
Combined TTI
Size 1/4" TxDOT
Size 1/4" TTI
Size 3/8" TxDOT
Size 3/8" TTI
Size #4 TxDOT
Size #4 TTI
Polished
Smooth
Low Roughness
Moderate Roughness
High Roughness

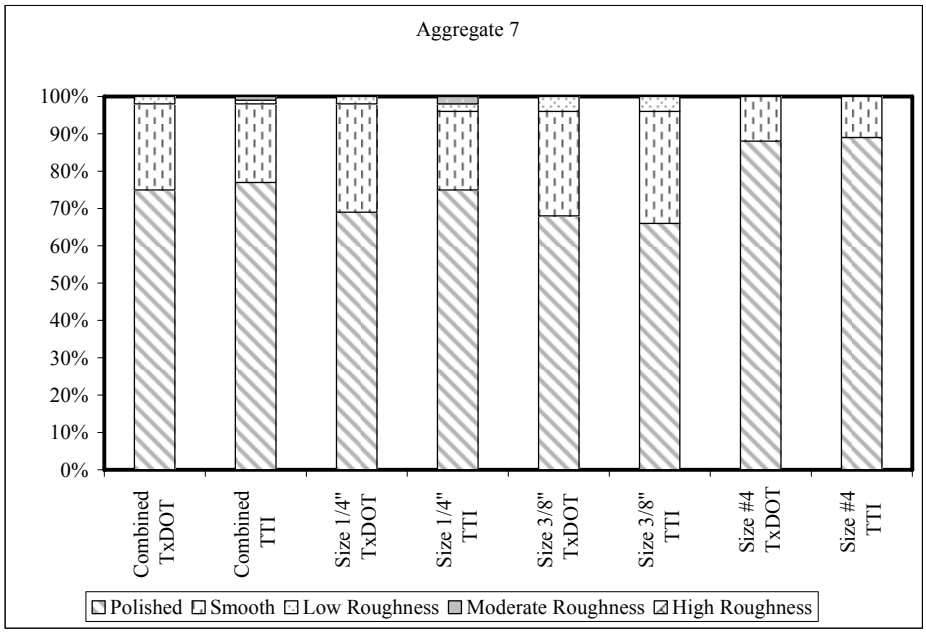
Aggregate 7
100%
90%
80%
70%
60%
50%
40%
30%
20%
10%
0%
Combined TxDOT
Combined TTI
Size 1/4" TxDOT
Size 1/4" TTI
Size 3/8" TxDOT
Size 3/8" TTI
Size #4 TxDOT
Size #4 TTI
Polished
Smooth
Low Roughness
Moderate Roughness
High Roughness

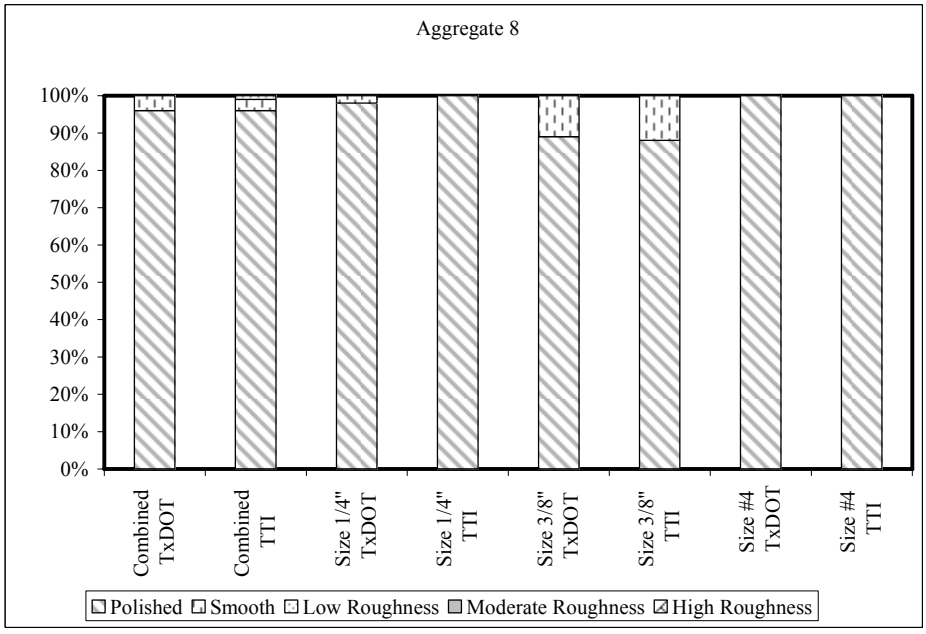
Aggregate 8
100%
90%
80%
70%
60%
50%
40%
30%
20%
10%
0%
Combined TxDOT
Combined TTI
Size 1/4" TxDOT
Size 1/4" TTI
Size 3/8" TxDOT
Size 3/8" TTI
Size #4 TxDOT
Size #4 TTI
Polished
Smooth
Low Roughness
Moderate Roughness
High Roughness

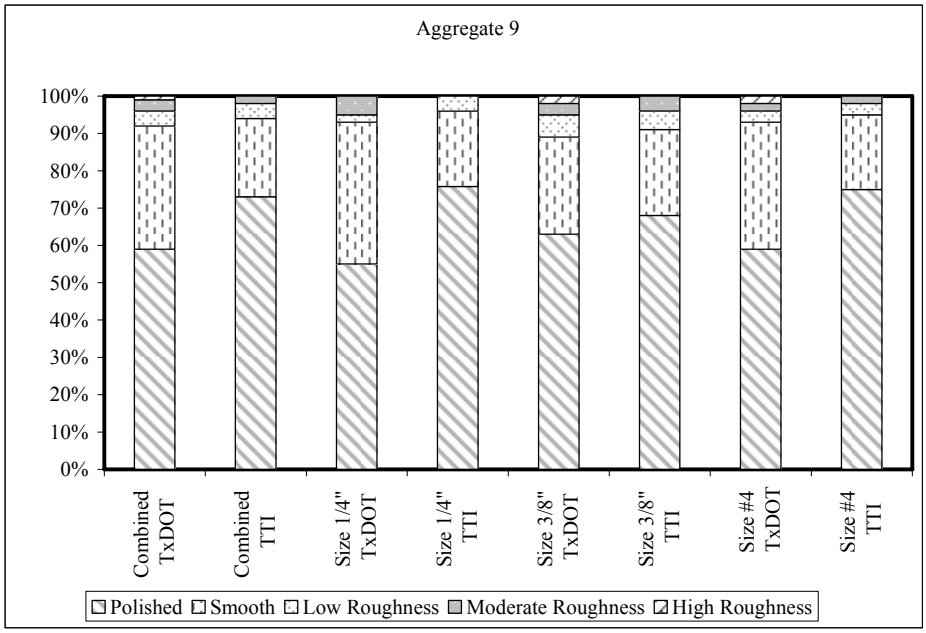
Aggregate 9
100%
90%
80%
70%
60%
50%
40%
30%
20%
10%
0%
Combined TxDOT
Combined TTI
Size 1/4" TxDOT
Size 1/4" TTI
Size 3/8" TxDOT
Size 3/8" TTI
Size #4 TxDOT
Size #4 TTI
Polished
Smooth
Low Roughness
Moderate Roughness
High Roughness

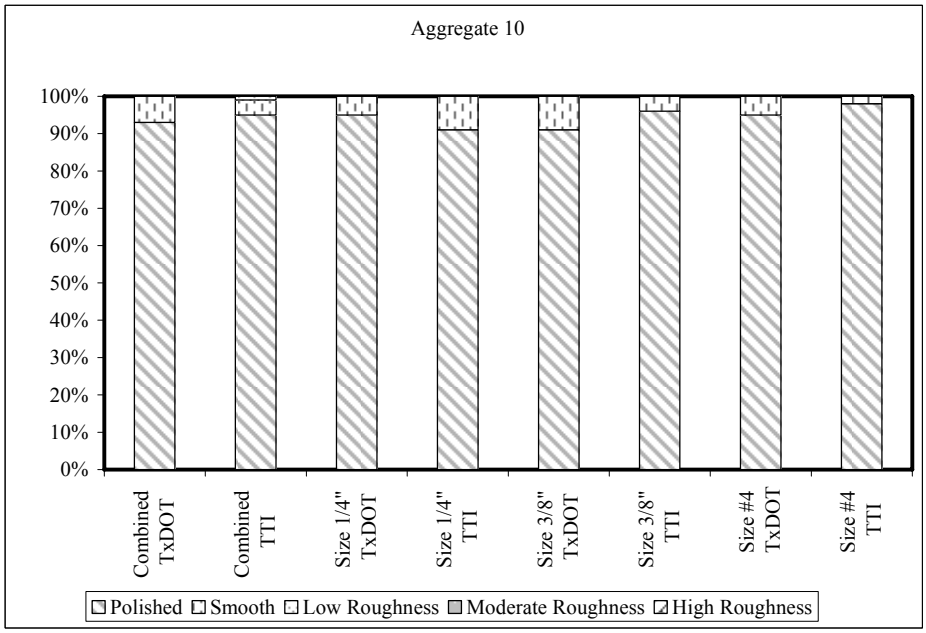
Aggregate 10
100%
90%
80%
70%
60%
50%
40%
30%
20%
10%
0%
Combined TxDOT
Combined TTI
Size 1/4" TxDOT
Size 1/4" TTI
Size 3/8" TxDOT
Size 3/8" TTI
Size #4 TxDOT
Size #4 TTI
Polished
Smooth
Low Roughness
Moderate Roughness
High Roughness

Angularity

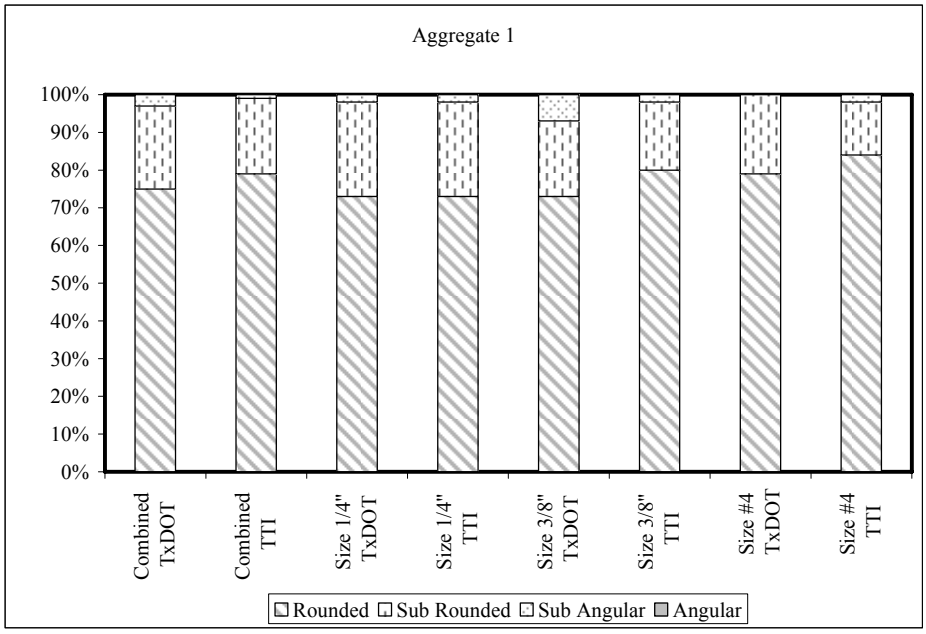
Aggregate 1
100%
90%
80%
70%
60%
50%
40%
30%
20%
10%
0%
Combined TxDOT
Combined TTI
Size 1/4" TxDOT
Size 1/4" TTI
Size 3/8" TxDOT
Size 3/8" TTI
Size #4 TxDOT
Size #4 TTI
Rounded
Sub Rounded
Sub Angular
Angular

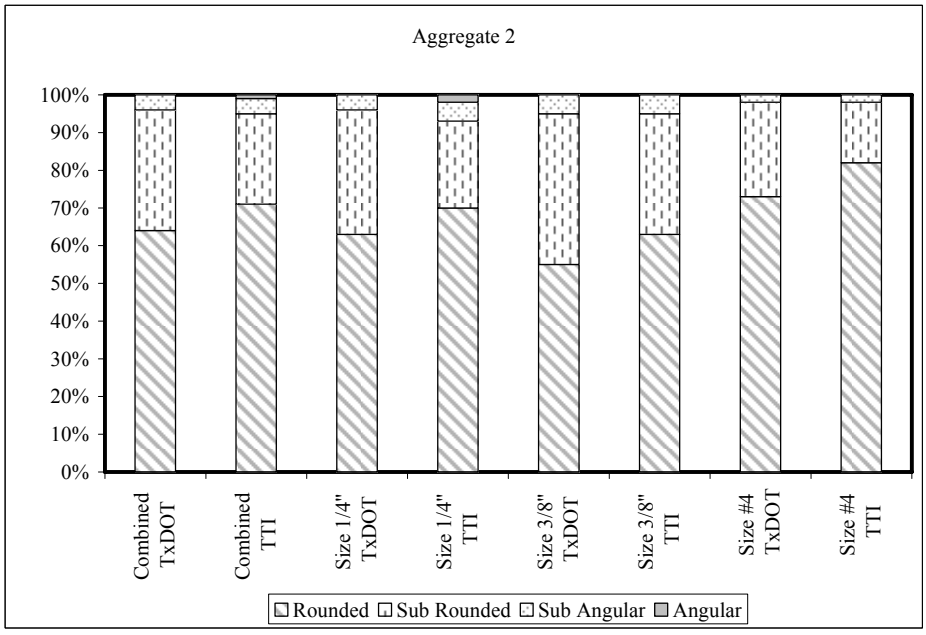
Aggregate 2
100%
90%
80%
70%
60%
50%
40%
30%
20%
10%
0%
Combined TxDOT
Combined TTI
Size 1/4" TxDOT
Size 1/4" TTI
Size 3/8" TxDOT
Size 3/8" TTI
Size #4 TxDOT
Size #4 TTI
Rounded
Sub Rounded
Sub Angular
Angular

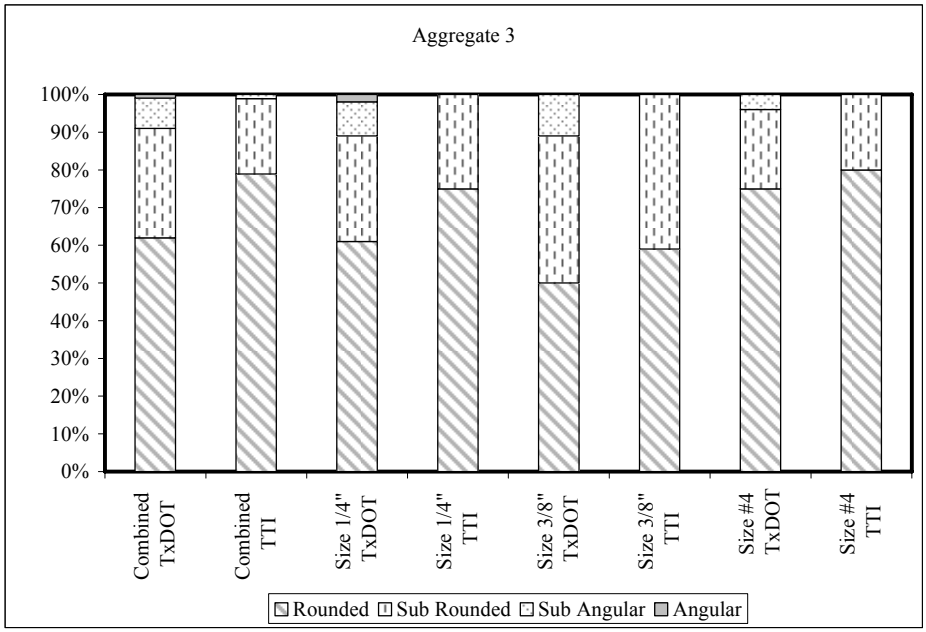
Aggregate 3
100%
90%
80%
70%
60%
50%
40%
30%
20%
10%
0%
Combined TxDOT
Combined TTI
Size 1/4" TxDOT
Size 1/4" TTI
Size 3/8" TxDOT
Size 3/8" TTI
Size #4 TxDOT
Size #4 TTI
Rounded
Sub Rounded
Sub Angular
Angular

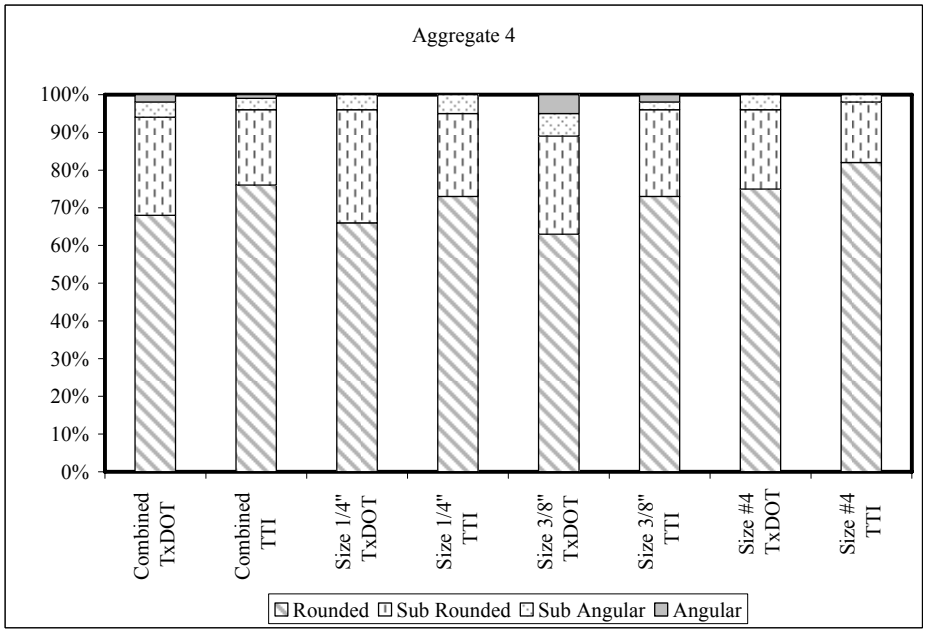
Aggregate 4
100%
90%
80%
70%
60%
50%
40%
30%
20%
10%
0%
Combined TxDOT
Combined TTI
Size 1/4" TxDOT
Size 1/4" TTI
Size 3/8" TxDOT
Size 3/8" TTI
Size #4 TxDOT
Size #4 TTI
Rounded
Sub Rounded
Sub Angular
Angular

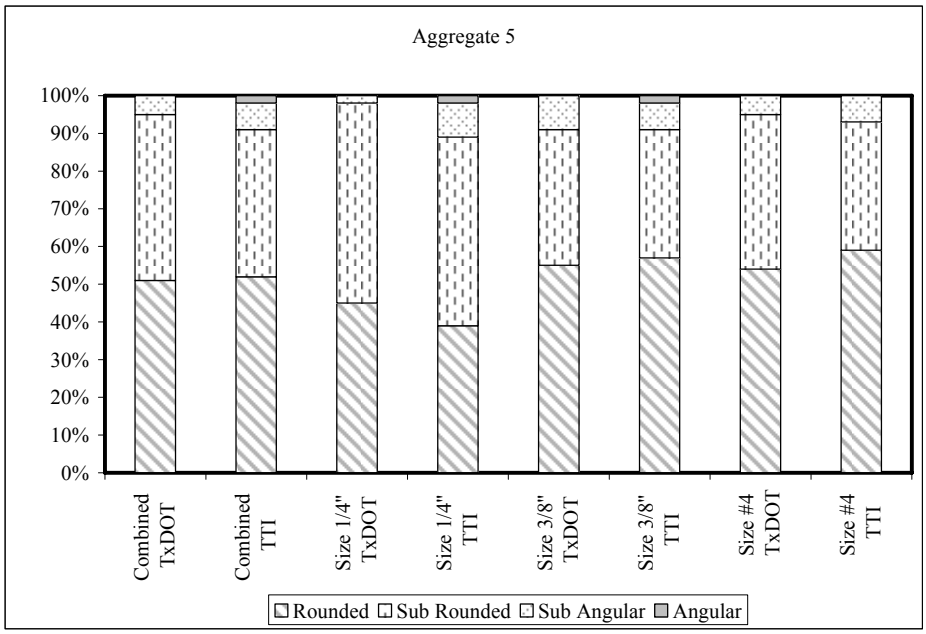
Aggregate 5
100%
90%
80%
70%
60%
50%
40%
30%
20%
10%
0%
Combined TxDOT
Combined TTI
Size 1/4" TxDOT
Size 1/4" TTI
Size 3/8" TxDOT
Size 3/8" TTI
Size #4 TxDOT
Size #4 TTI
Rounded
Sub Rounded
Sub Angular
Angular

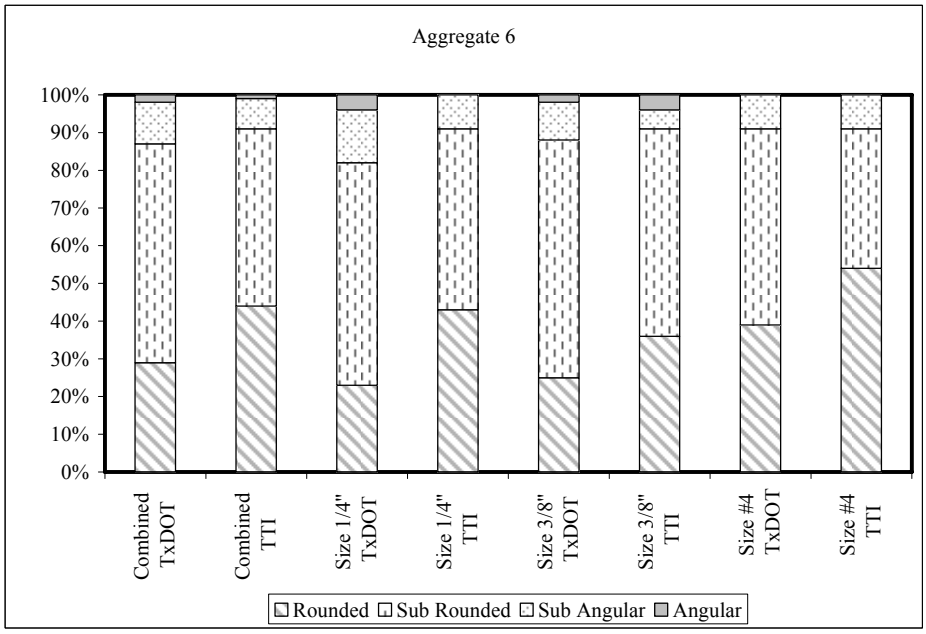
Aggregate 6
100%
90%
80%
70%
60%
50%
40%
30%
20%
10%
0%
Combined TxDOT
Combined TTI
Size 1/4" TxDOT
Size 1/4" TTI
Size 3/8" TxDOT
Size 3/8" TTI
Size #4 TxDOT
Size #4 TTI
Rounded
Sub Rounded
Sub Angular
Angular

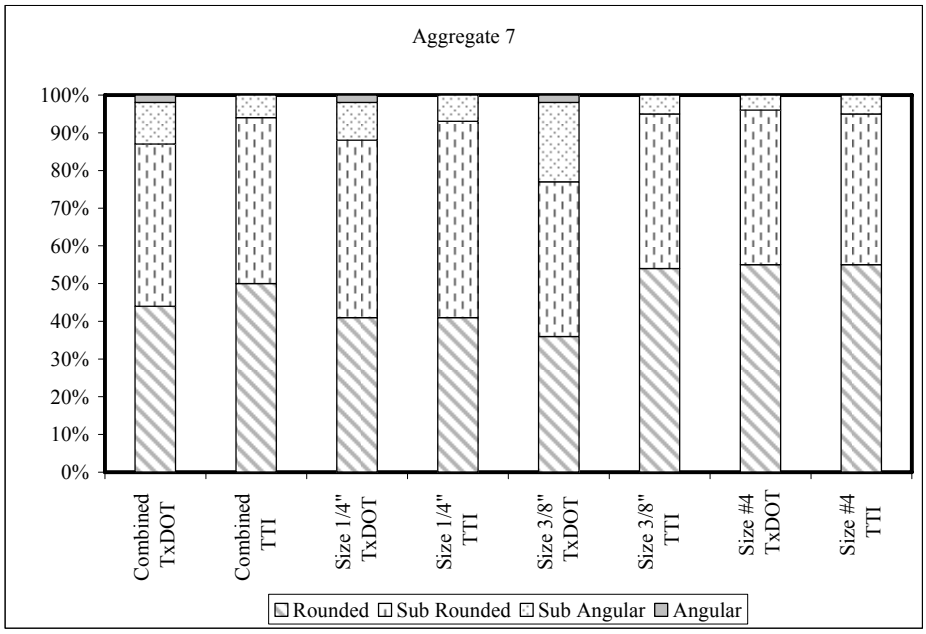
Aggregate 7
100%
90%
80%
70%
60%
50%
40%
30%
20%
10%
0%
Combined TxDOT
Combined TTI
Size 1/4" TxDOT
Size 1/4" TTI
Size 3/8" TxDOT
Size 3/8" TTI
Size #4 TxDOT
Size #4 TTI
Rounded
Sub Rounded
Sub Angular
Angular

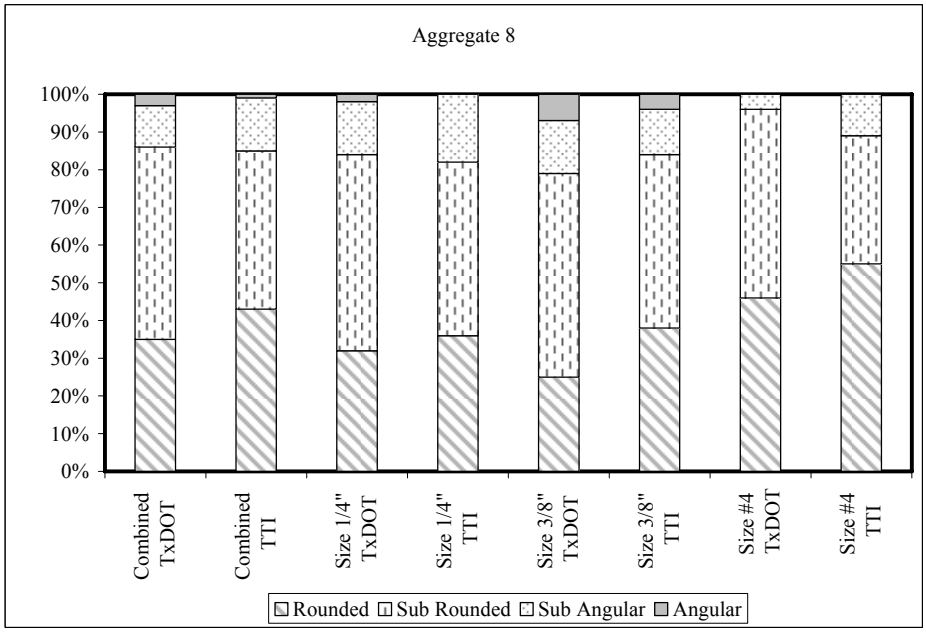
Aggregate 8
100%
90%
80%
70%
60%
50%
40%
30%
20%
10%
0%
Combined TxDOT
Combined TTI
Size 1/4" TxDOT
Size 1/4" TTI
Size 3/8" TxDOT
Size 3/8" TTI
Size #4 TxDOT
Size #4 TTI
Rounded
Sub Rounded
Sub Angular
Angular

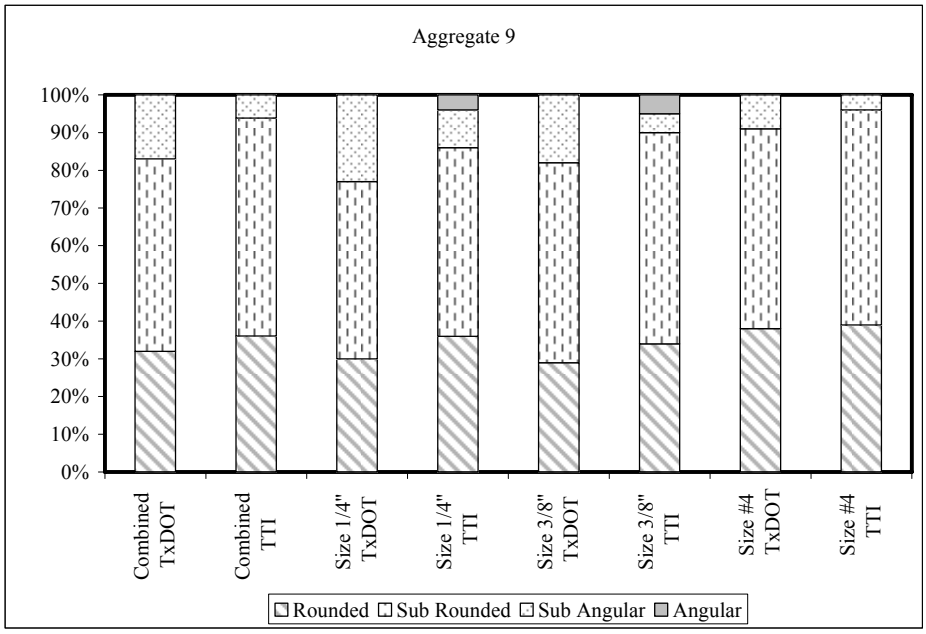
Aggregate 9
100%
90%
80%
70%
60%
50%
40%
30%
20%
10%
0%
Combined TxDOT
Combined TTI
Size 1/4" TxDOT
Size 1/4" TTI
Size 3/8" TxDOT
Size 3/8" TTI
Size #4 TxDOT
Size #4 TTI
Rounded
Sub Rounded
Sub Angular
Angular

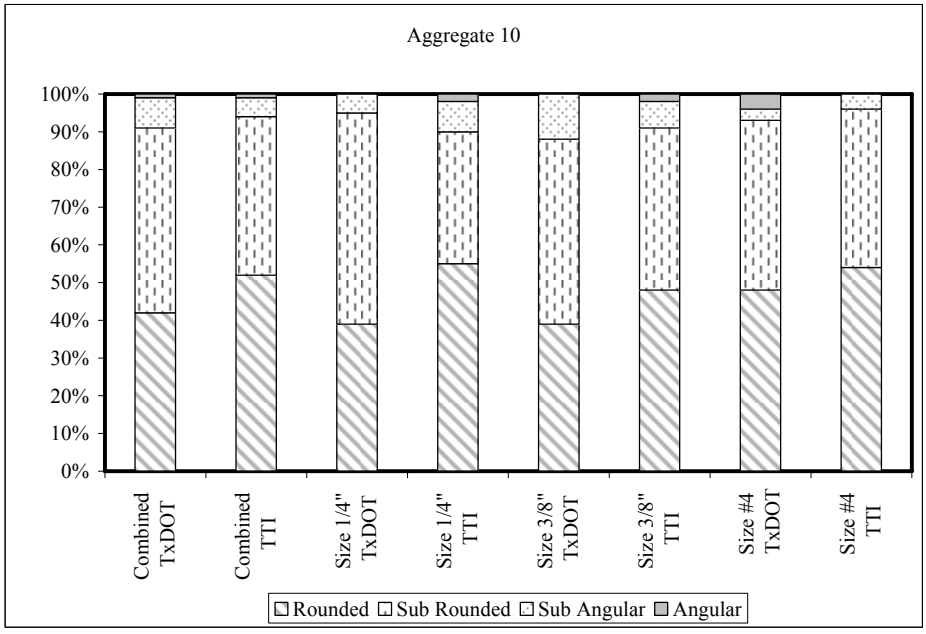
Aggregate 10
100%
90%
80%
70%
60%
50%
40%
30%
20%
10%
0%
Combined TxDOT
Combined TTI
Size 1/4" TxDOT
Size 1/4" TTI
Size 3/8" TxDOT
Size 3/8" TTI
Size #4 TxDOT
Size #4 TTI
Rounded
Sub Rounded
Sub Angular
Angular

Aggregate Coupons

Texture Coupons (some examples)

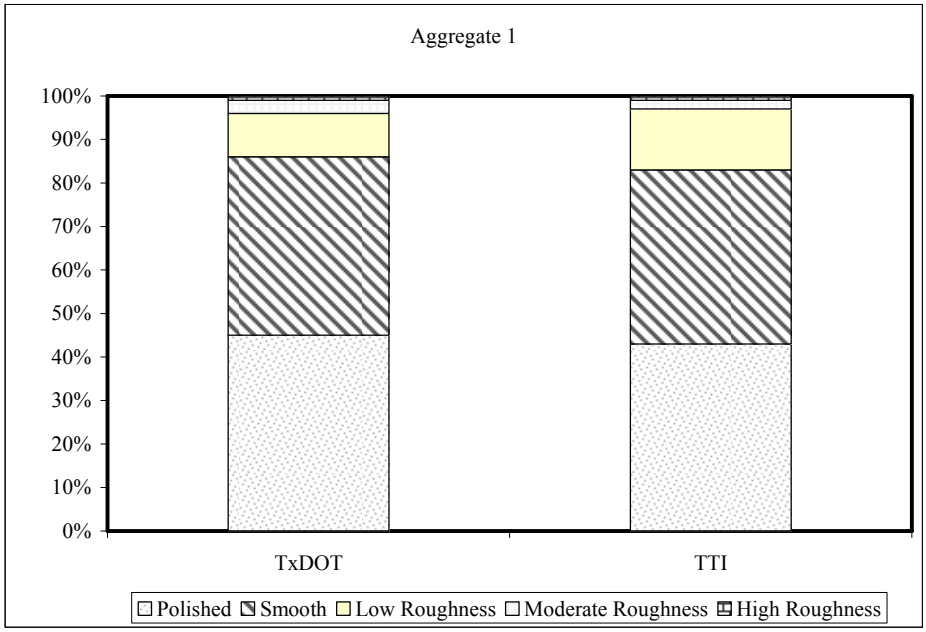

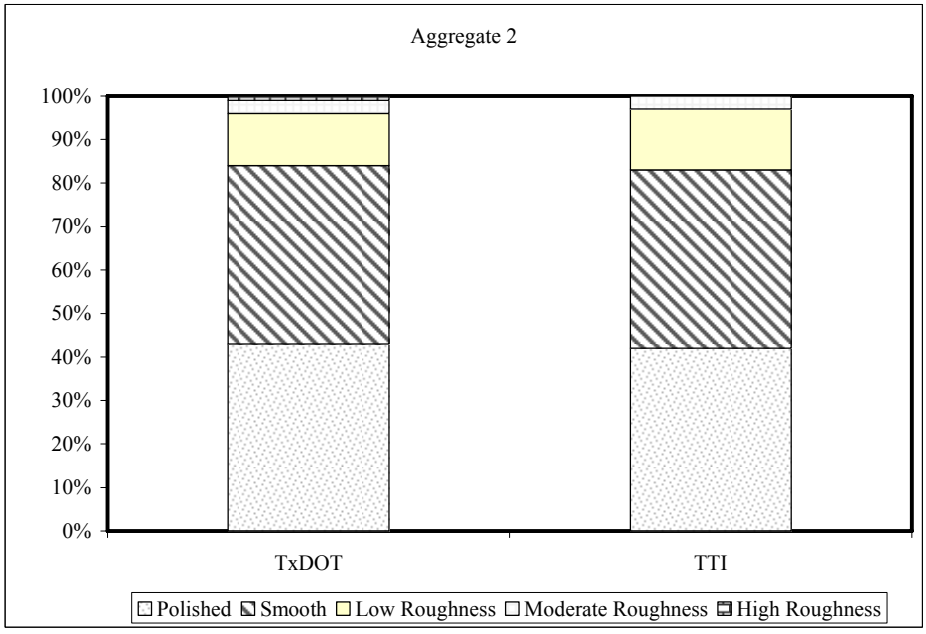

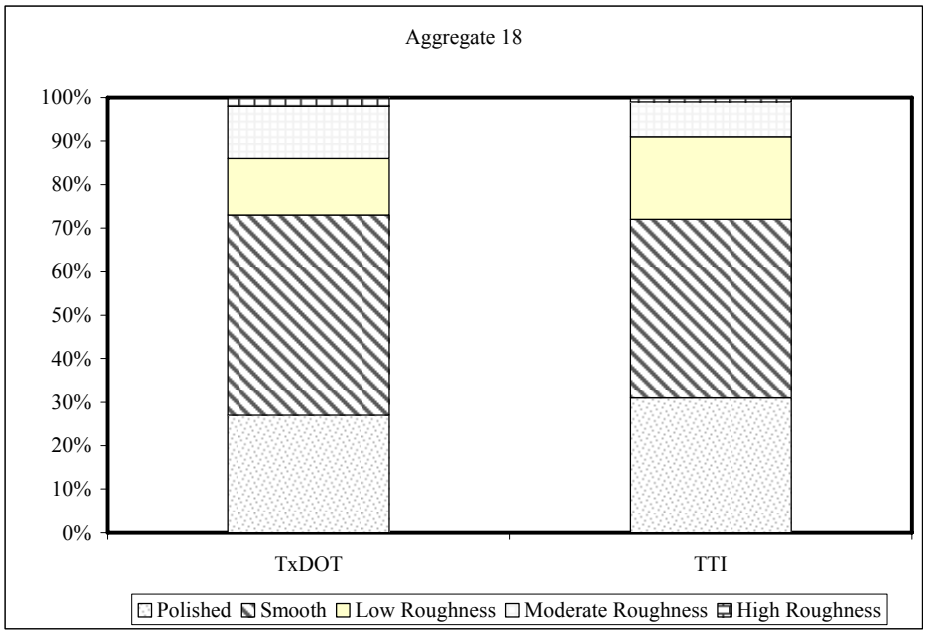
Aggregate 18
100%
90%
80%
70%
60%
50%
40%
30%
20%
10%
0%
TxDOT
TTI
Polished
Smooth
Low Roughness
Moderate Roughness
High Roughness

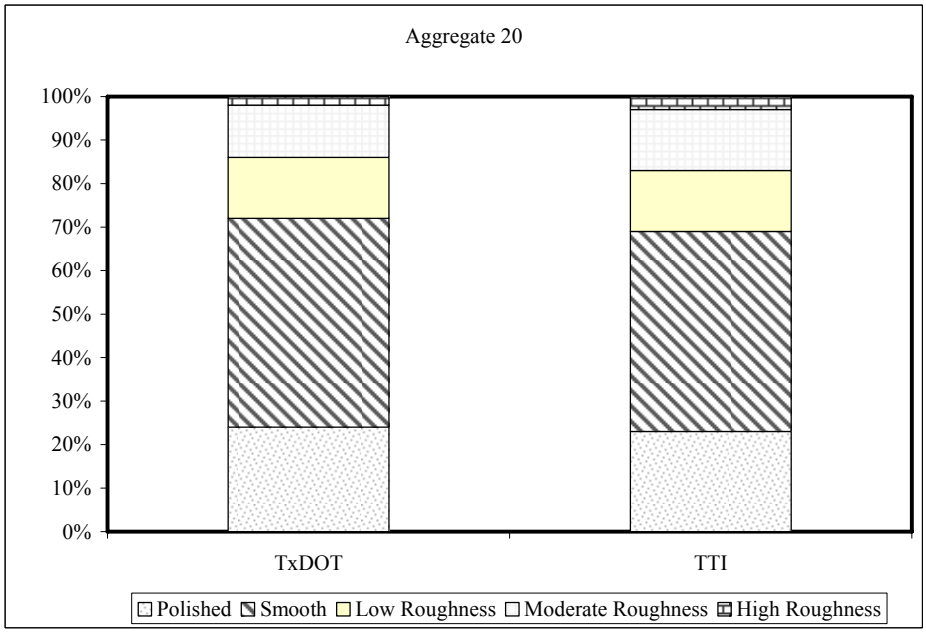
Aggregate 20
100%
90%
80%
70%
60%
50%
40%
30%
20%
10%
0%
TxDOT
TTI
Polished
Smooth
Low Roughness
Moderate Roughness
High Roughness

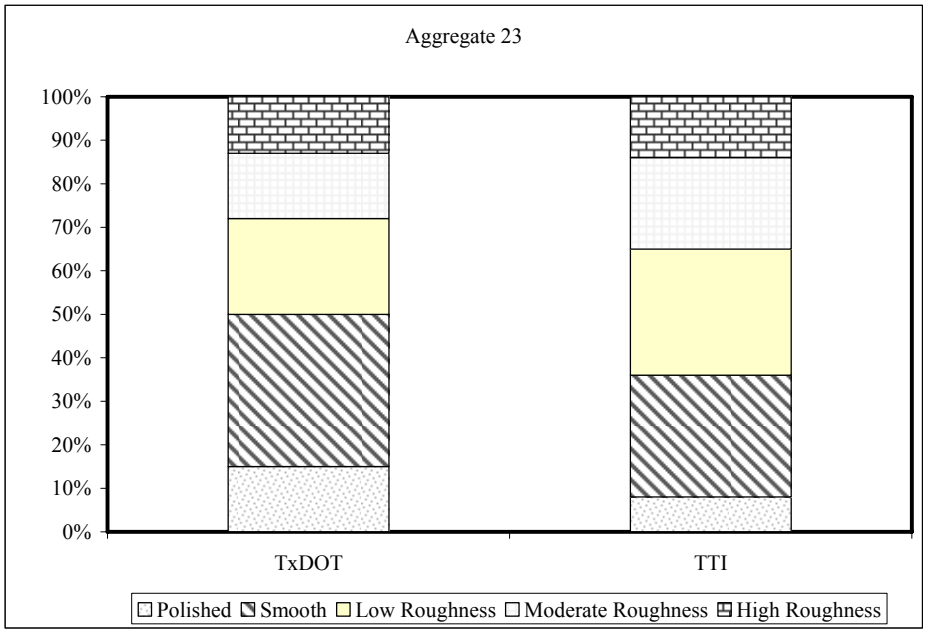
Aggregate 23
100%
90%
80%
70%
60%
50%
40%
30%
20%
10%
0%
TxDOT
TTI
Polished
Smooth
Low Roughness
Moderate Roughness
High Roughness

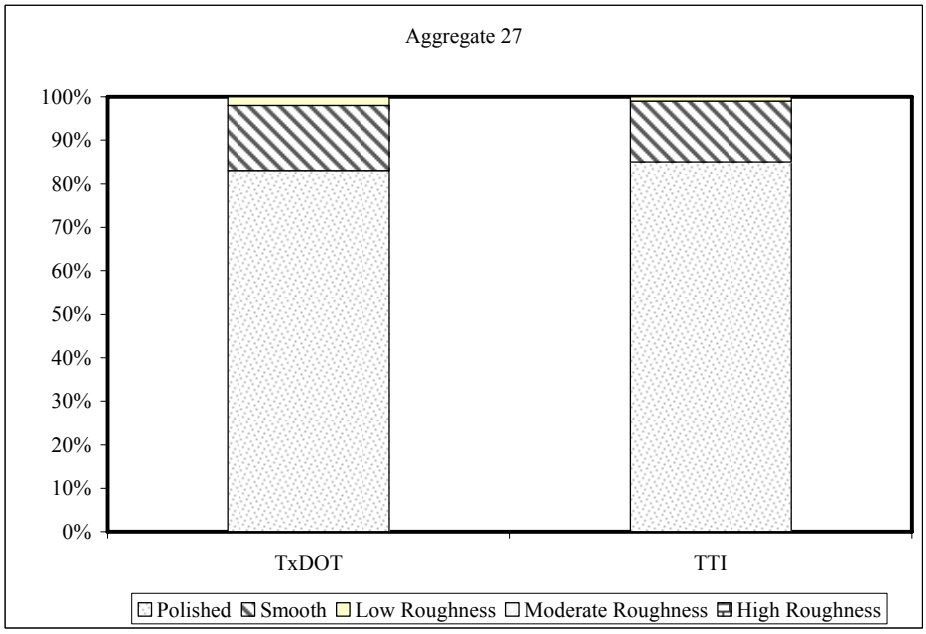
Aggregate 27
100%
90%
80%
70%
60%
50%
40%
30%
20%
10%
0%
TxDOT
TTI
Polished
Smooth
Low Roughness
Moderate Roughness
High Roughness

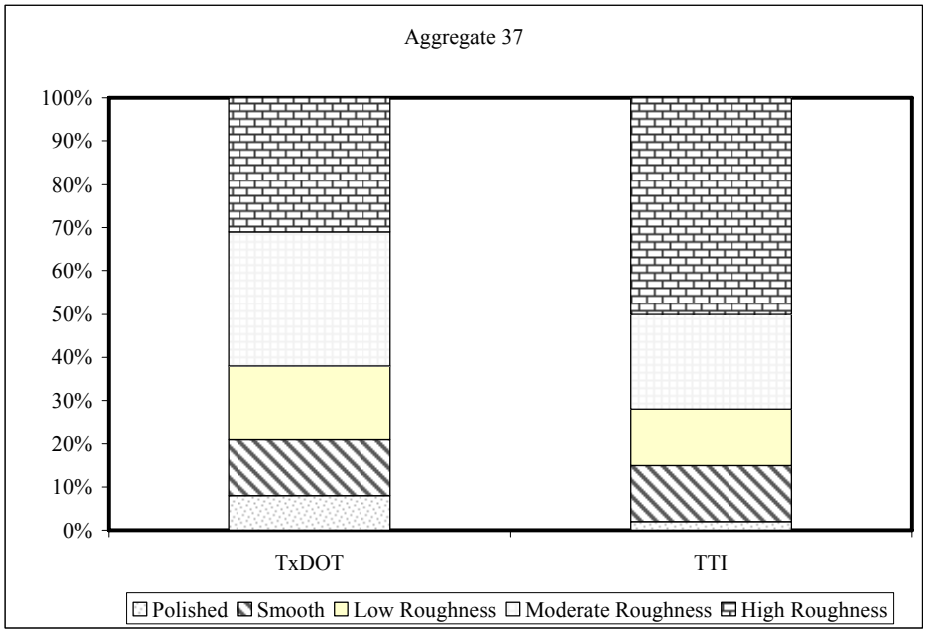
Aggregate 37
100%
90%
80%
70%
60%
50%
40%
30%
20%
10%
0%
TxDOT
TTI
Polished
Smooth
Low Roughness
Moderate Roughness
High Roughness

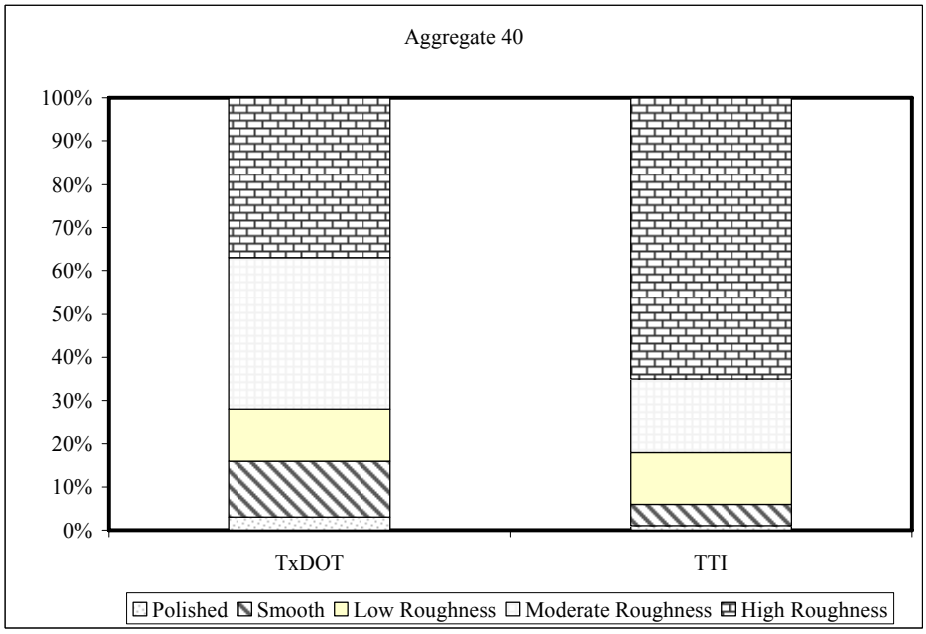
Aggregate 40
100%
90%
80%
70%
60%
50%
40%
30%
20%
10%
0%
TxDOT
TTI
Polished
Smooth
Low Roughness
Moderate Roughness
High Roughness

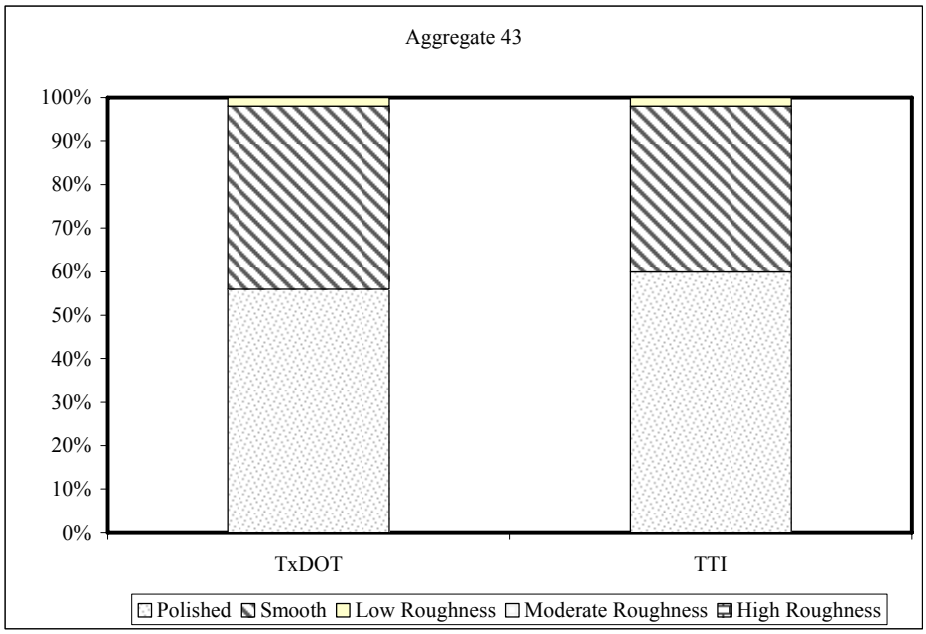
Aggregate 43
100%
90%
80%
70%
60%
50%
40%
30%
20%
10%
0%
TxDOT
TTI
Polished
Smooth
Low Roughness
Moderate Roughness
High Roughness

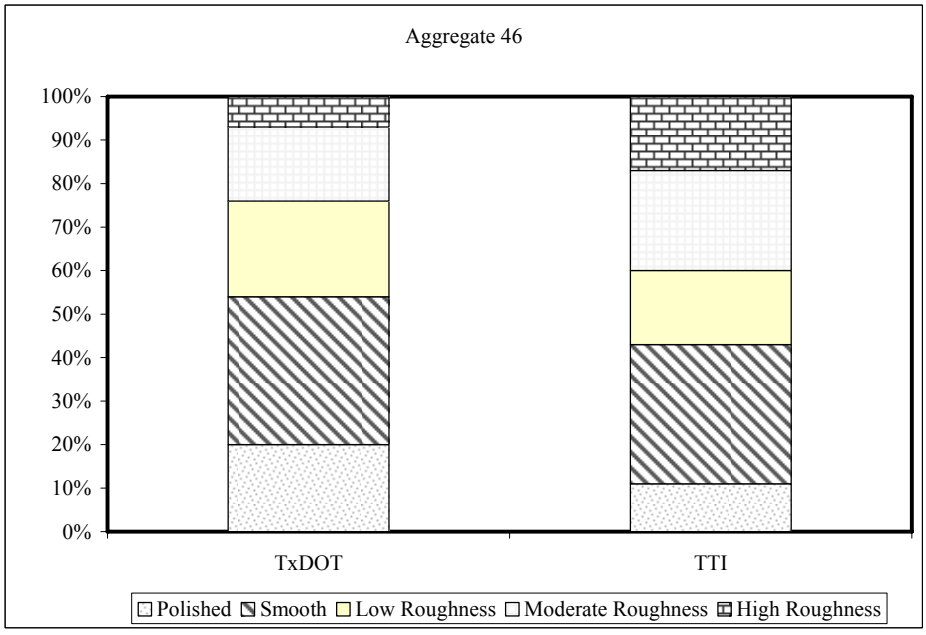
Aggregate 46
100%
90%
80%
70%
60%
50%
40%
30%
20%
10%
0%
TxDOT
TTI
Polished
Smooth
Low Roughness
Moderate Roughness
High Roughness

APPENDIX D

CHI-SQUARE SUMMARY TABLES

Aggregate Particles

Texture (summary tables)

Aggregate 1	Size Compared	Standard Residual Subclass					Chi-Square p-value
Texture		**1**	**2**	**3**	**4**	**5**	
TxDOT	Combined	-0.2	0.5	0.0			0.749
TTI		0.2	-0.5	0.0			
TxDOT	⅜"	0.3	-0.5	-1.0			0.263
TTI		-0.3	0.5	1.0			
TxDOT	¼"	-0.2	0.5				0.489
TTI		0.2	-0.5				
TxDOT	#4	-0.3	0.6	1.0			0.229
TTI		0.3	-0.6	-1.0			

Aggregate 2	Size Compared	Standard Residual Subclass					Chi-Square p-value
Texture		**1**	**2**	**3**	**4**	**5**	
TxDOT	Combined	0.0	0.0	0.0			1.000
TTI		0.0	0.0	0.0			
TxDOT	⅜"	0.0	0.3	-1.0			0.344
TTI		0.0	-0.3	1.0			
TxDOT	¼"	0.1	-0.4				0.602
TTI		-0.1	0.4				
TxDOT	#4	-0.1	-0.3	1.0			0.342
TTI		0.1	0.3	-1.0			

Aggregate 3	Size Compared	Standard Residual Subclass					Chi-Square p-value
Texture		**1**	**2**	**3**	**4**	**5**	
TxDOT	Combined	-0.2	-0.4	0.0			0.814
TTI		0.2	0.4	0.0			
TxDOT	⅜"	-0.6	1.6	0.0			0.062
TTI		0.6	-1.6	0.0			
TxDOT	¼"	-0.1	0.0	1.0			0.364
TTI		0.1	0.0	-1.0			
TxDOT	#4	-0.3	1.2				0.088
TTI		0.3	-1.2				

Aggregate 4	Size Compared	Standard Residual					Chi-Square P-value
		Subclass					
Texture		1	2	3	4	5	
TxDOT	Combined	-0.1	0.4				0.552
TTI		0.1	-0.4				
TxDOT	⅜"	-0.3	1.0				0.152
TTI		0.3	-1.0				
TxDOT	¼"	0.0	0.0				1.000
TTI		0.0	0.0				
TxDOT	#4	-0.1	0.2				0.733
TTI		0.1	-0.2				

Aggregate 5	Size Compared	Standard Residual					Chi-Square P-value
		Subclass					
Texture		1	2	3	4	5	
TxDOT	Combined	0.4	-0.6	0.5	-0.4	-0.7	0.580
TTI		-0.4	0.6	-0.5	0.4	0.7	
TxDOT	⅜"	0.4	-0.4	0.3	-1.4		0.184
TTI		-0.4	0.4	-0.3	1.4		
TxDOT	¼"	0.2	-0.6	0.6	0.3	-1.0	0.429
TTI		-0.2	0.6	-0.6	-0.3	1.0	
TxDOT	#4	0.3	-0.9	0.6			0.297
TTI		-0.3	0.9	-0.6			

Aggregate 6	Size Compared	Standard Residual					Chi-Square P-value
		Subclass					
Texture		1	2	3	4	5	
TxDOT	Combined	0.1	-0.3				0.651
TTI		-0.1	0.3				
TxDOT	⅜"	0.0	0.0				1.000
TTI		0.0	0.0				
TxDOT	¼"	0.1	-1.0				0.155
TTI		-0.1	1.0				
TxDOT	#4	0.0					
TTI		0.0					

Aggregate 7	Size Compared	Standard Residual					Chi-Square P-value
		Subclass					
Texture		1	2	3	4	5	
TxDOT	Combined	-0.1	0.2	0.4	-0.7		0.694
TTI		0.1	-0.2	-0.4	0.7		
TxDOT	⅜"	0.1	-0.2	0.0			0.952
TTI		-0.1	0.2	0.0			
TxDOT	¼"	-0.4	0.8	0.0	-1.0		0.317
TTI		0.4	-0.8	0.0	1.0		
TxDOT	#4	-0.1	0.1				0.825
TTI		0.1	-0.1				

Aggregate 8	Size Compared	Standard Residual					Chi-Square P-value
		Subclass					
Texture		1	2	3	4	5	
TxDOT	Combined	0.0	0.3	-0.7			0.565
TTI		0.0	-0.3	0.7			
TxDOT	⅜"	0.1	-0.1				0.825
TTI		-0.1	0.1				
TxDOT	¼"	-0.1	1.0				0.155
TTI		0.1	-1.0				
TxDOT	#4	0.0					
TTI		0.0					

Aggregate 9	Size Compared	Standard Residual					Chi-Square P-value
		Subclass					
Texture		1	2	3	4	5	
TxDOT	Combined	-0.9	1.2	0.0	0.3	0.7	0.253
TTI		0.9	-1.2	0.0	-0.3	-0.7	
TxDOT	⅜"	-0.3	0.3	0.2	-0.3	1.0	0.625
TTI		0.3	-0.3	-0.2	0.3	-1.0	
TxDOT	¼"	-1.2	1.6	-0.6	1.6		0.003
TTI		1.2	-1.6	0.6	-1.6		
TxDOT	#4	-1.0	1.3	0.0	0.0	1.0	0.110
TTI		1.0	-1.3	0.0	0.0	-1.0	

Aggregate 10	Size Compared	Standard Residual					Chi-Square P-value
		Subclass					
Texture		1	2	3	4	5	
TxDOT	Combined	-0.1	0.6	-0.7			0.399
TTI		0.1	-0.6	0.7			
TxDOT	⅜"	-0.3	1.0				0.152
TTI		0.3	-1.0				
TxDOT	¼"	0.2	-0.8				0.268
TTI		-0.2	0.8				
TxDOT	#4	-0.2	0.8				0.248
TTI		0.2	-0.8				

Angularity (summary tables)

Aggregate 1	Size Compared	Standard Residual Subclass				Chi-Square P-value
Gradient Angularity		**1**	**2**	**3**	**4**	
TxDOT	Combined	-0.2	0.2	0.7		0.549
TTI		0.2	-0.2	-0.7		
TxDOT	⅜"	-0.4	0.2	1.2		0.202
TTI		0.4	-0.2	-1.2		
TxDOT	¼"	0.0	0.0	0.0		1.000
TTI		0.0	0.0	0.0		
TxDOT	#4	-0.3	0.8	-1.0		0.169
TTI		0.3	-0.8	1.0		

Aggregate 2	Size Compared	Standard Residual Subclass				Chi-Square P-value
Gradient Angularity		**1**	**2**	**3**	**4**	
TxDOT	Combined	-0.4	0.8	0.0	-0.7	0.474
TTI		0.4	-0.8	0.0	0.7	
TxDOT	⅜"	-0.5	0.7	0.0		0.489
TTI		0.5	-0.7	0.0		
TxDOT	¼"	-0.4	0.9	-0.2	-1.0	0.234
TTI		0.4	-0.9	0.2	1.0	
TxDOT	#4	-0.5	1.0	0.0		0.287
TTI		0.5	-1.0	0.0		

Aggregate 3	Size Compared	Standard Residual Subclass				Chi-Square P-value
Gradient Angularity		**1**	**2**	**3**	**4**	
TxDOT	Combined	-0.6	1.1	1.6	0.7	0.070
TTI		0.6	-1.1	-1.6	-0.7	
TxDOT	⅜"	-0.6	-0.2	2.3		0.003
TTI		0.6	0.2	-2.3		
TxDOT	¼"	-0.8	0.3	2.1	1.0	0.006
TTI		0.8	-0.3	-2.1	-1.0	
TxDOT	#4	-0.3	0.1	1.4		0.123
TTI		0.3	-0.1	-1.4		

Aggregate 4	Size Compared	Standard Residual Subclass				Chi-Square P-value
Gradient Angularity		**1**	**2**	**3**	**4**	
TxDOT	Combined	-0.5	0.6	0.3	0.4	0.636
TTI		0.5	-0.6	-0.3	-0.4	
TxDOT	⅜"	-0.6	0.3	1.0	0.8	0.240
TTI		0.6	-0.3	-1.0	-0.8	
TxDOT	¼"	-0.4	0.8	-0.2	-0.4	0.429
TTI		0.4	-0.8	0.2	0.4	
TxDOT	#4	-0.4	0.6	0.6		0.437
TTI		0.4	-0.6	-0.6		

Aggregate 5	Size Compared	Standard Residual Subclass				Chi-Square P-value
Gradient Angularity		**1**	**2**	**3**	**4**	
TxDOT	Combined	-0.1	0.4	-0.4	-1.0	0.450
TTI		0.1	-0.4	0.4	1.0	
TxDOT	⅜"	-0.1	0.2	0.4	-1.0	0.504
TTI		0.1	-0.2	-0.4	1.0	
TxDOT	¼"	0.5	0.2	-1.5	-1.0	0.073
TTI		-0.5	-0.2	1.5	1.0	
TxDOT	#4	-0.3	0.6	-0.4		.547
TTI		0.3	-0.6	0.4		

Aggregate 6	Size Compared	Standard Residual Subclass				Chi-Square P-value
Gradient Angularity		**1**	**2**	**3**	**4**	
TxDOT	Combined	-1.2	0.8	0.5	0.4	0.169
TTI		1.2	-0.8	-0.5	-0.4	
TxDOT	⅜"	-1.0	0.5	0.9	-0.6	0.182
TTI		1.0	-0.5	-0.9	0.6	
TxDOT	¼"	-1.7	0.8	0.7	1.4	0.006
TTI		1.7	-0.8	-0.7	-1.4	
TxDOT	#4	-1.1	1.1	0.0		0.084
TTI		1.1	-1.1	0.0		

Aggregate 7	Size Compared	Standard Residual				Chi-Square P-value
		Subclass				
Gradient Angularity		1	2	3	4	
TxDOT	Combined	-0.4	-0.1	0.9	1.0	0.276
TTI		0.4	0.1	-0.9	-1.0	
TxDOT	⅜"	-1.3	0.0	2.2	1.0	0.001
TTI		1.3	0.0	-2.2	-1.0	
TxDOT	¼"	0.0	-0.4	0.5	1.0	0.426
TTI		0.0	0.4	-0.5	-1.0	
TxDOT	#4	0.0	0.1	-0.2		0.940
TTI		0.0	-0.1	0.2		

Aggregate 8	Size Compared	Standard Residual				Chi-Square P-value
		Subclass				
Gradient Angularity		1	2	3	4	
TxDOT	Combined	-0.6	0.7	-0.4	0.7	0.384
TTI		0.6	-0.7	0.4	-0.7	
TxDOT	⅜"	-1.2	0.6	0.3	0.6	0.231
TTI		1.2	-0.6	-0.3	-0.6	
TxDOT	¼"	-0.3	0.4	-0.5	1.0	0.376
TTI		0.3	-0.4	0.5	-1.0	
TxDOT	#4	-0.6	1.2	-1.3		0.028
TTI		0.6	-1.2	1.3		

Aggregate 9	Size Compared	Standard Residual				Chi-Square P-value
		Subclass				
Gradient Angularity		1	2	3	4	
TxDOT	Combined	-0.3	-0.5	2.2	-1.2	0.0035
TTI		0.3	0.5	-2.2	1.2	
TxDOT	⅜"	-0.4	-0.2	1.9	-1.6	0.005
TTI		0.4	0.2	-1.9	1.6	
TxDOT	¼"	-0.5	-0.2	1.6	-1.4	0.021
TTI		0.5	0.2	-1.6	1.4	
TxDOT	#4	-0.1	-0.3	1.0		0.353
TTI		0.1	0.3	-1.0		

Aggregate 10	Size Compared	Standard Residual				Chi-Square P-value
		Subclass				
Gradient Angularity		**1**	**2**	**3**	**4**	
TxDOT	Combined	-0.7	0.5	0.6	0.0	0.514
TTI		0.7	-0.5	-0.6	0.0	
TxDOT	⅜"	-0.7	0.4	0.8	-1.0	0.200
TTI		0.7	-0.4	-0.8	1.0	
TxDOT	¼"	-1.2	1.6	-0.6	-1.0	0.016
TTI		1.2	-1.6	0.6	1.0	
TxDOT	#4	-0.4	0.2	-0.3	1.4	0.204
TTI		0.4	-0.2	0.3	-1.4	

Aggregate Coupons

Texture Coupons (summary table)

Coupons	Size Compared	Standard Residual Subclass					Chi-Square P-value
Texture		**1**	**2**	**3**	**4**	**5**	
TxDOT	1	0.2	0.1	-0.6	0.3	0.0	0.921
TTI		-0.2	-0.1	0.6	-0.3	0.0	
TxDOT	2	0.1	0.0	-0.3	0.0	0.7	0.847
TTI		-0.1	0.0	0.3	0.0	-0.7	
TxDOT	3	0.1	-0.8	1.5	-0.8	0.7	0.094
TTI		-0.1	0.8	-1.5	0.8	-0.7	
TxDOT	4	3.1	-3.8	-1.5	-0.7		0
TTI		-3.1	3.8	1.5	0.7		
TxDOT	5	0.1	-0.4	0.5	0.4		0.762
TTI		-0.1	0.4	-0.5	-0.4		
TxDOT	6	-0.1	0.1	0.3	0.0		0.969
TTI		0.1	-0.1	-0.3	0.0		
TxDOT	7	0.1	-0.2	0.3	-0.7	0.7	0.683
TTI		-0.1	0.2	-0.3	0.7	-0.7	
TxDOT	8	-0.9	0.6	1.0	0.0	-1.0	0.17
TTI		0.9	-0.6	-1.0	0.0	1.0	
TxDOT	9	0.3	-0.3	0.4	-1.0		0.449
TTI		-0.3	0.3	-0.4	1.0		
TxDOT	10	-0.5	-0.4	0.7	1.5	0.7	0.119
TTI		0.5	0.4	-0.7	-1.5	-0.7	
TxDOT	11	0.0	0.1	-0.3	0.0	0.7	0.876
TTI		0.0	-0.1	0.3	0.0	-0.7	
TxDOT	12	-0.4	0.8	-0.6	0.0		0.495
TTI		0.4	-0.8	0.6	0.0		
TxDOT	13	0.3	-0.5	0.6			0.516
TTI		-0.3	0.5	-0.6			
TxDOT	14	0.2	-0.6	1.0			0.245
TTI		-0.2	0.6	-1.0			
TxDOT	15	-0.6	0.7	-0.3	0.3	0.0	0.714
TTI		0.6	-0.7	0.3	-0.3	0.0	
TxDOT	16	1.1	-0.6	-0.1	-1.2	0.7	0.143
TTI		-1.1	0.6	0.1	1.2	-0.7	
TxDOT	17	0.0	0.6	-0.7	-0.7	-0.7	0.451
TTI		0.0	-0.6	0.7	0.7	0.7	

Coupons	Size Compared	Standard Residual Subclass					Chi-Square P-value
TxDOT	18	-0.4	0.4	-0.8	0.6	0.4	0.588
TTI		0.4	-0.4	0.8	-0.6	-0.4	
TxDOT	19	1.0	-0.1	-0.4	-0.9	0.3	0.373
TTI		-1.0	0.1	0.4	0.9	-0.3	
TxDOT	20	0.1	0.1	0.0	-0.3	-0.3	0.981
TTI		-0.1	-0.1	0.0	0.3	0.3	
TxDOT	21	0.3	-0.7	1.2	0.0		0.245
TTI		-0.3	0.7	-1.2	0.0		
TxDOT	22	4.9	-2.4	-2.7	-1.8	-1.0	0
TTI		-4.9	2.4	2.7	1.8	1.0	
TxDOT	23	1.0	0.6	-0.7	-0.7	-0.1	0.297
TTI		-1.0	-0.6	0.7	0.7	0.1	
TxDOT	24	0.1	-0.2	0.5	0.0	-0.7	0.819
TTI		-0.1	0.2	-0.5	0.0	0.7	
TxDOT	25	0.7	-0.5	-0.2	-0.2	0.3	0.782
TTI		-0.7	0.5	0.2	0.2	-0.3	
TxDOT	26	-0.2	0.2	-0.3	0.6	0.0	0.901
TTI		0.2	-0.2	0.3	-0.6	0.0	
TxDOT	27	-0.1	0.1	0.4			0.822
TTI		0.1	-0.1	-0.4			
TxDOT	28	0.6	-0.1	-1.2	0.7		0.224
TTI		-0.6	0.1	1.2	-0.7		
TxDOT	29	0.3	0.1	-0.7	-0.4		0.68
TTI		-0.3	-0.1	0.7	0.4		
TxDOT	30	-0.2	0.4				0.558
TTI		0.2	-0.4				
TxDOT	31	0.2	-0.7	1.2			0.166
TTI		-0.2	0.7	-1.2			
TxDOT	32	-0.4	0.5	0.0	0.7		0.638
TTI		0.4	-0.5	0.0	-0.7		
TxDOT	33	0.3	-0.8	0.0			0.45
TTI		-0.3	0.8	0.0			
TxDOT	34	0.2	-0.4	0.4			0.698
TTI		-0.2	0.4	-0.4			
TxDOT	35	-0.1	0.3	-0.4			0.756
TTI		0.1	-0.3	0.4			
TxDOT	36	0.1	-0.1	0.3	-0.9	0.7	0.563
TTI		-0.1	0.1	-0.3	0.9	-0.7	
TxDOT	37	1.3	0.0	0.5	0.9	-1.5	0.038
TTI		-1.3	0.0	-0.5	-0.9	1.5	

Coupons	Size Compared	Standard Residual Subclass					Chi-Square P-value
TxDOT	38	0.4	-0.3	0.0	0.2	-0.7	0.809
TTI		-0.4	0.3	0.0	-0.2	0.7	
TxDOT	39	-0.4	-0.4	0.8	0.4		0.507
TTI		0.4	0.4	-0.8	-0.4		
TxDOT	40	0.7	1.3	0.0	1.8	-2.0	0
TTI		-0.7	-1.3	0.0	-1.8	2.0	
TxDOT	41	0.5	0.3	-0.9	-1.3	0.0	0.001
TTI		-0.5	-0.3	0.9	1.3	0.0	
TxDOT	42	0.2	-0.3	-0.7			0.547
TTI		-0.2	0.3	0.7			
TxDOT	43	-0.3	0.3	0.0			0.845
TTI		0.3	-0.3	0.0			
TxDOT	44	0.8	-0.6	-0.4	-0.4		0.459
TTI		-0.8	0.6	0.4	0.4		
TxDOT	45	-0.1	0.0	0.7			0.605
TTI		0.1	0.0	-0.7			
TxDOT	46	1.1	0.2	0.6	-0.7	-1.4	0.079
TTI		-1.1	-0.2	-0.6	0.7	1.4	
TxDOT	47	-1.5	1.0	1.0			0.013
TTI		1.5	-1.0	-1.0			
TxDOT	48	0.0	-0.1	0.7			0.598
TTI		0.0	0.1	-0.7			
TxDOT	49	0.1	0.0	-0.7			0.605
TTI		-0.1	0.0	0.7			
TxDOT	50	0.4	-0.7	-0.3	0.4		0.619
TTI		-0.4	0.7	0.3	-0.4		
TxDOT	51	-0.5	0.6	0.0	0.0		0.786
TTI		0.5	-0.6	0.0	0.0		
TxDOT	52	0.6	-0.9	0.6	-0.3		0.345
TTI		-0.6	0.9	-0.6	0.3		
TxDOT	53	0.7	-0.9	-0.8			0.136
TTI		-0.7	0.9	0.8			
TxDOT	54	0.1	-0.3	0.3	0.7		0.688
TTI		-0.1	0.3	-0.3	-0.7		
TxDOT	55	0.2	-0.3	-0.4			0.739
TTI		-0.2	0.3	0.4			
TxDOT	56	-0.1	-0.1	0.1	0.3		0.966
TTI		0.1	0.1	-0.1	-0.3		
TxDOT	57	0.4	-0.9	0.4	0.7		0.378
TTI		-0.4	0.9	-0.4	-0.7		

Coupons	Size Compared	Standard Residual Subclass					Chi-Square P-value
TxDOT	58	-0.3	0.0	-0.1	0.7	0.0	0.874
TTI		0.3	0.0	0.1	-0.7	0.0	
TxDOT	59	-0.1	0.3	-0.7		0.7	0.533
TTI		0.1	-0.3	0.7		-0.7	
TxDOT	60	0.1	-0.3	0.4	0.0		0.907
TTI		-0.1	0.3	-0.4	0.0		
TxDOT	61	-0.4	0.6	-0.3	0.7		0.543
TTI		0.4	-0.6	0.3	-0.7		
TxDOT	62	0.2	-0.6	0.4			0.593
TTI		-0.2	0.6	-0.4			
TxDOT	63	-0.1	0.3	-0.7			0.548
TTI		0.1	-0.3	0.7			
TxDOT	64	-1.0	1.2	0.7	0.7		0.085
TTI		1.0	-1.2	-0.7	-0.7		
TxDOT	65	-0.4	0.7	-0.3			0.507
TTI		0.4	-0.7	0.3			
TxDOT	66	-0.1	0.1	-0.6	1.0		0.441
TTI		0.1	-0.1	0.6	-1.0		
TxDOT	67	0.4	-0.7	-1.0	0.7		0.243
TTI		-0.4	0.7	1.0	-0.7		
TxDOT	68	0.6	-1.1	0.0			0.202
TTI		-0.6	1.1	0.0			
TxDOT	69	0.3	-0.2	-0.2	0.3		0.927
TTI		-0.3	0.2	0.2	-0.3		
TxDOT	70	0.7	-0.9	-0.5			0.192
TTI		-0.7	0.9	0.5			
TxDOT	71	0.2	-0.3	0.0	0.4		0.893
TTI		-0.2	0.3	0.0	-0.4		
TxDOT	72	0.5	-0.6	-0.7			0.344
TTI		-0.5	0.6	0.7			
TxDOT	73	0.1	-0.7	0.7	1.0		0.269
TTI		-0.1	0.7	-0.7	-1.0		
TxDOT	74	0.6	-0.5	-0.5	-0.7		0.439
TTI		-0.6	0.5	0.5	0.7		
TxDOT	75	-0.1	0.1	1.0		-0.7	0.384
TTI		0.1	-0.1	-1.0		0.7	

APPENDIX E

CHI-SQUARE FULL TABLES (ILLUSTRATION EXAMPLES)

Aggregate Particles

Texture (example)

1/4" size			Subclass					Total
			1	**2**	**3**	**4**	**5**	
Aggregate 5	TxDOT	Count	68	21	7	4	0	100
		Expected count	66	24	5.5	3.5	1	100
		Standard Residual	0.2	-0.6	0.6	0.3	-1.0	
	TTI	Count	64	27	4	3	2	100
		Expected count	66	24	5.5	3.5	1	100
		Standard Residual	-0.2	0.6	-0.6	-0.3	1.0	
Total		Count	132	48	11	7	2	200
		Expected count	132	48	11	7	2	200

Chi-Square Tests

	Value	**df**	**Asymp. Sig. (2-sided)**
Pearson Chi-Square	3.832(a)	4	.429
Likelihood Ratio	4.618	4	.329
Linear-by-Linear Association	.180	1	.671
N of Valid Cases	200		

a 4 cells (40.0 percent) have expected count less than 5. The minimum expected count is 1.00.

Angularity (example)

⅜" size			Subclass				Total
			1	2	3	4	
Aggregate 1	TxDOT	Count	73	20	7		100
		Expected count	76.5	19	4.5		100
		Standard Residual	-0.4	0.2	1.2		
	TTI	Count	80	18	2		100
		Expected count	76.5	19	4.5		100
		Standard Residual	0.4	-0.2	-1.2		
Total		Count	153	38	9		200
		Expected count	153	38	9		200

Chi-Square Tests

	Value	df	Asymp. Sig. (2-sided)
Pearson Chi-Square	3.203(a)	2	.202
Likelihood Ratio	3.368	2	.186
Linear-by-Linear Association	2.457	1	.117
N of Valid Cases	200		

a 2 cells (33.3 percent) have expected count less than 5. The minimum expected count is 4.50.

Aggregate Coupons

Texture Coupons (example)

			Subclass					Total
			1	2	3	4	5	
Aggregate 1	TxDOT	Count	45	41	10	3	1	100
		Expected count	44	40.5	12	2.5	1	100
		Standard Residual	0.2	0.1	-0.6	0.3	0.0	
	TTI	Count	43	40	14	2	1	100
		Expected count	44	40.5	12	2.5	1	100
		Standard Residual	-0.2	-0.1	0.6	-0.3	0.0	
Total		Count	87	81	24	5	2	200
		Expected count	87	81	24	5	2	200

Chi-Square Tests

	Value	df	Asymp. Sig. (2-sided)
Pearson Chi-Square	.924(a)	4	.921
Likelihood Ratio	.929	4	.920
Linear-by-Linear Association	.115	1	.735
N of Valid Cases	200		

a 4 cells (40.0 percent) have expected count less than 5. The minimum expected count is 1.00.

APPENDIX F

MICRO-DEVAL VARIABILITY (SPSS OUTPUT)

Linear Model (all data point)

Model Summary(b)

Model	R	R^2	Adjusted R^2	Std. Error of the Estimate
1	.961(a)	.924	.923	2.13666

a Predictors: (Constant), TxDOT
b Dependent Variable: TTI

Coefficients(a)

Model		Unstandardized Coefficients		Standardized Coefficients	t	Sig.	95 % Confidence Interval for B	
		B	Std. Error	Beta			Lower Bound	Upper Bound
1	(Constant)	.812	.450		1.807	.074	-.080	1.705
	TxDOT	.872	.025	.961	34.475	.000	.822	.922

a Dependent Variable: TTI

Residuals Statistics(a)

	Minimum	Maximum	Mean	Std. Deviation	N
Predicted Value	2.3816	31.2380	14.4507	7.40326	100
Residual	-13.1323	4.5410	.0000	2.12585	100
Std. Predicted Value	-1.630	2.268	.000	1.000	100
Std. Residual	-6.146	2.125	.000	.995	100

a Dependent Variable: TTI

Charts

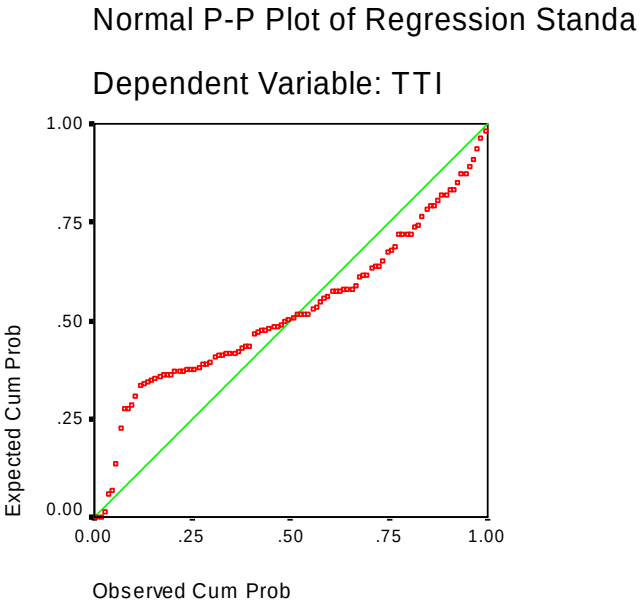
Normal P-P Plot of Regression Standa
Dependent Variable: TTI
Expected Cum Prob
Observed Cum Prob
0.00
.25
.50
.75
1.00

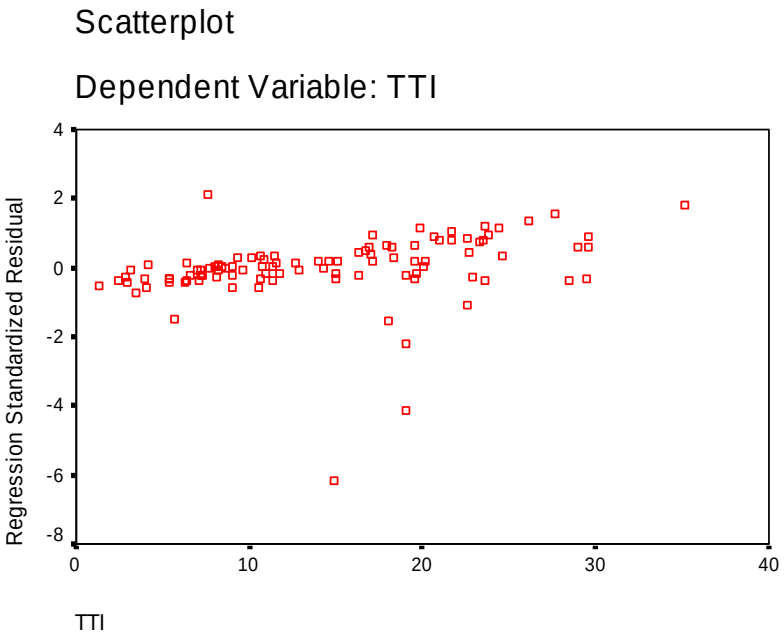
Scatterplot
Dependent Variable: TTI
Regression Standardized Residual
TTI
4
2
0
-2
-4
-6
-8
0
10
20
30
40

Linear Model (excluding outliers)

Model Summary(b)

Model	R	R^2	Adjusted R^2	Std. Error of the Estimate
1	.985(a)	.970	.970	1.34462

a Predictors: (Constant), TxDOT
b Dependent Variable: TTI

Coefficients (a)

Model		Unstandardized Coefficients		Standardized Coefficients	t	Sig.	95 % Confidence Interval for B	
		B	Std. Error	Beta			Lower Bound	Upper Bound
1	(Constant)	.234	.287		.817	.416	-.335	.804
	TXDOT	.924	.016	.985	56.040	.000	.891	.957

a Dependent Variable: TTI

Residuals Statistics(a)

	Minimum	Maximum	Mean	Std. Deviation	N
Predicted Value	1.8979	32.4866	14.3991	7.65087	98
Residual	-5.5515	4.9828	.0000	1.33767	98
Std. Predicted Value	-1.634	2.364	.000	1.000	98
Std. Residual	-4.129	3.706	.000	.995	98

a Dependent Variable: TTI

Charts

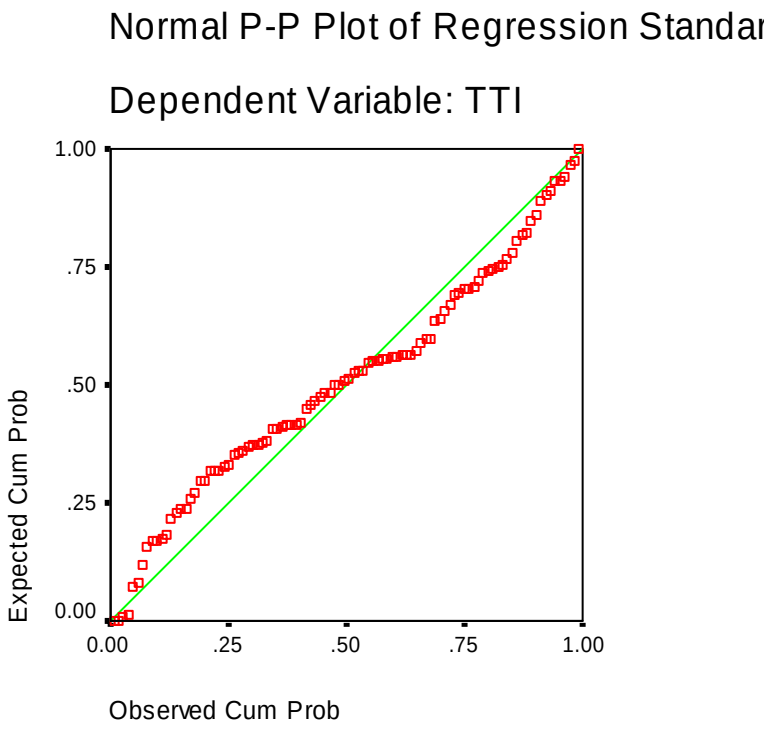
Normal P-P Plot of Regression Standar
Dependent Variable: TTI
Expected Cum Prob
Observed Cum Prob
1.00
.75
.50
.25
0.00
0.00
.25
.50
.75
1.00

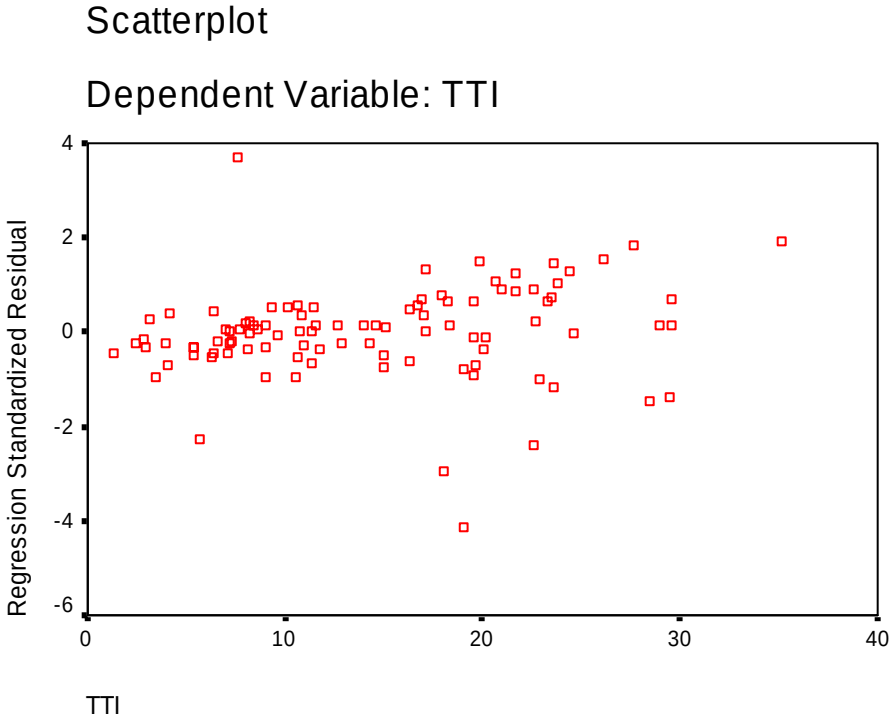
Scatterplot
Dependent Variable: TTI
Regression Standardized Residual
TTI
4
2
0
-2
-4
-6
0
10
20
30
40

APPENDIX G

DATABASE SUMMARY

Table G.1. Aggregate Mineralogy and Classification.

Sample Number	Material Code	Material Type
04-1205	O18	Crushed Limestone
04-1220	O18	Crushed Limestone
04-1277	O18	Crushed Limestone
04-1283	O18	Crushed Limestone
04-1285	O18	Crushed Limestone
04-1300	O18	Crushed Limestone
04-1307	O18	Crushed Limestone
05-0005	O19	Crushed Dolomite
05-0007	O18	Crushed Limestone
05-0009	O18	Crushed Limestone
05-0011	O32	Crushed Rhyolite
05-0014	O15	Partly Crushed Sil. & LS Gravel
05-0017	O14	Crushed Sil. & LS Gravel
05-0020	O11	Crushed Sil. Gravel
05-0029	O33	Crushed Rhyolite Gravel
05-0041	O48	Lightweight Aggregate
05-0048	O25	Partly Crushed LS & Sil. Gravel
05-0077	O14	Crushed Sil. & LS Gravel
05-0081	O19	Crushed Dolomite
05-0083	O19	Crushed Dolomite
05-0086	O29	Crushed Sandstone
05-0089	O18	Crushed Limestone
05-0093	O18	Crushed Limestone
05-0109	O18	Crushed Limestone
05-0129	O18	Crushed Limestone
05-0143	O18	Crushed Limestone
05-0149	O18	Crushed Limestone
05-0151	O18	Crushed Limestone
05-0161	O14	Crushed Sil. & LS Gravel
05-0178	O18	Crushed Limestone
05-0213	O18	Crushed Limestone
05-0216	O18	Crushed Limestone
05-0231	O24	Crushed LS & Sil. Gravel

Table G.1. Continued.

Sample Number	Material Code	Material Type
05-0235	O11	Crushed Sil. Gravel
05-0238	O14	Crushed Sil. & LS Gravel
05-0239	O14	Crushed Sil. & LS Gravel
05-0245	O17	Crushed Sil. & Calcareous Gravel
05-0247	O17	Crushed Sil. & Calcareous Gravel
05-0251	O18	Crushed Limestone
05-0266	O49	Crushed LS Rock Asphalt
05-0317	O50	Crushed Traprock
05-0320	O32	Crushed Rhyolite
05-0321	O18	Crushed Limestone
05-0337	O14	Crushed Sil. & LS Gravel
05-0338	O14	Crushed Sil. & LS Gravel
05-0347	O18	Crushed Limestone
05-0350	O18	Crushed Limestone
05-0365	O18	Crushed Limestone
05-0368	O18	Crushed Limestone
05-0397	O18	Crushed Limestone
05-0399	O18	Crushed Limestone
05-0493	O18	Crushed Limestone
05-0494	O18	Crushed Limestone
05-0496	O29	Crushed Sandstone
05-0519	O18	Crushed Limestone
05-0521	O49	Crushed LS Rock Asphalt
05-0532	O18	Crushed Limestone
05-0534	O18	Crushed Limestone
05-0535	O49	Crushed LS Rock Asphalt
05-0543	O14	Crushed Sil. & LS Gravel
05-0545	O18	Crushed Limestone
05-0630	O29	Crushed Sandstone
05-0643	O18	Crushed Limestone
05-0649	O18	Crushed Limestone
05-0693	O33	Crushed Rhyolite Gravel
05-0708	O29	Crushed Sandstone

Table G.1. Continued.

Sample Number	Material Code	Material Type
05-0715	O18	Crushed Limestone
05-0716	O18	Crushed Limestone
05-0719	O18	Crushed Limestone
05-0768	O19	Crushed Dolomite
05-0770	O19	Crushed Dolomite
05-0771	O29	Crushed Sandstone
05-0774	O18	Crushed Limestone
05-0800	O18	Crushed Limestone
05-0806	O18	Crushed Limestone
05-0822	O19	Crushed Dolomite
05-0824	O19	Crushed Dolomite
05-0826	O51	Crushed Granite
05-0828	O29	Crushed Sandstone
05-0832	O18	Crushed Limestone
05-0921	O18	Crushed Limestone
05-0922	O18	Crushed Limestone
05-0938	O51	Crushed Granite
05-0941	O11	Crushed Sil. Gravel
05-0943	O12	Partly Crushed Sil. Gravel
05-0946	O40	Quartzite
05-0992	O18	Crushed Limestone
05-0995	O18	Crushed Limestone
05-1002	O18	Crushed Limestone
05-1009	O21	Crushed Limestone Gravel
05-1183	O18	Crushed Limestone
05-1184	O18	Crushed Limestone
05-1190	O29	Crushed Sandstone
05-1194	O18	Crushed Limestone
05-1201	O18	Crushed Limestone
05-1205	O18	Crushed Limestone
05-1207	O18	Crushed Limestone
05-1210	O29	Crushed Sandstone
05-1213	O18	Crushed Limestone

Table G.1. Continued.

Sample Number	Material Code	Material Type
05-1221	O29	Crushed Sandstone
05-1222	O29	Crushed Sandstone
05-1223	O18	Crushed Limestone
05-1235	O18	Crushed Limestone
05-1236	O18	Crushed Limestone
05-1260	O18	Crushed Limestone
05-1262	O18	Crushed Limestone
05-1269	O18	Crushed Limestone
05-1274	O33	Crushed Rhyolite Gravel
05-1314	O18	Crushed Limestone
05-1319	O18	Crushed Limestone
05-1341	O49	Crushed LS Rock Asphalt
05-1354	O18	Crushed Limestone
05-1357	O18	Crushed Limestone
05-1358	O18	Crushed Limestone
05-1359	O18	Crushed Limestone
05-1360	O18	Crushed Limestone
05-1361	O18	Crushed Limestone
05-1383	O29	Crushed Sandstone
05-1389	O18	Crushed Limestone
05-1397	O18	Crushed Limestone
05-1412	O14	Crushed Sil. & LS Gravel
05-1419	O14	Crushed Sil. & LS Gravel
05-1422	O19	Crushed Dolomite
05-1423	O55	Crushed Slag
05-1425	O18	Crushed Limestone
05-1438	O18	Crushed Limestone
05-1452	O14	Crushed Sil. & LS Gravel
05-1458	O14	Crushed Sil. & LS Gravel
05-1468	O19	Crushed Dolomite
05-1475	O48	Lightweight Aggregate
05-1476	O18	Crushed Limestone
06-0004	O18	Crushed Limestone

Table G.1. Continued.

Sample Number	Material Code	Material Type
06-0009	O18	Crushed Limestone
06-0025	O14	Crushed Sil. & LS Gravel
06-0028	O18	Crushed Limestone
06-0031	O51	Crushed Granite
06-0041	O18	Crushed Limestone
06-0078	O50	Crushed Traprock
06-0082	O49	Crushed LS Rock Asphalt
06-0086	O18	Crushed Limestone
06-0087	O18	Crushed Limestone
06-0107	O18	Crushed Limestone
06-0116	O19	Crushed Dolomite
06-0121	O19	Crushed Dolomite
06-0136	O11	Crushed Sil. Gravel
06-0143	O11	Crushed Sil. Gravel
06-0162	O18	Crushed Limestone
06-0175	O14	Crushed Sil. & LS Gravel
06-0182	O18	Crushed Limestone
06-0196	O21	Crushed Limeston Gravel
06-0199	O19	Crushed Dolomite
06-0257	O18	Crushed Limestone

Table G.2. Gradient Angularity

Sample Number	TxDOT			TTI		
	Average Angularity		Percent Loss Ang.	Average Angularity		Percent Loss Ang.
	BMD	AMD		BMD	AMD	
04-1205	2326.20	2059.90	11.45%	2391.28	1852.14	22.55%
04-1220	2609.40	1863.00	28.60%	2240.59	1668.30	25.54%
04-1277	2548.20	1974.50	22.51%	2619.33	1924.13	26.54%
04-1283	2626.80	1948.60	25.82%	2261.70	2025.59	10.44%
04-1285	3213.10	2051.40	36.16%	2920.38	1809.61	38.04%
04-1300	2991.90	1581.50	47.14%	2555.70	1791.52	29.90%
04-1307	3156.20	1872.60	40.67%	2979.65	1899.69	36.24%

Table G.2. Continued.

Sample Number	TxDOT			TTI		
	Average Angularity		Percent Loss Ang.	Average Angularity		Percent Loss Ang.
	BMD	AMD		BMD	AMD	
05-0005	2821.70	1916.80	32.07%	2810.87	2488.04	11.48%
05-0007	2778.70	2140.50	22.97%	2341.73	2013.54	14.01%
05-0009	2565.50	1950.70	23.96%	2782.41	2179.63	21.66%
05-0011	2956.60	2517.30	14.86%	2860.44	2316.60	19.01%
05-0014	2947.20	2016.70	31.57%	2882.88	2372.51	17.70%
05-0017	2597.40	2071.50	20.25%	2499.45	2141.13	14.34%
05-0020	2699.40	2225.20	17.57%	2687.65	1874.24	30.26%
05-0029	2588.60	2081.00	19.61%	2619.93	2076.84	20.73%
05-0041	2204.90	1820.60	17.43%	2403.33	1583.58	34.11%
05-0048	2164.40	2101.10	2.92%	2425.10	1914.09	21.07%
05-0077	2753.90	2517.10	8.60%	2688.99	2276.43	15.34%
05-0081	2736.60	1996.60	27.04%	2533.27	2331.66	7.96%
05-0083	2642.40	2184.20	17.34%	2861.77	2313.58	19.16%
05-0086	2513.30	2229.20	11.30%	2696.34	1941.21	28.01%
05-0089	3072.30	2108.90	31.36%	2653.82	2391.61	9.88%
05-0093	2723.00	1693.30	37.81%	2560.39	1778.80	30.53%
05-0109	2746.60	2166.90	21.11%	2607.94	2157.20	17.28%
05-0129	2624.80	2085.60	20.54%	2383.92	1538.37	35.47%
05-0143	2489.70	1953.20	21.55%	3000.07	1949.25	35.03%
05-0149	2254.10	1897.40	15.82%	2527.23	1701.11	32.69%
05-0151	2849.60	1781.40	37.49%	2827.28	1905.71	32.60%
05-0161	2843.60	2392.30	15.87%	2953.53	2791.45	5.49%
05-0178	2935.20	1754.60	40.22%	2667.21	1894.66	28.96%
05-0213	2680.80	1949.90	27.26%	2340.39	1765.07	24.58%
05-0216	2798.80			2476.35	1844.10	25.53%
05-0231	2364.80	1983.90	16.11%	2274.41	1827.69	19.64%
05-0235	2616.00	2354.80	9.98%	2688.98	2119.71	21.17%
05-0238	2493.40	2174.70	12.78%	2680.61	1800.57	32.83%
05-0239	2799.80	2351.30	16.02%			-
05-0245	2343.80	2249.80	4.01%	2692.67	2030.63	24.59%
05-0247	2882.50	2443.90	15.22%	2842.35	2134.11	24.92%
05-0251	2764.90	2372.60	14.19%	2698.69	1898.01	29.67%

Table G.2. Continued.

Sample Number	TxDOT			TTI		
	Average Angularity		Percent Loss Ang.	Average Angularity		Percent Loss Ang.
	BMD	AMD		BMD	AMD	
05-0266	2737.50	2096.40	23.42%	3051.98	2008.19	34.20%
05-0317	2866.40	2106.40	26.51%	3146.42	1972.02	37.32%
05-0320	2805.60	2129.20	24.11%	2996.06	2376.54	20.68%
05-0321	2873.40	2064.20	28.16%	2923.72	1992.44	31.85%
05-0337	2953.80	2748.10	6.96%			-
05-0338	2402.00	1970.00	17.99%	2791.78	2371.86	15.04%
05-0347	2801.90	2185.00	22.02%	2876.84	1790.19	37.77%
05-0350	2305.80	2036.60	11.67%	2567.76	1665.28	35.15%
05-0365	3212.00	2166.40	32.55%	2885.56	1623.43	43.74%
05-0368	2829.20	2134.00	24.57%	2989.02	1549.76	48.15%
05-0397	2260.10	1664.40	26.36%	2397.32	1532.34	36.08%
05-0399	2926.20	1833.40	37.35%	2779.06	1691.40	39.14%
05-0493	2946.50			2513.85	1778.13	29.27%
05-0494	2849.60			2433.82	2046.02	15.93%
05-0496	3048.50	2304.40	24.41%	2403.70	1715.20	28.64%
05-0519	2468.20	2094.40	15.14%	2621.33	1735.61	33.79%
05-0532	2797.60	1966.00	29.73%	2250.64	1584.58	29.59%
05-0535	3097.40	1999.90	35.43%	2507.48	1767.41	29.51%
05-0543	2722.20			2464.62	2141.47	13.11%
05-0545	2520.30	1998.47	20.71%	2594.54	1758.04	32.24%
05-0630	2810.60			2554.70	1947.57	23.77%
05-0643	2624.10	1797.89	31.49%	2589.19	1720.87	33.54%
05-0649	2805.90	2173.27	22.55%	2423.10	1663.60	31.34%
05-0693	2862.90			2558.39	2174.95	14.99%
05-0708	2391.00			2332.68	1745.32	25.18%
05-0768	2765.67	1921.35	30.53%	2721.47	2124.05	21.95%
05-0770	2976.40	1964.65	33.99%	2533.94	2250.29	11.19%
05-0771	2760.30	2109.98	23.56%	2706.39	1834.72	32.21%
05-0774	2744.24	2131.08	22.34%	2390.28	2488.38	-4.10%
05-0822	2614.00	2456.58	6.02%	2773.04	2357.79	14.97%
05-0824	3083.10	2083.20	32.43%	2930.76	2148.49	26.69%
05-0826	3252.40	2522.88	22.43%	3187.28	2578.47	19.10%

Table G.2. Continued.

Sample Number	TxDOT			TTI		
	Average Angularity		Percent Loss Ang.	Average Angularity		Percent Loss Ang.
	BMD	AMD		BMD	AMD	
05-0828	2914.30	2102.62	27.85%	2308.91	2047.36	11.33%
05-0832	2454.50	1800.57	26.64%	2220.50	1897.34	14.55%
05-0921	2687.60	1850.54	31.15%	2705.40	2134.76	21.09%
05-0922	2693.80	1791.19	33.51%	2510.16	1894.66	24.52%
05-0938	3352.10	2640.77	21.22%	2739.89	2916.01	-6.43%
05-0941	2608.00	2347.75	9.98%	2764.32	1957.29	29.19%
05-0943	2813.40	2289.48	18.62%	2664.54	2041.35	23.39%
05-0946	2821.40	2462.60	12.72%	2836.66	2264.02	20.19%
05-0992	2791.80	2555.68	8.46%	2580.15	1903.37	26.23%
05-0995	2726.00	2067.79	24.15%	2895.59	1966.66	32.08%
05-1002	2603.40	2710.39	-4.11%	2748.92	1951.26	29.02%
05-1009	2226.19	2571.75	-15.52%	2439.83	1806.59	25.95%
05-1183	2913.30	1959.96	32.72%	2550.01	2059.75	19.23%
05-1184	2544.90	2103.28	17.35%	2283.12	2007.18	12.09%
05-1190	2611.70	2041.00	21.85%	2431.58	1833.39	24.60%
05-1201	2678.60	1859.50	30.58%	2805.18	1852.81	33.95%
05-1205	2842.80	2054.06	27.75%	2562.06	2098.26	18.10%
05-1207	2818.90	1845.63	34.53%	2476.34	1901.03	23.23%
05-1210	2746.10	2117.02	22.91%	2424.44	1962.98	19.03%
05-1213	2846.30	2155.86	24.26%	2743.56	1864.86	32.03%
05-1221	2755.62	1966.66	28.63%	2613.30	1911.07	26.87%
05-1222	2645.77	2094.24	20.85%	2658.51	1773.11	33.30%
05-1223	2768.67	1975.70	28.64%	2577.14	2103.62	18.37%
05-1235	2542.98	1936.52	23.85%	2381.24	1674.32	29.69%
05-1236	2681.28	1923.13	28.28%	2217.49	2063.77	6.93%
05-1260	2604.93	1817.65	30.22%	2387.94	1646.53	31.05%
05-1262	2835.32	1729.24	39.01%	2421.09	1679.01	30.65%
05-1269	2738.54	2106.63	23.07%			-
05-1274	2738.88	2171.94	20.70%	2703.72	2374.20	12.19%
05-1319	2795.80	2012.20	28.03%	2259.68	1852.81	18.01%
05-1360	2653.82	2108.98	20.53%	2219.50	2050.71	7.60%
05-1389	2571.44	2135.43	16.96%	2249.64	1726.90	23.24%

Table G.2. Continued.

Sample Number	TxDOT			TTI		
	Average Angularity		Percent Loss Ang.	Average Angularity		Percent Loss Ang.
	BMD	AMD		BMD	AMD	
05-1419	2637.41	2339.38	11.30%	2240.60	2200.08	1.81%
05-1422	2680.27	1910.74	28.71%	2435.16	1652.88	32.12%
05-1468	2773.70	2086.21	24.79%	2235.58	1881.61	15.83%
06-0009	2632.39	2064.44	21.58%	2331.01	1681.69	27.86%
06-0082	2763.65	1789.51	35.25%	2466.29	1720.53	30.24%
06-0086	2784.25	2086.21	25.07%	2446.87	1793.20	26.71%

Table G.3. Aggregate Surface Texture.

Sample Number	TxDOT			TTI		
	Average Texture		Percent Loss Txtr.	Average Texture		Percent Loss Txtr.
	BMD	AMD		BMD	AMD	
04-1205	246.80	135.40	45.14%			
04-1220	222.90	130.10	41.63%			
04-1277	387.20	204.90	47.08%			
04-1283	198.80	120.70	39.29%			
04-1285	323.50	194.70	39.81%			
04-1300	283.90	52.10	81.65%			
04-1307	109.10	88.30	19.07%			
05-0005	153.40	72.90	52.48%			
05-0007	83.70	55.00	34.29%			
05-0009	154.20	96.00	37.74%			
05-0011	99.50	87.50	12.06%			
05-0014	130.10	119.90	7.84%			
05-0017	115.70	105.20	9.08%			
05-0020	103.60	108.70	-4.92%			
05-0029	107.30	106.20	1.03%			
05-0041	73.40	67.30	8.31%	73.61	79.24	-7.65%
05-0048	112.30	103.30	8.01%			
05-0077	104.60	65.10	37.76%			
05-0081	73.60	79.50	-8.02%			

Table G.3. Continued.

Sample Number	TxDOT			TTI		
	Average Texture		PErcent Loss Txtr.	Average Texture		Percent Loss Txtr.
	BMD	AMD		BMD	AMD	
05-0083	73.60	80.70	-9.65%			
05-0086	124.00	94.00	24.19%			
05-0089	50.30	51.00	-1.39%			
05-0093	53.80	30.20	43.87%			
05-0109	51.10	61.10	-19.57%			
05-0129	201.20	134.80	33.00%	183.96	110.45	39.96%
05-0143	83.30	100.90	-21.13%			
05-0149	169.20	91.20	46.10%	158.40	88.82	43.93%
05-0151	115.70	92.60	19.97%			
05-0161	110.40	97.00	12.14%			
05-0178	72.30	42.10	41.77%	79.47	41.70	47.53%
05-0213	136.00	88.00	35.29%	126.58	85.10	32.78%
05-0216	92.20			79.67	50.32	36.84%
05-0231	143.30	113.60		115.52	86.18	25.40%
05-0235	165.30	128.00	22.57%	145.68	115.39	20.79%
05-0238	139.90	89.50	36.03%	143.79	75.91	47.21%
05-0239	173.00	137.10	20.75%			
05-0245	225.40	146.00	35.23%	171.11	124.71	27.11%
05-0247	174.20	131.20	24.68%	130.28	138.92	-6.63%
05-0251	217.60	130.10	40.21%	199.25	95.01	52.32%
05-0266	483.90	413.40	14.57%			
05-0317	140.50	125.90	10.39%			
05-0320	120.00	202.60	-68.83%			
05-0321	126.40	108.00	14.56%			
05-0337	166.20	126.00	24.19%			
05-0338	121.90	103.00	15.50%			
05-0347	86.80	76.00	12.44%	75.13	60.29	19.75%
05-0350	153.90	116.10	24.56%	150.44	109.14	27.46%
05-0365	129.50	97.10	25.02%	125.43	95.71	23.69%
05-0368	84.50	47.10	44.26%	63.74	52.64	17.42%
05-0397	120.50	73.40	39.09%	97.38	65.93	32.30%
05-0399	99.60	57.40	42.37%	81.21	51.36	36.76%

Table G.3. Continued.

Sample Number	TxDOT			TTI		
	Average Texture		Percent Loss Txtr.	Average Texture		Percent Loss Txtr.
	BMD	AMD		BMD	AMD	
05-0493	79.50			70.14	46.74	33.37%
05-0494	122.50			119.90	91.65	23.56%
05-0496	82.30	60.60	26.37%	59.40	51.60	13.13%
05-0519	168.70	114.80	31.95%	153.05	89.63	41.44%
05-0532	134.90	105.30	21.94%	106.48	78.63	26.16%
05-0535	454.50	270.80	40.42%	436.70	573.99	-31.44%
05-0543	150.40			122.26	124.40	-1.76%
05-0545	74.70	54.90	26.50%	64.70	56.09	13.31%
05-0630	111.60			89.24	81.10	9.12%
05-0643	133.80	84.29	37.00%	122.15	76.21	37.61%
05-0649	86.70	51.18	40.97%	79.00	47.80	39.49%
05-0693	174.70	84.18	51.82%	148.43	216.27	-45.70%
05-0708	117.80			102.54	92.94	9.36%
05-0768	112.56	108.34	3.75%	122.45	88.48	27.74%
05-0770	115.00	114.69	0.27%	116.23	105.29	9.41%
05-0771	180.99	111.78	38.24%	204.36	142.26	30.39%
05-0774	123.73	77.97	36.98%	122.39	77.95	36.31%
05-0822	167.80	103.28	38.45%	193.10	165.05	14.52%
05-0824	226.90	156.35	31.09%	241.16	168.92	29.96%
05-0826	184.90	157.48	14.83%	185.32	176.75	4.63%
05-0828	145.80	97.86	32.88%	133.43	122.85	7.93%
05-0832	213.80	111.37	47.91%	192.87	114.16	40.81%
05-0921	75.70	52.01	31.30%	75.21	45.84	39.05%
05-0922	103.50	85.78	17.12%	111.23	66.51	40.20%
05-0938	339.50	217.14	36.04%	328.70	305.02	7.20%
05-0941	120.20	91.18	24.14%	122.21	106.71	12.69%
05-0943	99.10	95.11	4.03%	92.62	83.75	9.57%
05-0946	144.70	78.67	45.63%	151.08	111.53	26.18%
05-0992	138.10	95.06	31.16%	135.81	92.20	32.11%
05-0995	122.00	63.71	47.78%	115.89	65.10	43.82%
05-1002	161.10	110.32	31.52%	151.64	101.14	33.30%
05-1009	103.35	98.89	4.32%	122.98	72.52	41.03%

Table G.3. Continued.

Sample Number	TxDOT			TTI		
	Average Texture		Percent Loss Txtr.	Average Texture		Percent Loss Txtr.
	BMD	AMD		BMD	AMD	
05-1183	99.20	64.14	35.34%	84.86	49.40	41.78%
05-1184	217.00	117.10	46.04%	186.29	102.88	44.77%
05-1190	90.40	77.59	14.17%	84.46	69.42	17.81%
05-1201	108.00	72.26	33.09%	108.80	61.55	43.42%
05-1205	197.60	82.52	58.24%	177.88	100.68	43.40%
05-1207	96.10	61.83	35.66%	86.78	46.97	45.88%
05-1210	91.00	77.61	14.72%	93.12	62.73	32.63%
05-1213	96.20	57.23	40.51%	81.79	42.92	47.52%
05-1221	104.36	81.37	22.03%	98.70	68.79	30.31%
05-1222	97.51	84.30	13.55%	94.68	71.20	24.80%
05-1223	83.73	54.50	34.92%	88.77	51.59	41.88%
05-1235	113.53	67.48	40.57%	102.55	74.16	27.68%
05-1236	102.03	62.61	38.64%	106.57	57.07	46.44%
05-1260	98.55	60.19	38.92%	83.00	51.22	38.28%
05-1262	142.68	113.14	20.70%	147.21	96.43	34.50%
05-1269	150.96	65.77	56.43%			
05-1274	184.37	185.16	-0.43%	218.51	197.25	9.73%
05-1319	124.83	79.27	36.49%	106.78	77.08	27.81%
05-1360	95.49	63.25	33.76%	89.16	60.09	32.61%
05-1389	208.73	117.56	43.68%	207.58	135.41	34.77%
05-1419	168.66	93.63	44.49%	207.33	107.48	48.16%
05-1422	157.82	95.40	39.55%	231.54	117.04	49.45%
05-1468	234.84	127.72	45.61%	234.04	149.27	36.22%
06-0009	126.93	80.86	36.30%	104.30	60.00	42.47%
06-0082	402.52	317.38	21.15%	489.76	606.21	-23.78%
06-0086	92.45	55.72	39.73%	73.18	45.18	38.27%

Table G.4. Aggregate Sphericity.

Sample Number	TxDOT			TTI		
	Average Sphericity		Percent Loss Sph.	Average Sphericity		Percent Loss Sph.
	BMD	AMD		BMD	AMD	
04-1205	0.670	0.687	-2.43%			
04-1220	0.671	0.694	-3.56%			
04-1277	0.651	0.662	-1.67%			
04-1283	0.688	0.646	6.12%			
04-1285	0.637	0.686	-7.64%			
04-1300	0.712	0.707	0.72%			
04-1307	0.695	0.690	0.72%			
05-0005	0.602	0.654	-8.72%			
05-0007	0.683	0.690	-1.00%			
05-0009	0.627	0.676	-7.75%			
05-0011	0.708	0.717	-1.31%			
05-0014	0.687	0.704	-2.38%			
05-0017	0.708	0.699	1.29%			
05-0020	0.682	0.704	-3.24%			
05-0029	0.733	0.718	2.04%			
05-0041	0.759	0.738	2.82%	0.815	0.750	8.00%
05-0048	0.674	0.648	3.80%			
05-0077	0.680					
05-0081	0.665	0.672	-0.97%			
05-0083	0.668	0.660	1.09%			
05-0086	0.709	0.665	6.20%			
05-0089	0.649	0.640	1.39%			
05-0093	0.684	0.700	-2.37%			
05-0109	0.680	0.671	1.31%			
05-0129	0.670	0.694	-3.62%	0.704	0.773	-9.82%
05-0143	0.647	0.672	-3.97%			
05-0149	0.690	0.683	1.03%	0.674	0.688	-2.17%
05-0151	0.673	0.672	0.21%			
05-0161	0.692	0.675	2.48%			
05-0178	0.640	0.672	-4.99%	0.659	0.735	-11.48%
05-0213	0.692	0.676	2.35%	0.738	0.713	3.33%
05-0216	0.637			0.685	0.641	6.37%

Table G.4. Continued.

Sample Number	TxDOT			TTI		
	Average Sphericity		Percent Loss Sph.	Average Sphericity		Percent Loss Sph.
	BMD	AMD		BMD	AMD	
05-0231				0.727	0.697	4.07%
05-0235	0.695	0.717	-3.03%	0.707	0.784	-11.00%
05-0238	0.693	0.683	1.44%	0.729	0.692	5.06%
05-0239	0.689	0.725	-5.24%			
05-0245	0.726	0.727	-0.22%	0.721	0.755	-4.70%
05-0247	0.699	0.711	-1.83%	0.676	0.795	-17.66%
05-0251	0.684	0.705	-3.16%	0.698	0.752	-7.66%
05-0266	0.724	0.695	3.96%			
05-0317	0.681	0.688	-0.93%			
05-0320	0.710	0.716	-0.92%			
05-0321	0.625	0.641	-2.55%			
05-0337	0.705	0.695	1.55%			
05-0338	0.714	0.679	4.84%			
05-0347	0.661	0.629	4.91%	0.650	0.699	-7.55%
05-0350	0.717	0.686	4.27%	0.699	0.740	-5.85%
05-0365	0.667	0.689	-3.30%	0.683	0.733	-7.43%
05-0368	0.627	0.635	-1.27%	0.668	0.681	-2.02%
05-0397	0.695	0.701	-0.88%	0.732	0.783	-6.92%
05-0399	0.647	0.682	-5.34%	0.651	0.730	-12.10%
05-0493	0.651			0.664	0.716	-7.96%
05-0494	0.667			0.677	0.670	0.99%
05-0496	0.590	0.638	-8.11%	0.681	0.660	3.00%
05-0519	0.673	0.611	9.19%	0.681	0.665	2.21%
05-0521						
05-0532	0.688	0.686	0.30%	0.688	0.673	2.06%
05-0534			-			
05-0535	0.699	0.677	3.13%	0.716	0.703	1.82%
05-0543	0.697			0.699	0.775	-10.82%
05-0545	0.644	0.695	-7.83%	0.662	0.664	-0.25%
05-0630	0.623			0.616	0.647	-5.10%
05-0643	0.690	0.705	-2.14%	0.683	0.695	-1.82%
05-0649	0.685			0.675	0.673	0.35%

Table G.4. Continued.

Sample Number	TxDOT			TTI		
	Average Sphericity		Percent Loss Sph.	Average Sphericity		Percent Loss Sph.
	BMD	AMD		BMD	AMD	
05-0693	0.685			0.747	0.696	6.75%
05-0708	0.690			0.650	0.748	-15.12%
05-0768	0.672	0.669	0.48%	0.660	0.668	-1.20%
05-0770	0.679	0.655	3.54%	0.663	0.668	-0.71%
05-0771	0.677	0.671	0.87%	0.665	0.706	-6.24%
05-0774	0.636	0.643	-1.10%	0.673	0.641	4.73%
05-0822	0.716	0.691	3.57%	0.663	0.696	-5.03%
05-0824	0.631	0.603	4.46%	0.615	0.659	-7.01%
05-0826	0.703	0.672	4.38%	0.682	0.693	-1.67%
05-0828	0.653	0.651	0.25%	0.646	0.677	-4.79%
05-0832	0.707	0.703	0.45%	0.721	0.684	5.18%
05-0921	0.679	0.640	5.85%	0.665	0.667	-0.27%
05-0922	0.703	0.648	7.91%	0.681	0.677	0.60%
05-0938	0.660	0.654	1.01%	0.617	0.622	-0.87%
05-0941	0.720	0.688	4.56%	0.695	0.731	-5.24%
05-0943	0.687	0.667	2.87%	0.669	0.736	-10.06%
05-0946	0.670	0.626	6.61%	0.623	0.642	-3.13%
05-0992	0.735	0.673	8.48%	0.686	0.713	-3.98%
05-0995	0.683	0.660	3.41%	0.631	0.661	-4.68%
05-1002	0.727	0.644	11.41%	0.702	0.697	0.62%
05-1009	0.706	0.676	4.25%	0.710	0.725	-2.15%
05-1183	0.670	0.638	4.71%	0.658	0.667	-1.33%
05-1184	0.675	0.655	2.91%	0.661	0.654	1.00%
05-1190	0.677	0.680	-0.46%	0.705	0.673	4.50%
05-1201	0.706	0.690	2.32%	0.676	0.678	-0.42%
05-1205	0.673	0.679	-0.87%	0.642	0.668	-4.12%
05-1207	0.719	0.670	6.80%	0.681	0.684	-0.40%
05-1210	0.634	0.629	0.85%	0.645	0.662	-2.72%
05-1213	0.697	0.668	4.05%	0.660	0.713	-8.11%
05-1221	0.665	0.666	-0.21%	0.633	0.678	-7.10%
05-1222	0.668	0.660	1.18%	0.649	0.700	-7.96%
05-1223	0.678	0.673	0.82%	0.655	0.654	0.16%

Table G.4. Continued.

Sample Number	TxDOT			TTI		
	Average Sphericity		Percent Loss Sph.	Average Sphericity		Percent Loss Sph.
	BMD	AMD		BMD	AMD	
05-1235	0.679	0.675	0.63%	0.683	0.695	-1.75%
05-1236	0.668	0.676	-1.26%	0.684	0.680	0.49%
05-1260	0.689	0.680	1.37%	0.709	0.725	-2.25%
05-1262	0.660	0.693	-4.88%	0.682	0.687	-0.85%
05-1269	0.682	0.694	-1.81%			
05-1274	0.659	0.679	-3.04%	0.713	0.703	1.40%
05-1319	0.667	0.650	2.53%	0.733	0.672	8.41%
05-1360	0.661	0.663	-0.37%	0.684	0.655	4.16%
05-1389	0.659	0.665	-0.90%	0.735	0.659	10.31%
05-1419	0.684	0.685	-0.07%	0.719	0.696	3.18%
05-1422	0.685	0.665	2.95%	0.672	0.682	-1.46%
05-1468	0.667	0.700	-4.91%	0.760	0.686	9.75%
06-0009	0.676	0.679	-0.35%	0.716	0.586	18.15%
06-0082	0.671	0.681	-1.41%	0.668	0.687	-2.92%
06-0086	0.644	0.624	3.15%	0.673	0.639	5.03%

Table G.5. Aggregate Durability and Deleterious Materials Test Results

Sample Number	Percent Loss MD		Mg. Soundness		Percent Loss L.A. Abrasion
	TxDOT	TTI	HMAC	Surface Treatment	
04-1205	17.0	16.9	9	5	
04-1220	18.3	16.3	8	4	
04-1277	17.6	17.0	17	14	
04-1283	24.3	24.4	20	16	
04-1285	20.5	20.6	15	10	
04-1300	21.0	19.5	18	15	
04-1307	30.7	29.5	25	19	
05-0005	13.0	11.7	6	5	
05-0007	12.5	10.5	5	4	
05-0009	11.4	10.8	6	5	
05-0011	7.9	7.2	5	4	

Table G.5. Continued.

Sample Number	Percent Loss MD		Mg. Soundness		Percent Loss L.A. Abrasion
	TxDOT	TTI	HMAC	Surface Treatment	
05-0014	9.3	9.0	8	5	
05-0017	10.9	9.0	9	7	
05-0020	9.2	5.7	7	5	
05-0029	6.2	5.3	13	10	
05-0041	27.6	22.5	10	14	
05-0048	12.0	11.3	7	6	
05-0077	1.8	1.3	2	2	
05-0081	7.2	7.0	3	2	
05-0083	8.6	8.4	5	3	
05-0086	16.3	17.1	18	16	
05-0089	7.2	6.6	6	5	
05-0093	31.1	19.1	20	15	
05-0109	34.9	35.1	42	35	
05-0129	11.0	10.9	8	7	
05-0143	15.5	14.2	7	6	
05-0149	15.9	15.1	11	9	
05-0151	16.7	16.3	18	16	
05-0161	7.3	6.4	11	8	
05-0178	21.7	20.1	25	22	
05-0213	16.7	15.0	8	7	25
05-0216	10.4	10.6	7	7	27
05-0231	8.3	8.2	5	5	21
05-0235	2.7	2.4	3	2	18
05-0238	10.2	9.6	5	4	19
05-0239	7.3		8	5	20
05-0245	2.8	3.2	3	2	18
05-0247	3.7	4.2	3	3	17
05-0251	11.4	11.5	6	5	23
05-0266	23.5	18.0	27	22	
05-0317	2.6	7.6	4	2	11
05-0320	8.1	7.1	11	7	19
05-0321	14.6	13.9	11	7	25
05-0337	11.2		16	14	23

Table G.5. Continued.

Sample Number	Percent Loss MD		Mg. Soundness		Percent Loss L.A. Abrasion
	TxDOT	TTI	HMAC	Surface Treatment	
05-0338	5.2	4.1	9	5	21
05-0347	31.5	29.5	34	27	33
05-0350	15.3	14.6	25	20	33
05-0365	26.4	24.6	30	25	33
05-0368	32.7	28.5	25	22	29
05-0397	19.4	18.4	11	9	27
05-0399	23.1	23.6	20	16	29
05-0493	30.9	29.0	26	21	30
05-0494	26.4	19.1	30	25	31
05-0496	31.2	14.9	57	50	43
05-0519	18.5	18.2	16	15	25
05-0521	19.6		30	20	35
05-0532	19.9	19.5	22	14	27
05-0534			27	18	28
05-0535	22.8	22.5	26	20	
05-0543	4.9	3.5	7	5	19
05-0545	33.7	29.5	27	20	31
05-0630		9.8	19	16	31
05-0643	21.5	19.1			
05-0649		24.9	18	14	30
05-0693	7.9	7.3			
05-0708	8.1	8.0	9	9	26
05-0715	9.1		22	19	32
05-0716			23	20	29
05-0719			29	26	32
05-0768	10.0	9.1	3	3	27
05-0770	9.0	9.3	3	3	22
05-0771	12.0	10.6	6	6	20
05-0774	6.0	6.4	3	3	21
05-0800	16.3		19	17	25
05-0806	11.8		7	7	19
05-0822	6.0	5.4	2	2	18
05-0824	9.0	8.6	3	3	21

Table G.5. Continued.

Sample Number	Percent Loss MD		Mg. Soundness		Percent Loss L.A. Abrasion
	TxDOT	TTI	HMAC	Surface Treatment	
05-0826	8.0	7.7	3	3	33
05-0828	6.0	5.3	5	5	26
05-0832	12.0	11.5	11	10	22
05-0921	24.0	23.3	28	25	29
05-0922	24.0	23.8	23	22	32
05-0938	4.4	4.0	2	2	28
05-0941	3.4	2.9	3	3	19
05-0943	3.0	2.8	4	4	21
05-0946	7.3	6.3	2	2	14
05-0992	17.0	16.7	6	6	31
05-0995	10.0	10.2	3	3	26
05-1002	22.2	19.5	19	13	26
05-1009	18.0	17.9	9	10	26
05-1183	24.1	23.5	23	20	30
05-1184		13.5	5	5	24
05-1190		8.6	20	12	32
05-1194	27.0		24	19	30
05-1201	17.0	14.9	4	4	27
05-1205	8.7	8.2	7	7	18
05-1207	27.0	27.7	30	23	31
05-1210	13.3	12.7	23	18	34
05-1213	26.0	22.9	25	20	30
05-1221	12.0	10.9	19	17	34
05-1222	9.0	8.1	9	9	29
05-1223	27.0	23.6	19	14	29
05-1235	25.8	26.2	19	17	30
05-1236	21.1	20.9	2	9	28
05-1260	21.4	21.7	23	14	29
05-1262	18.2	17.1	2	6	26
05-1274	7.5	7.2	0	6	18
05-1314	11.6		8	6	21
05-1319	22.0		11	7	29

Table G.5. Continued.

Sample Number	% Loss MD		Mg. Soundness		% Loss L.A. Abrasion
	TxDOT	TTI	HMAC	Surface Treatment	
05-1341	22.0		21	16	36
05-1357	20.0		12	11	28
05-1358	22.0		14	13	28
05-1359	22.8		11	9	29
05-1360	24.0	22.7	11	9	29
05-1361	23.0		20	15	30
05-1389		14.4			
05-1412	5.0		9	7	20
05-1419	14.0	12.9	27	24	24
05-1422	13.0	11.4	5	4	23
05-1423	6.0		1	1	13
05-1425	28.0		23	22	30
05-1468		9.2			
06-0004	26.0		17	15	30
06-0009	22.0	19.6	9	9	27
06-0025	10.0		10	8	25
06-0028	23.0		19	17	29
06-0031	5.0		3	4	23
06-0041	26.0		33	30	29
06-0078	20.0		24	16	14
06-0082	19.0	19.8	18	18	33
06-0086	22.0	20.1	21	22	30
06-0087	20.0		17	16	27
06-0107	15.0		16	16	25
06-0116	9.0		6	7	19
06-0121	14.0		8	10	25
06-0136	10.0				34
06-0143	7.0				19
06-0162	24.0		16	13	29
06-0175	7.0		9	10	18
06-0182	23.0		18	12	29
06-0196	20.0		19	17	26
06-0199	9.0		4	4	19

Table G.6. Other AQMP Measurements.

Sample Number	Percent >		Percent CFC>2	Flakiness	PV	
	3:1	5:1			Initial	Final
06-0257	22.0		17	16	28	
04-1205	1	1		19	39	22
04-1220	1	2		12	43	23
04-1277	5	4		16	42	23
04-1283	3	2		11	46	25
04-1285	2	2		16	49	24
04-1300	1	0		3	47	26
04-1307	2	0		4	50	25
05-0005	9	7		24		29
05-0007	7	4	99	13	42	23
05-0009	5	5		27	41	21
05-0011	3	2		7	50	33
05-0014	2	3	99	15	43	30
05-0017	3	2	97	12	42	31
05-0020	2	1	98	15	47	29
05-0029	2	2	85	11		
05-0041	0	0		2	50	48
05-0048	2	0	66	11		23
05-0077	1	0	94	6	41	25
05-0081	4	4		12		22
05-0083	8	4		20		23
05-0086	4	4		24	46	40
05-0089	6	5		27		24
05-0093	1	0		12		25
05-0109	2	1		9		25
05-0129	1	1		16	42	25
05-0143	2	2		28	40	21
05-0149	2	3		27		24
05-0151	2	0		27		24
05-0161	3	2	89	7	35	23
05-0178	1	1		17	45	27
05-0213	2	0		7	41	21
05-0216	7	0		22	41	25

Table G.6. Continued.

Sample Number	Percent >		Percent CFC>2	Flakiness	PV	
	3:1	5:1			Initial	Final
05-0231	2	1	86	12	36	24
05-0235	3	2	97	5	42	26
05-0238	2	0	86	7	40	25
05-0239	3	1	96	11	42	27
05-0245	0	0	86	15	42	25
05-0247	0	0	95	9	42	26
05-0251	1	0		4	40	21
05-0266	1	2		10		35
05-0317	1	0		22		29
05-0320	0	0		11		35
05-0321	6	3		33		25
05-0337	1	1	79	16		27
05-0338			61			24
05-0347				10		26
05-0350	1	1		12	45	33
05-0365	1	0		9	46	25
05-0368	1	1		15	48	27
05-0397	0	0		10		24
05-0399	3	1		7	43	26
05-0493	3	1		14		25
05-0494	3	0		10		23
05-0496	5	1		18		35
05-0519	2	1		19	42	23
05-0521	0	0		8	50	35
05-0532	0	0		8	46	28
05-0534					42	25
05-0535	0	0		5	51	35
05-0543	3	1	96	8	42	26
05-0545	3	2		10	46	27
05-0630	4	0		32	50	34
05-0643	1	0		6	45	27
05-0649	0	0		11	45	25
05-0693	0	0		11	46	32

Table G.6. Continued.

Sample Number	Percent >		Percent CFC>2	Flakiness	PV	
	3:1	5:1			Initial	Final
05-0708	6	1		25	47	35
05-0715					45	26
05-0716					44	25
05-0719					44	25
05-0768	2	0		14	40	23
05-0770	2	1		11		
05-0771						
05-0774	3	2		13		
05-0800			61		41	24
05-0806					44	31
05-0822	2	2		10		
05-0824	7	6		25		
05-0826	2	1		13		
05-0828	3	3		16		30
05-0832	3	2		17		27
05-0921	2	2		12		
05-0922	0	0		9	45	25
05-0938	3	2		19	41	26
05-0941	1	1	98	6	43	30
05-0943	1	1	91	5		
05-0946	8	6		20		
05-0992	1	0		3		24
05-0995	2	1		8		
05-1002	1	1		8	42	37
05-1009	0	0	95	3		
05-1183	2	1		6	43	25
05-1184	2	1		9	43	21
05-1190	5	4		15	48	
05-1194					43	25
05-1201	1	1		8		25
05-1205	3	3		14		31
05-1207	2	1		8		26
05-1210	8	8		25	47	32

Table G.6. Continued.

Sample Number	Percent >		Percent CFC>2	Flakiness	PV	
	3:1	5:1			Initial	Final
05-1213	1	1		7		26
05-1221	5	4		16	46	
05-1222	4	2		12	49	31
05-1223	1	1		7	43	23
05-1235	1	0		8		25
05-1236	1	1		7		25
05-1260	2	1		3		
05-1262	1	1		7	40	32
05-1269	1	1		15	47	
05-1274	1	1	100	8	45	30
05-1314	2	1		10	20	
05-1319	0	0		5		
05-1341	0	0		4	30	
05-1354						
05-1357	1	0		4		
05-1358	1	1		7		
05-1359	3	3		7		26
05-1360	1	2		9		25
05-1361	2	2		7		26
05-1412	2	4	95	7		
05-1419	1	1	98	4		
05-1422	2	1		8		
05-1423	1	1		1		
05-1425	2	2		8		
06-0004				4		23
06-0009	2	2		6		24
06-0025	1	1		6		
06-0028	2	2		15		20
06-0031		7		16		
06-0041				12		
06-0078		3		19		
06-0082	3	3		6		30
06-0086	8	7		15		21

Table G.6. Continued.

Sample Number	Percent >		Percent CFC>2	Flakiness	PV	
	3:1	5:1			Initial	Final
06-0087		2		9		21
06-0107	0	0		5		22
06-0116	2	2		9		26
06-0121		9		28		24
06-0136			100	16		
06-0143			90	3		
06-0162				7		25
06-0175		1	92	10		28
06-0182				3		20
06-0196			87	5		22
06-0199				7		26
06-0257				8		

Table G.7. Modified Angularity Summary.

Sample Number	TxDOT			TTI		
	Average Ang Mod		Percent Loss Ang Mod	Average Ang Mod		Percent Loss Ang Mod
	BMD	AMD		BMD	AMD	
04-1205	2723.26	1856.86	31.81%	2837.62	1874.87	33.93%
04-1220	3000.67	1791.79	40.29%	3000.11	1771.93	40.94%
04-1277	2909.11	1868.09	35.79%	2950.52	1977.80	32.97%
04-1283	2967.15	1746.30	41.15%	3039.58	1764.14	41.96%
04-1285	3508.81	2071.90	40.95%	3388.36	2114.35	37.60%
04-1300	2938.05	1590.52	45.86%	2655.18	1601.09	39.70%
04-1307	3320.66	1589.88	52.12%	3252.61	1702.94	47.64%
05-0005	3131.34	2157.82	31.09%	3079.95	2243.34	27.16%
05-0007	3048.51	2120.62	30.44%	2998.58	2074.90	30.80%
05-0009	3168.70	2193.40	30.78%	3057.21	2160.89	29.32%
05-0011	2567.77	2567.77	0.00%	3197.64	2604.69	18.54%
05-0014	2950.34	2453.75	16.83%	3011.37	2169.38	27.96%
05-0017	2664.01	2019.63	24.19%	2815.31	2168.95	22.96%
05-0020	3132.24	2178.32	30.45%	2926.72	2287.43	21.84%

Table G.7. Continued.

Sample Number	TxDOT			TTI		
	Average Ang Mod		Percent Loss Ang Mod	Average Ang Mod		Percent Loss Ang Mod
	BMD	AMD		BMD	AMD	
05-0029	2954.28	2143.18	27.46%	2915.49	2266.94	22.24%
05-0041	2321.05	1285.17	44.63%	2332.81	1329.99	42.99%
05-0048	2258.98	1766.02	21.82%	2371.38	1764.85	25.58%
05-0077	3029.10	2984.40	1.48%	3091.43	2791.60	9.70%
05-0081	3103.15	2186.07	29.55%	3194.86	2360.40	26.12%
05-0083	3159.67	2275.97	27.97%	3059.12	2193.20	28.31%
05-0086	2860.95	1900.60	33.57%	2734.55	1831.05	33.04%
05-0089	3076.53	2217.30	27.93%	3169.81	2327.35	26.58%
05-0093	2770.51	1770.52	36.09%	2818.53	1734.29	38.47%
05-0109	2967.75	1958.69	34.00%	2900.62	1949.67	32.78%
05-0129	2955.22	1997.31	32.41%	2797.51	1981.65	29.16%
05-0143	2866.36	1826.70	36.27%	2994.77	1868.82	37.60%
05-0149	2888.83	1844.59	36.15%	2763.48	1906.07	31.03%
05-0151	2979.70	1898.64	36.28%	3049.67	1906.26	37.49%
05-0161	2973.44	2836.87	4.59%	2879.18	2854.40	0.86%
05-0178	3147.99	1835.70	41.69%	3101.93	1858.76	40.08%
05-0213	3020.90	1911.34	36.73%	3002.96	1912.04	36.33%
05-0216	3062.77			3029.35	2073.25	31.56%
05-0231				2449.73	1652.40	32.55%
05-0235	2851.05	2743.04	3.79%	2839.87	2657.10	6.44%
05-0238	2587.89	1961.69	24.20%	2521.39	1852.33	26.54%
05-0239	2986.82	2436.17	18.44%			
05-0245	2955.66	2650.16	10.34%	2847.52	2563.67	9.97%
05-0247	3098.83	2561.59	17.34%	2953.07	2730.06	7.55%
05-0251	2855.27	2757.68	3.42%	2654.50	1712.21	35.50%
05-0266	3208.41	1712.47	46.63%	2970.85	1831.45	38.35%
05-0317	3185.17	2225.87	30.12%	3212.17	2228.24	30.63%
05-0320	3388.00	2389.94	29.46%	3192.02	2408.45	24.55%
05-0321	3067.77	1998.72	34.85%	3086.39	2107.40	31.72%
05-0337	3139.09	2676.95	14.72%			
05-0338	2692.61	1795.95	33.30%	2994.92	2654.59	11.36%
05-0347	3176.68	1998.43	37.09%	2996.89	2010.38	32.92%

Table G.7. Continued.

Sample Number	TxDOT			TTI		
	Average Ang Mod		Percent Loss Ang Mod	Average Ang Mod		Percent Loss Ang Mod
	BMD	AMD		BMD	AMD	
05-0350	2943.91	1851.51	37.11%	2900.15	1869.50	35.54%
05-0365	3416.27	2072.98	39.32%	3430.12	2071.74	39.60%
05-0368	3200.20	1881.26	41.21%	3023.72	1902.51	37.08%
05-0397	2860.36	1740.25	39.16%	2897.98	1677.25	42.12%
05-0399	3048.91	1698.41	44.29%	2906.93	1737.67	40.22%
05-0493	3093.18			3070.58	1946.48	36.61%
05-0494	3340.45			3197.17	2190.24	31.49%
05-0496	2624.19	2083.87	20.59%	2684.66	1997.93	25.58%
05-0519	2922.91	1955.92	33.08%	2803.28	1940.13	30.79%
05-0532	3000.46	1555.51	48.16%	2880.76	1570.19	45.49%
05-0535	3123.44	1628.75	47.85%	3032.05	1528.87	49.58%
05-0543	2906.21			2820.33	2556.95	9.34%
05-0545	3036.73	1923.27	36.67%	3052.54	1906.92	37.53%
05-0630	2979.95			2958.83	2266.18	23.41%
05-0643	2904.03	1703.40	41.34%	3031.57	1798.98	40.66%
05-0649	2788.92			2923.98	1744.71	40.33%
05-0693	3209.55			3307.12	2455.10	25.76%
05-0708	2771.35			2725.34	2044.79	24.97%
05-0768	3147.85	2282.02	27.51%	3158.71	2211.73	29.98%
05-0770	3042.83	2224.66	26.89%	3135.24	2030.84	35.23%
05-0771	2941.58	1859.30	36.79%	2936.49	1906.72	35.07%
05-0774	3047.41	2416.80	20.69%	3069.83	2297.66	25.15%
05-0822	3137.25	2670.74	14.87%	3008.95	2760.88	8.24%
05-0824	3182.12	2345.43	26.29%	3157.55	2266.77	28.21%
05-0826	3406.05	2767.79	18.74%	3523.23	2932.79	16.76%
05-0828	2798.92	2040.50	27.10%	2806.69	2127.38	24.20%
05-0832	2877.08	1999.99	30.49%	2890.27	1982.16	31.42%
05-0921	3176.90	2050.84	35.45%	3017.52	1774.23	41.20%
05-0922	2940.30	1910.36	35.03%	2888.07	1737.41	39.84%
05-0938	3279.25	2681.73	18.22%	3278.82	2831.25	13.65%
05-0941	2999.88	2628.16	12.39%	2994.70	2520.44	15.84%
05-0943	2859.53	2479.91	13.28%	2830.56	2510.91	11.29%

Table G.7. Continued.

Sample Number	TxDOT			TTI		
	Average AngMod		Percent Loss AngMod	Average AngMod		Percent Loss AngMod
	BMD	AMD		BMD	AMD	
05-0946	3257.83	2558.27	21.47%	3224.17	2563.01	20.51%
05-0992	3298.09			3189.40	1907.88	40.18%
05-0995	3051.85	2201.44	27.87%	3131.24	1993.28	36.34%
05-1002	2976.90			2782.05	1738.58	37.51%
05-1009	2491.79			2355.26	1460.55	37.99%
05-1183	3008.07	1860.14	38.16%	2970.85	1956.66	34.14%
05-1184	2807.32	1803.29	35.76%	2808.02	1809.77	35.55%
05-1190	2733.56	2066.53	24.40%	2816.46	2141.05	23.98%
05-1201	2851.66	1718.26	39.75%	2936.46	1869.29	36.34%
05-1205	2910.65	2132.94	26.72%	2937.24	2250.02	23.40%
05-1207	2940.39	1881.31	36.02%	2880.20	1817.08	36.91%
05-1210	2802.69	2232.77	20.33%	2840.76	2175.40	23.42%
05-1213	2984.22	1902.37	36.25%	2890.96	1739.55	39.83%
05-1221	2748.13	2169.16	21.07%	2785.28	2102.91	24.50%
05-1222	2687.71	2054.98	23.54%	2725.96	1998.00	26.70%
05-1223	3053.75	1900.55	37.76%	3044.18	1922.25	36.85%
05-1235	2905.92	1624.20	44.11%	2914.53	1697.84	41.75%
05-1236	2804.02	2010.35	28.30%	2794.86	1936.00	30.73%
05-1260	2969.71	1889.52	36.37%	2841.91	1798.38	36.72%
05-1262	2906.02	1570.40	45.96%	2883.40	1834.20	36.39%
05-1269	2934.63	1837.24	37.39%			-
05-1274	3275.33	2401.96	26.67%	3191.16	2473.88	22.48%
05-1319	3111.08	1943.35	37.53%	3054.49	1842.97	39.66%
05-1360	2938.38	1960.64	33.27%	2862.61	1980.36	30.82%
05-1389	2823.28	1873.13	33.65%	2755.14	1872.14	32.05%
05-1419	2943.42	2632.77	10.55%	2871.23	2609.94	9.10%
05-1422	2867.17	1900.45	33.72%	2885.94	1922.83	33.37%
05-1468	2872.47	2047.90	28.71%	2940.79	2019.49	31.33%
06-0009	3076.78	1785.73	41.96%	2872.65	1894.10	34.06%
06-0082	2766.98	1747.48	36.85%	2712.25	1650.99	39.13%
06-0086	3092.34	2041.00	34.00%	2978.50	2130.01	28.49%

Table G.8. Average of Texture Levels 4 and 5.

Sample Number	TxDOT			TTI		
	Average Texture		Percent Loss Txtr.	Average Texture		Percent Loss Txtr.
	BMD	AMD		BMD	AMD	
04-1205	160.61	99.33	38.15%			
04-1220	150.64	91.25	39.43%			
04-1277	257.41	148.24	42.41%			
04-1283	148.71	89.02	40.14%			
04-1285	205.27	130.52	36.41%			
04-1300	181.23	36.89	79.64%			
04-1307	66.29	56.34	15.01%			
05-0005	115.25	60.74	47.29%			
05-0007	70.23	44.18	37.09%			
05-0009	126.51	73.76	41.70%			
05-0011	99.94	91.39	8.55%			
05-0014	102.57	95.41	6.99%			
05-0017	89.00	84.55	5.00%			
05-0020	82.64	87.32	-5.66%			
05-0029	84.69	87.83	-3.71%			
05-0041	110.85	88.18	20.45%	113.14	112.55	0.52%
05-0048	83.19	78.96	5.08%			
05-0077	74.88					
05-0081	55.54	56.46	-1.65%			
05-0083	57.90	62.12	-7.29%			
05-0086	104.31	92.43	11.39%			
05-0089	48.96	49.68	-1.48%			
05-0093	39.51	26.67	32.49%			
05-0109	39.91	49.51	-24.06%			
05-0129	151.12	100.95	33.20%	177.19	99.50	43.84%
05-0143	57.64	65.32	-13.33%			
05-0149	120.65	68.95	42.85%	134.12	79.00	41.10%
05-0151	74.43	66.34	10.87%			
05-0161	86.91	81.22	6.55%			
05-0178	59.82	41.42	30.75%	62.85	36.31	42.23%
05-0213	89.92	61.30	31.83%	102.92	72.27	29.78%
05-0216	59.23			58.08	36.96	36.37%

Table G.8. Continued.

Sample Number	TxDOT			TTI		
	Average Texture		Percent Loss Txtr.	Average Texture		Percent Loss Txtr.
	BMD	AMD		BMD	AMD	
05-0231				117.02	89.86	23.21%
05-0235	134.05	105.00	21.67%	141.69	100.30	29.21%
05-0238	106.73	69.90	34.50%	134.03	74.90	44.12%
05-0239	140.44	100.72	28.29%			
05-0245	177.05	116.15	34.40%	167.33	99.58	40.49%
05-0247	147.74	102.64	30.53%	148.02	107.50	27.37%
05-0251	147.31	96.34	34.60%	161.17	79.64	50.59%
05-0266	381.68	392.58	-2.86%			
05-0317	153.50	136.05	11.36%			
05-0320	93.23	150.67	-61.61%			
05-0321	84.76	77.28	8.82%			
05-0337	141.60	93.40	34.04%			
05-0338	100.36	75.52	24.75%			
05-0347	69.61	59.82	14.07%	66.24	55.90	15.61%
05-0350	106.62	78.57	26.31%	128.45	86.52	32.64%
05-0365	89.56	65.30	27.09%	99.68	74.39	25.37%
05-0368	58.50	39.18	33.03%	65.66	52.70	19.72%
05-0397	83.04	56.73	31.68%	93.07	59.50	36.07%
05-0399	69.17	43.37	37.30%	74.78	45.68	38.92%
05-0493	58.05			61.26	48.97	20.06%
05-0494	85.27			96.99	71.08	26.71%
05-0496	71.42	50.62	29.13%	71.07	54.45	23.38%
05-0519	109.58	75.30	31.28%	132.23	79.94	39.55%
05-0521						
05-0532	90.11	72.46	19.59%	86.80	65.56	24.47%
05-0534						
05-0535	467.90	216.34	53.76%	325.49	357.57	-9.85%
05-0543	117.77			115.69	95.90	17.10%
05-0545	55.50	41.88	24.54%	61.01	53.33	12.60%
05-0630	115.17			114.41	94.27	17.61%
05-0643	93.73	61.17	34.74%	104.57	68.98	34.03%
05-0649	61.92			69.15	50.83	26.49%

Table G.8. Continued.

Sample Number	TxDOT			TTI		
	Average Texture		Percent Loss Txtr.	Average Texture		Percent Loss Txtr.
	BMD	AMD		BMD	AMD	
05-0693	137.49			131.28	157.09	-19.66%
05-0708	129.58			132.77	114.48	13.77%
05-0768	75.22	67.08	10.82%	84.17	70.44	16.31%
05-0770	103.29	82.20	20.42%	104.52	94.73	9.37%
05-0771	197.46	105.23	46.71%	223.05	162.03	27.36%
05-0774	138.81	70.98	48.87%	141.32	86.88	38.52%
05-0822	150.27	85.11	43.36%	192.69	154.67	19.73%
05-0824	188.19	120.85	35.78%	243.54	174.30	28.43%
05-0826	137.82	103.70	24.76%	146.81	124.45	15.23%
05-0828	157.02	96.63	38.46%	184.38	152.09	17.51%
05-0832	157.79	90.98	42.34%	162.46	108.68	33.11%
05-0921	47.66	34.09	28.48%	56.31	38.26	32.06%
05-0922	76.55	59.69	22.03%	88.44	64.76	26.78%
05-0938	232.15	147.21	36.59%	235.66	213.88	9.24%
05-0941	91.10	63.25	30.57%	105.55	89.55	15.15%
05-0943	78.29	64.90	17.10%	81.87	68.29	16.59%
05-0946	168.29	70.12	58.33%	223.58	131.67	41.11%
05-0992	91.76	60.83	33.70%	96.45	75.35	21.87%
05-0995	74.39	42.62	42.72%	77.22	50.51	34.59%
05-1002	118.68	81.74	31.12%	133.35	98.49	26.14%
05-1009	81.94	74.18	9.48%	112.33	75.31	32.96%
05-1183	63.48	42.14	33.61%	59.99	45.95	23.40%
05-1184	142.10	84.09	40.83%	141.62	96.20	32.07%
05-1190	89.07	67.07	24.70%	101.06	84.45	16.44%
05-1201	77.63	50.48	34.98%	86.44	59.79	30.83%
05-1205	176.04	75.53	57.10%	187.75	119.61	36.29%
05-1207	61.53	44.03	28.44%	65.61	48.15	26.62%
05-1210	95.93	71.14	25.84%	113.74	77.82	31.58%
05-1213	61.43	41.91	31.78%	67.59	42.47	37.16%
05-1221	101.04	71.57	29.16%	119.72	78.45	34.47%
05-1222	95.50	76.25	20.16%	115.04	88.50	23.07%
05-1223	57.89	40.08	30.77%	66.90	48.18	27.98%

Table G.8. Continued.

Sample Number	TxDOT			TTI		
	Average Texture		Percent Loss Txtr.	Average Texture		Percent Loss Txtr.
	BMD	AMD		BMD	AMD	
05-1235	72.70	47.56	34.59%	84.46	64.56	23.56%
05-1236	70.30	47.67	32.19%	85.70	55.49	35.25%
05-1260	66.55	42.66	35.91%	68.40	49.44	27.72%
05-1262	95.42	80.14	16.02%	121.24	91.09	24.86%
05-1269	100.25	47.09	53.02%			
05-1274	131.06	136.63	-4.24%	175.37	153.94	12.22%
05-1319	77.78	54.86	29.48%	78.04	60.11	22.98%
05-1360	69.08	52.12	24.55%	75.51	50.79	32.74%
05-1389	140.51	96.90	31.04%	161.26	106.41	34.01%
05-1419	128.58	72.05	43.96%	177.96	89.51	49.70%
05-1422	134.72	94.50	29.86%	246.63	121.75	50.63%
05-1468	194.19	113.73	41.43%	214.90	143.08	33.42%
06-0009	81.30	63.74	21.60%	77.38	56.58	26.88%
06-0082	279.45	212.72	23.88%	344.68	375.79	-9.03%
06-0086	64.52	37.33	42.14%	60.41	38.39	36.46%